

DEVELOPMENTAL AND FUNCTIONAL INFLUENCES ON  
COVARIANCE IN THE MANDIBLE

by

Megan Anne Holmes

A dissertation submitted to Johns Hopkins University in conformity with the  
requirements of the degree of Doctor of Philosophy.

Baltimore, Maryland

October, 2015

## Abstract

The mandible is a morphologically complex structure shaped by multiple demands including function and development. It is difficult to untangle the extent to which complex external influences and internal constraints impact mandibular shape. The study of covariance plays an essential role in understanding the development and evolution of complex morphologies like the mandible. Determining the pattern and magnitude of covariance elucidates the degree to which traits are developmentally and/or functionally correlated while illuminating the extent of morphological constraints. The hypotheses of this dissertation address whether and to what extent covariance 1) changes in the mandible over ontogeny and whether these changes are linked to function, and; 2) is different between primates with distinct dietary demands.

Two samples were collected to address these hypotheses, separately. The first was an ontogenetic sample of mutant mice and wild-type littermates. Ontogenetic comparisons of covariance were conducted between wild-type age groups, as well as between age-matched wild-type and mutant cohorts. The second sample consisted of four closely related platyrrhines, belonging to Cebidae (*Cebus apella*; *Saimiri sciureus*) and Pitheciidae (*Pithecia pithecia*; *Callicebus torquatus*). Within-clade pair-wise comparisons of covariance were conducted between primates that possess mechanically challenging diets and those that do not. Procrustes superimposition techniques were applied to three-dimensional landmarks collected from the mandibles of each individual. Procrustes data were used to compare patterns and magnitudes of covariance within each sample.

Results showed that pattern and magnitude of covariance changed throughout ontogeny in mice. Patterns shifted between peri-weaning and adult mice, coincident with a transition to an adult diet. Thus, early developmental constraints may deter selective pressures. Comparisons of mutant and wild-type mice, as well as primate dietary groups revealed similar patterns of covariance between groups. In contrast, magnitude of covariance varied drastically in each group comparison. Previous studies also document these trends in other model mice and across taxonomic groups within mammals. This indicates that patterns of covariance are conserved, likely via stabilizing selection on development and functional constraints. Plasticity in magnitudes of covariance, however, likely facilitates morphological diversity. Lastly, primates that consumed hard foods possessed higher magnitudes of covariance, further suggesting an important role for function in determining mandibular shape.

## **Acknowledgments**

Thank you to my family for your patience. Thank you to my friends for your support. Thank you to my mentors for your guidance. No one succeeds alone. I could not have achieved any of this without you.

## Table of Contents

Abstract.....	ii
Acknowledgements.....	iv
List of Tables.....	ix
List of Figures.....	xi
 Chapter 1: Introduction and Background.....	 1
1.1 Introduction.....	1
1.2 The Structure of Covariance.....	3
1.2.1 Morphological Integration and Modularity.....	6
1.2.2 Covariance in the Mandible.....	14
1.3. Functional Morphology of the Mandible.....	26
1.4 Challenge: Interpreting Mandibular Shape.....	31
1.4.1 Addressing the Challenge.....	31
1.5 Hypotheses.....	33
1.5.1 Covariance of Shape Changes over Ontogeny.....	35
1.5.2 Covariance of Shape Differs between genotype.....	37
1.5.3 Covariance of Shape will be different among primates will different masticatory loading regimes.....	39
Chapter 2: Materials and Methods.....	42
2.1. Developmental Mutant Sample – Crouzon Mice.....	43
2.1.1. Fibroblast Growth Factor receptor 2 – Crouzon Syndrome.....	44
2.1.2 Crouzon Mouse Data Collection.....	48
2.1.3 Mouse Ages.....	50
2.2 Functional Sample – Primates.....	51
2.2.1 Primate Sample Selection.....	53
2.2.2. Crown Platyrrhines - Taxonomy.....	53
2.2.3 Cebidae and Pitheciidae Diet.....	55
2.2.4. Primate Data Collection.....	62
2.3 Data Collection.....	67
2.3.1 Landmark Selection.....	67
2.3.2 Generalized Procrustes Analysis.....	72

2.4 Error Study for Landmark data .....	76
2.4.1 Developmental Sample: Landmark Measurement Error Analysis .....	77
2.4.2 Functional Sample: Landmark Measurement Error Analysis .....	78
2.4.3 Colony-based Shape Differences .....	81
2.5 Statistical Analyses .....	87
2.5.1 Covariance Matrix Comparison .....	91
2.5.2 Scaled Variance of the Eigenvalue .....	97
2.5.3. RV coefficient .....	99
Chapter 3: Results and Discussion – Developmental Hypotheses .....	102
3.1. Results .....	102
3.1.1. Ontogenetic Shape and Size Variation .....	102
3.1.2. Patterns of Covariance over Ontogeny .....	109
3.1.3. Magnitude of Covariance over Ontogeny .....	117
3.2. Discussion .....	120
3.2.1. Ontogenetic Changes in Mandibular Morphology .....	120
3.2.2 Patterns of Covariance Change at Specific Ontogenetic Times .....	123
3.2.3 Magnitude of Covariance Changes over Ontogeny .....	126
3.2.4 Summary .....	131
Chapter 4: Results and Discussion – Mutation Hypotheses .....	135
4.1. Results .....	135
4.1.1. Genotype Shape and Size Variation .....	135
4.1.2. Patterns of Covariance across Genotypes .....	144
4.1.3. Magnitude of Covariance across Genotypes .....	153
4.2. Discussion .....	165
4.2.1 Dynamic interaction of shape and size between the WT and HT mice. ....	165
4.2.2 Only Magnitude of Covariance is Altered Between Wild-type and Crouzon Mice ...	169
4.2.3 Summary .....	174
Chapter 5: Results and Discussion – Functional Hypotheses .....	176
5.1. Results .....	<b>176</b>
5.1.1. Shape Variation .....	176
5.1.2 Patterns of Covariance .....	182
5.1.3. Magnitude .....	189
5.2 Discussion .....	<b>193</b>
5.2.1 Mandibular Morphological Diversity .....	194
5.2.2. Covariance Patterns Are Conserved Across Primate Groups. ....	197
5.2.3. Magnitude of Integration Differs Amongst Primate Mandibles. ....	201

5.2.4 The Mandible Has A Hierarchical Covariance Structure. ....	207
5.2.5 Summary .....	209
Chapter 6: Overall Conclusions .....	212
6.1 Interpretations of Mandibular Covariance from both Samples.....	<b>212</b>
6.1.1 The Mandible is a Nested Hierarchical Structure .....	213
6.1.2 Pattern of Covariance is conserved while Magnitude of Covariance is Plastic .....	214
6.1.3 Covariance Changes over Ontogeny .....	215
6.1.4 Function Influences Covariance.....	217
Literature Cited .....	221
Curriculum Vitae.....	260

## List of Tables

Table 2.1	List of mouse model sample ages and genotype.....	50
Table 2.2	New World Monkey sample.....	62
Table 2.3	List of landmarks used in both the mouse and primate samples.....	70
Table 2.4	Total number of landmarks for both sample sets (k).....	72
Table 3.1	Covariance matrix repeatability, observed and adjusted correlations compared between WT age groups.....	111
Table 3.2	Calculations of observed variance for each separate age group.....	113
Table 3.3	Table of RV coefficients for ontogenetic mouse sample.....	119
Table 4.1	Covariance matrix repeatability, observed and adjusted correlations compared between WT and HT age-cohorts.....	145
Table 4.2	Calculations of observed variance for each separate age group.....	146
Table 4.3	Pairwise correlation of 2-Block PLS scores from raw data within WT and HT age-cohorts.....	147
Table 4.4	Pairwise correlation of 2-Block PLS scores from scaled data within WT and HT age-cohorts.....	148
Table 5.1	MANCOVA results investigating the influence of sex and allometry on mandibular shape in each primate genus.....	181
Table 5.2	Covariance matrix repeatability, observed and adjusted correlations for <i>Cebus</i> – <i>Saimiri</i> and <i>Pithecia</i> – <i>Callicebus</i> .....	182
Table 5.3	Calculations of observed variance for each separate primate genus.....	184
Table 5.4	Pairwise correlation of 2-Block PLS scores between the alveolar and ramal regions in the mandible.....	184



Table 5.5	Table of RV coefficients from each primate genus.....	193
-----------	---	-----

## List of Figures

Figure 1.1	Image illustrating pleiotropic interactions from gene to units of traits.....	9
Figure 1.2	Image depicting anatomy of the mammalian mandible.....	15
Figure 2.1	Size and shape differences among adult WT and HT mandibles using Euclidean Distance Matrix Analysis.....	47
Figure 2.2	Mouse sample growth series.....	51
Figure 2.3	Platyrrhini phylogenetic tree.....	54
Figure 2.4	Mandibles of the four species used in this analysis.....	63
Figure 2.5	Positions used to capture mandibular surfaces using the NextEngine scanner.....	66
Figure 2.6	Image depicting landmarks used to capture mouse mandibular morphology.....	69
Figure 2.7	PCA scatterplots demonstrating the distinction of specimens .....	80
Figure 2.8	Principal Component Analysis scatterplot of colony differences for E17.5 mice.....	82
Figure 2.9	Principal Component Analysis scatterplot of colony differences for P14 mice.....	83
Figure 2.10	Principal Component Analysis scatterplot of colony differences for P42 mice.....	84
Figure 2.11	Two conventional modular structures demonstrated on adult mouse mandibles.....	90

Figure 3.1	Principal Component Analysis scatterplot of WT mouse mandibles of each age range.....	104
Figure 3.2	Boxplot showing the distribution of mandibular size (ln CS) among each of the WT age groups.....	107
Figure 3.3	Wireframes show the average shape of each WT age group.....	109
Figure 3.4	Scatterplots of WT PLS1 & PLS2 scores from ontogenetic 2-Block PLS analyses. ....	115
Figure 3.5	SVE scores for WT mice over ontogeny.....	118
Figure 4.1	PCA scatterplot of WT and HT embryonic mice (E17.5).....	136
Figure 4.2	PCA scatterplot of WT and HT embryonic mice (P14).....	138
Figure 4.3	PCA scatterplot of WT and HT embryonic mice (P42).....	140
Figure 4.4	Box-plots comparing mandibular size (ln CS) between WT and HT mice within each age range.....	141
Figure 4.5	Scatterplots representing WT and HT mandibular shape change associated with static allometry within each age cohort.....	143
Figure 4.6	Scatterplots of WT and HT age-cohorts for PLS1 axes scores.....	149
Figure 4.7	Wireframes depicting the pattern of shape change associated with the greatest amount of covariance between the alveolar and ramal region in WT and HT age-cohort mandibles.....	151
Figure 4.8	Raw SVE scores for WT and HT embryonic (E 17.5) mice.....	154
Figure 4.9	Raw SVE scores for WT and HT peri-weaning (P 14) mice.....	155
Figure 4.10	Raw SVE scores for WT and HT adult (P 42) mice.....	156
Figure 4.11	Scaled SVE scores for WT and HT embryonic (E17.5) mice.....	157

Figure 4.12	Scaled SVE scores for WT and HT peri-weaning (P14) mice.....	158
Figure 4.13	Scaled SVE scores for WT and HT adult (P42) mice.....	159
Figure 4.14	SVE scores for JHU bred WT and HT embryonic (E 17.5) mice....	161
Figure 4.15	SVE scores for JHU bred WT and HT peri-weaning (P 14) mice...	162
Figure 4.16	SVE scores for JHU bred WT and HT adult (P 42) mice.....	163
Figure 4.17	17 Histogram showing the distribution (up to 90%) of the percent of variance over principle component axes for mouse colonies.....	164
Figure 5.1	Principal Component Analysis scatterplot of PC1 and PC2 scores for all primates.....	177
Figure 5.2	Shape changes within sister-taxa cohorts.....	178
Figure 5.3	Images demonstrating ln CS differences between primate taxa and between within-taxa sex.....	180
Figure 5.4	Scatterplots of PLS1 scores from 2-Block PLS analyses of <i>Cebus</i> – <i>Saimiri</i> and <i>Pithecia</i> – <i>Callicebus</i> .....	187
Figure 5.5	Scatterplots of PLS2 scores from 2-Block PLS analyses of <i>Cebus</i> – <i>Saimiri</i> and <i>Pithecia</i> – <i>Callicebus</i> .....	188
Figure 5.6	SVE scores for the Cebid cohort using three different landmark configurations based on the global mandible, landmarks representing the Bi-module configuration and the Mesenchymal configuration.....	190

Figure 5.7	SVE scores for the Pithecinne cohort using three different landmark configurations based on the global mandible, landmarks representing the Bi-module configuration and the Mesenchymal configuration.....	191
------------	--	-----



# Chapter 1: Introduction and Background

## 1.1 Introduction

Evolutionary studies focused on the mammalian mandible have traditionally highlighted its functional, morphological and developmental complexity. The mandible must generate and withstand bite forces necessary to masticate mechanically resistant foods and for paramasticatory behaviors, such as combat in seals (e.g., Jones *et al.*, 2013) or tools use in humans (e.g., Spencer and Demes, 1993; Holmes and Ruff, 2011). The mandible must also articulate with the cranial base at the temporomandibular joint (TMJ), provide appropriate attachment sites for muscles of mastication, house deciduous and developing dentition and place those teeth in occlusion with the maxillary dentition. Lastly, development of the mandible involves multiple osteo- and chondrogenic precursor cell populations, as well as, mesenchymal condensations. Thus, it may not be surprising that it is difficult to untangle the extent to which these complex external influences and internal constraints impact mandibular shape, especially among primates.

Despite these complexities, mandibular shape is regularly studied in evolutionary anthropological studies and evolutionary biology, at large. This may be due to three general reasons. First, the mandible is well represented in the primate fossil record. Paleoanthropologists rely on the mandible to provide information on the diet and phylogeny to reconstruct species-level dietary behavior. Second, mandibular morphology provides the same information concerning extant species while allowing for the direct observation of dietary behaviors. Third, the mandible provides an excellent opportunity to study the juxtaposition of function and genetic pleiotropic influence in one structure. Several studies have looked at the external influences of differing diets on mandibular

form in experimental designs (Bouvier and Hylander, 1982; McFadden and McFadden, 1986; Corruccini and Beecher, 1982; 1984; Hylander and Johnson, 1994; Lieberman et al., 2004; Ravosa et al., 2007; 2008; Vinyard, 2008; Menegaz et al., 2010, Iriarte-Díaz et al., 2011; Ross et al., 2012; Anderson *et al.*, 2014; Scott et al., 2014) and in natural settings (Daegling, 1989, 1992; Ravosa, 1996; Taylor, 2002; Vinyard et al., 2003; Badyaev and Forseman, 2004; Daegling and Grine, 2004; Badyaev, 2005; Badyaev *et al.*, 2005; Perry and Wall, 2008 Taylor et al., 2009; Vinyard and Taylor, 2010; Perry *et al.*, 2014). Other analyses focused on the internal developmental-genetic effects on size and shape variation in the mandible (Atchley *et al.*, 1985a, b; Bailey, 1986; Zelditch, 1988; Zelditch and Carmichael, 1989 a, b; Atchley and Hall, 1991; Cheverud *et al.*, 1991; Mezey *et al.*, 2000; Klingenberg *et al.*, 2004), including studies that explored the modifications of specific genetic pathways responsible for mandibular size and shape (Atchley *et al.*, 1990; Vogl *et al.*, 1993; Cheverud *et al.*, 1997; Leamy *et al.*, 1997; Klingenberg and Leamy, 2001; Leamy *et al.*, 2008; Jones *et al.*, 2008; Renaud *et al.*, 2010; Fish *et al.*, 2014).

Understanding the ontogenetic (internal) and functional (external) impacts on the shape and variation of the mandible is extremely important. If the jaw is to be utilized to elucidate how mechanisms of evolutionary biology work then it must be known how selective pressures have evolved to constrain mandibular morphology. Similarly, functional anatomy is used to generate hypotheses about how the mandible has been optimally adapted to withstand particular diets or other ecological factors. If the degree of plasticity-to-constraint of the mandibular form is unclear, then theories that do not take this factor into account are less likely to accurately explain complex mandibular



morphology. Here a series of hypotheses will be tested by studying patterns of covariance in the mandible. Objectives include defining how ontogenetic changes and differing masticatory demands might influence variance and covariance in the mandible.

## **1.2 The Structure of Covariance**

Studying the structure of covariation within skeletal structures is a useful and well known method to explore the factors involved in complex morphologies. Olson and Miller (1958) termed the covariance found among traits as *morphological integration*. The central theory behind morphological integration assumes that complex structures are comprised of several interdependent traits. Variation in one trait may result in coordinated variation in others. Covariation of anatomic units can be the result of variation in genetic, developmental or functional determinants. Olson and Miller (1958) introduced a quantitative way in which to test *a priori* hypotheses of covariation among traits via correlation coefficients. Cheverud (1982, 1984, 1996 a, b) later expanded upon these theoretical underpinnings by testing them against quantitative genetic theory. These analyses demonstrated that developmentally and functionally integrated traits would be genetically integrated, and thus co-inherited, allowing for the evolution of correlated traits at the population level.

Covariation in the craniofacial complex can give insight into species diversity and evolutionary trends as each character or trait must be viewed as part of a system, not an independent entity. This is especially significant when conducting cladistic analyses which rely on the ability to identify independent, homologous traits (Lieberman, 1995,

1999). Investigations of covariation structure are also useful for establishing trends in species diversity and evolutionary biology in general. Previous analyses have examined phenotypic covariance structure in the skull across broad taxonomic groups within mammals, including primates and carnivores, which have linked patterns of integration with morphological diversification and adaptive radiations (Marroig and Cheverud, 2001; Marroig *et al.*, 2004; Goswami, 2006; Drake and Klingenberg, 2010; Meloro *et al.*, 2011; Marroig *et al.*, 2009; Oliveira *et al.*, 2009; Porto *et al.*, 2009; Shirai *et al.*, 2010; Joganic *et al.*, 2012).

Patterns of covariation have also been helpful in analyses of developmental evolutionary biology for determining the processes behind phenotypic variability (Willmore *et al.*, 2007). A large number of these analyses have been conducted on model organisms to gain insight on how variation is mediated from the genotype to the phenotype (Zelditch and Carmichael, 1989a, b; Hallgrímsson *et al.*, 2004, 2006; Willmore *et al.*, 2006, 2009; Zelditch *et al.*, 2006; Gonzalez, *et al.*, 2011; 2014; Burgio *et al.*, 2012; Fish *et al.*, 2012; Parsons *et al.*, 2012; Renaud *et al.*, 2013; Anderson *et al.*, 2014). Phenotypic integration also has clinical relevance, it has been used to determine the influence of particular mutations or surgery on craniofacial dysmorphology (Richtsmeier *et al.*, 2005; Richtsmeier *et al.*, 2006; Richtsmeier and DeLeon, 2009; Martínez-Abadías *et al.*, 2010). Despite the powerful utility of model organisms as platforms to investigate the structure of covariance, very few of these analyses have been conducted on an ontogenetic sample.

A recent study by Gonzalez *et al.*, (2011) explored how the structure of covariance changed over ontogeny in the skull of rats (*Rattus norvegicus albinus*). One of the main hypotheses postulated that nutrient deprivation during fetal growth would increase the amount of variance in the crania of developing rats, leading to an alteration in the pattern and degree of integration seen within shape of the skull. In order to test their hypotheses, rats were deprived of nutrient rich blood while *in utero*, then data on cranial shape were collected from birth (P0) to 21 days of age (P21).

Nutrition deficiency, which Gonzalez *et al.*, (2011) found resulted in greater amounts of variance when compared to controls. Variance was also greatest in the youngest individuals (P0 to P17), as expected, though this dissipated as the specimens neared P21. Results from covariance matrix comparisons between successive age groups demonstrated low correlation scores ( $R = \sim 0.20$ ) suggesting that the structure of covariance in shape was changing throughout postnatal development. Furthermore, the largest discrepancies were found when the youngest (P5) and oldest (P21) rats were compared. Not only was this disparity between ages detectable in the way in which cranial traits were integrated, it was also found in the degree to which the skull was integrated.

Overall, the trends found in this study suggested that the structure of covariance in rat crania changes significantly with age, which the authors attributed to temporally dynamic covariance patterns. Environmental disturbances, such as nutrition deficiency, will thus have varying degrees of influence on phenotype or shape depending on when they occur along growth trajectories. The influence of nutrient deprivation enacted on fetal rats resulted in ongoing variance further suggesting that adult phenotypes are highly

dependent on environmental influences experienced during development. Interestingly, phenotypic covariance in the basicranium is considered to be rather constrained so that response to environmental disturbances may be slightly muted (e.g., Goswami, 2006; Goswami and Polly, 2010; Singh *et al.*, 2012; Goswami *et al.*, 2014). The mandible however, is considered to be a relatively plastic bone which responds to environmental stimuli through life (e.g., Badyaev *et al.*, 2005; Young *et al.*, 2010; Renaud *et al.*, 2010, 2015; Holmes and Ruff, 2011; Scott *et al.*, 2014). Yet, very few ontogenetic analyses have been conducted which specifically aim to determine the ways in which covariance changes in the mandible as it develops. The purpose of this project is to utilize this powerful methodology to further learn how the mandible is formed and how covariance changes over ontogeny.

### 1.2.1 Morphological Integration and Modularity

Morphological structures are considered to covary in a hierarchical manner (e.g., Bolker, 2000; Hallgrímsson *et al.*, 2009). In other words, while morphological integration can span various components of an organism, levels of covariation among traits may be higher within components than among them. These internally integrated units are referred to as modules. Morphological integration and modularity are closely related phenomena that share implications for evolutionary biology. Namely, the relationship between integration and modularity may determine the ease and direction in which organisms will respond to selection (Wagner and Altenberg, 1996; Hansen, 2003; Wagner *et al.*, 2007; Hansen and House, 2008).

Integration and modularity are inherently related; however it is important to understand the key differences between these two concepts. One important mechanism that previous authors have suggested results in morphological integration is the selection for pleiotropy (the ability of one gene to affect multiple structures) among traits (Lande, 1979; Ehrich et al., 2003; Cheverud et al., 2004; Kenney-Hunt et al., 2008). The reasoning is that pleiotropy among traits creates a coordinated signaling system and shared developmental effects. Modularity, on the other hand, requires a division in the signaling systems, whether via adaptive selection or mutation, that spans multiple traits (Klingenberg, 2008a; Hallgrímsson et al., 2009). Thus, because modularity is associated with a break in pleiotropy, developmental effects are no longer shared among traits. This dissociation among traits does not necessarily mean that correlations across the entire structure become absent, only that the correlations among components are significantly weaker than those found within them.

Basic differences between morphological integration and modularity underlie assumptions of how they channel the introduction of variation. Whereas morphological integration limits the potential for variation of a structure, thus constraining the phenotype, modularity has been suggested to allow the phenotype to remain more susceptible to selective pressures, by allowing selection to modify some units of complex morphological structures while other units remain unchanged (Wagner, 1996; Raff and Sly, 2000; Hansen, 2003; Klingenberg, 2005; Hansen and Houle, 2008). This is the case whether modification is due to adaptive pressures or mutation. (Lande, 1980a; Wagner and Altenberg, 1996; Jones et al., 2014). The ability to dissociate units of traits means

that direct selection on one unit will not have deleterious effects on indirectly selected units (Needham, 1933; Bonner, 1988). This increases the ability for biological organisms to respond to adaptive selection, termed ‘evolvability’ (Wagner and Altenberg, 1996; Hansen, 2003; Wagner et al., 2007).

Evolvability, as a dispositional concept, is facilitated by an elevated presence of modularity in contrast to overall inter-trait integration (Hansen and Houle, 2008). Recent empirical analyses have been dedicated to unraveling how covariance in natural populations relates to evolvability and the response to selection. Results overwhelmingly suggest that higher levels of modularity, relative to integration, are associated with increased response to selective pressures and thus greater evolvability (Marroig et al., 2009; Goswami et al., 2014). Conversely, larger overall morphological integration was shown to be more constrained under selection. This however, does not detract from the adaptive importance of integration as a means to co-select developmentally and functionally linked traits (Armbruster et al., 2014).

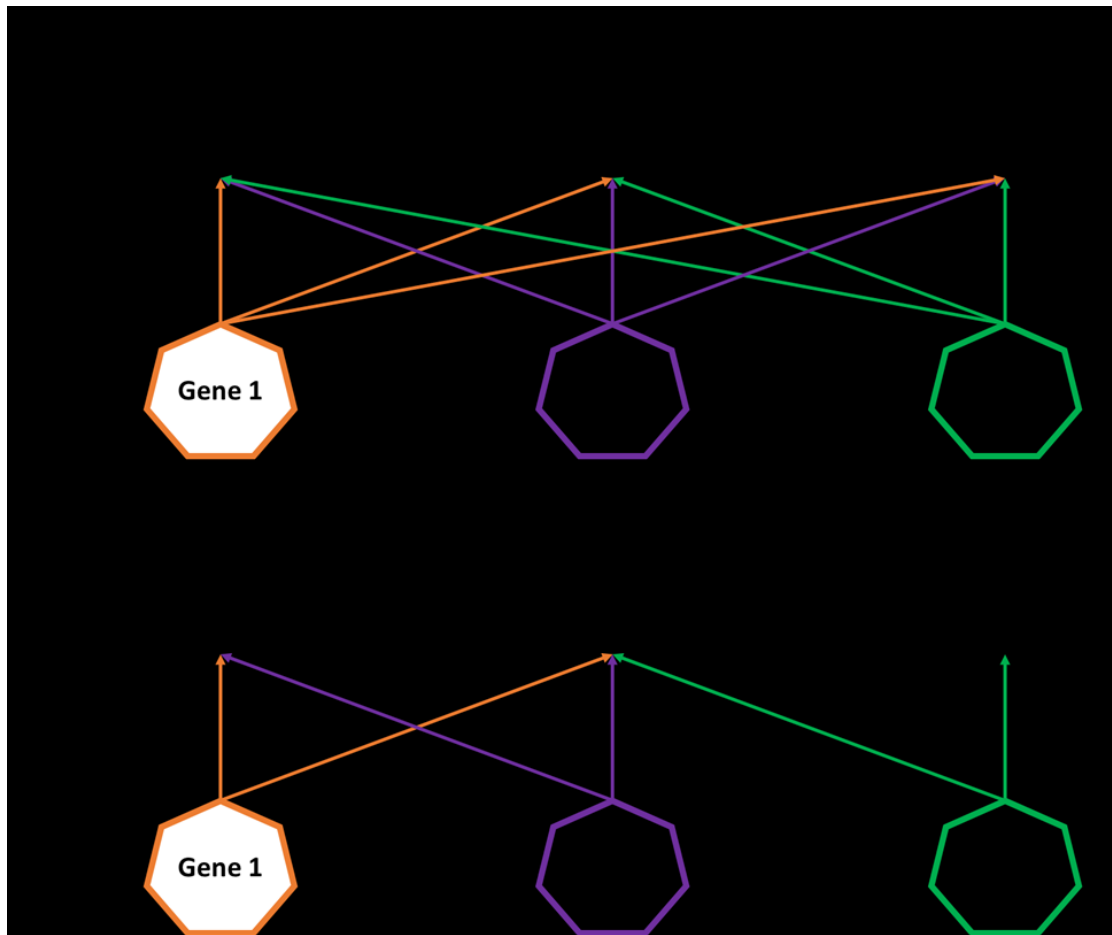


**Figure 1.1** Image illustrating pleiotropic interactions from gene to units of traits. This schematic is a simplification of pleiotropic signaling pathways associated with A) morphological integration and B) modularity. Three separate genes are represented by each heptagon. Three units of multiple traits are represented by the black rectangles. The color coordinated arrows connecting each gene to respective units represent signaling pathways (developmental factors). Solid black arrows indicate strong correlation between traits, while hatched black arrows indicated weakened correlation between traits. A) Pleiotropic signaling patterns of all three genes affect each unit equally, resulting in morphological integration between each unit. B) A change in signaling pathway minimizes pleiotropic effects shared between unit 3 and the other units. This results in a weakened pattern of integration between unit 3 and the other units and engenders a modular structure of covariance.

The organization of covariance, whether highly integrated or modular, influences the response to selection as stated above. In turn, selective pressures have also been shown to mold inter-trait relationships and the stability of that relationship (Wagner and Altenberg, 1996; Jones et al., 2003, 2007; Estes and Arnold, 2007; Wagner et al., 2007;

Jamniczky and Hallgrímsson, 2009; Jones et al., 2014). Lande and colleagues (1980a, b; Lande and Arnold, 1983) suggested that stabilizing selection, which favors average phenotypes over extremes, decreases population variance. Decrease in variance caused by stabilizing selection has long been associated with constraint and further extrapolated to induce long-term stability in the structure of covariance (Armbruster et al., 2014). In a simulation study, Melo and Marroig (2015) applied separate selective pressures such as directional and stabilizing selection, to a group of traits modeled as modules. Results from these tests showed that directional selection was essential in creating modular structures, which could conceivably occur via breaks in pleiotropic patterns. Stabilizing selection on the other hand, was critical in maintaining the organization of modularity within simulated biological systems.

In summary, structures such as the skull and the mandible are hierarchically arranged with integrated inter-trait relationships at larger organizational levels and modular relationships at smaller levels. The proportion of morphological integration to modulatory may determine the evolvability of a species or population. In particular, wide-spanning modularity has been theoretically and empirically linked to an amplified response to selective pressures largely due to the autonomous nature of modules. Lastly, the maintenance of morphological integration and modularity within the overall organization of covariance has been attributed to stabilizing selection, which may buffer against the introduction of increased modularity within a population.



### *Developmental and Functional Covariance*

Developmental and functional covariance are inherently related to each other and are thought to evolve together as functionally viable traits are inherited (Olson and Miller, 1958; Cheverud, 1982; 1984; 1996a; Chernoff and Magwene, 1999; Zelditch *et al.*, 2006; 2008; 2009; Wagner *et al.*, 2007; Klingenberg, 2014). Developmentally and functionally linked traits may be integrated due to shared genetic selection (Lande, 1980) or as independent traits selected together (Cheverud *et al.*, 2004). Given the plasticity found in bone, stabilizing selection may be advantageous for avoiding deleterious variation and thus constraining functionally linked traits through evolving genetic pleiotropy (Young and Hallgrímsson, 2005; Jamniczky and Hallgrímsson, 2009). Thus covariance in functional traits can be moderated by selecting for specific developmental pathways, inherently linking the two patterns of covariance. However, the degree to which one affects the other is not fully resolved in the literature (Wainwright *et al.*, 2005; Breuker *et al.*, 2006; Young *et al.*, 2007; Klingenberg, 2008; Klingenberg *et al.*, 2010).

Developmental covariance is generated as a result of traits sharing similar developmental pathways, sharing similar embryonic cellular origins (Atchley and Hall, 1991; Atchley, 1993) or in several other ways. Shared signaling among tissues, such as mesenchymal condensations, means that any variation derived from that signal will result in shared variance (or covariance) between those two tissues. This has been shown to result from pleiotropic signaling (Cheverud, 1996a; Ehrich *et al.*, Cheverud *et al.*, 2004; Klingenberg 2008a). If a modification in pleiotropic signaling were to occur in which one of the mesenchymal condensations is differentially affected, that shared covariance is weakened. For instance, epistatic interactions in which one gene is dependent on another

are known to have pleiotropic effects on developmental processes (Rice, 1998; Rutherford, 2000; Wolf *et al.*, 2005; Kenney-Hunt *et al.*, 2008; Pavlicev *et al.*, 2008; Sikkink *et al.*, 2015). Adjustments in epistatic interactions that affect those developmental pathways therefore have the ability to dissociate traits that were previously integrated, resulting in a modularity among traits.

Functional covariance arises under biomechanical influence in which traits that function together are inherited together which can lead to the selection for optimal performance (Albertson *et al.*, 2005; Young *et al.*, 2007). Optimal performance may be the outcome of increased integration in which traits are involved in shared biomechanical actions between two units. Conversely, decreased integration between traits resulting in modularity may result from dissociation of functional requirements (Makendonska *et al.*, 2012; Menegaz, 2013; Anderson *et al.*, 2014; Jamniczky *et al.*, 2014). Muscle-bone interactions and other mechanisms that induce mechanical forces (e.g., biting) are cited as functional factors that generate processes of covariance (Zelditch *et al.*, 2006; Hallgrímsson *et al.*, 2007). Forces on bone from muscle and other soft tissues create peak loads and strains that influence the rate of absorption and deposition in bone, which in turn generates shared variance possibly resulting in functional covariance (Klingenberg, 2008; Zelditch *et al.*, 2009). Depending on whether traits perform one or multiple functions may dictate the degree of functional integration or modularity.

In a study of covariance in the craniofacial complex of capuchin monkeys, increased integration was found to correlate with mechanically resistant diets (Makedonska *et al.*, 2012). Based on the morphology of the masticatory apparatus several previous analyses suggest that *Cebus apella* habitually processes food items with

resistant material properties while other *Cebus* spp. (*C. olivaceus* and *C. albifrons*) more frequently consume less resistant foods (e.g., Kinzey, 1974; Cole, 1992; Daegling, 1992; Anapol and Lee, 1994; Wright, 2005). Distinction in *Cebus* craniofacial morphology related to dietary differences are further supported by observational analyses (e.g., Wright, 2005; Wright *et al.*, 2009). Thus, the predictions were that because hard items are vital for the *C. apella* dietary regime, selection for a masticatory apparatus that could withstand such forces would reduce variation. Reducing variation through stabilizing selection would therefore increase the level of integration within the craniofacial complex in *C. apella*, but not in their “soft diet” counterparts. It was also suggested that primates experiencing high and repetitive masticatory forces would also result in large amounts of integration across the skull due to the coordinated response of bone to high strains. However, in *Cebus* spp. that do not habitually incur these loads, the skull would be less constrained by mechanical demands and therefore decrease the level of integration.

Makedonska *et al.*, (2012) collected shape data on mechanically important traits in the skull of multiple closely related capuchin monkeys, including *C. apella*, in order to test these hypotheses. Results did find that in inter-species comparisons, *C. apella* possessed significantly greater amounts of integration in the craniofacial complex which they related to characteristic high mechanical loads in that species. However, no conclusion was made on whether tighter integration was the result of stabilizing selective pressures or due to the plastic and non-heritable biomechanical responses of bone.

### 1.2.2 Covariance in the Mandible

A description of basic mandibular anatomy and development are essential in order to understand spatiotemporal organization of covariance. Figure 1.1 displays the basic anatomic terminology for the mammalian mandible. As mentioned previously, the mandible is a complex bone. In order for the mandible to function properly it must house dentition, articulate with the cranium at the temporal bone (temporomandibular joint), match the maxilla in size and shape for dentition to occlude and act as an attachment site for several muscles of mastication. The mammalian mandible is a bilateral bone with a right and left side, each side has both a medial (lingual) and lateral aspect (buccal). The right and left mandibles meet anteriorly at the mandibular symphysis which can be either fused or unfused in mammalia. The main body of the mandible is distal and includes the symphysis and the alveolar bone which surrounds the dentition. Proximally the ascending ramus serves to articulate the mandible to the cranium and as a major site of masticatory muscle attachment. Three different processes exist in the ramus, the condylar, coronoid and angular. The head of the condyle articulates with the skull at the temporomandibular joint and is connected to the descending ramus through the condylar neck where the lateral pterygoid muscle inserts. The temporalis muscle inserts on the coronoid process which is located anterior to the condyle. Inferiorly, the angular process is the site of masseteric and medial pterygoid muscle attachment.

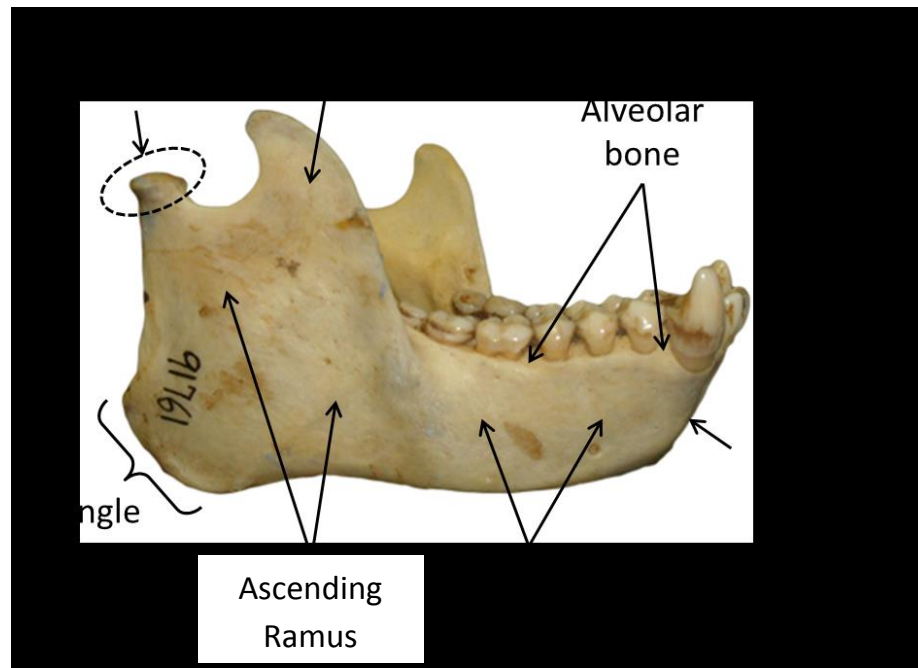


**Figure 1.2 Image depicting anatomy of the mammalian mandible. A *Cebus apella* mandible is used to demonstrate the mandible. The mandibular body, or horizontal ramus, is comprised of the alveolar bone where the dentition resides and the symphysis. The symphysis is fused in many primates but is unfused in mice. Posteriorly, the ascending ramus of the mandible contains three processes for muscle attachment: coronoid (temporalis muscle), angular (masseter and medial pterygoid muscles) and condylar (lateral pterygoid muscle). The condylar head (within the dashed circle) articulates with the cranium at the temporomandibular joint. Muscles attachments also cover the ascending ramus in general and are present on both the medial and lateral aspect of the mandible. The body, symphysis and alveolar bone are intramembranous bone while the ramus is derived from intramembranous and endochondral precursor cells. Specifically the three processes arise from secondary cartilage which caps the intramembranous bone of the ramus, much like long bone epiphyses (Hall, 1999).**

During development, neural-crest cells (NCC) migrate toward the first pharyngeal arch where the mandible begins its growth (Atchley and Hall, 1991; Lee *et al.*, 2001; Hall, 2003; Ramesh and Bard, 2003). NCC eventually differentiate into chondrogenic and osteogenic cells so that adult mandibular bone is derived both endochondrally and intramembranously. Meckel's cartilage is the earliest structure formed in the mandible and is thought to be important scaffolding for later embryonic and fetal development (Oka *et al.*, 2006). Several mesenchymal condensations surround the Meckel's cartilage

during intra-uterine development. Two arise from osteoblasts and eventually form the body and alveolar bone. Precursor cells of the alveolar bone also differentiate into odontoblasts to form the dentine and it is widely held that the interaction between these two cell types helps form the alveolar bone (Fleischmannova *et al.*, 2010; Radlanski *et al.*, 2015). Mesenchymal condensations that form the three processes are intramembranous with caps of secondary cartilages, similar to the epiphyses of long bones (Atchley and Hall, 1991; Hall, 2003). As intramembranous and endochondral bone growth continues, the Meckel's cartilage eventually dissipates (Lee *et al.*, 2001).

#### *Developmental and Functional Mandibular Modules*

Morphological modular units in the mandible have previously been described as either developmental, functional or both. The ascending ramus and body (referred to as the alveolus) are considered as two modules that correspond to skeletal areas that are both functionally and developmentally distinct. In the context of function, the ascending ramus represents the location of insertion for muscles of mastication (Atchley and Hall, 1991; Zelditch, 2008, 2009). Strains produced by muscular loading are known to influence ossification during growth and development and thus mold resulting bone shape (Herring and Lakars, 1982; Herring, 1993; Huiskes, 2000). In contrast, the alveolar region, which encompasses the body, represents another functional unit characterized by strains transmitted via the dentition (Herring, *et al.*, 2001). The ascending ramus and alveolus originate as several mesenchymal condensations making up the three ramal muscular processes – the angular, condylar and coronoid processes – and molar and incisive units of the alveolar region (Atchley and Hall, 1991; Hall, 2003; Ramaesh and Bard, 2003).

Atchley and Hall (1991) referred to each condensation as a morphogenetic unit and argued that as separate cell aggregations each represent independent modules.

#### *Covariance as an Analytical Tool - Rodents*

Numerous investigations into the developmental, functional and evolutionary underpinnings of covariance have used the rodent mandible as an exemplar for complex morphology. Bailey (1986) conducted a study exploring the influence of particular genes on morphogenesis of the mandible using a strain of recombinant inbred mice. Results demonstrated a strong correlation between specific chromosomal regions and anterior and posterior portions of the mandible, respectively. These results were corroborated by a series of studies which used Quantitative Trait Loci (QTL) analyses to map pleiotropic signaling pathways to particular regions of the mandible by comparing genetic expression with linear measurement, or more recently, geometric morphometric techniques. A majority of these studies identified two main modular units within the mandible: the ascending ramus and the alveolar body (Atchley *et al.*, 1985a; Cheverud *et al.*, 1991, 1997, 2004; Leamy, 1997; Mezey *et al.*, 2000; Klingenberg *et al.*, 2003, 2004; Burgio *et al.*, 2012), while others noted no clear delineation between these two areas (Klingenberg and Leamy 2001; Klingenberg *et al.* 2001; Zelditch *et al.* 2008, 2009; Roseman *et al.*, 2009). Klingenberg *et al.* (2003, 2004) suggested that the discrepancy between their earlier and later studies was a consequence of interpreting modularity of QTL effects as a “black-or-white issue” which obscures the complex hierarchical nature of structure of covariance. Zelditch *et al.* (2008, 2009) conducted both *a priori* and exploratory analyses, testing the presence of multiple models of modularity including models based on

mesenchymal condensations, muscular insertions and the alveolar/ascending ramus Bi-modular model. They found only weak evidence to support any of these predicted models, which was also attributed to the complexities of covariation structure.

The multiple cellular condensations of the mandible are considered fundamental modular units and have been identified by several studies of the rodent mandible (Atchley and Hall, 1991; Atchley, 1993; Duarte, 2000; Cheverud *et al.*, 2004; Willmore *et al.*, 2009). Developmental modules, being internally conserved, are predicted to correlate with population-level genetic covariation. A variety of analyses, therefore, have used developmental modules to study adaptive radiations and evolutionary integration among related taxa (Monteiro *et al.*, 2005; Young and Badyaev, 2006; Goswami and Polly, 2010; Monteiro and Nogueira, 2010). However, one common thread among their results also suggests that function exerts a strong influence on the structure of covariation.

Monteiro and Nogueira (2010) examined mandibular modules in a large taxonomic sample of phyllostomid bats with differing dietary regimes. They found that patterns of covariation differed significantly among only bats with highly specialized diets. These conclusions suggest that differences in developmental modularity are associated with evolutionary radiations, unless selection (in this case, due to diet or function) is strong enough to override those patterns of covariation. Differences in patterns of covariation have also been found to correlate with masticatory specializations in squirrels (Zelditch *et al.*, 2008, 2009) and shrews (Badyaev and Forseman, 2004; Badyaev *et al.*, 2005; Young *et al.*, 2007).



Indeed, several analyses have used both the alveolar/ramal and the mesenchymal modular systems to describe adaptive evolution in mice. Muñoz-Muñoz *et al.*, (2011) found that geographic isolation and chromosomal reorganization among distantly related mice were highly correlated with shape differences in the ramal (“ascending ramus”) region of the mandible but not in the alveolar region. They concluded that results supported the presence of two modules in the mandible and that higher correlation in the ramus meant that it was more modular, perhaps more constrained, as well. More constraint in the ramus was attributed to its complex developmental origins and importance as scaffolding for several masticatory muscles.

Renaud *et al.*, (2015) studied the structure of mandibular covariance in mice that have invaded new habitats in which dietary demands have shifted. They found that covariance in the mandible changed related to dietary shifts. Similarly, Anderson *et al.*, (2014) demonstrated that modularity in the mouse mandible is reorganized when mice are fed diets of differing mechanical resistance. Mice fed a “soft diet” displayed much lower degrees of integration throughout the entire mandible. Results here reinforce those found by Makedonska *et al.*, (2012) in that degree of integration is linked to the material properties of food masticated by the subject. In addition, when covariance between modular mesenchymal regions was analyzed, “hard” and “soft” diet mice differed in the regions which showed significant correlations. Plasticity in the mouse mandible thus accommodated differing dietary loads. In the case of the higher loads, the mandible becomes more integrated overall, possibly to increase biomechanical efficiency. Soft diets on the other hand, resulted in a lack of constraining integration, which they added, may make the mandible susceptible to new selective pressures. In each of these studies

and others (Garcia *et al.*, 2014; Jojić *et al.*, 2012; Renaud *et al.*, 2012) the relative independence of the mandibular modules increases the ability for the mandible to adapt to novel functional demands.

#### *Covariance as an Analytical Tool - Primates*

Few analyses have directed questions of integration or modularity toward the primate mandible. Singh *et al.*, (2014) completed a study in which patterns of ontogenetic and allometric variation in the mandibles of humans, chimps and bonobos were analyzed and compared. Part of this study hypothesized that allometric differences among taxa would be localized to either the alveolar or ramal modules. Indeed, Singh (2014) found that growth of the anterior alveolus and posterior ramus were ontogenetically divergent between groups. Specifically, the ramus demonstrated disparate growth trajectories among humans, chimps and bonobos while growth trajectories in the anterior alveolus remained similar among taxa. Polanski (2011) examined the covariation of linear measurements in an ontogenetic sample of modern human mandibles. Similar to Daegling (1996) he found that different components of the mandible were decoupled during growth, further supporting a modular pattern. Each of these analyses supports a relatively modular structure in the primate mandible, dividing it into a ramal and an alveolar unit.

Dissociated growth patterns in the primate mandible suggest that separate developmental and functional influences are present, providing evidence for modularity in the primate mandible. Ontogenetic autonomy between the ramus and alveolus, or any other mandibular module, allows growth trajectories to diverge among species,

facilitating adaptive evolution. Indeed, if dietary demands change within a group of primates, they may undergo selective pressure for increased masticatory muscles mass or perhaps larger surface areas for post-canine dentition. Modular regulation of the ramal and alveolar regions could enable adaptability in one region without negatively affecting the other.

In a recent study, it was hypothesized that differential use of dentition between Neanderthals and modern humans would result in differential integration within the mandible (Harvati *et al.*, 2011). Because Neanderthals are noted for paramasticatory use of their anterior dentition, it was speculated that the pattern and magnitude of covariance between the alveolus and ramus would reflect this specialized paramasticatory behavior. However, no difference in integration was found; Neanderthal and modern human mandibular integration was in fact quite similar.

The pattern of covariance within the alveolus and ramus of Neanderthals and modern humans contrasts with the ontogenetic analyses which identify modular signals (Daegling, 1996; Polanski, 2011; Singh *et al.*, 2014). One possible explanation is that disparate patterns and magnitudes of covariance within the mandible of separate taxa can best be seen in an ontogenetic context. The phenotypic structure of the adult mandible is the product of covariance generated over development, it is possible that multiple and distinct covariance generating processes may result in similar adult phenotype. Thus, the best way to tease out differences in the pattern and/or magnitude of covariance between taxa is to look at ontogenetic trajectories. Another explanation may be that paramasticatory behavior may not be enough of a covariance generating process to induce difference among mandibular modularity in the alveolus and ramus. It would be

beneficial to conduct similar covariance analyses on a group of closely related primates with divergent mandibular morphologies due to significant dietary specializations in order to determine if diet is a significant covariance generating process and to determine whether it alters covariance in any way between species. Adding an ontogenetic component to these analyses would further elucidate the unique developmental trajectories that produce covariance differences in adult primate mandibles.

### *The Palimpsest Model*

Hallgrímsson and colleagues (2009) have presented a foundational approach to the study and interpretation of covariance in biological structures that addresses confounding factors encountered by researchers. Their concern was twofold. First, it is imperative to acknowledge that there is a fundamental difference between pattern and process in covariation structure. The methodology used to determine the presence of covariation is dependent upon the amount of variation that exists (Hallgrímsson et al., 2009; Klingenberg, 2010). Different developmental mechanisms may generate indistinguishable patterns of covariation (Mitteroecker and Bookstein, 2007; Mitteroecker, 2009). It is therefore essential to have a full understanding of the developmental processes creating variation in the morphology of interest. Keeping a clear separation between the processes that generate covariation and observable patterns of covariation is vital for maintaining questions with biological significance.

Second, multiple processes generate covariation within a structure during growth, making it difficult to clearly delineate among them. The “palimpsest” is used as a metaphorical model to describe the difficulties in deciphering integrated and modular

units within complex traits (Hallgrímsson et al., 2009). Difficulties arise when one must consider the multiple continuous processes that are inherent to the formation of such structures throughout ontogeny and into adulthood. For instance, mandibular size and shape are known to be influenced by precursor mesenchymal condensations, dental growth and bone-muscle interaction. Each of these influences is spatiotemporally unique while at the same time overlapping each other in space and time, thus obscuring the importance that each influence has on the resultant adult shape.

Several important and illustrative analyses have demonstrated how developmental processes mitigate the structure of covariance. Hallgrímsson and colleagues (2006) set out to demonstrate that mutations in developmental mechanisms will increase phenotypic variance in the mutated sample and alter the structure of covariance. The purpose of this study was to empirically test the theoretical underpinnings of canalization which have been related to direct genetic influence from specific “chaperone” genes or as an outcome of complex developmental-genetic interactions in which multiple factors play a role in stunting unwanted variance. In order to specifically target these questions, they chose a loss-of-function mutation, the brachymorph (*bm*) mutation, because it does not directly control any developmental mechanisms. Another attractive component of the *bm* mutation is that it is differentially expressed through out skull. It disrupts and stunts chondrocranial growth and has differential degrees of mutative effect on parts of the skull derived from separate precursor cells. Therefore changes in variance and covariance seen in the skull of mutant mice should be specific to the basicranium which is chondrocranially derived.

Shape data were collected on the skulls of *bm* mutant mice and wildtype controls, with data sets divided into a global set representing the entire skull and smaller subsets representing the face, neurocranium and basicranium. The landmark subsets were chosen to represent regions of the skull derived from either chondrogenic or osteogenic cells. Analyses were conducted to test for significant differences in phenotypic variance between *bm* and wildtype samples. Pattern and magnitude of covariance of the entire skull and between subsets were also compared between samples.

Variance was significantly greater in *bm* crania ( $p < 0.001$ ) and this was most evident in the chondrocranially derived basicranium. Matrix comparisons fell outside 95% confidence intervals, suggesting significant difference in population covariance structure. Finally, *bm* mice possessed a significantly greater degree or magnitude of covariance ( $p < 0.01$ ) in the skull, as well as in the cranial subsets. Results supported the hypotheses that *bm* mutation would increase phenotypic integration and alter covariance in the skull. This project provides direct evidence that canalization is a multifactorial property of the developmental-genetic architecture.

More recently an analysis was conducted using another mutation that disturbs growth in the cranium (Martínez-Abadías *et al.*, 2011). Martínez-Abadías and colleagues used a transgenic mouse model, heterozygous for *Fgfr2* mutations, to demonstrate that the FGF/FGFR signaling pathway is a significant contributor to covariance in the skull. Two separate *Fgfr2* gain-of-function mutations (*Fgfr2*<sup>+/*S252W*</sup> and *Fgfr2*<sup>+/*P253R*</sup>) were chosen to compare the structure of covariance among peri-natal mouse skulls and their wild-type littermates. These particular mutations are associated with cranial dysmorphology mutations connected to Aperts syndrome due to premature suture

closure. A foreshortened face relative to the neurocranium, which is also relatively globular are typical phenotypic characteristics of Apert mice. Facial retraction is often attributed to early fusion of bony connections between the face and neurocranium which stunts facial growth.

Two main conjectures were made for their study. First, that morphological integration between the neurocranium and face may dissipate the dysmorphic effect of Aperts syndrome via canalizing factors inherent to integration. Second, if the FGF/FGFR signaling pathway is critical to skull development then transgenic specimens should possess greater amounts of covariance per the palimpsest model. In order to test these hypotheses, shape data were collected from the skulls of newborn mice (P0) with either *Fgfr2* mutation and then compared to their respective wildtype littermates. Both the pattern of covariance and the amount (magnitude) of covariance between the face and the neurocranium were analyzed.

Results demonstrated that the way in which the face and neurocranium were integrated (pattern) was similar between mutants and non-mutants. In contrast, the amount of integration (magnitude) between the two units was much higher in the mutant mice. Martínez-Abadías and colleagues concluded that, as expected, the pattern of integration between the face and neurocranium was conserved, suggesting that the way in which traits covary between the two units would mitigate any outstanding dysmorphic effects attributable to Apert syndrome. However, the amount of integration between the face and neurocranium was much larger in the mutant mice. According to the palimpsest model this would suggest that the FGF/FGFR2 pathway is an important covariance generating factor.

Hallgrímsson *et al.*, (2006) and Martinez-Abadías *et al.*, (2011) both explore the contribution of mutation to variance and covariance in the skull. These studies provide evidence that disturbances in important developmental pathways increase variance in the skull and alter the way in which components of the skull are integrated. However, both of these studies focused on one time point in age, without capturing the continuous changes that occur throughout ontogeny. Recognizing the difference between how covariation is produced and how it is measured is critical. This project is designed to explicitly target different covariation-generating processes by testing for changing patterns of covariation at separate ontogenetic stages, therefore attempting to address each of these issues. It will address the way in which covariance changes over ontogeny and how the introduction of mutation to an important bone developing signaling pathway affects the pattern and magnitude of covariance in the mandible. This study will also show how differing biomechanical demands in separate groups result in disparate covariance-generating processes.

### **1.3. Functional Morphology of the Mandible**

Functional morphology of the mandible has been studied with the intent to link behavioral use of the masticatory complex to its shape or form. The principle that form follows function suggests that mandibular shape is the result of functional adaptation to the loading environment (Hylander, 1975; 1979; Biewener and Bertram, 1993, Turner and Burr, 1993). A number of experimental analyses across Mammalia have been conducted in order to determine the effects of differing diets on the craniofacial complex. These studies have used food items of varying mechanical resistance to elicit different



peak strains in bone and characterize jaw kinematics (Bouvier and Hylander, 1981; McFadden *et al.*, 1986; Beecher and Corruccini, 1981; 1983; Corruccini and Beecher, 1982; Hylander and Johnson, 1994; Lieberman *et al.*, 2004; Ravosa *et al.*, 2007; 2008; Vinyard, 2008; Menegaz *et al.*, 2010; Iriarte-Díaz *et al.*, 2011; Ross *et al.*, 2012; Scott *et al.*, 2014). It is well understood from these analyses that increased mechanical resistance of food items results in greater muscle activity and higher peak strains which in turn promote remodeling of bone to reinforce structural stability in the mandible.

Functional morphologists have utilized what is known about the response of bone to biomechanical stressors to inform hypotheses of how mandibular shape should vary in primates with diverse loading environments. Cross-taxonomic comparative analyses of diverse mandibular lever mechanics, jaw robusticity and masticatory muscle architecture have demonstrated a relationship between morphology and behavior across multiple primate species (Hylander, 1979; Bouvier, 1986a; Demes and Creel, 1988; Daegling, 1989, 1992; Taylor, 2002; Vinyard *et al.*, 2003; Daegling and Grine, 2007; Taylor *et al.*, 2009; Taylor and Vinyard, 2010; Vinyard and Taylor, 2010). However, generalizing mandibular shape to fit within certain dietary categories often results in analyses that are either contradictory or do not find coherent associations between shape and diet. Characteristic mandibular morphology associated with particular dietary demands are not consistent across primate clades (Bouvier, 1986a, b; Ravosa, 1996; Daegling and McGraw 2000; Taylor, 2000, 2002). This suggests that, at least in primates, external mandibular morphology can respond in multiple ways to masticatory behaviors. Thus, shape of the mandible in primates is not always a reliable indicator of masticatory efforts.

Similarly, internal geometry of the mandible does not completely correlate with biomechanical stressors and variation. The distribution of cortical bone around the mandible is thought to remodel in response to the types of torsion and bending experienced (Daegling 1992, 2002, 2007; Daegling and Hotzmann, 2004). Indeed, in edentulous mandibles it has been demonstrated that the reduction of significant occlusal force contributes to changes in bone material property and mass (Dechow *et al.*, 2010). However, more recent cross-taxonomic comparisons have demonstrated no significant link between internal geometry and hardness/toughness of diet (Daegling, 2007; Daegling and McGraw, 2007). Interestingly, outside of non-human primates there seems to be a strong relationship between these factors in Rodentia (Ravosa *et al.*, 2007; Menegaz, 2013; Scott *et al.*, 2014) and geographically distinct or dietarily diverse modern human populations (Holmes and Ruff, 2011; von Cramon-Taubadel, 2011; Holton *et al.*, 2014; Hoover *et al.*, 2015). The confounding evidence for biomechanical implications on mandibular external and internal variables likely reflects the fact that broad dietary categories are not refined enough to determine mandibular shape. More specialized variables such as the way in which food items are approached may have a larger implication (Ross *et al.*, 2012). In addition, mandibular cortical bone is anisotropic, suggesting that it will respond to stress and strain differently between separate regions of the bone (Dechow and Hylander, 2000; Schwartz-Dabney and Dechow, 2003). Cortical bone material properties are therefore an important aspect for constructing functional interpretations of internal geometry of the mandible.

The influence of dental size and eruption sequence is another possible confounding factor in interpreting mandibular morphology. Dental development and ensuing size may have a close relationship with mandibular size and shape. Posterior and anterior dental crown size has been proposed to regulate mandibular corpus size and robusticity in primates (Wood, 1978; Smith, 1983; Daegling, 1996; Taylor, 2000). Empirical analysis of that hypothesis has returned with conflicting results. Plavcan and Daegling (2006) found that crown size was not significantly correlated with external measures of the mandible across multiple species of primates. The aid of CT scans has allowed more recent analyses to refocus the question of spatial demands on both crown and root sizes as well as internal space of the mandible. Many of these studies linked anterior dental development with strong spatial demands in the mandibular symphysis in human and non-human primates (Cobb and Panagiotopoulou, 2011; Suwa et al., 2011; Fukase, 2011, 2012). On a larger scope, it has also been suggested that molecular signaling pathways of the dental and mandibular growth have evolved over time to create an integrated system (Boughner and Hallgrímsson, 2008; Gómez-Robles and Polly, 2011; Dean and Cole, 2013). The project presented here will not directly address the relationship of dental development to mandibular morphology; however more hypothesis driven analyses need to be completed before the true co-dependence between these factors is understood.

The analysis presented here tests hypotheses related to how dietary diversity and heavy mechanical demands are reflected in the structure of covariance in the primate mandible and what this might tell us about mandibular morphology. Studying covariance is an effective way to elucidate the factors that are mitigating response of primate

mandibles to external stimuli. As we have seen in the literature presented here, high levels of integration in the craniofacial complex are often the result of chewing mechanically resistant foods (Makedonska *et al.*, 2012; Anderson *et al.*, 2014). Increased integration over the entire mandible may then dampen the ability of different regions to vary on their own in response to further external stimuli. Because the mandible operates mechanically as a lever, strain will be experienced at both the bite point, whether that is positioned at the incisors or molar row, as well as at the temporal mandibular joint (Hylander, 1975, 1978; Greaves, 1978). Occlusal loads will be distributed throughout the mandibular bone, on both the working and balancing side. (Hylander, 1979). Thus, hypothesized modules would in fact act as a single unit to respond to stress and strain. Bone remodeling due to shared masticatory stress would then be similar leading to larger magnitudes of covariance across the mandible. However, covariance in the mandible may exhibit a more hierarchical structure. Response to muscular loading in the ramus may necessitate the ability to respond to covariance generating patterns unique to the ramus. Similarly, covariance generating factors unique to the alveolus, such as dental development could lead to a unique pattern of covariance in the alveolus. Regionally distinct demands would then result in a degree of dissociation between the ramus and alveolus. The same could be true for mechanical stimuli unique to the alveolus and/or the mesenchymal modules that have also been proposed in the literature. Understanding the different patterns and magnitudes of covariance in mandibles in conjunction with functional demands clarifies how the mandible responds to external stimuli. This project will attempt to address these questions in a sample of dietarily diverse primates.

## **1.4 Challenge: Interpreting Mandibular Shape**

This introduction has highlighted the importance of studying mandibular shape to decipher dietary behaviors and adaptive response to those behaviors. It has also delineated the degree of uncertainty as to what factors are actually contributing to mandibular shape. First, the way in which mandibular covariance changes over ontogeny is relatively unknown despite the utility in using that knowledge to make predictions about morphology. Second, there are conflicting indications about the ability to correlate form-function in the primate mandible. This impedes the process of forming predictions about how diet can influence mandibular shape and how those predictions can be applied to extinct and extant primates. Third, studies of covariance structure within the primate mandible can help address confounding functional morphologies. Yet, very few analyses have focused on covariance in the primate mandible and, as of now, no analyses have explicitly addressed these questions in the context of function.

### **1.4.1 Addressing the Challenge**

Clarifying the manner in which different components of a structure covary to either constrain it or allow it to adapt under selective pressures is an important goal in evolutionary biology. The purpose of this study is to examine the combined contribution of development and function in the mandible by identifying specific patterns of covariation. Several aspects of the research design for the project presented here make it unique and powerful.

One of the most effective ways to approach these issues is to conduct research on patterns of covariation within a sample where age and developmental mechanisms can be controlled, for instance in an ontogenetic series of inbred mice (Hallgrímsson et al., 2009; Mitteroecker and Bookstein, 2009; Mitteroecker, 2009; Klingenberg, 2010). The project completed here is one of the few to approach the development of covariation in mandibular shape using an ontogenetic sample. Additionally, Hallgrímsson et al. (2009) demonstrated that major determinants of covariation can be identified by testing levels of integration in a sample in which normal developmental processes have been compromised. When variance is introduced to a developmental process it could respond in one of two ways depending on whether it significantly contributes to covariance. A developmental process that does contribute to covariance will channel the new variance so that those traits that already demonstrated a degree of covariance will be even more integrated. However, in developmental processes that do not already significantly contribute to covariance, the newly introduced variance will be dispersed randomly amongst traits leading to a diminished level of integration. Therefore, if integration or magnitude of covariance is higher in the mutant model when compared to a control sample, those processes are developmentally important. In the project presented here underlying developmental processes are targeted by utilizing a mutant mouse model as an additional ontogenetic sample.

Few studies of primate mandibular functional morphology have taken the structure of covariance into account. Here we use a sample of diverse platyrrhines to examine questions related to how differing diets influence integration and modularity in the mandible. Additionally, there are relatively few three-dimensional morphometric

analyses comparing mandibular shape among New World Primates (Rosenberger *et al.*, 2013). Thus, new data about morphological diversity in the platyrrhine mandible will be added to the field. Lastly, large-scale research has been conducted on the diversity of covariance within the primate skull which has led to important conclusions about the level of constraint and plasticity direction adaptive evolution. This project will be one of the first to explicitly study these patterns in the primate mandible thus adding essential information to what is already known about the skull.

## **1.5 Hypotheses**

The purpose of this dissertation is to test three main inter-related hypotheses surrounding covariation structure in the mandible. Each of these hypotheses will explore the pattern and magnitude of integration within and between samples. Patterns of covariance explain the way in which traits covary, for instance the associated shape changes observed between the alveolar and ramal regions described above. Magnitude of covariance on the other hand describes the intensity of integration among traits, as in how much integration exists between two units.

An ontogenetic sample of mice was used to test the first two main hypotheses focused on the structure of covariance over development. The first of which used wild-type mice exclusively while the second incorporated an age-matched transgenic mutant mouse model (described in further detail in Chapter 3) for comparative reasons. Three important developmental stages, embryonic, peri-weaning and adult were selected in order to test whether covariance changed depending on age-specific growth processes or masticatory behaviors. Ossification is still occurring in the embryonic mandibles, dental

crypts are developing to accommodate dentition and they have not experienced masticatory loads. Peri-weaning mandibles are fully ossified, but the dentition is still erupting and they have not experienced prolonged mechanical stress from an adult diet. Adult mandibles have attained full adult size, all dentition has erupted and come in to occlusion and they have been experiencing adult masticatory loads for several weeks.

The first main hypothesis was separated into two sub-hypotheses, the Developmental Hypotheses A ( $\mathbf{H_{DVA}}$ ) and Developmental Hypotheses B ( $\mathbf{H_{DVB}}$ ). Both of which predicts that covariance is developmentally dynamic and will change as the mandible grows. Specifically,  $\mathbf{H_{DVA}}$  will address patterns of covariance between the developmental stages used here while  $\mathbf{H_{DVB}}$  will address the way in which magnitudes of covariance change over ontogeny.

The second set of hypotheses and sub-hypotheses are centered on how covariance is influenced by a developmental perturbation. These are named Mutant Hypothesis A ( $\mathbf{H_{MTA}}$ ) and Mutant Hypothesis B ( $\mathbf{H_{MTB}}$ ). An ontogenetic sample of wild-type and mutant mice will be used to test these hypotheses. Similar to the previous set of hypotheses,  $\mathbf{H_{MTA}}$  will explicitly address if patterns of covariance are altered in mutant mice while  $\mathbf{H_{MTB}}$  will address whether mutant mandibles differ in magnitudes of integration.

The third hypothesis and concomitant sub-hypotheses were ascribed to the Functional Hypothesis A and B ( $\mathbf{H_{FXA}}$  and  $\mathbf{H_{FXB}}$ ) set and will be tested using a sample of adult platyrrhines. Primate choice was based on habitual dietary behaviors experienced by closely related taxa (described in further detail in Chapter 3). These hypotheses are related to the influence of diet on overall covariance of the mandible and whether the



structure of covariance is altered or remains the same in primates with heavy mechanical loads.  $H_{FXA}$  concerns the pattern of covariance between the primates that habitually experience heavy mechanical loads and those that do not.  $H_{FXB}$  predicts that high stress and strain in the mandible will produce greater intensity of covariance and result in significantly different magnitudes of covariance between samples.

### 1.5.1 Covariance of Shape Changes over Ontogeny

A series of hypotheses has been designed to test the overall question of how structure of covariation changes over ontogeny, moving from intrinsic (developmental) to extrinsic (functional, somatic) influences. This will be tested in the wildtype sample to assess normal growth patterns.

#### *Developmental Patterns of Covariance*

**$H_{DVA0}$ :** Patterns of mandibular covariance are dissimilar between each age group.

If this null hypothesis is rejected, it would suggest that the pattern of covariance does not change during growth and development in the mandible. However, it is expected that  **$H_{DVA0}$**  *will not* be rejected which can be interpreted to mean that patterns of covariance *do* shift during ontogeny.

**$H_{DVA1}$ :** Patterns of covariance are dissimilar between embryonic and peri-weaning mice.

If this hypothesis is rejected, it would suggest that the patterns of covariance from the embryonic to the peri-weaning developmental stage does not result in different patterns of covariance. However, it is expected that  **$H_{DVA1}$**  *will not* be rejected which can be interpreted to mean that patterns of covariance *do* change

from the embryonic to the peri-weaning mandible. This suggests that patterns of covariance change before the onset of a fully incorporated diet. Moreover, covariance is being led by intrinsic factors preparing the mandible for future loading regimes before they are substantially exerted on the jaw.

**H<sub>DVA2</sub>**: Patterns of covariance are dissimilar between the peri-weaning and adult mice.

If this hypothesis is rejected it would suggest that the adult patterns of covariance in the mandible are the same as the peri-weaning developmental stages.

However, it is expected that **H<sub>DVA1</sub>** *will not* be rejected which can be interpreted to mean that patterns of covariance *do* change after weaning. If patterns of covariance are similar among the embryonic and peri-weaning mice, though both differ from the adults, then this would suggest that patterns of covariance will alter only after prolonged exposure to an adult diet.

#### *Developmental Magnitude of Covariance.*

**H<sub>DVB0</sub>**: The magnitude of covariance is that same at all developmental stages.

If this null hypothesis is rejected it would suggest that the intensity of integration among component parts changes during growth and development in the mandible.

**H<sub>DVB1</sub>**: The magnitude of covariance is the same between embryonic and peri-weaning mandibles.

If this null hypothesis is rejected, it would suggest that the intensity of integration changes significantly between the embryonic and peri-weaning developmental

stages. It is predicted that peri-weaning mice will possess significantly greater magnitudes of covariance, before the onset of a fully incorporated diet. Taken in conjunction with  $H_{DV\Delta 1}$ , this would suggest that mandible becomes more integrated as a consequence of preparing for future loading regimes before they are substantially exerted on the jaw.

**$H_{DV\Delta 2}$ :** The magnitude of covariance is the same between the between the peri-weaning and adult mice.

If this null hypothesis is rejected, it would suggest that the magnitude of covariance significantly changes after weaning and the introduction of an adult diet. It is predicted that adult mice will have significantly greater magnitudes of covariance. This would further support previously reported results that showed greater amounts of integration when biomechanical stressors are introduced on the mandible and the skull (Makendonska *et al.*, 2012; Anderson *et al.*, 2014).

### 1.5.2 Covariance of Shape Differs between Genotype

Similar to the set of hypotheses above, this set of hypotheses will address how covariance changes over ontogeny, but will now examine the difference between genotypes rather than ages. The main purpose of these sets of hypotheses is to determine if perturbations caused by mutations in a developmental pathway, first, change the structure of covariance and, second, if developmental perturbations are overlaid later in ontogeny when adult diet becomes an important aspect of morphology.

### *Mutant Patterns of Covariance*

**H<sub>MTA0</sub>**: Within each age range, the pattern of covariance is dissimilar between wildtype and mutant mice.

If this null hypothesis is rejected, it would suggest that, despite mutation in an important developmental signaling pathway, the structure of covariance is maintained between genotypes.

### *Mutant Magnitude of Covariance*

**H<sub>MTB0</sub>**: Magnitudes of covariance do not differ between wild-type and mutant mice at any age.

If this null hypothesis is rejected, it would suggest that the developmental perturbation in the mutant mice (described in Chapter 3) is not a covariance generating factor.

**H<sub>MTB1</sub>**: Alternatively, mutant mice possess significantly greater magnitudes of covariance within each age range.

This alternative hypothesis tests the assumption that the developmental perturbation in the mutant is a significant covariance generating factor in mandibular covariance. When a disruption is introduced into a developmental signaling pathway known to influence covariance, increased levels of variance will result in a more integrated structure (larger magnitudes) when compared to the normal system (Hallgrímsson *et al.*, 2009).

**H<sub>MTB2</sub>**: Alternatively, mutant mice possess a significantly larger magnitude of covariance when comparing embryonic mice, only; and, no difference will be present after weaning.

This alternative hypothesis suggests that though disruptions to developmental signaling will produce a more integrated mandibular structure, these differences will be overlaid and obscured after the introduction of large functional demands.

### 1.5.3 Covariance of Shape will be Different among Primates with Different Masticatory Loading.

Questions regarding mandibular adaptations to function in primates with contrasting diets are addressed here. These sets of hypotheses suggest that primates possessing masticatory apparatuses that are subjected to habitual, heightened occlusal loads will have a more integrated mandibular covariance structure due to coordinated response of bone, dentition and musculature. These hypotheses do not specifically address whether distinct structures of covariance are due to adaptive evolutionary responses or due to in vivo plastic remodeling. Here, only the presence of divergent patterns and magnitudes is tested; results will inform hypotheses for future studies.

#### *Functional Patterns of Covariance*

**H<sub>FXA0</sub>**: Patterns of covariance are dissimilar between primates that regularly incur heavy masticatory loads and primates that do not.

If this null hypothesis is rejected, it would suggest that the way in which mandibular traits covary does not differ between primates, despite differences in dietary behaviors.

### *Functional Magnitude of Covariance*

**H<sub>FXB0</sub>**: The magnitude of covariance does not differ between primates that regularly incur heavy masticatory loads and primates that do not.

If this null hypothesis is rejected, then the strength of covariance among traits does not differ between primates with differing diets.

**H<sub>FXB1</sub>**: Alternatively, primates that regularly incur heavy masticatory loads possess greater magnitudes of covariance than those that do not.

The alternative hypothesis suggests that increased occlusal loads leads to larger amounts of stress and strain. Heavier strain leads to coordinated bone remodeling in the mandible and thus greater magnitudes of covariance.



## Chapter 2: Materials and Methods

The objectives of this project required a sample selection that controlled for age and introduced a developmental perturbation relevant to the mandible (age- and genotype-match). Another sample was needed to test for functional effects of varied diets in primates. In order to meet the requirements, two quite different sample sets were chosen: 1) a transgenic mouse model of known developmental stages exhibiting cranial and mandibular dysmorphology and 2) a set of phylogenetically related adult New World monkeys in the family Cebidae. Each sample was specifically chosen to address explicit hypotheses of this dissertation.

The mouse model is essential because it provides the opportunity to select for specific developmental stages that are important to growth of the mandible. The nuances of covariance over ontogeny, as previously mentioned, can become concealed as growth continues or remain as detectable aspects of adult covariance. Either scenario can obfuscate the processes that contributed to the structure of covariance during growth and development and into adulthood. The ontogenetic sample thus further provides a controlled dataset to examine significant influences on mandibular shape and covariation over development ( $H_{DVA-B}$ ). In addition, a controlled *mutant model* mouse sample affords an experimental model to empirically test the organization of covariation within the mandible when a developmental perturbation is present ( $H_{MTA-B}$ ). Using a mouse model to address the hypotheses presented here may be problematic because they possess a highly derived mandible (Boell and Tautz, 2011), there is a long history of experimental data that demonstrates the importance of these models in our understanding of evolutionary developmental biology (Bailey, 1986; Atchley and Hall, 1991; Cheverud *et*



*al.*, 1991, 1997, 2004; Klingenberg *et al.*, 2003, 2004; Willmore *et al.*, 2009). Lastly, the primate sample constitutes a natural experiment to determine if patterns and magnitudes of covariation in the mandible are responding to distinct mechanical loads differentially between primates with varying diets. Observing these relationships in a natural population also contributes to the discussion of how covariation influences evolvability of organismal structures and helps to accumulate knowledge for future hypothesis testing.

## **2.1. Developmental Mutant Sample – Crouzon Mice**

Transgenic model mice carrying a fibroblast growth factor receptor 2 (FGFR2) mutation are used in this dissertation. This section introduces the ontogenetic mutant mouse sample directed at the ontogenetic hypotheses posed here, including information pertaining to the genotype and phenotype of the *Fgfr2* mutation, as well as sample collection and rationale for the age stages chosen. Experimental animal models carrying an *Fgfr2* mutation are an integral part of research surrounding morphological integration and modularity, mainly because of recent and important evidence that demonstrates that this gene significantly influences covariance structure (Richtsmeier *et al.*, 2006; Martínez-Abadías *et al.*, 2011; Hünemeier *et al.*, 2014). Multiple studies have been published recently focused on determining how covariance is structured in the crania and how we might use this to answer evolutionary biological questions (Marcucio *et al.*, 2011; Perrine *et al.*, 2014; Percival *et al.*, 2014).

### 2.1.1. Fibroblast Growth Factor receptor 2 – Crouzon Syndrome

Mutations in the *Fgfr2* gene are well documented in the clinical literature and are most often associated with craniosynostotic disorders which occur in 1 out of ~ 3,000 human births; each clinical presentation varying in intensity (Wilkie, 1997; DeLeon *et al.*, 2001; Eswarakumar *et al.*, 2006). Craniosynostotic syndromes are the result of premature fusion of sutures in the neurocranium, basicranium and face, culminating in insufficient room for growth of soft tissue growth. Several human craniosynostotic diseases, such as Pfeiffer, Apert and Crouzon syndromes are associated with mutations located in Fibroblast Growth Factor Receptor (FGFR) tyrosine kinase genes (Bresnick and Schendel, 1995; Muenke and Schell, 1995; Wilkie, 1997; Ornitz and Marie, 2002; Eswarakumar *et al.*, 2004; Morris-Kay and Wilkie, 2005; Eswarakumar *et al.*, 2006). FGFR is a multigene family, FGFR1-4, expressed in the epithelia and mesenchyme in multiple organs throughout the body (Hughes, 1997).

The mouse model utilized for this project possesses a missense mutation in *Fgfr2*<sup>C342Y/+</sup> which is specifically related to Crouzon syndrome. Like many other mutations related to craniosynostosis, the Crouzon mutation is located at the third immunoglobulin-like (Ig) domain on the extracellular portion of the receptor. The Ig domain is dominated by Cys-Cys bonds; consequently, Crouzon syndrome is associated with a Cystine substitution, specifically Cys342Tyr. This substitution causes the constitutive activation of *Fgfr2* tyrosine kinase (Galvin *et al.*, 1996; Perlyn *et al.*, 2006a, b). Over-activation of *Fgfr2* results in a complex cascade of events that affects the proliferation of osteoprogenitor cells, influencing both intramembranous and

endochondral growth during early bone formation (Bresnick and Schendel, 1995; Iseki *et al.*, 1997; Morris-Kay and Wikie, 2005; Perlyn *et al.*, 2006a, b).

Phenotypic manifestations of this syndrome in humans include midfacial hypoplasia, exophthalmos, hypertelorism and mandibular Class III malocclusion (Kreiborg, 1981; Kreiborg and Björk, 1982). Transgenic mouse models carrying the *Fgfr2c*<sup>C342Y/+</sup> mutation have been widely used to better understand the molecular underpinnings and cellular response to this disease because they share the same aspects of dysmorphology present in humans (Eswarakumar *et al.*, 2006; Perlyn *et al.*, 2006a; Heuzé *et al.*, 2014a). Despite the focus on cranial dysmorphology little attention has been paid to the effect of *Fgfr2c*<sup>C342Y/+</sup> on mandibular growth and development. A small number of orthodontic studies focus on the presentation of Class III malocclusion caused by maxillary hypoplasia and sagittal growth of the mandible (Costaras-Volarich and Pruzansky, 1984; Kreiborg and Aduss, 1986; Bachmayer *et al.*, 1986; Carinci *et al.*, 1994; Cutting; 1995; Meazzini *et al.*, 2005; Wery *et al.*, 2015). In many of these analyses it is mentioned that the mandible in Crouzon patients is relatively small compared to unaffected patients (see Reitsma *et al.*, 2012 for contrasting results) and is rotated antero-inferiorly (Meazzini *et al.*, 2005, but see Wery *et al.*, 2015). Most of these clinical analyses have documented size and shape of the Crouzon mandible using traditional linear measurements from lateral cephaloradiographs (Costaras-Volarich and Pruzansky, 1984; Kreiborg and Aduss, 1986; Bachmayer *et al.*, 1986; Carinci *et al.*, 1994; Cutting; 1995; Meazzini *et al.*, 2005; Wery *et al.*, 2015).

Previous analyses conducted by this author looked at the three-dimensional form of the Crouzon mouse in an ontogenetic sample (Holmes *et al.*, 2011; 2013). Mandibles belonging to mice carrying the *Fgfr2c*<sup>C342Y/+</sup> were found to be significantly smaller in many antero-posterior dimensions when compared to wild-type littermates. This further supports the orthodontic research presented above. In addition, significant differences in shape in both the ramal and alveolar regions were reported (Holmes *et al.*, 2011; 2013) (Figure 2.1). This further illuminates the significance of *Fgfr2c*<sup>C342Y/+</sup> for mandibular growth and development.

*FGF* ligands and *FGFR* tyrosine kinase represent a family of related genes which interact to promote cellular proliferation and differentiation, and thus play a significant role in morphogenesis in vertebrate development. Expression of these developmental signals varies within cranial regions and introduction of a mutation in one of these proteins will consequently differentially affect separate aspects of the skull, changing the relationships among anatomical parts (Heuzé *et al.*, 2014b). Biological models exhibiting *Fgf* and *Fgfr* perturbations create an exciting opportunity to construct many experimental analyses that explore the role of intramembranous and endochondral growth in evolutionary development. Several authors have noted the global influence of FGF genes and their receptors on origination of vertebrate traits including the head (Coulier *et al.*, 1997; Bertrand *et al.*, 2011), as well as magnitudes of covariance among facial structures and coordination of brain-face development (Richtsmeier *et al.*, 2006; Marcucio *et al.*, 2011; Griffin *et al.*, 2013; Hunemeier *et al.*, 2013). Recent studies on *Fgfr2* mutations in particular have defined it as a covariation-generating developmental mechanism (Martínez-Abadías *et al.*, 2010, 2011). The dysmorphology seen in *Fgfr2c*<sup>C342Y/+</sup>

mandibles and the ongoing research demonstrating the significant role this family of genes has in coordinating developmental processes make the Crouzon mouse model ideal for experimental designs investigating the ontogeny of covariation structure.

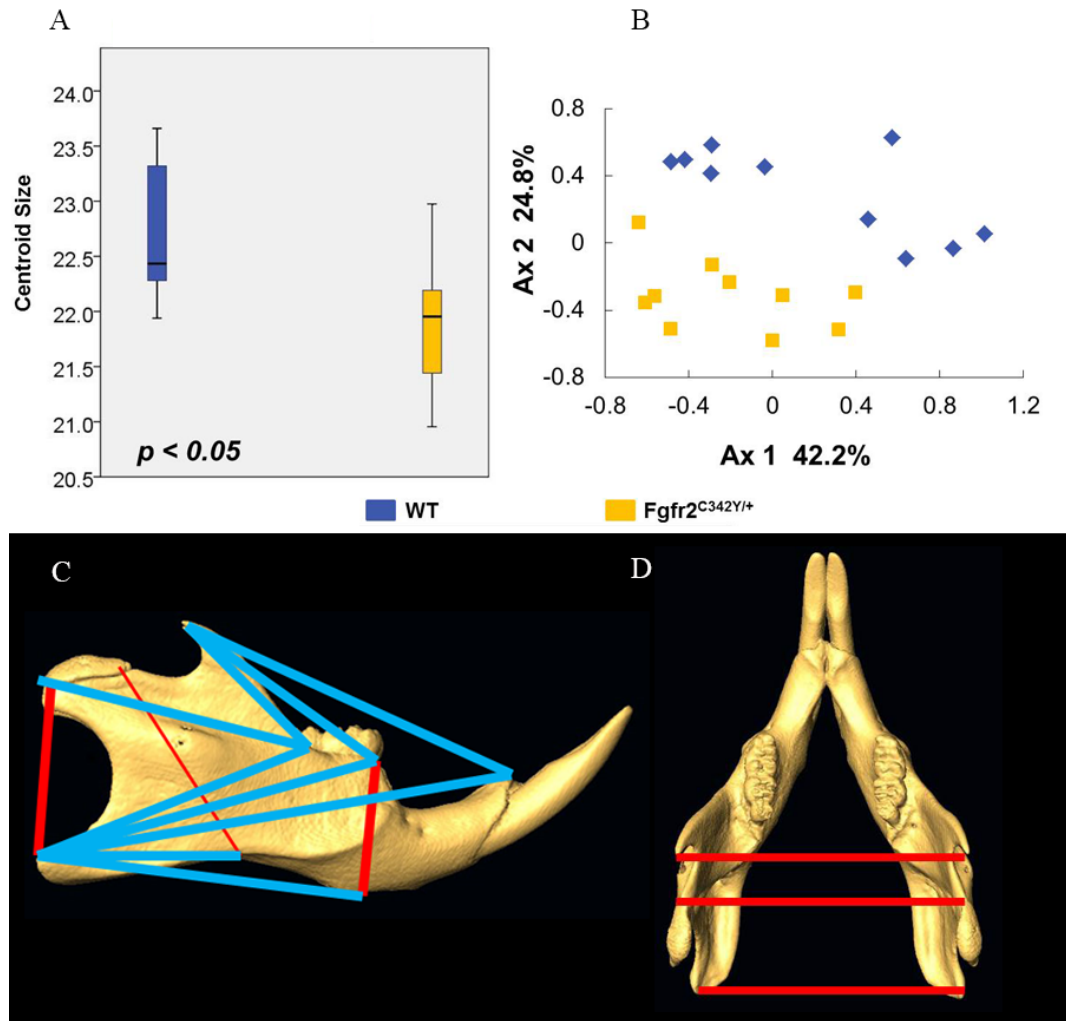


Figure 2.1. Size and shape differences among adult WT and HT (*Fgfr2<sup>C342Y/+</sup>*) mandibles using Euclidean Distance Matrix Analysis. Results from Holmes *et al.* (2011). A) Bar graph showing that HT mice were significantly smaller than WT; B) Principal Coordinate Analysis demonstrating a clear separation in shape between the two genotypes; C) sagittal and superior view of an adult mouse, blue lines indicate distances that are significantly smaller in HT mice while red indicate where HT mice were significantly larger.

### 2.1.2 Crouzon Mouse Data Collection

*Fgfr2c*<sup>C342Y/+</sup> mice (HT) and their wildtype (WT) littermates were maintained on a CD1 background house by the DeLeon Lab at the Broadway Research Building Animal Facility, Johns Hopkins Medical Institution. Genetic variation is dampened in inbred laboratory mice which causes logistical problems in calculating phenotypic covariation (Vinyard and Payseur, 2008; Hallgrímsson *et al.*, 2009). CD1 strains are useful in this instance as they have a mixed genetic background. Matings were organized with male mutant heterozygotes and female wildtypes; careful attention was paid to avoid sibling breeding. All genotyping was conducted by a commercial vendor, Transnetyx, Inc (Cordova, TN). Adult tail and fetal hind-limb biopsies were collected then shipped to Transnetyx, Inc. where a real-time PCR used specific probes designed to recognize the *Fgfr2c*<sup>C342Y/+</sup> mutation in the delivered specimens.

In order to visualize the mandible, each specimen was scanned in a high-resolution micro computed tomography machine ( $\mu$ CT). Specimen preparation for  $\mu$ CT scanning was a multi-tiered process involving specimen sacrifice, decapitation, chemical fixation and shipping. All mouse euthanasia procedures were done according to IACUC standards. Postnatal mice were first anaesthetized before undergoing cervical dislocation at which time the head was severed from the main body at the cervical region taking great care to avoid destroying any cranial tissue. Prenatal mice necessitated in utero collection. Pregnant dams were euthanized in the same manner described above. Intra-abdominal dissection was used to gain access to fetal mice, each still contained within their own embryonic sac. Subsequent to separating each fetus from the uterus they were then

decapitated at the lower cervical level. Specimen heads were fixed separately in 10% formalin and placed overnight on a laboratory rocker to ensure full perfusion.

Catalogued and fixed mouse heads were then shipped to the Louisiana State University School of Veterinary Medicine, Department of Comparative Biomedical Sciences located in Baton Rouge, LA. Here each specimen was  $\mu$ CT scanned at a resolution appropriate for size, age and bone density. Scan parameters used were 55kVp and cubic voxel resolution of 30 $\mu$ m for adult heads and 20 $\mu$ m for peri-weaning and fetal heads. All scans were saved as DICOM files and an LSU server was used to upload and share files.

Post  $\mu$ CT scan processing was completed using Amira (Mercury Computer Systems, Berlin, Germany), a multifaceted software that contains many different modules for visualizing and processing volume data as well as manipulating and quantifying 3D objects. Full skull DICOM files were uploaded in Amira where they could be visualized as a 3D surface and inspected for any abnormalities or scanning errors. After visual approval, the mandibles of each skull were segmented away from the rest of the material and saved as a separate data file. To segment an object, voxels of a particular density are assigned to a material specified by the user. All other material were deleted from the file, leaving only the mandible. Saved mandibular volume data was then “smoothed” using a computer automated algorithm, and saved in a surface file format to be imported into Geomagic Studio software (Raindrop Geomagic, Research Triangle Park, NC) for landmark collection.

### 2.1.3 Mouse Ages

Three specific age ranges were used: late embryonic stage (E17.5), two weeks old (P14 – peri-weaning) and 6 weeks of age (P42 – adults). Thus the sample encompasses a large range of growth appropriate for addressing changing developmental influences on the mandible. The youngest age groups provide information on mandibular growth and morphology before biomechanical function becomes a confounding factor in establishing modules structured on mesenchymal condensations. By contrast, the latter age groups represent a period when multiple influences are affecting mandibular variation and morphology. Sex was recorded when possible. Target sample size for all three age ranges was 30 mice of either genotype, however, the younger mice have smaller numbers (Table 2.1, Figure 2.2).

**Table 2.1. List of mouse model sample ages and genotype.**

Age	WT	MT ( <i>Fgfr2c</i> <sup>C342Y/+</sup> )	TOTAL
E17.5	23	17	40
P14	26	26	52
P42	30	30	60
TOTAL	79	73	152



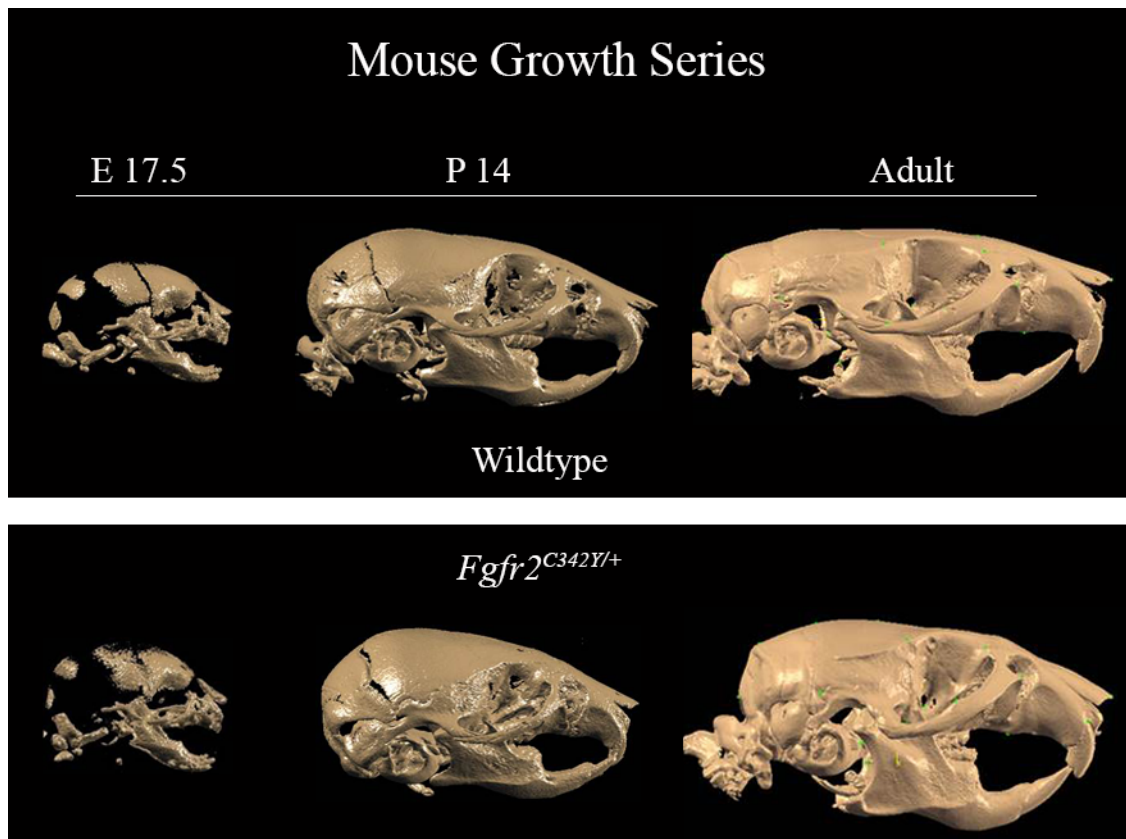


Figure 2.2. Mouse sample growth series. Illustration of WT (top) and HT (bottom) crania at each age range (left to right: E17.5, P14, Adult or P42) from  $\mu$ CT scans. Not to scale.

## 2.2 Functional Sample – Primates

The following section introduces the primate sample, utilized to test hypotheses under  $H_{\text{FXN}}$ . Rationale of sample selection is addressed. In addition, information on primate dietary ecology and phylogeny is described below followed by a description of data collection techniques and curation details.

The relationship between selective pressure and the structure of covariance in the mandible, or body in general, is highly complex. As stated above, there is a delicate balance in natural populations between adaptive influence and stabilizing selection, which can have significant implications for morphological integration and/or modularity.

Because covariation structure is a composite of developmental, functional and evolutionary mechanisms it has been difficult to construct analytical designs that empirically test the role of adaptation on integrated or modular structures. Thus, few analyses have addressed these questions head-on. Those that have, utilized samples from natural populations in order to compare covariance structure as an adaptive response to diverse environmental and mechanical demands (Badyaev and Forseman 2004; Badyaev *et al.*, 2005; Monteiro *et al.*, 2005; Young and Badyaev, 2006; Young *et al.*, 2007; Zelditch *et al.*, 2009; Goswami and Polly, 2010; Monteiro and Nogueira, 2010; Makedonska *et al.*, 2012; Klingenberg and Marugán-Lóbon, 2013). One experimental analysis focused more closely on short-term influences of differing dietary demands on covariance in the mandible. Anderson *et al.*, (2014) demonstrated that mice fed soft diets had significantly lower levels integration in the mandible than controls. These distinctions were found in the mic after only three weeks of being fed a different diet, suggesting that changes in covariance occurs as a result of bone remodeling during life. Whether the patterns and magnitudes of covariance in the primate mandible are due to long-term adaptive pressures or environmental pressures experienced *in vivo* is not explicitly addressed here. However, by utilizing a sample of closely related primates with disparate dietary behaviors it can be first determined whether differences in covariance exist within the mandible. Further interpretations of whether differences are due to selective pressures or the plasticity of bone response to stress can be made from there.

### 2.2.1 Primate Sample Selection

Two pairs of New World monkey (NWM) species from the family Cebidae were used for the primate sample. There are several reasons why these taxa are an excellent sample for the current project. NWM taxonomy and phylogeny are fairly well established and, as a group, NWM are highly diversified in habitat and morphology (Marroig and Cheverud, 2001, 2005; Schneider *et al.*, 2001, 2013). Cranial diversity in NWM is especially pertinent, given that several analyses have shown a strong correlation between cranial morphology and dietary habits (Ackermann and Cheverud, 2000; Marroig and Cheverud, 2001; 2004; 2005). The four cebids chosen here are *Cebus apella*, *Saimiri sciureus*, *Callicebus torquatus*, and *Pithecia pithecia*. Specimens were paired according to their associated clades: *C. apella* and *S. sciureus* were paired as members of the Cebidae clade; *C. torquatus* and *P. pithecia* were paired as members of the Pitheciidae clade.

### 2.2.2. Crown Platyrrhines - Taxonomy

New World Monkeys belong to the infraorder Platyrrhini, which exclusively inhabit the Central and South America; consisting of at least 16 genera and over 125 species (Groves, 2001; Ryland and Mittermeier, 2009; Wildman *et al.*, 2009; Kay, 2015). Much work in the past three decades has been dedicated to improving the resolution of the NWM phylogeny. The accumulation of morphometric (HersHKovitz, 1977; Rosenberger, 1984; Ford, 1986; Kay, 1990, 2014), molecular (Baba *et al.*, 1979; Schneider *et al.*, 1993, 1996; Stringer, 2003; Ray *et al.*, 2005; Schneider and Sampaio, 2014) and phylogenomic (Wildman *et al.*, 2009; Perelman *et al.*, 2011) analyses have

resulted in a well mapped phylogenetic framework with few remaining debates surrounding extant species (Figure 2.3). Three families have been recognized, Pitheciidae (sakis, uakaris and titi monkeys) as the basal clade and then Cebidae (capuchins, squirrel monkeys, marmosets, tamarins and owl monkeys) and Atelidae (spider, woolly, howler and woolly spider monkeys) as sister taxa.

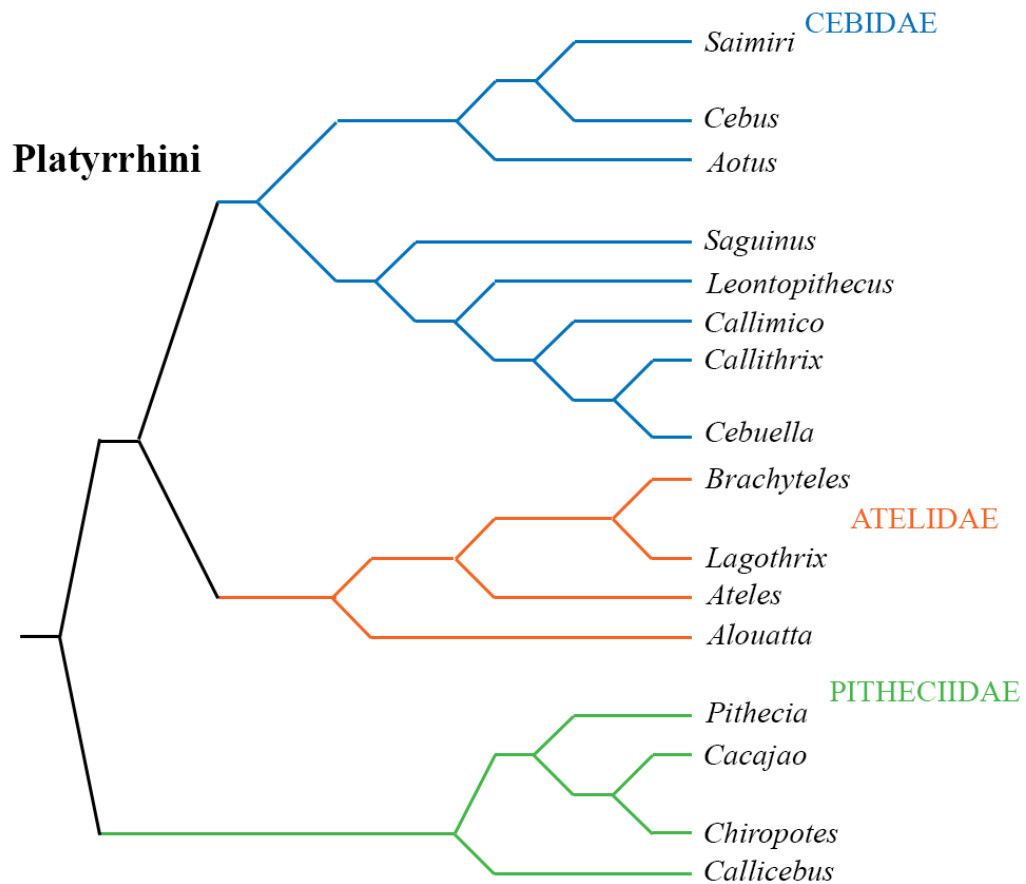


Figure 2.3. Platyrrhini phylogenetic tree. The three accepted platyrrhine clades, Cebidae, Atelidae and Pitheciidae along with branching patterns are shown here (adapted from Kay, 2014).

Contemporary unresolved issues in NWM taxonomy include the assignment of genera to new names (Wildman *et al.*, 2009; Perelman *et al.*, 2011; Alfaro *et al.*, 2012; Schneider and Sampaio, 2015). For instance, it has been recently argued that the robust *C. apella* should be assigned a new, unique genus name. Boubli *et al.*, (2012) and Alfaro *et al.*, (2012) suggested that *C. apella*, the most robust of all *Cebus* species, is so morphologically and ecologically distinct from the remaining gracile species that it should be as a separate genus *Sapajus*. They argued that repeated periods of isolation occurred between the robust and gracile cebines, wherein *C. apella* remained in the Atlantic Forest while other *Cebus spp.* remained in the Amazon Basin. This, therefore, accounts for the relatively unique hard diet acquired by *C. apella* as well as the concomitant morphological differences. They also stated that it was only recently that *C. apella* reinhabited the Amazon Basin, thus obfuscating their original generic designation. Given that only one species of *Cebus* is being utilized in this study and that the position of *C. apella* remains within the Cebidae clade, whether or not robust cebines should be reassigned to a new genus is irrelevant to the questions posed here.

### 2.2.3 Cebidae and Pitheciidae Diet

The primates sampled here were purposefully chosen as pairs, exhibiting either durophagous or non-durophagous diet, with each pairing residing in the clade Pitheciidae (*Pithecia* and *Callicebus*) or Cebidae (*Cebus* and *Saimiri*). The extent to which fruit composes the diet varies among genera and even species. Furthermore, most NWM must supplement their diet with other food materials in order to ingest requisite amounts of protein. NWM also occupy a wide body size range, which may dictate the type of diet

consumed for caloric intake (Fleagle *et al.*, 1981; Kay, 1984; Robinson and Redford, 1986; Janson and Boinski, 1992; Hawes and Peres, 2014). This generally leads small-bodied platyrrhines to engage in insectivory and/or gummivory while large-bodied primates use seed predation or folivory. However, these are general rules, and most NWM will engage in generalist foraging strategies. Even so, Norconk *et al.* (2009) recently reported metabolic energy intake is relatively stable within each clade, such that when ranked by nutritional richness, *Cebus* and *Saimiri* rank closely together, as do *Pithecia* and *Callicebus*.

### *Cebidae*

The cebid species used here are well studied in the anthropological literature because they offer an excellent natural comparison of sympatric species that are markedly different in both body size and diet (Podolsky, 1990; Garber and Leigh, 1997). *Saimiri* is substantially smaller than *Cebus* (*Saimiri* 0.699-1.02 kg; *Cebus* 2.52-3.65 kg), a factor which has been used to partially explain the disparate foraging strategies utilized by these two Amazonian neighbors (Smith and Jungers, 1997). Indeed, *C. apella* habitually masticates and ingests mechanically resistant objects while *S. sciureus* ingests a much larger percentage of insects (79-97% of diet, compared to 16-33% in *C. apella*) (Janson and Boinski, 1992; Norconk *et al.*, 2009; Zimble-DeLorenzo and Stone, 2011). Dissimilarity in body size is largely the product of genus specific growth patterns. Despite differences in adult body size, capuchins and squirrel monkeys are born at similar weights. However, the ratio of infant birth weight to mother's weight is remarkably high in *Saimiri*. This, paired with a high velocity of growth in the pre-weaning period suggests

that *Saimiri* attains the majority of its adult body size quite rapidly (Ross, 1991; Hartwig, 1996; Garber and Leigh, 1997; Stone, 2006; Marroig, 2007; MacKinnon, 2013). In contrast, *Cebus* species are characterized by an average NWM birth weight coupled with a prolonged and slow postnatal growth rate.

*C. apella* and *S. sciureus* display moderate sexual size dimorphism and sexual dimorphism in cranial shape (Anapol and Lee, 1994; Garber and Leigh, 1997; Marroig, 2007). Prolonged male growth has often been cited as a significant contributor to size differences (Leigh, 1992; Garber and Leigh, 1997). Interestingly, Anapol and Lee (1994) found that temporalis muscle lever arm is longer while the masseter lever arm is shorter in *S. sciureus* males compared to females. Given the closer position of the masseter to the axis of rotation at temporal-mandibular joint it is likely that this trait can afford wider gapes in males for canine display, a common feature in many other primates include *C. apella* (Anapol and Lee, 1994; Taylor and Vinyard, 2009).

The *Cebus spp.* have traditionally been divided into two general groups, the robust “tufted” capuchin (*C. apella*, *C. libidinosus*, *C. nigrinus*) and the gracile “non-tufted” capuchin (*C. olivaceus*, *C. albifrons*, *C. capuchinus*). Though each group likely participates in soft-object eating, it is the robust capuchins that are known for breeching mechanical resistant foods. Of these, *C. apella* has been repeatedly shown to masticate the hardest food materials, on the most consistent basis (Kinzey, 1974; 1992). Though *Cebus spp.* are generalists (Terborgh, 1983), several field studies have documented *C. apella* partaking in hard-object feeding during dry seasons. Palm seeds are a very important resource during the dry seasons and are encased in a hard outer shell. Interestingly, while other gracile capuchins use tools to open palm nuts, tufted capuchins

employ their dentition to open the hard outer shell of the palm nut (Visalberhi *et al.*, 2008). In addition, the robust *C. apella* has been observed using their dentition to tear open tough bark on tree limbs in an effort to find insects or to open tough pericarps of husked fruits (sclerocarpal harvesting) (Izawa and Mizuno, 1977; Anapol, 1994).

Many studies suggest that dietary habits exhibited by *C. apella* have led to a quantifiably more robust masticatory apparatus than that of other cebids. Estimation of masseter and temporalis lever mechanics based on cranial (Wright, 2005) and mandibular measurements (Norconk *et al.*, 2009), comparisons of mandibular corpus dimensions, cross-sectional properties and cortical thickness (Cole, 1992; Daegling, 1992; Anapol and Lee, 1994), as well as masticatory muscle architecture (Taylor and Vinyard, 2009), have demonstrated a clear relationship of diet with *C. apella* mandibular size and shape. Characteristics include relatively larger corporal dimensions and muscular mass when compared to congener species, broad mandibular corpus at M<sub>1</sub>, and a disproportionately larger temporalis lever arm compared to masseteric lever arm. *C. apella* mandibular configuration is therefore well built to generate and withstand large occlusal loads.

*Saimiri*, in general, are the most insectivorous of the neotropical primate genera with little to no record of seed predation (Norconk *et al.*, 2009). Though habitat ranges overlap among squirrel monkeys and capuchins, *Saimiri*'s smaller size is advantageous when navigating tree canopy areas with smaller branches (Podolsky, 1990). This allows them to forage in areas unavailable to other large-bodied primates. *Saimiri* dexterity also plays a key role in grabbing insects from the air and open surfaces as well as digging through dried or rotted bark, a skill that is developed quite early in juveniles (Janson and Boinski, 1992; Stone, 2006). Fruit also comprises a portion of *S. sciureus* diet, 3-20%



(Zimblér-DeLorenzo and Stone, 2011). However, fruits selected tend to be much smaller and softer than those chosen by *Cebus* (Podolsky, 1990; Janson and Boinski, 1992).

Dietary differences between the two cebids used here are represented in mandibular morphology. As mentioned above, *Cebus* displays a remarkably robust mandible, whereas *Saimiri* is considered to be more gracile. Corporal dimensions in *Saimiri* were thinner medio-laterally and shorter supero-inferiorly when compared to other platyrrhines (Janson and Boinski, 1992). In fact, several authors have used *S. sciureus* as low-bite force standard for comparison when hypothesizing about cortical and trabecular bone distribution (Vinyard and Ryan 2006; Ryan *et al.*, 2010).

### *Pitheciidae*

The other platyrrhine taxa to be studied here are members of the family Pitheciidae. Four genera exist within Pitheciidae: *Pithecia*, *Cacajao*, *Chiropotes* and *Callicebus*. The first three are closely related and can be grouped within pitheciines while *Callicebus* is considered the closest sister taxon. As with other platyrrhines, fruit is a large part of pitheciid dietary composition and pitheciids might ingest the largest percentage of fruit in all of the neotropical primates. *Pithecia*, *Cacajao*, and *Chiropotes* share a specialization in seed predation to the exclusion of *Callicebus*.

*Pithecia* (sakis) and *Callicebus* (titi monkeys) are the smaller two genera of Pitheciidae (*Pithecia*: 1.58-1.94 kg; *Callicebus*: 1.21-1.28 kg) and possess little to no sexual dimorphism (Kinzey, 1992; Smith and Jungers, 1997). Compared to their Cebidae counterparts, there is a noticeable dearth of research in the life history pattern or foraging technique of sakis and titi monkeys, especially in *C. torquatus*. However, more scientific

attention is currently being allocated to this group in conjunction with recent conservation efforts (Garber *et al.*, 2013). What is known, though, reemphasizes the fascinating diversity found in NWM. For instance, *Callicebus* are monogamous with substantial resources provided by the father. During weaning, the supplemental calories provided by the father allow for a rapid growth rate in infants while lowering energy expenditure by titi mothers. In contrast, *Saimiri* is profoundly dependent on maternal nutrition (Garber, 1995).

Regarding subsistence patterns, *P. pithecia* (white-faced sakis) can be classified as frugivore-granivores. *P. pithecia* is heavily invested in seed predation from both ripe and unripe fruits (Kinzey and Norconk, 1993; Norconk, 1996). Of the three pitheciines, *P. pithecia* participates in granivory the least and will often fall back on leaves and other leafy vegetation (Norconk *et al.*, 2009). As with other sclerocarpal harvesters, white-faced sakis must puncture tough exocarp with their incisors or canines to access the soft pulp. The seeds contained within have been described mostly as pliable (Kinzey, 1992). However, Norconk and Veres (2011) note that, despite seed plasticity they also demonstrated a high crushing threshold. High occlusal loads are therefore exerted on the anterior dentition and molar row of *P. pithecia*.

*C. torquatus sensu lato* is also predominately frugivorous (55-80%); however they rely more on the soft pulp or mesocarp (~50%) rather than seeds. *Pithecia*, on the other hand, relies on the seeds of fruit (~60%) (Norconk, 2009). Dispersible fruits and arils, which are high in lipids and protein, comprise a large portion of *C. torquatus* diet (Kinsey, 1992; Norconk *et al.*, 2009; Ledogar *et al.*, 2013). In addition, recent studies have also documented a substantial amount of insectivory in many *Callicebus spp.* as an

alternative protein source (Heymann and Nadjafzadeh, 2013). Titi monkey size should preclude high levels of insectivory; however, Kinzey (1978) suggested that this may be due to their sandy habitat, which is devoid of fresh leafy supply.

Dietary differences are again evident between *P. pithecia* and *C. torquatus* when comparing mandibular form as it relates to force production and resistance. Wright (2005) compared mechanical advantage in the posterior molar row in a sample of platyrrhines. Results showed *C. apella* and *P. pithecia*, two “hard-object” feeders, falling out together with the highest values while *C. torquatus* was among the lowest. Symphyseal robusticity was also noted in *P. pithecia* along with a tall mandibular body, both of which are thought to be an adaptation to parasagittal bending (Anapol and Lee, 1994). *C. torquatus* on the other hand is consistently characterized as possessing a gracile masticatory apparatus (Norconk *et al.*, 2009).

In summary, the primate sample is composed of two cohorts within two separate clades, Cebidae and Pitheciidae. Within Cebidae, the cohort includes *C. apella*, the most robust of the capuchins and the smaller-bodied, gracile *S. sciureus*. Many comparative analyses have utilized these two taxa due to their difference in body size and diet. Contrasts between the Pitheciidae cohort are less stark. *P. pithecia* and *C. torquatus* are closer in body size than the Cebids chosen here. In addition, though *P. pithecia* is considered to habitually incur “intermediate” loads compared to other pitheciids, they are still generally larger than those habitually generated by *C. torquatus*.

#### 2.2.4. Primate Data Collection

Three-dimensional surface scans were collected of *Cebus apella*, *Saimiri sciureus*, *Pithecia pithecia* and *Callicebus torquatus* adult mandibles housed at either the American Museum of Natural History (AMNH), Division of Mammals or the National Museum of Natural History (NMNH), Division of Mammals. Mandibles were chosen based on three criteria: 1) damage was not present on any of the relevant surfaces; 2) sex was known and documented for that specimen; and 3) third molar eruption was complete, indicating that the specimen had attained full adulthood (Table 2.2, Figure 2.4).

**Table 2.2. New World Monkey sample.**

Species	Male	Female	TOTAL
<i>Cebus apella</i>	15	15	30
<i>Saimiri sciureus</i>	14	15	29
<i>Pithecia pithecia</i>	13	14	27
<i>Callicebus torquatus</i>	15	15	30
TOTAL	57	59	116

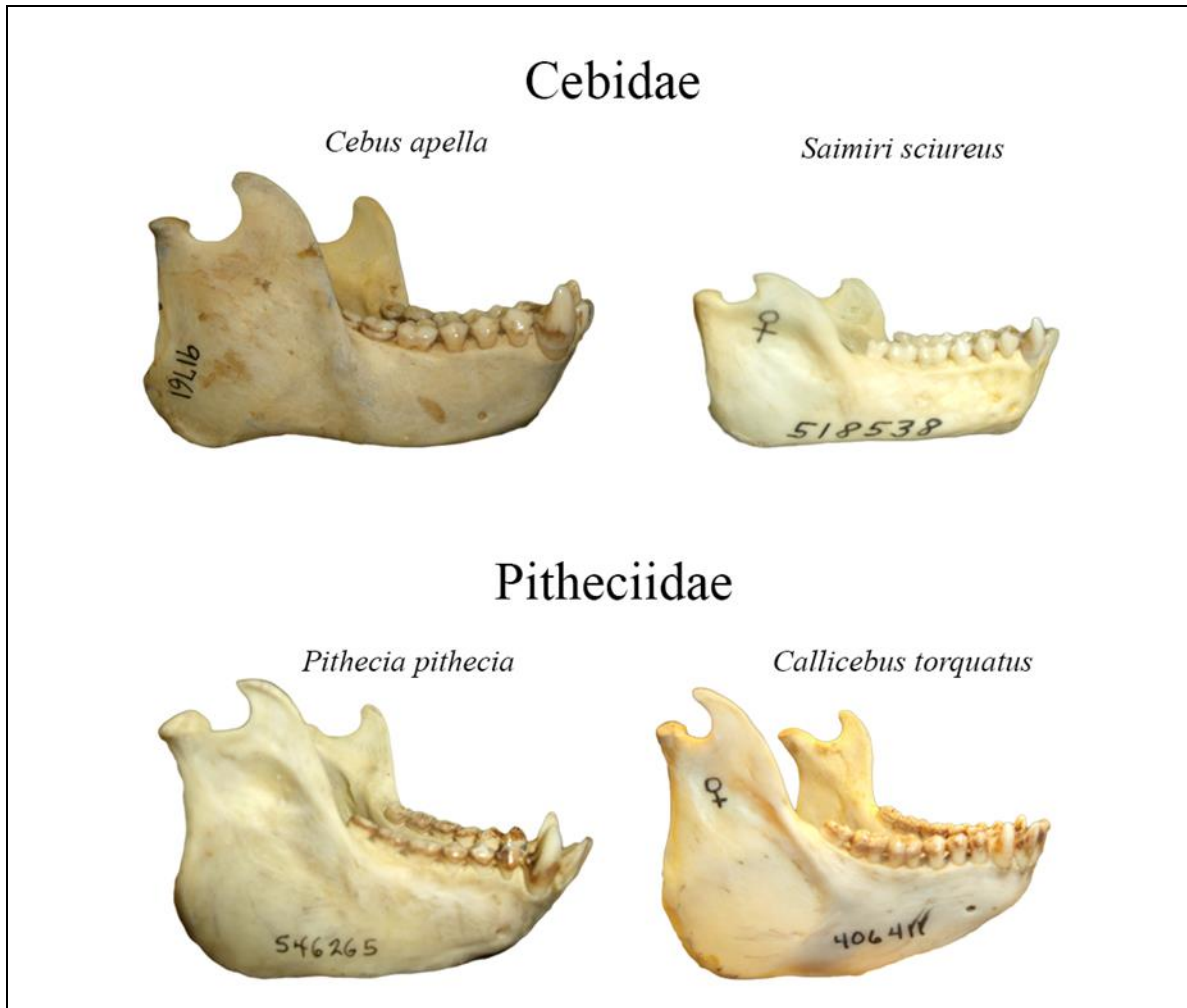


**Figure 2.4.** Mandibles of the four species used in this analysis, *C. apella*, *S. sciureus*, *P. pithecia* and *C. torquatus*. All images are of female mandibles.

A NextEngine Desktop 3D Scanner (model 2020i) along with NextEngine ScanStudio Pro HD software (NextEngine, Malibu, CA) was used to capture 3D surface images of each mandible. The NextEngine collects high-resolution color images of object surfaces via two parallel optical lasers which capture objects as point clouds (160,000 points per inch capable). The same scanning protocol was followed for each mandible. Software was set to “Macro” mode (0.005 inch accuracy, 40,000 ppi). Mandibles were affixed in putty on a rotating table during the scanning procedure to ensure minimal

movement. ScanStudio HD was set to collect 16 images (maximum possible) in a 360° rotation.

It is important to note the utility of generating 3D surfaces with the NextEngine scanner. While use of a microscribe to collect landmarks is highly efficient, it was considered less than ideal for this project. Mandibles lack a sufficient number of easily identifiable biological landmarks which are much more common on the skull (i.e. cranial sutures) and many of the mandibles used here are relatively small objects. These factors have been shown to lead to high measurement error when using a microscribe. Much lower measurement error can be attained with accurately collected 3D images (Sholts *et al.*, 2011).

Images were taken of the mandible in two separate positions on the rotating table, in order to capture its complex shape (Figure 2.5). Images from both positions eventually underwent a meshing procedure in order to create a 3D surface, which is described below. Supero-inferior (SI) scans were taken by fixing the angles of the mandible in putty on the rotating table, with the inferior border of the mandible at ~60°. Medio-lateral (ML) scans were taken by fixing the mandible in putty, with the anterior half of the inferior border of the mandible fixed in putty, parallel with the floor. Care was taken not to obscure the symphysis or angle in this view. Scanning each mandible in two separate views allowed me to accurately image both the buccal and mesial aspects, in addition to thin edges such as the inferior border of the corpus and the edge of the angle. Sixteen images were taken of the mandible in both positions to capture the entire mandibular surface.

The “raw” scans of the ML and SI view, each amalgamation of the 16 images captured, were then imported into ScanStudio HD software to create a single fused mesh model of each view. Raw scan were aligned with user selected preferences to create a model. Next, all unwanted data (i.e., pieces of rotating table or putty) were deselected from the image. Aligned models were then fused (0.003 inch maximum deviation) after selecting an optimized resolution ratio. Fully fused ML and SI mesh models were then saved as .ply files and imported into Geomagic.

Geomagic software allows one to merge multiple sets of 3D surface files. Here, MI and SL surface .ply files (~750,000 triangles each) were merged by manually placing matching landmarks on corresponding surfaces. The software then matches the two sets of landmarks to determine the position of either surface and then combines the surfaces. A separate automated registration process was then conducted to reduce any noise or scan deviation (average 0.05 mm deviation), resulting in a merged scan of an entire mandible. Each mandible scan was then further processed by manually filling in small holes or deleting unwanted surfaces, until deemed ready for landmark placement. Once completed each file was saved in the .ply file format.

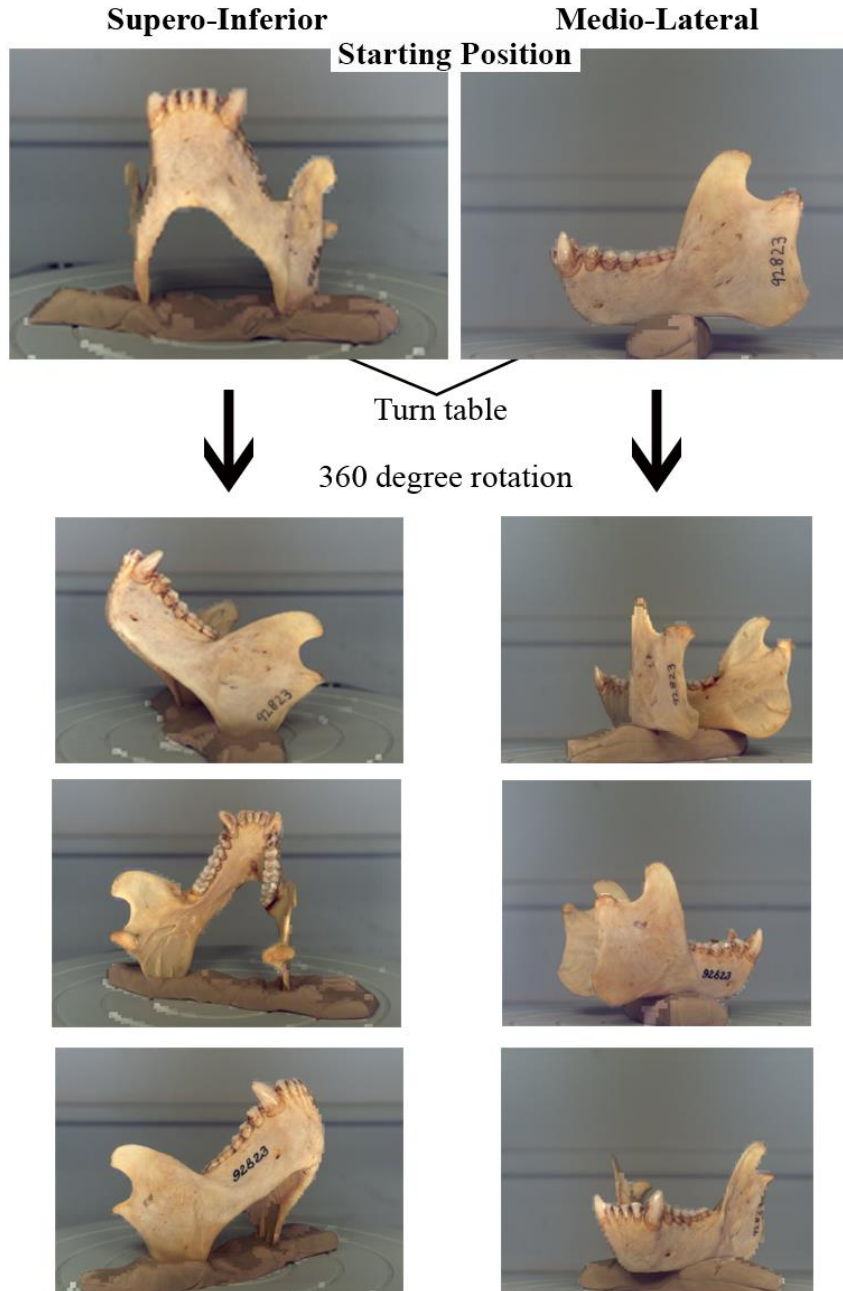


**Figure 2.5** Positions used to capture mandibular surfaces using the NextEngine scanner. Each mandible was scanned twice, in two separate views in order to ensure all aspects were imaged and converted in polygonal surfaces. In the supero-inferior view the mandibular is positioned at a  $\sim 60^\circ$  by fixing the angle of mandible in putty. In the medio-lateral view, the inferior edge of the mandible was placed relatively parallel to the turn table. The anterior 2/3 of the mandible was fixed in putty without obscuring the symphysis. Once each mandible was in place, the turn table rotates  $360^\circ$  while taking 16 separate images. Those images were then converted into polygonal surfaces and merged into a 3D surface.



## 2.3 Data Collection

### 2.3.1 Landmark Selection

Three-dimensional landmark coordinates were collected on the complete, rendered surface of the mandibles in both data sets within the Geomagic platform. Landmarks were carefully chosen to reflect developmentally and biomechanically relevant morphologies, as well as overall mandibular shape. The majority of landmarks between the mouse and primate samples were similar; however, due to anatomical differences a small number of separate landmarks were chosen to reflect the shape of each sample (Figure 2.6; Table 2.3 and 2.4). When selecting landmarks it is essential to ensure that they are homologous across specimens and are based on reliable anatomical markers in order to reduce the amount of variance introduced by landmark collection error. Different definitions exist for particular landmark types depending on the criteria used to locate them (Bookstein, 1997; Lele and Richtsmeier, 2001; Zelditch *et al.*, 2012). Type I landmarks represent intersection of bone, the most common example of which is the junction of two or more sutures. Type II landmarks can be located on extreme points such as an apex of a curve or farthest distance on a projection. Type III landmarks are based on defined, arbitrary measurements such as the center of a joint surface. In addition, semilandmarks may also be placed along curves or surfaces to capture shapes that do not afford easily identifiable homologous landmarks.

Mandibles are notoriously devoid of type I landmarks, which are considered to be the most reliable. For this reason, it was necessary to compile a set of points largely comprised of type II landmarks. Semilandmarks were used in order to capture variation in shape along the curve of the posterior aspect of the ramus and the gonial angle in

primates. In mice, semilandmarks were used to capture the curve of the posterior aspect of the ramus, the gonial angle and incisal alveolus (Figure 2.6). Semilandmarks are highly appropriate for defining shape along curves such as these, especially in ontogenetic studies where the boundaries of bony deposition are of interest (Zelditch *et al.*, 2012).

Conventionally, semilandmarks are not only placed equidistantly along the desired curve, but are also allowed to “slide” (see pg. 77) along the curve in an effort to avoid assumptions of spacing in structures that will vary in size and shape (Gunz *et al.*, 2005). If the same numbers of landmarks are placed equidistantly along two curves that are of different size or shape the landmarks will not match and result in local shape differences that are not biologically meaningful. In other words, sliding semilandmarks are manipulated within the statistical analysis in order to optimize matching landmarks among specimens, or create “homologous curves” rather than exact landmarks (Zelditch *et al.*, 2012).

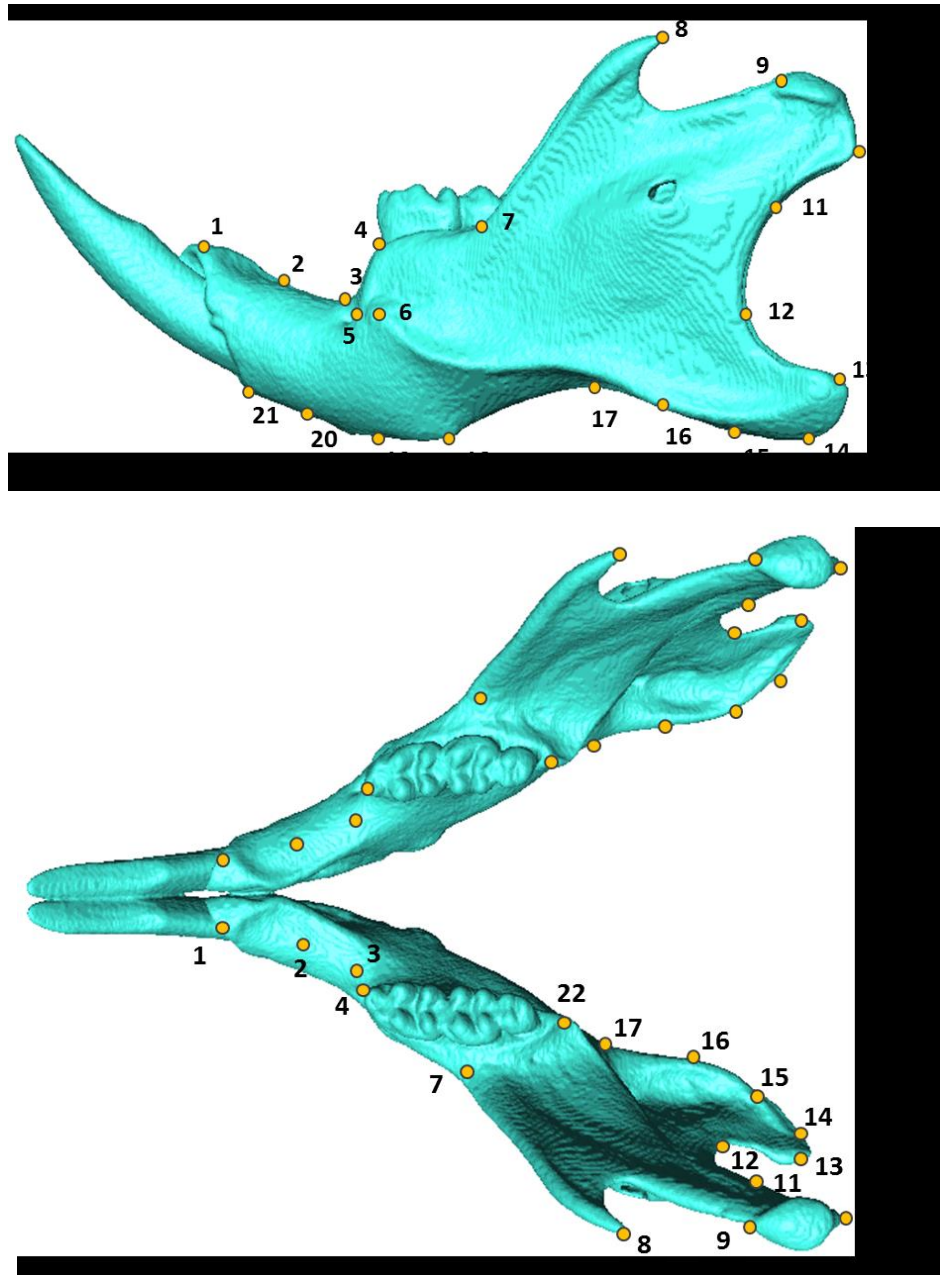


**Figure 2.6** Image depicting landmarks used to capture mouse mandibular morphology. A) sagittal view of mouse mandibular landmarks; B) superior view depicting all bi-lateral landmarks. Landmark names for the left side, only: (1) LASI (2-3) sliding semi-landmarks for left upper incisor curve; (4) LAMR; (5) LMAF; (6) LMSM; (7) LCMJ; (8) LSCD; (9) LACD; (10) LPCD (11-16) sliding semi-landmarks for the posterior ramus and angle; (17) LABJ; (18) LIRA; (19-20) sliding semilandmarks for the left lower incisor curve; (21) LAII; (22) LPMR (see Table 2.3 for full landmark name and descriptions)

**Table 2.3. List of landmarks used in both the mouse and primate samples.**

Traditional landmarks			
Mouse	Primate	Name	Definition
X	X	ASI	Anterior Superior Incisor – anterior superior most point on the symphyseal alveolar bone, located between the central incisors. Primates: this is a midline landmark; Mice: this landmark is bilateral, located on the most anterior central projection of the superior incisal bone.
X		PSI	Posterior Superior Incisor – junction between the incisal alveolus and the anterior - inferior edge of the molar row.
X	X	AII	Anterior Inferior Incisor- anterior inferior most point on the symphyseal alveolar bone, located between the central incisors. Primates: this is a midline landmark; Mice: this landmark is bilateral, located on the most anterior central projection of the inferior incisal alveolar bone.
X		AMR	Anterior Molar Row - located on the superior alveolar bone in line with the first molar. This landmark should be near the dento-enamel junction.
X	X	MAF	Mandibular Foramen - point taken on the posterior rim of the mandibular foramen.
X	X	CMJ	Coronoid Molar Junction - located where the coronoid meets the molar row. This point should be placed at the most anterior intersection.
X		PMR	Posterior Molar Row - the most posterior projection on the alveolar bone of the molar row.
X	X	SCD	Superior Coronoid - superior most point on the mandibular coronoid
X	X	ACD	Anterior Condyle - anterior most point of the condyle, taken in the midline.
X	X	PCD	Posterior Condyle - posterior most point of the condyle, taken in the center. In primates this landmark is included in the angular sliding semi-landmarks
X	X	IRA	Inferior Ramus - Primates: this point is taken as the inferior most point on the ramus in line with the center of the first molar; Mice: the landmark is located on the inferior most projection of the mandibular body, which is easily identifiable.
X	X	ABJ	Angle Body Junction - junction of the mandibular angle and body, taken on the inferior rim of the body.
X	X	MSM	Masseter Muscle - point located at the anterior-most, bony projection of the masseteric insertion area.
Semilandmark Curves			
X	X	Angle	PCD to ABJ – taken along the edge of the angle.
X		Superior Incisor	ASI to PSI – taken along the midline of the curve.
X		Inferior Incisor	AII to IRA – taken following the prominent bony ridge between these two points.

An X indicates whether the landmark was collected for that particular group. Traditional landmarks and their definitions are listed first, the majority of which are bilateral with two exceptions. ASI and AII are midline landmarks in primates because they have fused symphyses, whereas mice lack a fused symphysis. Semilandmarks are also listed below along with definitions.

The starting point of each angular curve for both mice and primates began at the most posterior edge of the mandibular condyle, in the midline (PCD). Curves were traced within Geomagic from PCD all the way along the edge of the angle to the inferior junction between the angle and the body of the mandible (ABJ) (see Figure 2.6 and Table 2.4). PCD and ABJ thus acted as anchor points for the curves. Semilandmarks, all points between the anchors, were then projected onto that tracing and extracted for further processing (primates, k=60; mice, k=20; including anchor points). Semilandmarks were then resampled down to fewer landmarks using the “Resample” executable program. “Resample” enables the resampling of semilandmarks along a curve into a user defined number of equidistantly spaced points. Semilandmark numbers were essentially halved for after resampling (post resample: primates, k=15; mice k=8; including anchor points) in order to minimize overrepresentation of the mandibular angle within the overall landmark configuration.

Similar steps were taken when selecting and collecting semilandmarks for the incisal curve, a predominant feature of murine mandibles. Two curves, one superior and one inferior, were collected here. The superior incisal curve begins at the anterior most projection of the alveolar bone superior to the incisor (ASI) and ends at the junction between the incisal alveolus and the anterior - inferior edge of the molar row (PSI). This curve was placed along the midline to fully represent the extent of the incisal bend. The inferior incisal curve runs from the anterior most projection of the inferior incisal alveolus (AII) to the inferior most ridge of the mandibular body (IRA) which is very well defined in murine mandibles. Points along this curve were not placed solely in the midline, but followed an anatomical ridge which extends from either point. As with the

angular curve, initial point collection for the superior and inferior incisal curves oversampled landmarks (superior incisal curve, k=5; inferior incisal curve, k=10; including anchor points). Subsequently, the landmarks were resampled to smaller numbers of equidistantly placed semilandmarks (superior incisal curve, k=3; inferior incisal curve, k=4; including anchor points). All semilandmarks were individually checked to assure they were placed in correct anatomical order after resampling.

The choice to reduce semilandmark number was based on numerous trials in which different numbers of landmarks were used. After visualizing curves for this each of these trials, semilandmark number was chosen for the best representation of the each particular curve while minimizing the number needed. Variation in size and shape was also considered here especially in the NWM which possess highly distinctive gonial angle shapes. Therefore a balance was made between using enough landmarks to capture taxonomic variance and minimizing landmark number.

Table 2.4. Total number of landmarks for both sample sets (k).

	<b>Traditional Landmarks</b>	<b>Sliding Semilandmarks</b>	<b>Total</b>
<b>Mice</b>	<b>26 (bilateral)</b>	<b>18 (bilateral)</b>	<b>44</b>
<b>Primates</b>	<b>16 (bilateral) + 2 (midline) = 18</b>	<b>26 (bilateral)</b>	<b>44</b>

### 2.3.2 Generalized Procrustes Analysis

Subsequently, all landmarks underwent Generalized Procrustes Analysis (GPA). This geometric morphometric approach is a commonly used method for exploring shape variation in complex structures. Analyses of shape variation are equivalent to estimations

of covariance in biological form, and GPA has become a prevalent technique to quantify shape variables (Dean *et al.*, 2004; Slice, 2007; Mitteroecker and Gunz, 2009; Zelditch *et al.*, 2012). Shape variables are derived from a partial Procrustes superimposition which is applied to the selected landmarks. There are three steps to partial Procrustes superimposition including rotation, translation and scaling. Landmarks of each specimen are superimposed by first finding the centroid of each specimen and then aligning all centroids. Once the centroids are aligned the specimens are *translated*. Landmark configurations are then *scaled* by dividing each individual landmark coordinate by that specimen's Centroid Size (CS). CS (sum of the squared distances from each landmark to the centroid) is an estimate of overall size independent of shape. Specimens are then *rotated* into optimal alignment based on the average shape of all specimens (Rohlf and Slice, 1990; Zelditch *et al.*, 2004; Mitteroecker and Gunz, 2009). The result is multivariate shape information in form of Procrustes coordinates. Multivariate analyses of shape differences are then conducted by quantifying the deviation of these new coordinates from the average shape coordinates. Procrustes coordinates can be used in a variety of analytical techniques, including covariance matrices, Principal Components Analysis (PCA) and other data reduction techniques.

Despite the ubiquity of GPA there are some inherent, underlying flaws that need to be mentioned. Landmark variance, due to the computations that result in rotation and translation, has been found to be unreliable when using Procrustes superimposition (Lele and Richtsmeier, 1990). Superimposing the landmarks by minimizing the sum of squared distances between equivalent landmarks of each specimen changes the natural variance of each landmark in two ways. First it assumes that variance is equally distributed across all

landmarks. Therefore, Procrustes analyses will allocate variance to landmarks that are not prone to variance while simultaneously removing variance from those landmarks that are prone to error (Richtsmeier *et al.*, 2005). Second, the superimposition method biases variance found in landmarks depending on where they are located relative to the centroid. Such that variance is reduced in landmarks that are farther away but increased in closer landmarks (Lele, 1993).

The model used for Procrustes superimposition assumes that biological variance of each landmark is small enough that these complications do not fundamentally distort the data. Yet, several authors have found fault in the superimposition methods, especially statistical analyses of covariance and measurement error (Corner *et al.*, 1992; Richtsmeier *et al.*, 1995; Richtsmeier *et al.*, 2005; von Cramon-Taubadel *et al.*, 2007). Lele (1993) and colleagues (Lele and Richtsmeier, 2001) devised a separate approach to analyzing shape differences among specimens, the Euclidean Distance Matrix Analysis (EDMA). This method is coordinate-free precluding the need for object rotation thus removing problems associated with superimposition. EDM is based on the distances between landmarks and results in a matrix of these differences. Mean form and localized variation of specified landmarks can then be assessed. EDM analyses will be conducted in the future to complement the analyses reported here. The potential issues the Procrustes derived analyses and future approaches using EDM are discussed later in further sections of Chapter 2 and Chapter 6.



### *Sliding Semilandmark Curves*

After resampling, all landmarks associated with a curve in this analyses underwent a “sliding” protocol to produce sliding semilandmarks which are used to capture complex curves (Bookstein *et al.*, 2003; Zelditch *et al.*, 2012). Sliding semilandmarks are slid using the tangent line of the curve. First, equidistant landmarks are placed along the chosen curve with a homologous starting point across specimens. Tangent vectors are calculated for each semilandmark along the curve. The semilandmark then slides along the tangent direction until the net bending energy is minimized among specimens (Bookstein, 1997; Gunz *et al.*, 2005; Perez *et al.*, 2006; Mitteroecker and Gunz, 2009). Bending energy is a scalar quantity used to define the action of a point on a curve and the movement of that point along a tangent vector Gunz *et al.*, 2005).

Semilandmarks were slid using the Geomorph R package written and made freely available by Adams and Otárola-Castillo (2013). Whole landmark configurations were loaded into the Geomorph package and run through the “gpagen” code which produces a Generalized Procrustes analysis. Using the same program, semilandmark points were slid using Bookstein’s benign energy protocol (Gunz *et al.*, 2005; Perez *et al.*, 2006). Once a Procrustes superimposition was performed and semilandmarks were slid, an output file was created containing the resulting Procrustes coordinates and centroid sizes for each specimen. This file could then be utilized within other morphometric software packages (i.e., MorphoJ) and R coding.

## 2.4 Error Study for Landmark data

Measurement error analyses are fundamental for any morphometric study (Corner et al., 1992; Richtsmeier et al., 1995). Since the basis of morphometric analyses is often dependent on quantifying and allocating degrees of intra- and inter-sample variance, the amount of variance introduced by observer error must be taken into account. Precision and repeatability analyses were conducted here to evaluate intra-observer landmark placement. Precision refers to the data collector's accuracy in placing landmarks on the same specimens over multiple trials. Repeatability, on the other hand, measures the ability of the collector to locate landmarks reliably across specimens representing diverse morphologies, relative to actual differences (Corner et al, 1992; Kohn and Cheverud, 1992). Precision and repeatability was investigated in both samples in order to assure that landmarks could be located across a diverse set of mandibles.

As mentioned previously, a Procrustes analysis introduces unknown error to landmark variance. The process of superimposition biases the amount of variance given to a landmark relative to its location near the centroid and it allocates variance equally across landmarks despite biological differences in variance. However, sliding semilandmarks were used in this project to capture the shape of complex curves. Curve landmarks were slid based on the minimum bending energy criterion which necessitates the step of Procrustes superimposition (Bookstein, 1997; Gunz *et al*, 2005). By default, error analyses on the raw coordinates must exclude the slid semilandmarks. Therefore, it was decided that separate precision and repeatability measurement error analyses would be conducted. To truly determine the precision of landmark placemen, precision analyses were conducted on raw landmark data. Repeatability analyses on the other hand were

conducted on Procrustes coordinate data in order to include the sliding semilandmarks. In addition, shape data were deemed acceptable here because the most important aspect of repeatability is that variation is greater between samples than within. Future analyses will include measurement error studies of repeatability using EDMA mean form for both mice and primates. Additionally, a distance based repeatability study will be conducted on multiple primate scanning episodes in order to detect any error in the process of merging two views of the mandible.

#### 2.4.1 Developmental Sample: Landmark Measurement Error Analysis

Raw coordinate data was collected from the mandibles of ten adult WT mice, in three trials each. Trials were conducted by the same observer and separated by a week. Sliding semilandmarks were excluded from these analyses. Average landmark location was calculated for all landmarks within each specific trial set. The distance formula was used to calculate landmark distance among all three trials and then these values were averaged across trials. The deviation of landmarks from the mean in each trial was determined. Deviations among trial landmarks greater than 0.3 mm were considered to be error prone. This measure was chosen to represent less than 3% of average adult WT mandibular length.

Nearly 21% of raw landmark coordinate deviations reached the 0.3 mm level of error. In fact, more than 50% of the landmarks had an average deviation less than 0.1 mm. Raw coordinate landmarks that deviated more than 3 mm includes the IRA and PCD (between 0.37 and 0.45 mm). Both of these landmarks are placed on faintly curved boney projections which may introduce observer error if not viewed in the same plane

upon each collection bout. Care was taken to place the mandible within the same viewing planes upon further landmark collection.

A PCA was performed on a subset of the adult WT mice using the Procrustes coordinate error study data set. The PCA plot, produced in MorphoJ software (Klingenberg, 2011), revealed that each trial clustered closely together and separate trials could be easily delineated from each other (Figure 2.7). Principal component scores were derived from the PCA and utilized as variables in a Multivariate Analysis of Variance (MANOVA) to estimate measurement repeatability, the goal of which is to determine the proportion of variance due to inter-individual differences. For purposes of repeatability, the desired outcome is significantly greater variance among-individuals. The resulting MANOVA, similar to the PCA, did demonstrate very significant among individual difference (Wilk's Lambda:  $p < 0.0001$ ) suggesting a high degree of repeatability.

#### 2.4.2 Functional Sample: Landmark Measurement Error Analysis

Precision analyses were conducted on each primate species used for this study, *C. apella*, *S. sciureus*, *P. pithecia* and *C. torquatus*. Five specimens were chosen within each group at random. Three separate landmarking trials were completed on each of the five specimens chosen within all four groups. Raw landmark coordinates were used, therefore excluding sliding semilandmarks. The same method used to calculate landmark deviation described in the mouse sample above was used here. Deviations among trial landmarks greater than 1.0 mm were considered to be error prone. This measure was chosen to represent less than 3% of mandibular length in the smallest primate sample used here, *S. sciureus*.

The lowest amount of error was found in the *Saimiri* mandibles (6% of deviation above 1.0 mm) while *Cebus* had the largest amount of error among trials (33% of deviation above 1.0 mm). *Pithecia* and *Callicebus* more closely resembled each other, each possessing around 20% of deviations above 1.0 mm. The landmarks most commonly prone to error across primates included ABJ and PCD. As in the mouse precision analysis, landmark collection may be predisposed to error when obtaining the posterior most aspect of the condyle (PCD; maximum deviation = 1.66 mm). Again, collection of this landmark may depend on the orientation of the mandible between collection bouts. In contrast, the inferior junction of the gonial angle and the horizontal ramus (ABJ; maximum deviation = 1.5 mm) is not always a well-defined anatomical landmark. In the future, this landmark may need to be averaged over multiple trials in order to reduce variation.

Similar to the repeatability error analysis described above, three separate landmark trials were replicated on three randomly chosen *P. pithecia* over non-consecutive days. For each landmark trial, the primate mandible surfaces were re-merged. Measurement error is therefore accounting for variance generated by both merging episodes as well as landmark repeatability. A PCA was performed on the resulting landmark configurations, visually validating the separation of trials in shape space (Figure 2.7). These differences were, again, statistically corroborated through a MANOVA using principal component scores as the dependent variables (Wilk's Lambda:  $p < 0.001$ ) suggesting a high degree of repeatability.

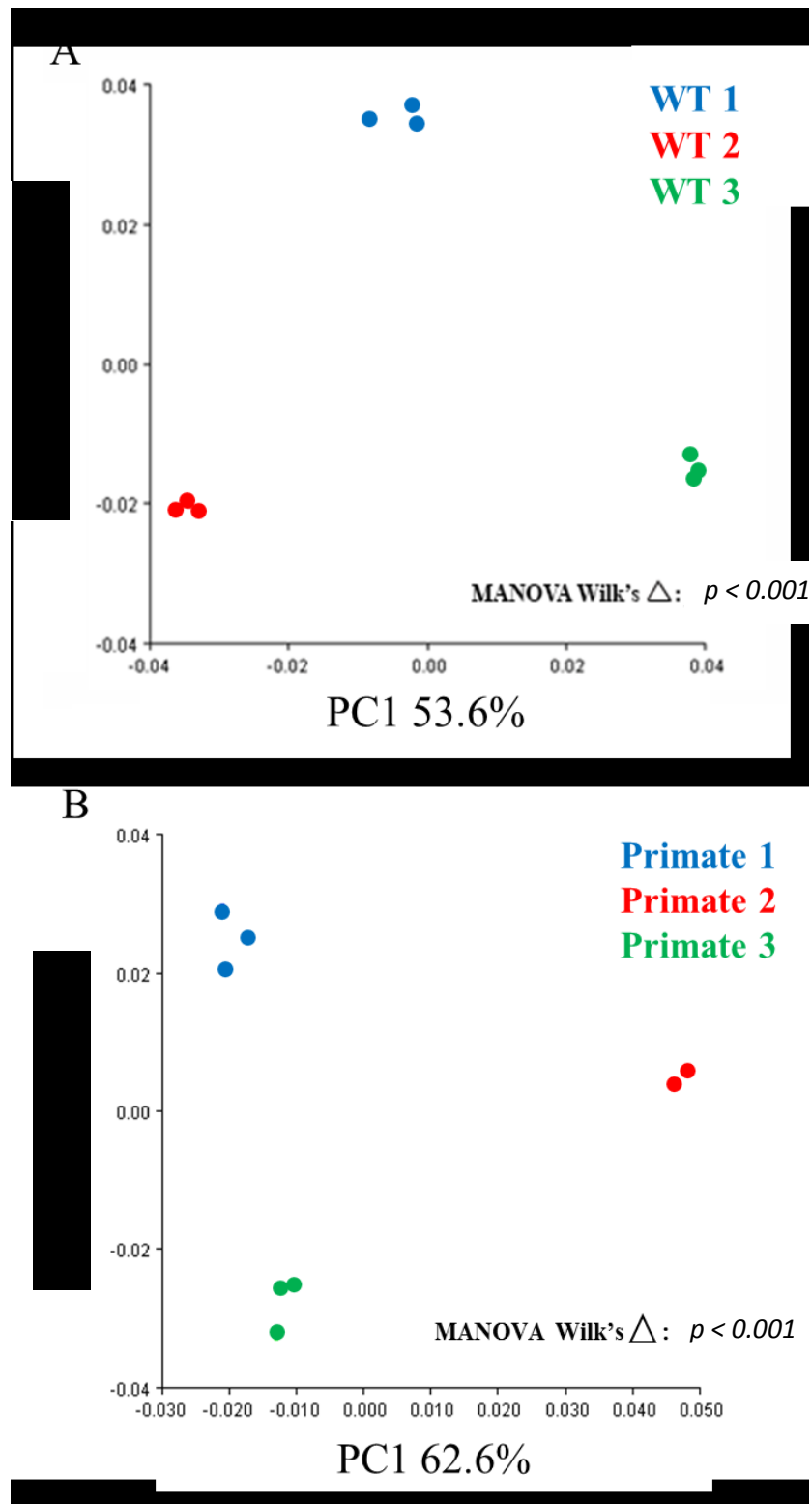
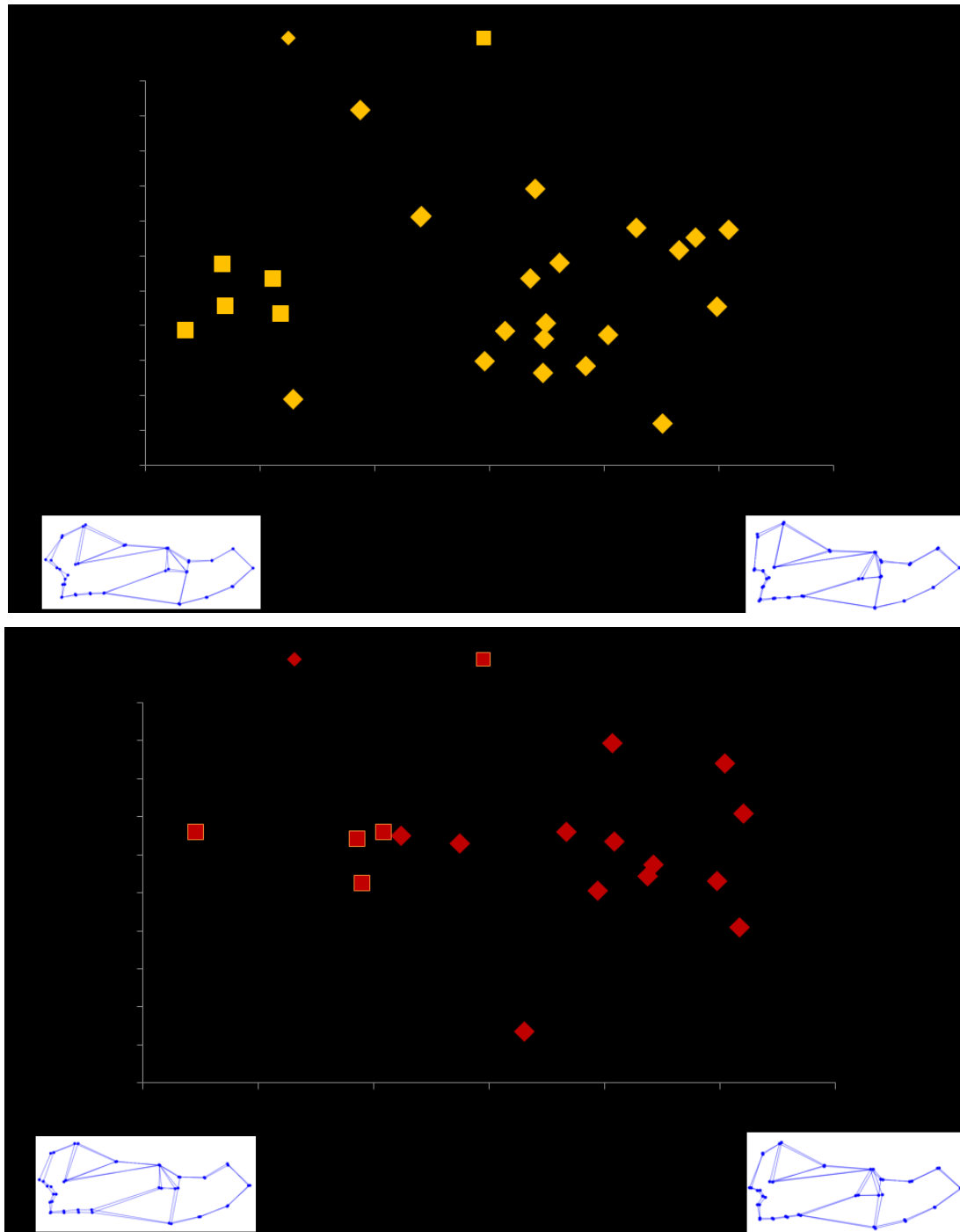


Figure 2.7 Principal Component Analysis scatterplots demonstrating the separation of specimens for A) developmental model measurement error trials and B) functional model measurement error trials. Wilk's Lambda from a MANOVA of principal component scores shows that variability is greater among groups than within groups.

### 2.4.3 Colony-based Shape Differences

The mice used in this study were bred and maintained in two separate facilities from separate colonies at Johns Hopkins University School of Medicine (JHU) and Washington University School of Medicine (WashU). Comparison of the size and shape of mice from each colony was essential to ensure that the amount of variance calculated within each age group and genotype was not unduly influenced by differences among colonies. Principal component analyses did in fact demonstrate a separation in overall shape between mice of different colony origin. This distinction was evident within each age group and genotype (Figure 2.8 – 2.10).

PCA scatterplots of E17.5 by Genotype and Colony



**Figure 2.8** Principal Component Analysis scatterplot of colony differences for E17.5 mice. A) E17.5 WT mouse mandibles and B) E17.5 HT mouse mandibles. This plot demonstrates the differences that can be seen in mandibular shape based on which colony the mice were reared in. The square symbol represents mice housed and bred in the Washington University facilities and the diamond represents mice housed and bred in the Johns Hopkins Facilities. Wireframes represent those shapes at the lowest and highest loading specimens on PC1.



# PCA scatterplots of P14 by Genotype and Colony

A.

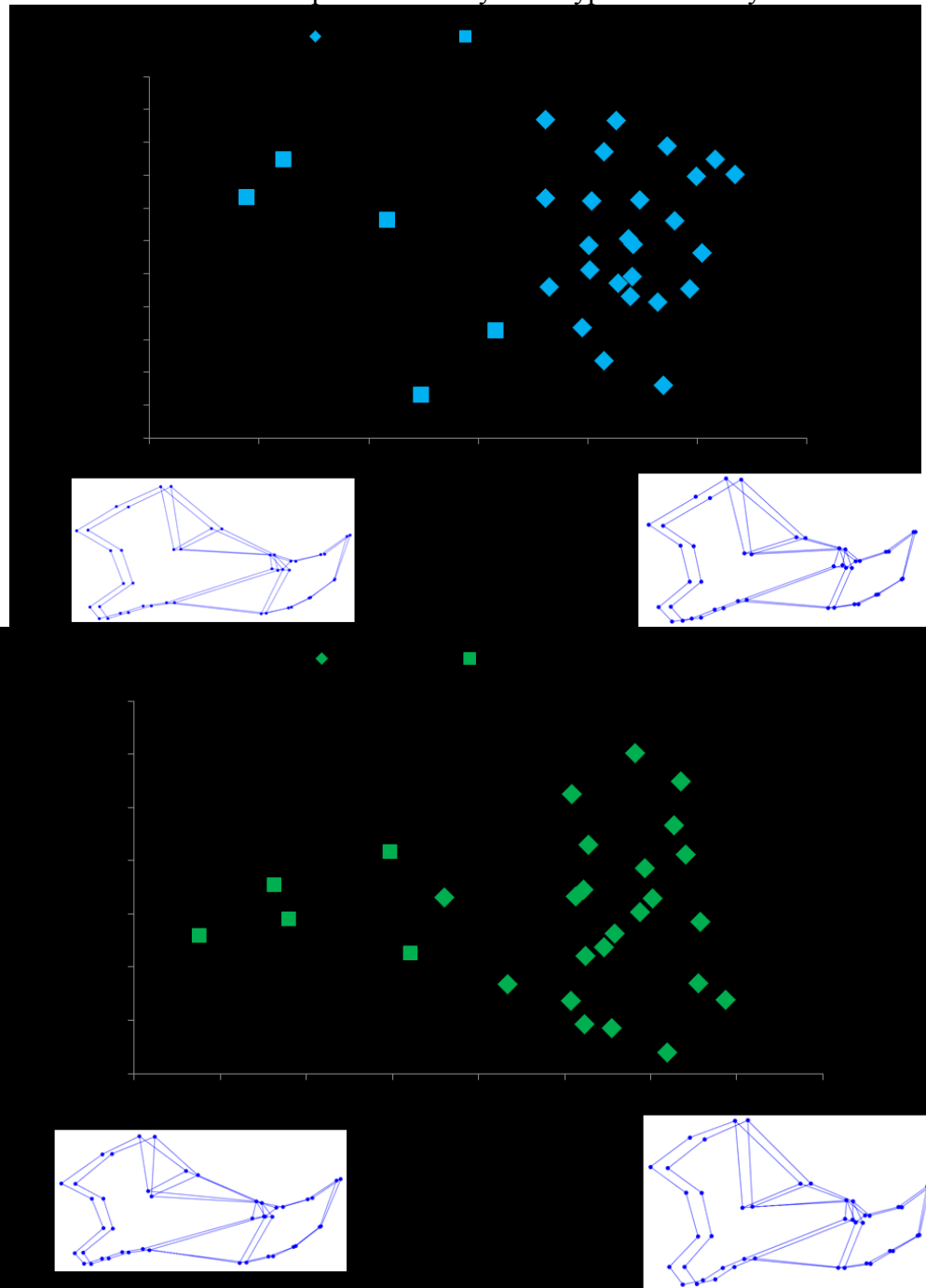


**Figure 2.9** Pricipal Component Analysis scatterplot of colony differenes for P14 mice A) P14 WT mouse mandibles and B) P14 HT mouse mandibles. This plot demonstrates the differences that can be seen in mandibular shape based on which colony the mice were reared in. The square symbol represents mice housed and bred in the Washington University facilites and the diamond represents mice housed and bred in the Johns Hopkins Facilities. Wireframes represent those shapes at the lowest and highest loading specimens on PC1.

# PCA scatterplots of P42 by Genotype and Colony

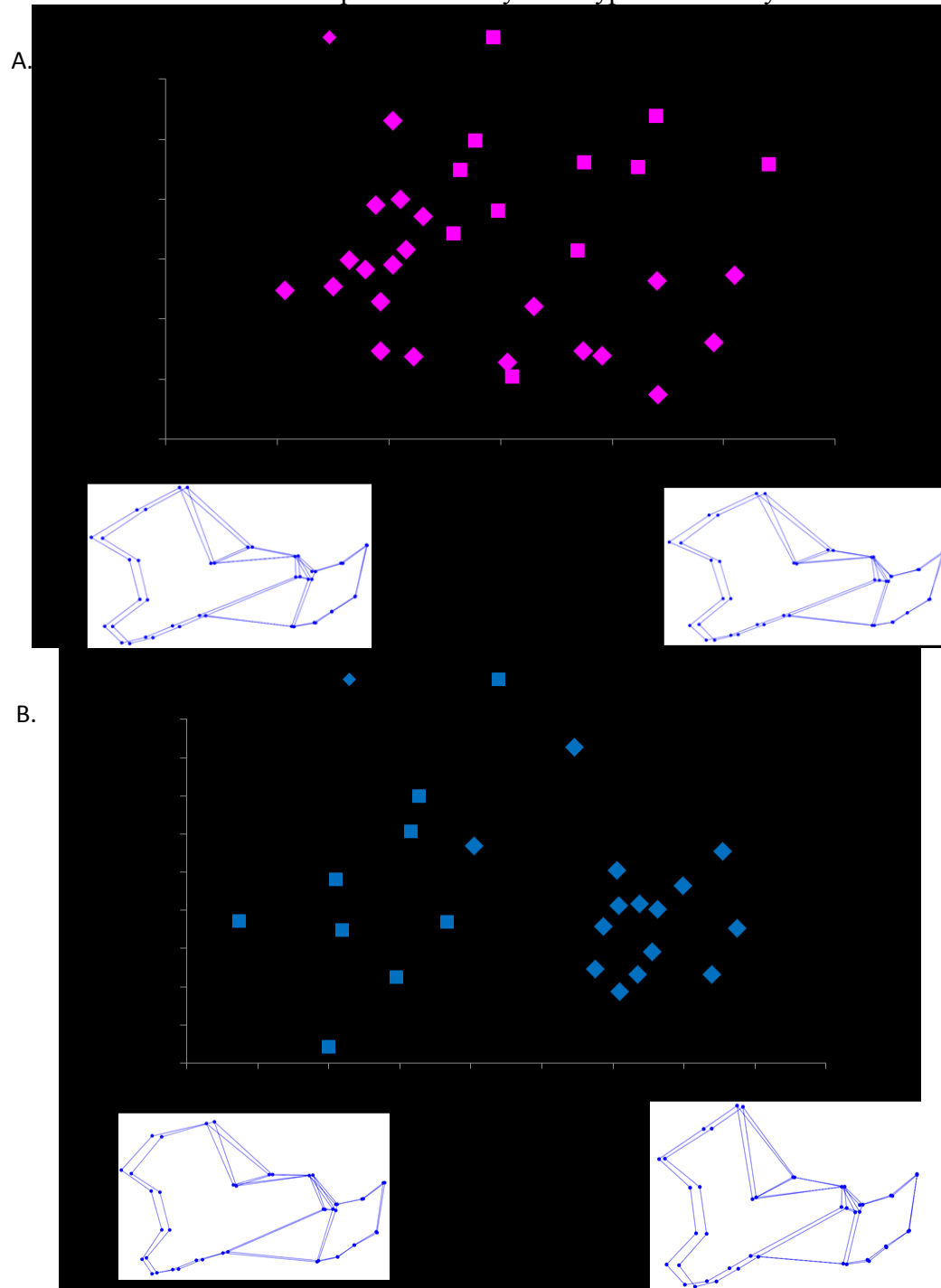


**Figure 2.10** Pricipal Component Analysis scatterplot of colony differenes for P42 mice. A) P42 WT mouse mandibles and B) P42 HT mouse mandibles. This plot demonstrates the differences that can be seen in mandibular shape based on which colony the mice were reared in. The square symbol represents mice housed and bred in the Washington University facilites and the diamond represents mice housed and bred in the Johns Hopkins Facilities. Wireframes represent those shapes at the lowest and highest loading specimens on PC1.

Colony-based shape differences were largely consistent across each genotype, meaning that aspects of morphology that separated the WT mouse colonies were similar to those found in the HT colony. The largest shape differences seen among the embryonic mice seemed to be in the orientation of the condyle, curvature of the angle and the ratio between length of the body and the incisor region. In general, the WashU specimens tended to display an elongate mandibular body with a relatively shorter incisor and a more horizontally oriented condyle. In contrast, the JHU mice have a vertically oriented condyle, a deeper curve of the angle and a longer incisor (Figure 2.8). Among the peri-weaning mice, greater morphological disparity is present in the HT group than WT, however, the pattern is still the same. JHU mice possess a taller ramal region due to heightened coronoid and condylar location. In addition the angle also has a greater superior-inferior height and is inflected more inferiorly creating a greater degree of ventral flexion at the junction between the angle and mandibular body. JHU specimens also display a more antero-inferior position of the coronoid and posteriorly molar region, effectively elongating the coronoid but shortening the molar row when compared to the WashU specimens. This also leads to an antero-posterior elongation of the WashU mandibular body, similar to that seen in the embryonic mice. Lastly the JHU mice exhibit an incisor with an increased superior flexion (Figure 2.9).

In the adult mice, the HT sample continues to display the greater amount of shape disparity while the WT are not as clearly demarcated. In addition, when shape changes were compared, WT colonies did not display obvious differences in morphology. HT samples on the other hand differ in patterns similar to those described above. Again we see that the mandible in mice raised in the JHU colony have a taller angle, longer and

more inferiorly inflected angle paired with increased height of the coronoid and condyle. WashU mice continue to have an antero-posteriorly elongate mandibular body relative to the incisor (Figure 2.10).

It is uncertain what could be causing this difference between the two colonies and why that difference would be present at the earliest stages of ontogeny in both genotypes but then becomes less obvious in adult WT colony comparisons. Diets were the same between either colony, each receiving pellet food. Maternal effect could be initiating the early morphological differences between the two colonies. It should also be noted that the WT mice come from a CD1 background which is outbred so that there is inherently more genetic diversity in the sample. General patterns of somatic growth and bone remodeling could then “correct” these differences, resulting in similar mandibular shape, at least within the WT mice. HT mice on the other hand seem to either remain distinct or possibly continually diverge to a greater degree. It is difficult to discern between the two options without a more robust ontogenetic sample. Due to these differences, however, all analyses were conducted using two datasets. The first dataset is comprised of the whole sample, including both colonies and is the basis for the majority of the results and discussion here. The second dataset consists of only the mice bred and reared at the Johns Hopkins facilities, as this is the larger sample. Differences in results from both datasets are reported below when they occurred.

## 2.5 Statistical Analyses

The research design of this dissertation is framed around the quantification of covariance structure within mandibles and how covariance may differ between the mandibles of different groups. The pattern (the way in which traits covary) and magnitude (the strength of covariance among traits) are tested here to investigate and compare the structure of covariance. Four main analyses were conducted here: 1) comparison of covariance matrices (pattern); 2) comparison of two-block PLS analyses and scatterplots (pattern); 3) comparison of scaled variance of the eigenvector (magnitude), and; 4) comparison of the correlation coefficient of variance, or  $R_v$  coefficients (magnitude). These analyses and their implications are discussed in more detail below.

Covariance matrices, the main data format for analyses conducted throughout this study, were generated from the Procrustes transformed data using MorphoJ software. Overall shape comparisons between mice and primates, separately, were conducted using PCA scatterplot and wireframe deformations. PCA scatterplots were used to visualize and compare the range of shape-space occupied by different mouse, as well as primate groups. Wireframe deformations were utilized to localize and compare mandibular shape differences that occur among the groups.

Effects of size on shape (allometric effects) can influence covariance in the mandible because somatic growth can be an overall integrating factors. This is especially true during ontogeny when allometry may amplify measures of integration. Because of the different composition of samples used here, two separate analyses were used to test for an allometric effect of size. Allometric analyses for the mouse sample were conducted

using a multivariate regression of shape variables on a single factor, following recommendations from Mitteroecker and Gunz (2009). Procrustes coordinates from Generalized Procrustes fit of the mouse sample were treated as dependent variables and regressed against the natural logarithm of centroid size (ln CS). By transforming CS to its natural logarithm, the influence of age-dependent size is reduced, which is considered the “optimal measure of allometry” in ontogenetic data (Mitteroecker et al., 2004; Mitteroecker and Gunz, 2009).

Multiple factors, however, were of interest for the primate sample. Such factors include, genus, sex and size of the mandible (ln CS). Therefore another approach was taken to consider each of the variables simultaneously. A Multivariate Analysis of Covariance of all taxa was performed controlling for sex and ln CS and using principal component (PC) scores as dependent shape variables. The first 35 PC scores were used as they described 99% of mandibular variation in the primate sample. Using PC scores as shape variables, rather than using Procrustes coordinates, was beneficial because it reduces large sets of variables while still representing a large amount of shape variance (Cobb and O’Higgins, 2007; Pierce et al., 2008). Procrustes coordinates, on the other hand, are appropriate shape variables when conducting a multivariate regression because multivariate regressions are unaffected by the number of dependent shape variables (Mitteroecker and Gunz, 2009). As a rule, if allometric influences were found to be significant, supplementary analyses were conducted using residual scores as scaled data in order to minimize allometric effects. The one exception to this were the analyses conducted on the wild-type ontogenetic sample for the hypotheses **H<sub>DVA-B</sub>**. Because increase in size is such an integral aspect of developmental changes it was deemed too

important to remove from the data for this project. Future analyses, however, will explore the influence of allometry on mandibular ontogenetic covariance.

Many of the following statistical tests were completed using multiple, separate landmark configurations, including comparisons of the scaled variance of the eigenvalue and comparison of  $R_V$  coefficients. Competing hypotheses of how covariance is arranged in the mandible between two separate sets of hypothetical modules, “Bi-modular” model vs. “Mesenchymal” model, were discussed in the Introduction. If these distinctions exist, they may persist throughout ontogeny or, in accordance with the Palimpsest Hypothesis, each may be detectable only at very specific points in development. Therefore, when relevant, both models were used to test hypotheses, along with the total landmark configurations. This adds a further dimension to my dissertation as it allows me to approach my hypotheses on several levels and to test competing hypotheses in the literature.

Definitions from the aforementioned literature were used to construct each modular model, as represented on mice in Figure 2.11. The “Bi-modular” model consists of two modules representing first, the area of insertions for muscles of mastication (ascending ramus), and second, the area of dental loading (alveolar region) (Atchley et al., 1985a; Leamy, 1994; Mezey et al., 2000; Ehrich et al., 2003; Klingenberg et al., 2003, 2004). The “Mesenchymal” model consists of five modules representing embryonic mesenchymal condensations, the three posterior processes (angular process, condylar process and coronoid process) and the alveolar condensation divided into a molar and incisor region (Monteiro et al., 2005; Zelditch et al., 2008; Willmore et al.,

2009; Monteiro and Nogueira, 2010). To ensure modular morphology is maintained, a minimum of three landmarks were required for each modular configuration (Figure 2.11).

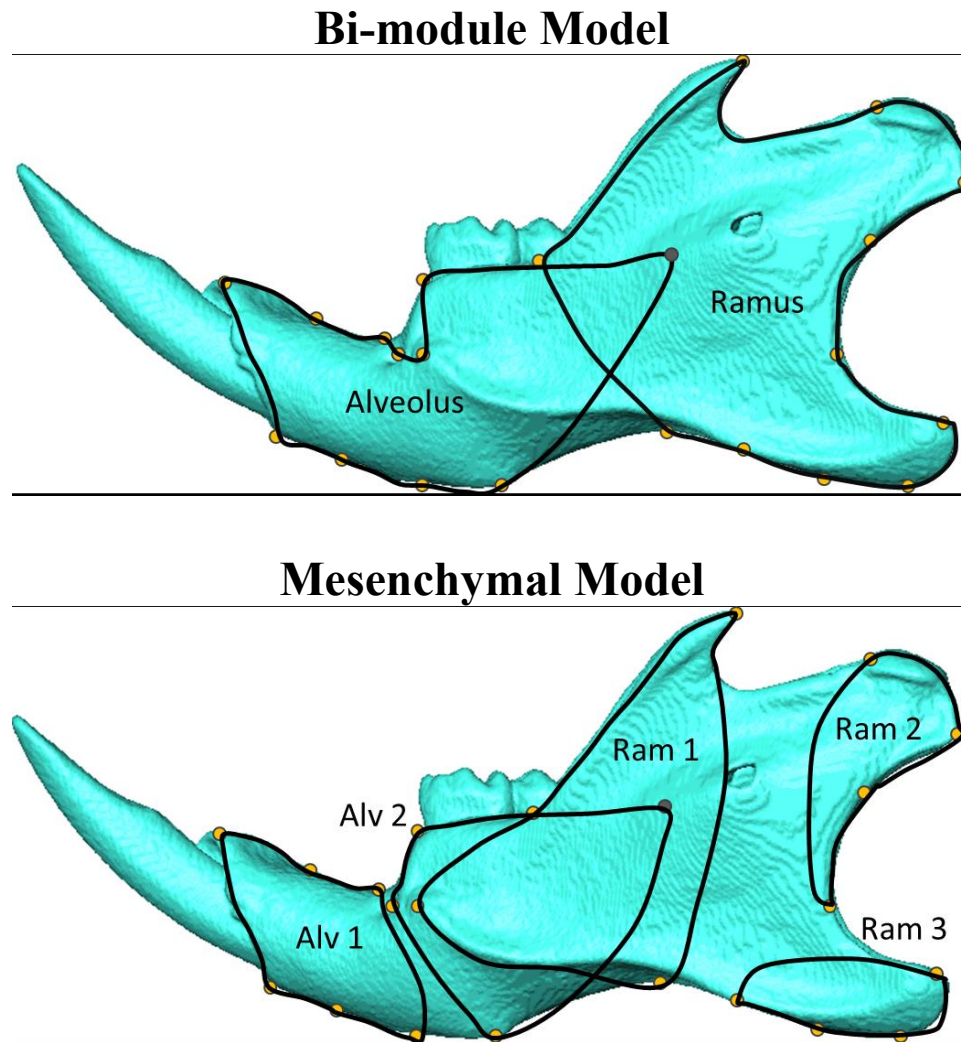


Figure 2.11 Two conventional modular structures demonstrated on adult mouse mandibles. Modular structure was constructed based on published models. A) Bi-module model which separates the alveolus and the ramus as two functionally separate modules; B) Mesenchymal module model consisting of Alveolus 1 (incisal alveolus), Alveolus 2 (molar alveolus), Ramus 1 (coronoid/ masseteric insertion), Ramus 2 (condyle), Ramus 3 (angle). The Mesenchymal model is based on the mesenchymal organization of the developing mandible, particularly the three developing processes.



As noted before, Procrustes superimposition may introduce biologically irrelevant variance to the landmarks under study here. Statistical analyses of covariance become inflated because variance is partitioned equally across all landmarks. For example, consider the shape of the coronoid, its height, width and depth. In this scenario the landmark describing height is highly variable. In contrast, those landmarks describing width and depth are more consistent and tend to covary when shape change occurs. Logically, landmarks associated with height of the mandible will be less correlated with landmarks associated with width and depth, of the coronoid. However, because the process of Procrustes superimposition is to minimize the sum of the squared distances between landmarks, the variance of each landmark describing coronoid shape is distributed amongst them thus inflating the correlation one might expect between height, width and depth.

Complications may also arise from using Procrustes analysis as a basis for analyzing covariance with different landmark configurations. The process of centering (or translating) coordinates to a common coordinate space during superimposition is arbitrary (Lele and Richtsmeier, 2001; Richtsmeier *et al.*, 2005). Therefore, when different landmark configurations undergo centering step different mean shape will be estimated and this in turn informs the. In result, the true variance/covariance structure is difficult to identify. Despite complications in the Procrustes model, it remains the most prevalent method for analyzing patterns of covariance and can still provide interesting and valuable information. Use of Procrustes analyses also allows for comparison with other similar works. Future analyses however, will explore relationships of covariance with EDMA methods.

### 2.5.1 Covariance Matrix Comparison

Two separate analyses were applied to test hypotheses surrounding patterns of covariance in the mandible: 1) Variance/Covariance matrices (also referred to as covariance matrix or V/CV for simplicity); and 2) Two-block PLS analyses (2B PLS). Covariance matrices were compared across samples, using multiple pair-wise comparisons, to test whether patterns of integration were similar among the groups of interest here. Matrices were computed from shape data in the form of Procrustes coordinates derived from the MorphoJ program. Covariance matrices are symmetrical matrices that retain information about multivariate data. They contain both the variance seen in each variable (along the diagonal) and the covariance between each pair of variables (off diagonal). Comparing covariance matrices for two separate groups with the same traits will determine if those traits covary in the same way in each group. For example, if the condylar landmarks (ACD and PCD) and the sliding semilandmarks defining the gonial angle covary in the same manner between samples then it may be determined that they share a similar pattern of covariance. Thus by using Procrustes coordinates as the variables, patterns of shape covariance can be determined across the mandible and compared between groups.

Matrix comparisons were conducted using the Random Skewers method which takes the covariance matrices in question and applies random vectors to each and compares the responses. The expectation is that if covariance matrices are similar they will respond similarly to the same vector application (Cheverud, 1996b; Marroig and Cheverud, 2001; Cheverud and Marroig, 2007; Goswami and Polly, 2010). Random vectors (1000x) were applied to the two matrices being compared, and correlations of the

response were computed for each vector. The average of those correlations was taken as the observed correlation ( $R_{obs}$ ). Permutation tests were calculated to determine statistical significance. Covariance comparisons are tested against the null hypothesis of no similarity (Marroig and Cheverud, 2001). Additionally, scaling patterns are unique to each row and associated column of a covariance matrix so a generalized randomization procedure would be inappropriate. The Monte Carlo, a permutation method, was chosen for resampling because it retains the structure of the matrix and it has been reliably used in the past (Cheverud, 1996b; Marroig and Cheverud, 2001; Cheverud and Marroig, 2007; Porto *et al.*, 2009).

Repeatability correlations ( $t$ ) of each covariance matrix were calculated before any comparisons were made. Calculating the repeatability of a covariance matrix estimates whether the sample used is a reliable representation of the population because it provides the proportion of variance within the sample due to error in individual matrix elements. Covariance matrices are self-correlated in order to calculate repeatability values. Random skewers and the Monte Carlo method were used for the repeatability correlations, as well.

The observed correlations between two V/CV matrices for each groups can also be adjusted ( $R_{adj}$ ) for small sample size using the repeatability measure ( $R_{obs}$ ) with the following formula:

$$R_{adj} = R_{obs}/R_{max}; R_{max} = (t_a t_b)^{1/2}$$

Where  $t_a$  and  $t_b$  are two separate matrices and  $R_{max}$  is the maximum average correlation that can be expect between those matrices (Marroig and Cheverud, 2001). The observed matrix correlations,  $R_{obs}$ , are then corrected for the maximum matrix correlation  $R_{max}$

resulting in the adjusted correlation,  $R_{adj}$ . All analyses were completed using the statistical software R (<http://www.r-project.org>).

Covariance matrix comparisons were designed as follows in order to test specific hypotheses about the patterns of covariance among the groups used here:

**H<sub>DVA</sub>**: In order to test whether patterns of integration changed over ontogeny pair-wise comparisons of covariance matrices were made between all WT age groups.

WT E17.5 v P14

WT E17.5 v P42

WT P14 v P42

**H<sub>MTA</sub>**: In order to test whether patterns of integration were different between genotypes, pair-wise comparisons of covariance matrices were made between HT and WT mice within each age cohort.

E 17.5: WT v HT

P 14: WT v HT

P 42 WT v HT

**H<sub>FxA</sub>**: In order to test if patterns of integration altered due to differing dietary demands pair-wise comparisons of covariance matrices were made between primate species.

Cebids: *Cebus* v *Saimiri*

Pitheciids: *Pithecia* v *Callicebus*

### *Two-Block Partial Least Squares Analysis*

Two-block Partial Least Squares analyses (2-B PLS) were also applied to the data in order to ascertain patterns of covariance in the mandible amid the samples. Unlike the comparison of covariance matrices which looked at mandibular shape data as a whole, 2-B PLS affords the ability to look at patterns of covariance between two sub-sets of shape data (or modules) within the mandible. 2-B PLS are commonly implemented to study evolutionary or developmental integration between component parts (Klingenberg et al., 2001, 2003; Bookstein et al., 2003; Bastir and Rosas, 2005; Mitteroecker and Bookstein 2008; Makedonska et al., 2012; Martínez-Abadías et al., 2011; Singh et al., 2012).

Similar to PCA, a 2-B PLS analysis uses a Singular Value Decomposition (SVD) to calculate the singular value (eigenvalue) and a pair of singular axes (eigenvectors) of a covariance matrix between the two units under examination. The first set of singular axes corresponds to the first singular value. Singular axes represent the maximum covariance between the units and are ordered from the largest amount of covariance to the least (Rohlf and Corti, 2000; Goswami and Polly, 2010; Zelditch et al., 2012; Klingenberg and Marugán-Lobón, 2013). In essence, PLS analyses consider the shared covariance between two blocks of shape data and extract the multivariate axes that represent the greatest amount of covariance between them. Shape deformation can also be computed to depict how the correlated changes in shape between the two blocks vary along each singular axis (or PLS axis).

One of the greatest benefits of 2B-PLS analysis is that it relays similarity of the integration among different groups. Here it was used to assess how the Bi-modular model (alveolus and ramus) of the mandible was integrated across samples. In order to control

for mean shape due to the multiple samples in each test, pooled within-group covariance matrices were utilized to produce group-centered scores (Mitteroecker and Bookstein, 2008; Mitteroecker and Gunz, 2009; Singh et al., 2012) . Furthermore, 2B-PLS analyses were constructed by performing simultaneous Procrustes fit for all landmarks before partitioning them into separate alveolar and ramal units. Using the entire configuration retains information about the coordinated variation of the whole structure as well as between the two units (Zelditch et al., 2012; Klingenberg and Marugán-Lobón, 2013). All PLS analyses performed for these analyses were completed in MorphoJ software (Klingenberg, 2011).

Patterns of covariation between the alveolus and ramus were visualized in two ways. First, scatterplots of the PLS axes of the alveolus and ramus were generated using the group-centered scores. Distribution of each group along the axes demonstrates the amount of overlap in patterns of integration. Separation of any particular group in the scatterplot suggests that they do not share the same trajectory of integration as the other(s). Second, wireframe deformations were computed to demonstrate the coordinated changes in shape between the alveolus and ramus. 2B-PLS analyses were designed as follows in order to test specific hypotheses:

**H<sub>DVA</sub>**: All age groups within the WT were assembled into one 2B-PLS (pooled within-age) to compare patterns of integration between the alveolus and ramus as the mandible develops during ontogeny.

**H<sub>MTA</sub>**: WT and HT mice were grouped together within each age-cohort (pooled within genotype), respectively. Age cohorts underwent 2B-PLS analyses in order

to see if patterns of integration between the two units were similar between genotypes at any given developmental stage.

**H<sub>FXN</sub>**: Primate PLS analyses grouped cebids and pitheciids (pooled within-genus), respectively, in order to assess patterns of integration within closely related species with differing mechanical demands in the mandible.

### 2.5.2 Scaled Variance of the Eigenvalue

Magnitude of covariance among mandibular traits is calculated as the Scaled Variance of the Eigenvalues (SVE). Eigenvalues define the amount of variance along an eigenvector (i.e., principal component axis) within a covariance matrix. Thus if the total variance is described by the first few eigenvalues, then the variance of eigenvalue is large, indicating that the variance of traits is coordinated and restricted to only a few eigenvectors. This would suggest that the traits are highly integrated and thus the magnitude of covariance is high. Conversely, trait variance that is dispersed over several eigenvalues and eigenvectors describes uncoordinated variance and is thus considered sparsely integrated, or possessing a low magnitude of covariance (Wagner, 1990; Hallgrímsson *et al.*, 2009).

Variance of the eigenvalues was determined for this project using pooled within-group covariance matrices constructed from Procrustes coordinates. Following Hallgrímsson *et al.*, 2009, variance of the eigenvalue was then scaled by the mean eigenvalue in order to control for undue variance resulting in the SVE value. Magnitude of integration was then contrasted between groups using pair-wise comparisons tests. In order to determine significant differences, bootstrapping methods were used to resample

the data (1000x) within-group. The distribution of resampled SVE values was compared to determine standard deviation and significance ( $\alpha = 0.05$ ). All analyses were completed using the statistical software R (<http://www.r-project.org>).

Comparisons were completed using SVE values calculated for all landmarks (global), for each alveolar and ramal module (Bi-module model), and for each Mesenchymal module. Because multiple statistics (8 different landmark configurations) were being completed on a single dataset, p-values underwent Bonferroni correction ( $\alpha = 0.006$ ). Bonferroni correction was applied by taking the decided upon  $\alpha$  value ( $p=0.05$ ) and dividing it by the number of related observations in a test. In order to test specific hypotheses about the magnitude of integration in the samples used here, pair- wise comparisons were constructed as follows:

**H<sub>DVB</sub>**: In order to test whether magnitude of covariance changed over ontogeny pair-wise comparisons of SVE were made between all WT ages.

WT E17.5 v P14

WT E17.5 v P42

WT P14 v P42

**H<sub>MTB</sub>**: In order to test whether magnitudes of covariance were different between genotypes, pair-wise comparisons of covariance matrices were made between HT and WT mice within each age-cohort.

E 17.5: WT v HT

P 14: WT v HT

P 42 WT v HT



**H<sub>FXB</sub>:** In order to test if magnitude of covariance altered due to differing dietary demands, pair-wise comparisons of covariance matrices were made between primate species.

Cebids: *Cebus* v *Saimiri*

Pitheciids: *Pithecia* v *Callicebus*

### 2.5.3. **R<sub>v</sub>** coefficient

Magnitude of covariance was also explored within the Bi-modular and Mesenchymal models. Klingenberg (2009) introduced the  $R_v$  coefficient as a method to test the strength of integration within proposed modules while taking the covariance of the whole structure into account.  $R_v$  coefficients are calculated by taking the sum of the squared covariances between proposed modules and then scaling it by the sum of the total variance within each module. The resulting value ranges between 0 – 1, 0 representing an absence of covariance and 1 representing complete covariance. In addition, the null hypothesis of independence between modules can be tested by generating modules with randomly chosen landmarks and comparing the amount of covariance with the original dataset. Permutations (1000x) of randomly assigned modules are created and the  $R_v$  coefficients for each iteration are calculated. The proportion of  $R_v$  coefficients from the random alternative model are then compared to the original hypothetical model. If the hypothetical model can truly be detected within the dataset than its  $R_v$  coefficient will be smaller than the majority of alternative permutations (Drake and Klingenberg, 2010).

The analyses conducted here utilized the  $R_v$  coefficient for two purposes. First,  $R_v$  coefficients were used to determine the magnitude of covariation that exists within each of the different modular models. Secondly, permutation tests were applied in order to test the significance of each module at different ages in mice, and in primates with differing diets. Analyses of  $R_v$  coefficients were designed as follows in order to test specific hypotheses:

**H<sub>DVB</sub>:** In order to test whether the modular signal was greater than overall integration in the mandible at each ontogenetic stage,  $R_v$  coefficients were calculated for the Bi-modular and Mesenchymal models at each WT age range.

**H<sub>FXB</sub>:**  $R_v$  coefficients were computed within each primate species in order to test the strength of both modular models in adult primates and whether these structures differed in conjunction with diet.



## Chapter 3: Results and Discussion – Developmental Hypotheses

### 3.1. Results

The first set of analyses test the null hypothesis that patterns of covariance are dissimilar between age groups ( $H_{DVA}$ ) and the second set predicted that the magnitude of covariance would increase as the mice aged ( $H_{DVB}$ ). Further sub-hypotheses suggested that changes, or lack-thereof, in the patterns and magnitudes of covariance are largely influenced by the timing of other developmental factors such as the growth of dentition or the introduction of an adult diet. If mandibular structure of covariance reflects adult patterns and magnitudes before reaching that stage it may suggest an intrinsic factor preparing the mandible for an adult diet ( $H_{DVA1}$  and  $H_{DVB1}$ ). On the other hand, if the structure of covariance in adults is found only in adults it would suggest that functional influence on covariance does not appear until those mechanical loads are experienced ( $H_{DVA2}$  and  $H_{DVB2}$ ).

#### 3.1.1. Ontogenetic Shape and Size Variation

The mouse mandible changes significantly from the prenatal stage to adulthood. Figure 3.1 depicts the position of each WT age group in shape space, including the wireframe deformations representing the average shape within age groups. The majority of shape variation occurs along PC1 (85.48%) the pattern of which is described below. All age groups are clearly separated from each other, with the embryonic mice loading much higher on PC1 than the peri-weaning and adult mice. On a wide scale, shape change over ontogeny results in a dramatic increase in height of the ramus, length of the angle and the relative antero-posterior position of the molar and incisor alveolar regions.

A large difference is discernable as the mandible grows from the embryonic to the peri-weaning mouse. Within the alveolar portion of the mandible, embryonic mice display a posteriorly positioned molar row paired with an elongate incisal alveolus. For comparison, in the peri-weaning mice the posterior and anterior molar rows are displaced anteriorly along with the mandibular foramen and anterior attachment of the masseter. At the same time, the portion of the alveolus that houses the incisor shows superior inflection. The net effect of these shape changes is an anteriorly displaced alveolus while maintaining the ratio between the molar and incisal region is maintained. This suggests a disproportionate amount of growth in the posterior ramus. In addition, the incisor has a more acute superior curve. Supero-inferior depth of the alveolus between the two age groups seems to be relatively consistent within the entire alveolar region. The curvature of the incisor region is most likely following the trajectory of the incisor as it emerges from the alveolus.

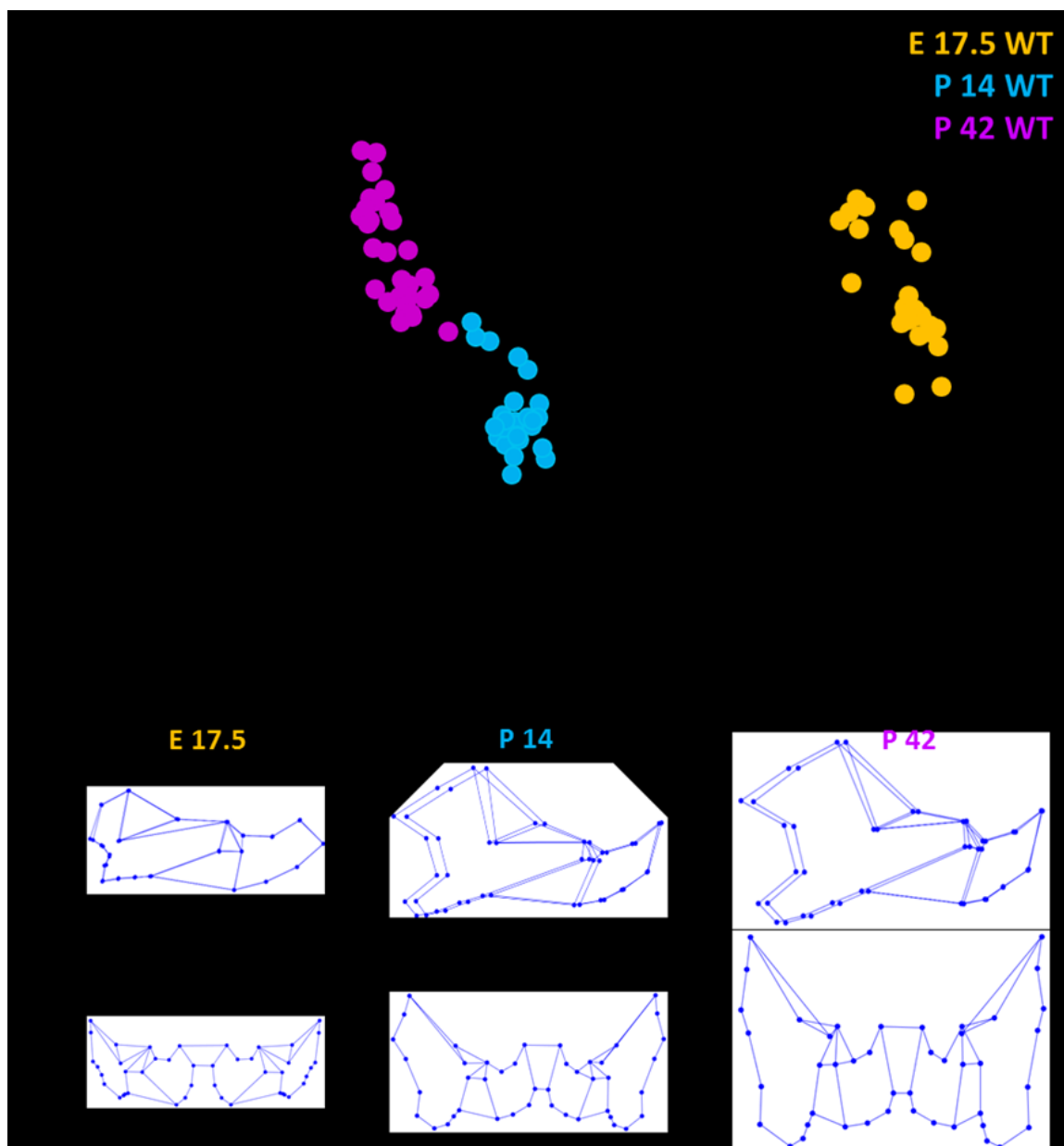


**Figure 3.1** Principal Component Analysis scatterplot of WT mouse mandibles of each age range. Wireframes depicting the average shape of the mandible in each age range are located below the scatterplot. Shape change can be seen from lateral view (A – P) in order to visualize antero-posterior shape change and the frontal view (M – L) in order to visualize medio-lateral shape change.

Ramal height relative to the molar row is greatly increased in the peri-weaning mice as compared to the embryonic specimens. This is due to superior displacement of the tip of coronoid and height of the anterior and posterior condylar points. In fact, the posterior aspect of the condyle reorients superiorly relative to the anterior edge of the condyle, effectively rotating the position of the condyle from vertical to more horizontal. As ramal height is increasing, the body of the coronoid is translating anteriorly along with the molar row. However, the degree of translation is not proportional, being greater in the molar row than in the coronoid, culminating in a narrower coronoid process relative to the rest of the ramal region.

Length of the angle also increases drastically between the embryonic and peri-weaning mice, as the angle grows posteriorly. Increase in angular length is matched by an inferior flexion, creating a marked turn between the angle and the mandibular corpus. The combined lengthening of the angle along with the heightening of the ramus coincides with a deeper curve along the posterior border of the ramus. From the frontal view, the angle appears more flared medially. Interestingly, this reflects an overall trend of the peri-weaning mandible to appear relatively narrower than the embryonic mandible. This is true from the incisor all the way posteriorly to the ramus; in fact, medio-lateral narrowing of the bi-ramal width is particularly pronounced.

The pattern of growth is maintained when comparing mandibular shape of the peri-weaning mice with that of the adults. Elongation of the mandible is occurring by an anterior shift in the molars. This is paired with a posterior translation of the angle, condyle and the posterior border of the ramus. The ramus is further lengthened antero-posteriorly due to the anterior aspect of the coronoid tracking with the molar row. The

ramus also continues to increase in height by superior movement of the superior-most point of the coronoid and the condyle. In addition, the angle continues to increase its inferior flexion as it elongates posteriorly. Lastly, the adult WT mandible is narrower medio-laterally relative to the peri-weaning WT mandible, continuing the contraction observed between the embryonic and peri-weaning mandibles. As the mandible grows in absolute, size medio-lateral width will increase from embryonic to adult size. The apparent narrowing within the posterior aspect of the mandible in Procrustes shape space suggests that, in comparison to embryonic shape, other aspects of the maturing mandible outpace increasing bi-gonial and bi-condylar width. It is possible that width is closer to adult values earlier in development and that lengthening of the mandible has a longer trajectory during post-natal growth.

As growth in size is an inherent aspect of ontogeny, WT mandibles were expected to increase in size sequentially from each age group. A one-way ANOVA was conducted to determine if size did indeed change among age groups (Figure 3.2). Results show that as the WT mandible grows it does increase in size and that overall size is significantly ( $p < 0.0001$ ) greater as age progresses. Additionally, there is a large increase from embryonic mandibular centroid size (median: 2.69) compared to peri-weaning (median: 3.34) and adult sizes (median: 3.53).



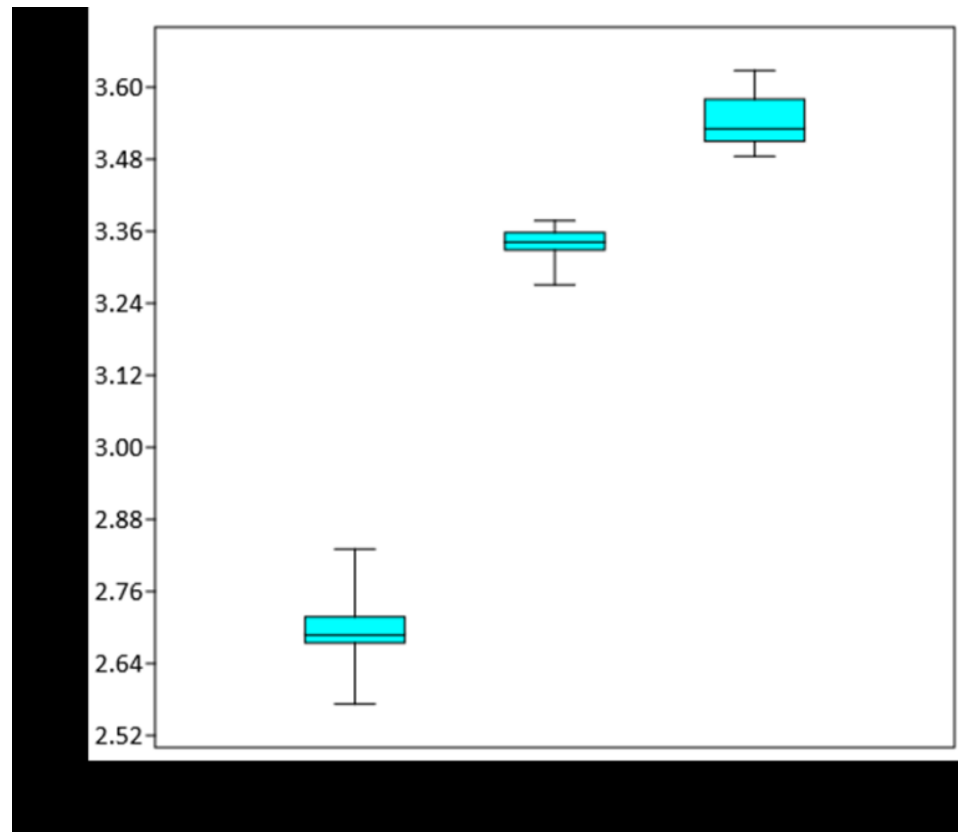


**Figure 3.2** Boxplot showing the distribution of mandibular size (ln CS) among each of the WT age groups

As size increases with age it will likely have an allometric effect on shape. A multivariate regression was run in order to determine if size significantly influenced mandibular shape. Procrustes coordinates from the age-pooled PCA were used as dependent variables and regressed on ln CS. A permutation test with 10,000 random iterations was performed to test the significance of the relationship between shape variables (Procrustes coordinates) and ln CS. Procrustes coordinates have been noted as highly appropriate for developmental analyses when both size and shape are of biological importance (Mitteroecker *et al.*, 2004). Multivariate regression is also useful for this analysis because it is unaffected by the number of dependent shape variables

(Mitteroecker and Gunz, 2009). As expected, there is a highly significant correlation between shape and size ( $p < 0.0001$ ) with 83.63% of the total variation accounted for by the regression. Though there is a significant allometric effect on shape in the growing mandible, scaled data are not reported on below because it is precisely this type of variance that is important for further analyses.

Procrustes distances were calculated between the mean forms for each age group to determine shape transformations. Results demonstrated significant differences among age groups, indicating that a large amount of shape change occurs over ontogeny (Figure 3.3). The largest Procrustes distance was found between the embryonic and adult mice (0.2331) while the smallest was found between peri-weaning and adult mice (0.0842). A similar trend was found in the size scaled data (0.2248; 0.0747, respectively). This suggests that as the mice age, their mandibles become more similar in shape, even when allometric influence is taken into account.

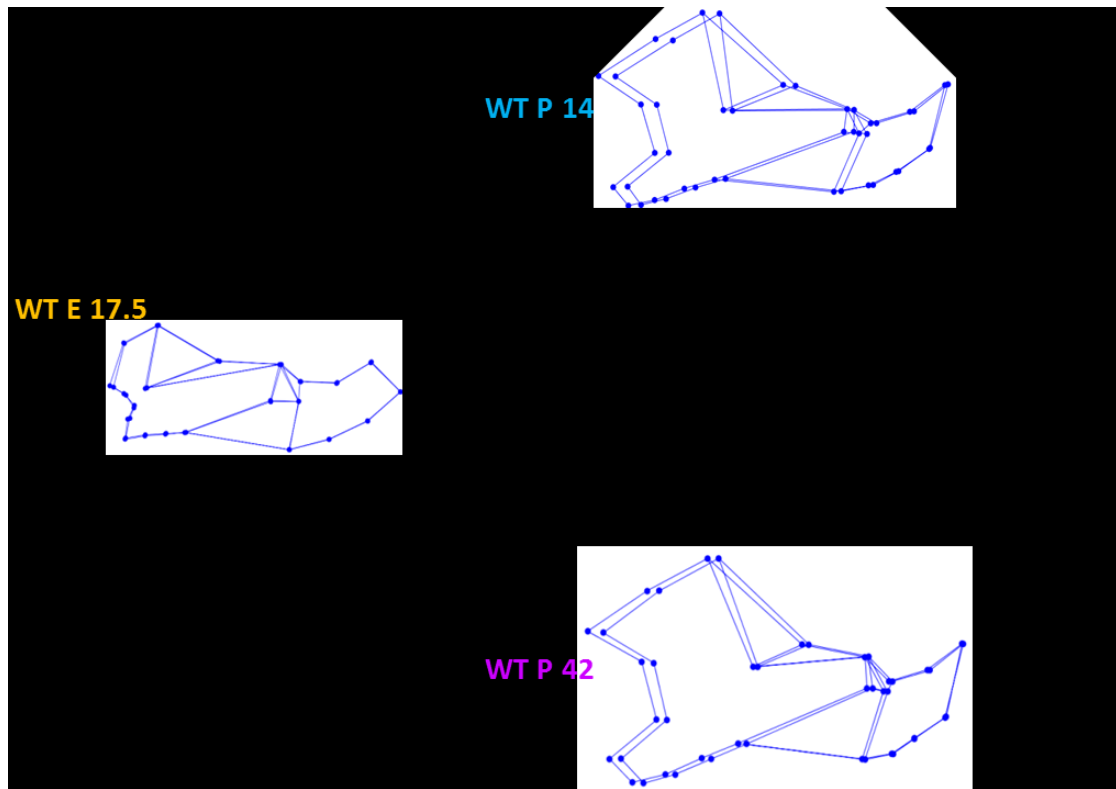


**Figure 3.3** Wireframes show the average shape of each WT age group. Arrows indicate comparisons of average shape between each age group, calculated as Procrustes distances. Procrustes distance was compared between A) E 17.5 vs P14; B) E 17.5 vs P 42; and C) P 14 vs P 42.

### 3.1.2. Patterns of Covariance over Ontogeny

The first set of objectives, Developmental Hypothesis A (**H<sub>DVA</sub>**), was concerned with how structure of covariance in the mouse mandible changes over ontogeny.

Explicitly the question was whether pattern of covariance and/or the magnitude of covariance altered in the mandible as it transitioned from embryonic shape to full adult morphology while experiencing concomitant internal and external pressures. Patterns of covariance were investigated by comparing matrix correlations generated from Procrustes coordinates between each age group using Random Skewers. Patterns of covariance were further analyzed by conducting a 2-Block PLS analysis which calculates the amount of

covariance between two units (alveolar and ramal modules were used here) and allows one to recreate the relative changes in shape that are most integrated between them. For these particular analyses, the pattern of integration over ontogeny was focused on rather than on the magnitude of integration. The latter aspect of the  $H_{DVA}$ , the change in magnitude of covariance over ontogeny, was investigated by calculating the Scaled Variance of the Eigenvalue (SVE). Here one can compare the magnitude of covariance within selected traits between one age group and the next. SVE was compared between each age group using three separate landmark configurations based on previously established modular designs in the literature: 1) the Global landmark configuration uses all landmarks; 2) the Bi-modular configuration partitions landmarks to represent alveolar and ramal modules and; 3) the Mesenchymal configuration partitions landmarks to represent mesenchymal condensations (see Figure 2.11). SVE was calculated for each of these modules and compared between age groups. Lastly, in order to test the goodness of fit for each of these modular configurations,  $R_v$  coefficients were calculated separately within the embryonic, peri-weaning and adult WT mice. Analyses were conducted on raw data using the entire sample as well as within the JHU-only sample. Results are discussed in the section below, JHU-sample results will be discussed only if outcomes were different from the whole sample analyses.

#### *Variance/ Covariance Matrix Correlations*

Patterns of covariance were compared between age groups within the WT mice. V/CV matrices were generated in order to assess global patterns of covariance within each developmental period and to contrast these patterns between periods. Three pair-

wise comparisons were made: 1) E17.5 to P14; 2) E17.5 to P42; and 3) P14 to P42.

Covariance matrix repeatability values were high across the three ages ( $t = 0.8364 - 0.8968$ ) suggesting that measurement error was sufficiently minor (Marroig and Cheverud, 2001). Table 3.1 shows all the matrix repeatability tests and observed and adjusted matrix correlations found from the WT and HT comparisons.

**Table 3.1 Covariance matrix repeatability, observed and adjusted correlations compared between WT age groups. Bold values, on the diagonal, are matrix repeatability correlations, below the diagonal are observed correlation values, and above the diagonal are adjusted correlation values. Italicized values represent matrices that were statistically similar ( $p < 0.05$ ). Matrix correlation comparisons using only the JHU bred mice resulted in statistically significant similarity among matrices. In each case, the JHU bred matrix repeatability, observed and adjusted correlations did not differ greatly from the whole-sample dataset.**

	E 17.5 WT	P 14 WT	P 42 WT
E 17.5 WT	<b>0.836422</b>	0.191895	0.131146
P 14 WT	0.166198	<b>0.896805</b>	0.134871
P42 WT	0.112884	0.120207	<b>0.885786</b>

Observed and adjusted matrix correlation values were extremely low for all WT age comparisons. Despite low vector correlation values between WT embryonic and peri-weaning mandibles, permutation tests were still significant suggesting similarity in covariance structure ( $R_{obs} = 0.1662$ ;  $R_{adj} = 0.1919$ ;  $p = 0.035$ ). In contrast, vector correlations were not significant when comparing both embryonic and peri-weaning mandibles to those of adults ( $p = 0.085$ ;  $p = 0.089$ , respectively), so that the null hypothesis of dissimilarity between groups cannot be rejected. Results from the JHU-only sample did not differ from those presented above.

### *Two-Block PLS*

Two-Block PLS analyses of all developmental stages were conducted using the Bi-modular model to observe ontogenetic patterns of covariance within the mandible. Covariance was specifically investigated between the alveolar region as Block 1 and the ramus as Block 2. Analyses were conducted using all WT age members. Age groups were pooled in order to diminish the influence of the mean shape differences between mandibles at separate developmental stages (Mitteroecker and Bookstein, 2008; Singh *et al.*, 2012). Two-Block PLS analyses conducted with the JHU-only sample resulted in similar statistical outcomes, therefore they will not be discussed below.

Another possible confounding factor when interpreting PLS analyses of multiple groups occurs when the degree of variance within groups is unequal. Heterogeneous amounts of variance can skew the data to result in greater measures of covariance than actually exists among the units or “blocks” under examination. In order to determine if unequal amounts of variance were influencing the interpretations of this analysis, the distribution of variance was calculated and compared between each sample (Table 3.2). The sum of the squared Procrustes distance of specimens within a sample was used as the measure of variance. Pair-wise permutation tests (900x) were then conducted using the residuals from the mean of the two groups to test the null hypothesis that the distribution of variance is no greater within each group than would be expected at random. Results showed that WT embryonic mouse mandibles possessed a significantly larger breadth of shape variance (0.00237 SS) when compared to either peri-weaning or adult mice. In contrast, peri-weaning and adult mice did not differ significantly. Therefore, the following interpretations of PLS analyses and further conclusions are made with caution.

**Table 3.2 Calculations of observed variance for each separate mouse age group. Bold values along the diagonal are the observed variance (SS) measures with each age. Above the diagonal are the observed absolute value differences ( $\Delta V$ ) in the variances between age groups in pair-wise comparisons.**

	E 17.5 WT	P 14 WT	P 42 WT
E 17.5 WT	<b>0.00237</b>	0.00127*	0.00094*
P 14 WT		<b>0.00110</b>	0.00033
P 42 WT			<b>0.00143</b>
* Indicates a significant difference in $\Delta V$ .			

The first two PLS axes described over 90% of covariance between the alveolar and ramal regions of the mandible in WT mice (Figure 3.4). Percentages of explained covariance were drastically lower following the first two axes ( $< 3\%$ ) therefore PLS1 and PLS2 are focused on here. Correlation coefficients between the two mandibular units were significant and relatively strong in both PLS1 ( $r > 0.95$ ;  $p < 0.001$ ) and PLS2 ( $r > 0.88$ ;  $p < 0.001$ ). This suggests that the alveolus and ramus are significantly integrated over ontogeny in WT mice. Though PLS1 represents shape change associated with the greatest amount covariance, PLS2 also captured very large amount of coordinated shape change and will thus both patterns of covariance were described below.

Scatterplots of PLS scores for the two blocks of data under examination, the alveolar region and ramus, illustrate the relationship of PLS axes between the two blocks. This can be extremely helpful in detecting different levels of covariance when multiple groups are being used. Plots were created using group-centered scores based on age category which removes the influence of different average shapes due to developmental stages. Scatterplots of PLS1 and PLS2 scores for all 2-Block PLS analyses, along with

wire deformations depicting associated shape changes in the alveolus and ramus can be found in Figure 3.4.



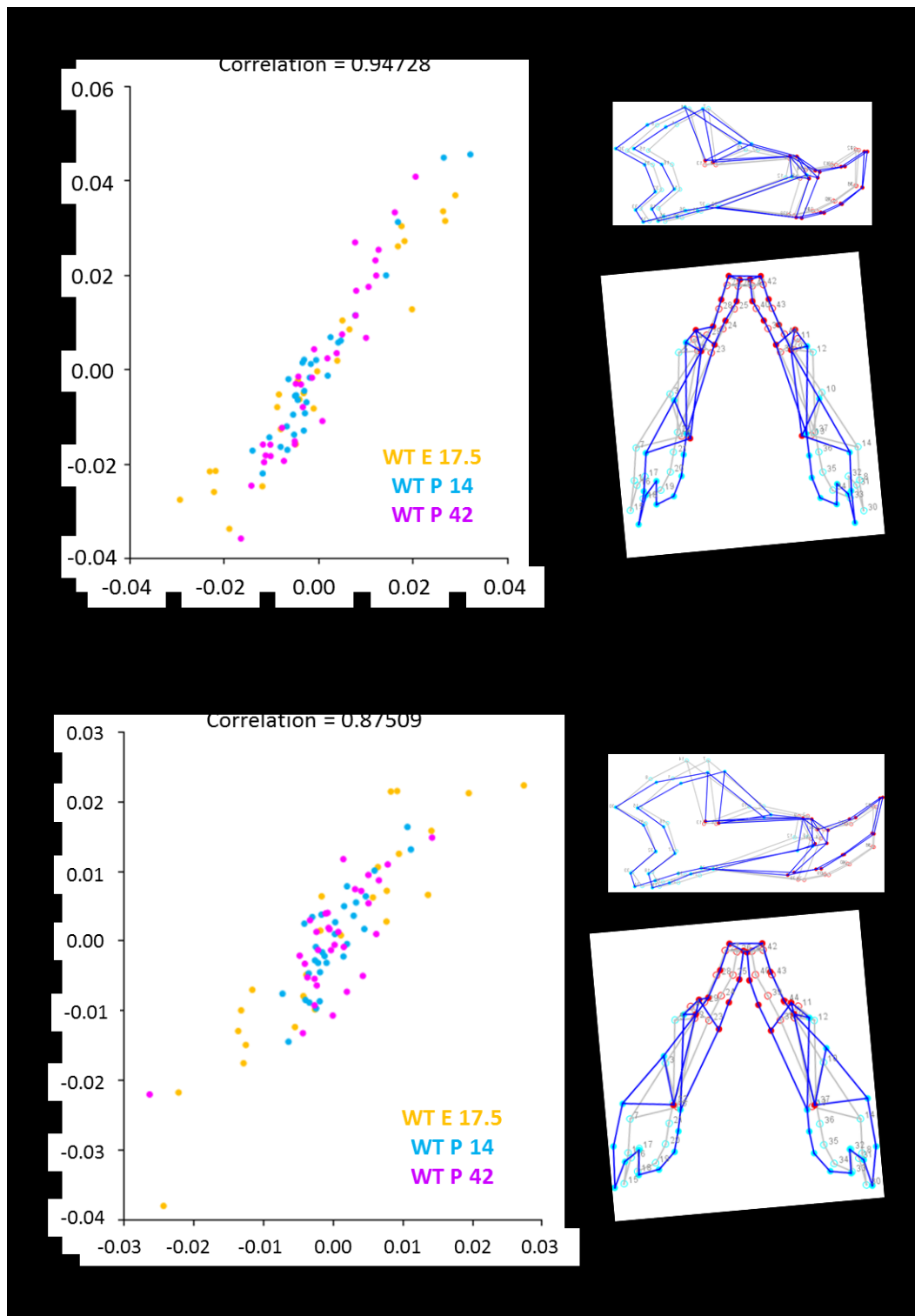


**Figure 3.4** Scatterplots of WT PLS1 & PLS2 scores from ontogenetic 2-Block PLS analyses. Scatterplots evaluate the amount of covariance shared in the Bi-modular model within all three age groups. Shape changes associated with patterns of integration between the alveolar and ramal modules are shown as wireframes.

A scatterplot of PLS1 (82.665%) scores for WT mice of all three age groups (Figure 3.4) demonstrate a large amount of overlap among ages, though the embryonic mice differentiate at the maximum and negative values. This suggests similar patterns of shape change associated with the covariance occurring between the alveolar region and ramus over ontogeny. In contrast, peri-weaning and adult mice tend to cluster together in PLS2 (9.523%) scatterplots while embryonic mice are much more dispersed. Larger dispersal within the embryonic mice in both PLS1 and PLS2 scatterplots is likely related to the large degree of overall shape variance found in the embryonic mouse mandible.

Associated shape change between the two blocks along PLS1 axes correspond to an anteriorly displaced alveolar region and posteriorly translated ramus, creating a more antero-posteriorly elongate mandible (Figure 3.4). As the alveolus shifts the anterior masseteric muscle marking and mandibular foramen follow suit, effectively creating a larger surface area for the masseter to insert. This is paired with an inferiorly rotated incisal curve and a coronoid that has been reoriented postero-inferiorly. Medio-lateral width between the right and left dental rows remained constant despite an apparent narrowing between the right and left descending ramus.

Patterns of shape integration along the PLS2 axes were quite different. Mandibles on the second PLS axis combined an overall supero-inferior shortening of the mandible, in both the alveolus and the ramus. Overall antero-posterior length did not change but bi-condylar width was increased. However, bi-gonial width remained constant, resulting in a laterally flared condylar region. The masseteric insertion translated anteriorly, while the molar row and posterior border of the ramus remained relatively static. Thus even though

the shape of the mandible along PLS2 does not correspond with lengthening, the masseter insertion area still becomes larger.

### 3.1.3. Magnitude of Covariance over Ontogeny

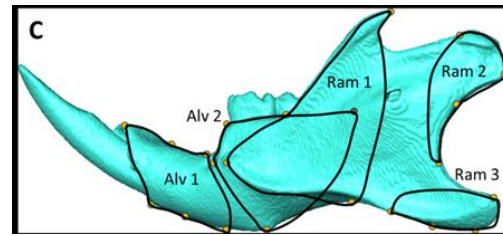
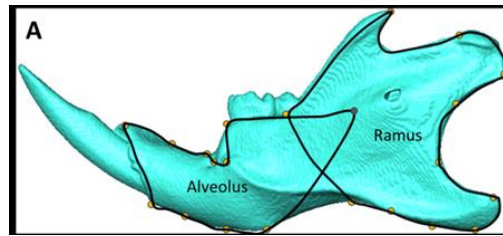
The magnitude of covariance was found for each age group by calculating the Scaled Variance of the Eigenvalue (SVE). Subsequent pair-wise comparisons were made between age groups in order to evaluate how levels of covariance might change over ontogeny. Multiple landmark configurations were used to explore this data, including global landmark configuration, landmarks partitioned into alveolar and ramal modules and lastly, landmarks partitioned into the Mesenchymal modules.

Among wild-type mice there was a discernable pattern in the magnitude of covariance within different mandibular components using raw data (Figure 3.5). Embryonic mice almost always possessed significantly greater levels of integration followed by the peri-weaning age group and then adult mice with the smallest values. This was true the alveolar module and most of the Mesenchymal modules yet differed in the ramal regions. Within the global and Bi-modular landmark configurations, though embryonic mice still had the largest SVE scores in the ramus as a whole, the adult mice possessed the second largest SVE scores so that the patterns of integration were no longer sequential with age group. In addition the angle of the mandible also did not follow any particular age dynamic. Peri-weaning angle landmarks are more integrated than those of either embryonic or adult mice. The JHU-only sample demonstrated the same pattern in SVE values. Significant differences were present between each pair-wise age

comparison. Embryonic mice possessed the greatest magnitude of covariance in the majority of landmark partitions while adult mice had the least.

#### Bi-module Configuration (2 partitions)

#### Mesenchymal Configuration (5 partitions)



WT 17.5    WT P14    WT P42

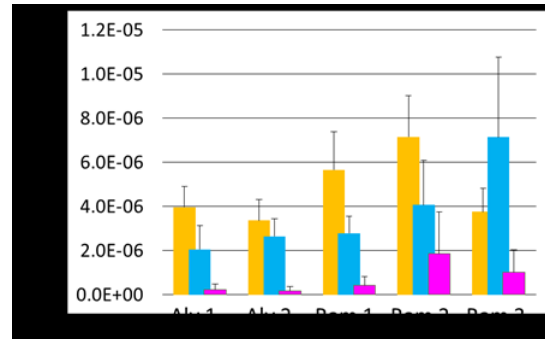
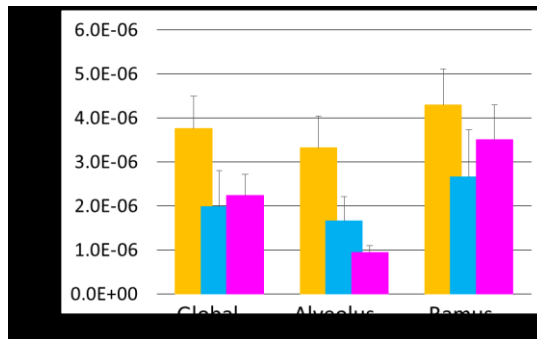


**Figure 3.5 SVE scores for WT mice over ontogeny.** Three different landmark configurations were used based on the global mandible, landmarks representing the Bi-module configuration and the Mesenchymal configuration. SVE was calculated for each module and subsequently compared between each age group using a bootstrap permutation test. All pair-wise comparisons were significantly different after Bonferroni correction ( $\alpha = 0.006$ ;  $p < 0.0001$ ). A) Example of Bi-module landmark configuration with alveolar (1,  $k=22$ ) and ramal (2,  $k=22$ ) partitions; B) Bar-graph showing global and Bi-modular raw SVE scores between age groups comparisons; C) Example of Mesenchymal landmark configuration with two alveolar (1,  $k=12$ ; 2,  $k=8$ ) and three ramal (1,  $k=8$ ; 2,  $k=8$ ; 3,  $k=8$ ) partitions; D) Bar-graph showing Mesenchymal SVE scores for ontogenetic comparisons.

### *R<sub>v</sub> Coefficients*

$R_v$  coefficients were calculated within each specific age group to test hypotheses related to the modular configuration of the mandible as it develops. Bi-modular and Mesenchymal models (Table 3.3) were separately applied to the analysis as hypothetical modular configurations. Covariance among the proposed modules was then compared to alternative configurations (permuted 10,000x), with landmarks chosen at random so that any covariance among traits is due to chance. If the  $R_v$  coefficients of hypothesized modules are consistently lower or weaker than the randomized configurations then the hypothesis of modularity is supported.

**Table. 3.3 Table of  $R_v$  coefficients for ontogenetic mouse sample.  $R_v$  coefficient scores and p-values (from permutation test of random modules) for all hypothetical modules in each age group, representing both raw and scaled data sets. Significant values are italicized.**

Age	Bi-module model		Mesenchymal model	
	$R_v$ coefficient	p-value	$R_v$ coefficient	p-value
WT E17.5	0.845295	0.0669	<i>0.652021</i>	<i>0.0000</i>
WT P14	0.851070	0.1532	<i>0.614247</i>	<i>0.0000</i>
WT P42	0.798562	<i>0.0300</i>	<i>0.576926</i>	<i>0.0000</i>

$R_v$  coefficients between the alveolar region and the ramus were quite high ( $R_v > 0.70$ ) indicating a strong integration between each unit. Embryonic and peri-weaning Bi-modular  $R_v$  coefficients were higher than the majority of randomized partitions ( $P = 0.066$  and  $0.153$ , respectively; Table 3.3) while the adult  $R_v$  coefficient was significantly lower ( $P = 0.03$ ). Therefore, the proposed Bi-modular configuration can be supported in the adults, but not in the younger WT mice. In contrast, when the Mesenchymal Model was investigated  $R_v$  scores were moderate, ranging from  $0.57 - 0.65$  and consistently

smaller than the majority of alternative configurations ( $P < 0.0001$ ). Hypothetical Mesenchymal models are thus highly supported at each developmental stage. The fact that both modular models proposed were significantly represented in the adult mandible further bolster the argument that covariance is a hierarchical structure.

### **3.2. Discussion**

#### **3.2.1. Ontogenetic Changes in Mandibular Morphology**

Mandibular shape change was apparent as wild-type mice aged from the embryonic to peri-weaning to full adult shape. Similarly, wild-type mandibles shifted dramatically in centroid size from each age. This is not unexpected as the mandible must transition from an ossifying bar of cartilage to a fully functional adult bone that must accommodate dental growth, muscular growth, and the onset of masticatory stress and strain induced by both muscular and occlusal loading. The fact that the peri-weaning wild-type and Crouzon mandibles were much closer in size and shape to the adults than they were to the embryonic mice suggests that a large portion of changes in size and shape occur within the first two weeks of life.

Previous analyses of the size and shape of the mouse mandible have generally focused on adult shape, whether from samples ranging from wild-caught mice from natural populations to laboratory mice, as well as genetically altered laboratory mice. The use of laboratory mice has allowed researchers to design a variety of studies that compare mandibular size and shape between wild-type strains, mice with different diets and transgenic mice. These analyses have provided important information regarding how the

mandible responds to different environmental influences as well as developmental perturbations induced by mutations. However, surprisingly few post-natal analyses of size and shape change in the growing mouse mandible have been completed. This analysis adds to a body of research that is severely lacking.

The results of the shape analyses conducted here correspond to those found by Swiderski and Zelditch (2013). In their study, they investigated the ontogenetic shape trajectory of *Mus musculus*. The periods of growth used in this analysis, between the embryonic and peri-weaning and subsequently the peri-weaning and adult mice can be considered as a first and second stage, respectively. There are distinct differences in the way shape changes within those two stages. The first stage displays a massive shift in shape largely in the ramus. Transition from embryonic to peri-weaning stages results in a large expansion of the ramus. In addition, the three posterior processes mature in shape to resemble the adult mandible. Transition in shape in the second stage is similarly largely represented in the ramus, though at this point there is a relative deepening of the body of the mandible below the molar row and a greater curvature of the incisor. Swiderski and Zelditch (2013) also reported that from post-natal day 1 (P 1) to post-natal day 15 (P 15) the greatest amount of morphological change was located in the ramus. First, shape changed by an overall expansion of the ramus until the first week, and then subsequent maturation occurred in the coronoid, condylar and angular processes in the second week of life. They also noted that shape of the molar and incisal region was nearly established by the second week and that any change after was related to depth of horizontal ramus or the body inferior to the molar row. They suggested that these shape changes reflected the mandible responding first to dental growth and then to muscular growth.

The growth pattern seen among the mice used for this study does seem to follow a two-tier system that tracks dental growth and then muscular growth. Previously, other research has attempted to correlate dental growth with mandibular growth, especially with the argument that mandibular shape is largely mediated by the spatial demands of dentition (Wood, 1978; Smith, 1983; Daegling, 1996; Taylor, 2000; Plavcan and Daegling, 2006; Boughner and Hallgrímsson, 2008; Cobb and Panagiotopoulou, 2011; Suwa *et al.*, 2011; Fukase, 2011, 2012; Gómez-Robles and Polly, 2011; Dean and Cole, 2013). Some studies have found that there is a strong spatial relationship between growing dentition and mandibular size or shape (Cobb and Panagiotopoulou, 2011; Suwa *et al.*, 2011; Fukase, 2011, 2012) while others have discounted this (Plavcan and Daegling, 2006). Other recent studies have provided some evidence that there are broad molecular underpinnings jointly signaling to both mandibular and dental growth. Results from this analysis do generally support the idea that mandibular shape over development is partly driven by growing dentition. For instance, even during the earliest stages of molar and incisal development, the dental crypts have already created space for the incoming dentition. This is further bolstered by the fact that the mandibular body deepens after dentition has come into occlusion in the peri-weaning mice. This would corroborate the idea that the mandibular body then needs to accommodate the growing molar roots, as well as biomechanical loads. Despite these findings, without any direct comparison of dental size and shape with mandibular size and shape in these analyses the degree to which one affects the other is difficult to determine. These questions will be addressed in future projects.



Muscular growth is also known to highly influence shape of the mandible, particularly in the posterior region where the muscles insert. Experimental analyses where muscles of mastication were extirpated during development revealed decreased mandibular growth and altered mandibular shape, especially in areas of muscular attachment (Moss and Meehan, 1970; Herring, 1993; Spyropoulous *et al.*, 2002). Other analyses that reduced muscular loading on the mandible, whether due to diet or genetic alteration also discovered significant differences in mandibular size and shape (Jones *et al.*, 2007; Anderson *et al.*, 2014). Thus the continued ontogenetic shape changes in the coronoid, condyle and angle are likely due to the presence and activation of muscular tissue. This then most likely transitions over to mechanical pressure and strain as bone remodels and becomes deeper to accommodate the elongating molar roots.

### 3.2.2 Patterns of Covariance Change at Specific Ontogenetic Times

Mandibular covariation changes over ontogeny within the mouse sample used here, as evidenced by comparisons of the covariance matrices. Covariance seems to be generally similar from the embryonic to the peri-weaning stages though neither was similar with the adults. The null hypothesis ( $H_{DVA0}$ ) can be rejected since adults diverged in patterns of covariance. In addition, the first alternative hypothesis ( $H_{DVA1}$ ) can be completely rejected because embryonic and peri-weaning covariance patterns could not be distinguished from each other. However, because the adults were not found to be similar in mandibular patterns of covariance the second alternative hypothesis ( $H_{DVA2}$ ) was not rejected.

It has been suggested that the onset of function is related to changes in the structure of covariance (Klingenberg *et al.*, 2003; Hallgrímsson *et al.*, 2009; Zelditch *et al.*, 2009). Even more, it is well established that varying dietary demands experienced during growth and development will modify the bone density and shape of the rodent masticatory apparatus (Mavropoulos *et al.*, 2005; Tanaka *et al.*, 2007; Renaud *et al.*, 2010; Anderson *et al.*, 2014). In the mandible function would include the combination of stress and strain from occlusal forces, muscular forces and joint reaction at the temporal mandibular joint. M1 and M2 are fully erupted from the gingiva in the peri-weaning mice; presumably they are beginning to use their mandible to ingest an adult diet. Yet, patterns of covariance were similar between the embryonic and peri-weaning mice. This suggests that the continued development of musculature and erupting dentition are not changing the way in which different components of the mandible are integrated. However, adults were not similar in covariance patterns when compared to either the embryonic or peri-weaning mandibles. The deposition and resorption of bone after prolonged adult diets likely results in the reorganization of covariance patterns. This suggests that function is playing a large role in organizing the adult pattern of covariance.

Ontogenetic changes in the pattern of covariance have been documented in the skull of rodents, humans and other mammalia (Zelditch, 1988; Zelditch *et al.*, 2006; Ackermann, 2005; Mitteroecker and Bookstein, 2009; Polanski, 2011; Goswami *et al.*, 2013) with covariance modifying through late-stage ontogeny but stabilizing in adulthood (Zelditch and Carmichael, 1989b; Zelditch *et al.*, 1992). It is possible that early changes in covariance are the result of developmental covariance generating factors while static covariance in adulthood may be the influence of function, particularly masticatory

function, stabilizing integration. The results here generally support previous analyses in that correlations were quite low between different age group patterns of covariance. However, the only instance in which covariance in the mandible was not statistically similar was found when comparing embryonic and peri-weaning mice to adults.

The gap between peri-weaning and adult mice is nearly a month (28 days) in which large amounts of growth and development occur. It is likely that adult muscle force has not been realized yet in the peri-weaning, mice so as force becomes greater than experienced before, patterns of covariance change. In other words, the brunt of force and its effect on bone is generating changes in patterning observed here. A comparison of covariance patterns and estimates of bite force, such as muscular physiological cross-sectional area or the calculation of mechanical advantage would help to further prove this. Previously it was suggested that mandibular covariance pre-empted adult functional demands by developing earlier than the necessary function (Zelditch, 1988; Zelditch *et al.*, 1992). The results here do not support this given that adult patterns of covariance do not appear until well after weaning. Possibly, this is due to the lack of developmental stages between peri-weaning and adult mice. It should also be noted that their sample consisted of rats (*Rattus norvegicus* and *Sigmodon fulviventer*) was not solely focused on the mandible which may also add to the differences in results.

When patterns of covariance are explored by the integration between the alveolus and ramus a more homogenous picture emerges. As the mandible develops, these two units are well integrated at each developmental stage; the first PLS axis left less than 20% of covariance unexplained. Indeed, the way in which the alveolar and ramal units are integrated is characteristic of mandibular growth itself. Two hall mark features of

ontogenetic change represented by covariance between the alveolus and ramus are an antero-posterior lengthened mandible and a greatly expanded ramus. As the palimpsest argument suggests, depending on what structural level or time period you are investigating covariance, you will receive differing signals. That can be evidenced here as we see a global configuration that suggests that adults are fundamentally different than the other two age groups but when a broader time sequence is considered, they are quite similar.

### 3.2.3 Magnitude of Covariance Changes over Ontogeny

The magnitudes of covariance found in the mandible were found to differ between each development stage so that the null hypothesis of no difference can be fully rejected. The two alternative hypotheses posited that either: (**H<sub>DVB1</sub>**) only embryonic and peri-weaning mice would possess differing magnitudes of variance, or; (**H<sub>DVB2</sub>**) differences would only be present between the adult mice and younger ages. These hypotheses were made in order to test whether intrinsic developmental factors (**H<sub>DVB1</sub>**) or functional influences (**H<sub>DVB2</sub>**) were producing observed magnitudes of covariance. Alternative hypotheses can only be partly supported here give that in the majority of cases each age is significantly different from each other.

WT embryonic mice have the greatest amount of integration in all instances save one, the angular process module. This degree of integration then begins to decline as age increases suggesting that covariance generating properties are decreasing with age, being dampened with age or more sources of localized variation are being produced. Previous

analyses have noted a stark drop in post-natal intra-*population* variance in the cranium of rodents and shrews (Nonaka & Nakata, 1988; Riska *et al.* 1984; Zelditch, 2005; Zelditch *et al.*, 2004; 2006; Gonzalez *et al.*, 2011; Goswami *et al.*, 2012). Others have documented increases of intra-*individual* variance, via fluctuating asymmetry, when the developmental process are disturbed in some way whether it be through experimental mutation or dietary insufficiencies (Mooney *et al.*, 1985; Hallgrímsson, 1999; but see Gonzales *et al.*, 2014 for rebuttal). The results in this study concerning differences in the distribution of variance of each age group support the idea that phenotypic variance is greater in younger, healthy mice which in turn is dampened by other developmental factors (Table 3.2). Thus variance-covariation generating signals are quelled and we see that the mandible loses intensity of integration as age increases.

It has also been suggested that increases in variance seen in younger specimens was due to varying rates of development among different individuals (Hallgrímsson, 1999). So that, though two mice may have the same age they are at different points on a growth trajectory resulting in vastly different size or shape and contributing to the amount of variance within that age group. Once maturity is reached small differences are muted as all individuals have reached a base-line of growth. It may be more beneficial then to use certain developmental markers, such as dental eruption, to measure intra-population levels of variance over ontogeny.

The Bi-modular model was not consistently apparent in the mice while the Mesenchymal model was. Two interesting trends developed. First, integration between the alveolar and ramal regions was strongest in the embryonic and peri-weaning mice. This was the opposite of what was expected. It was originally proposed here that before

the onset of adult masticatory forces, modules derived from separate embryonic origins would be detectable whereas after adult function initiated the mandible would be more integrated as a whole. Adult modular configuration would either demonstrate the Bi-modular model, overlapping the smaller Mesenchymal modules, or have a completely integrated mandible. It seems instead that as each component develops and becomes associated within its own role in chewing, the alveolar region and ramus become more differentiated with age. Other authors have noted the presence of two modules, which engendered the traditional view of the mandible (Atchley *et al.*, 1985; Cheverud and Leamy, 1985; Atchley, 1987; Cheverud *et al.*, 1997; Klingenberg *et al.*, 2004; but see Klingenberg *et al.*, 2003; Roseman *et al.*, 2009 for rebuttal).

Second, the Mesenchymal model was present at each age range. In line with the above arguments, these results were also unexpected. Originally it was thought that the covariance generating signal from the Mesenchymal modules would be overlaid or dampened by more integrating factors due to functional use of the mandible. However the fact that the mesenchymal signal can be found at all age ranges merely suggests that there is a strong developmental signal from the Mesenchymal modules. Representation of the integration between within the Bi-modular model and representation of the Mesenchymal model does not necessarily need to be mutually exclusive. It is far more likely that all signals of the variance-covariance structure can be detected depending on the trait level you are using and the a priori questions you are asking.

Allometry in the mandible might be masking the degree of modularity present, especially in adults. Certainly, by taking away the overall integrating factor of sheer size different levels of covariance can be partitioned out. Future analyses will consider size

corrected data, as it may show that integration is driven by growth factors. Somatic growth may also impact the amount variance at younger age ranges while process of development is ongoing.

The appearance and strength of modularity in the skull has been found both to increase (Zelditch and Carmichael, 1989a; Goswami and Polly, 2010; Goswami *et al.*, 2012) and decrease (Zelditch *et al.*, 1992) during ontogeny. Selection pressures change throughout ontogeny, therefore response to selective pressures are contingent upon the timing and intensity of covariance (Zelditch and Carmichael, 1989b; Hall, 1999; Hallgrímsson *et al.*, 2007). If overall integration is higher in the mandible early in ontogeny then that might constrain morphological evolution. On the other hand, an early appearance of mandibular modularity could evade developmental constraints, thus facilitating evolutionary response. The analyses presented here are not completely comparable with these previous studies considering that the proportion of overall integration to units of modularity were not calculated. Results from the SVE comparisons found that as age increases not only does the intensity of integration decrease in the mandible as a global whole but it also decreases within each modular level. Additionally, the overlap in modular signals identified by  $R_v$  coefficients suggest that the organization and intensity of modularity are detectable depending on what structural level is being investigated. Therefore it cannot be said with confidence that modularity decreases or increases with age relative to the global covariance structure versus separate modular models.

Porto *et al.*, (2009, 2013) recently devised a metric, the modularity index, to compare the magnitude of integration within specified modules while taking the magnitude of the remaining traits into account. In this new method, matrix correlations were computed between correlation matrices from morphometric data and theoretical matrices that reflected different hypothetical arrangements of modules. Hypothetical modular designs were based on functionally and developmentally related characters. Subsequently, a ratio of the average correlation in integrated traits to non-integrated traits was calculated, creating the modularity index. Since the modularity index is a ratio it allows one to measure the degree of modularity within a structure controlled for by the degree of integration throughout the structure.

It is possible that by controlling for overall integration the relative differences in magnitude seen between age groups may either diminish or re-pattern. Diminished magnitudes of covariance over ontogeny might suggest that developmental processes that control the pattern of covariance need to be more flexible during growth and development than the strength of which they covary. However, this is deemed unlikely in light of previous analyses on the crania mentioned above. The latter option suggests that if investigating relative degrees of modularity using the modularity index may reverse the patterns seen here. Meaning that it is possible that adults would then possess larger amounts of modularity, which would again match previously mentioned analyses. Future analyses will incorporate the modularity index to answer these questions.



### 3.2.4 Summary

Covariance structure changes drastically among the mandibles of developing mice. Indeed, coordinated shape change between the alveolar and ramal regions reflects developmental processes relevant to each developmental stage, such as the growth of dentition and muscular insertion areas. Patterns of covariance are altered between the peri-weaning and adult developmental stages suggesting that the onset of an adult diet significantly modifies the way in which traits are coordinated. This might be interpreted to mean that the strength of covariance is greater in the adult magnitude is reaction to habitually higher loads but this was not the case. Though function is implicated in the alteration of mandibular patterns of covariance, adults displayed the smallest magnitudes of covariance so that the strength of covariance between traits decreases into adulthood. Furthermore, both the Mesenchymal and Bi-modular models were detectable in the adult mice, suggesting that early developmental modules are present up to adulthood. Covariance is therefore a complex and hierarchical process during ontogeny in the mandible. This agrees with previous analyses that promote studying the “process” of covariance generation rather than the “pattern” because the structure of covariance is continually being modified as new variance is generated.

The hypotheses set forth and tested here were mainly interested in the influence of mesenchymal configurations and masticatory function governing the pattern and magnitude of integration. These are not the only aspects of mandibular growth however, and other factors should also be mentioned. Somatic growth for instance, as discussed in the previous sections, has been noted to contribute to covariance in the cranium and mandible. Simple allometric changes in shape related to size likely assert largely

integrative patterns in the mandible. This may be especially poignant when considering the large shift in overall size between the embryonic and peri-weaning mandible. The analyses conducted here did not take allometric effects into account. Further analyses controlling for size differences between age groups may in fact demonstrate a clear difference in patterns of covariance between younger mice.

Additionally, the importance of dental growth cannot be ignored. Though one might expect that the timing of the bulk of dental growth best coincides with early ontogenetic changes in covariance patterns, again, significant differences in covariance were only found between the younger mice. Yet, this does not preclude the influence of dental growth on the mandible in from peri-weaning to adulthood. Certainly, the continued elongation of the molar roots along with the emergence of third molar as the mouse mandible transitions from weaning to a consistent adult diet exerts influence on covariance. Specifically one might argue that dental growth would increase the pattern and magnitude within the alveolar module as a whole. In addition, as just simple growth of the dentition and masticatory muscles continues into adulthood the separate mechanical demands may change the way in which the ramus and alveolus covary regardless of mechanical loads exerted on the mandible.

The ability for overall integration and modularity to modify over ontogeny, whether it be in the pattern or magnitude of covariance, is an important concept. As stated previously, if traits are more integration during early ontogeny, that might constrain the response to selection pressures that act during development. It would seem from the way that the patterns of covariance are conserved during earlier developmental stages that perhaps developmental constraints conserve morphological variance in the

mandible. However, developmental constraints may be overridden by the introduction of functional constraints after an adult diet has been achieved. This may also be partly supported by the consistent change in the magnitudes of covariance of the mandible. As the mandible ages overall integration decreases relieving the mandible of particular constraints.

### *Future Directions*

- 1) Determine the degree of integration between the developing dentition and mandibular shape.
- 2) Conduct studies of ontogenetic allometry to determine the way size influences covariance in the developing mandible.
- 3) Test if the covariance magnitudes estimated here remain as significant when compared to other module magnitudes within the same population (per Porto *et al.*, 2009; 2013).



## Chapter 4: Results and Discussion – Mutation Hypotheses

### 4.1. Results

According to the Palimpsest model, as previously stated, developmental factors that contribute to the generation of covariance within a structure will increase the strength of covariance when a perturbation to that factor occurs. The focus of this chapter is on the contribution of an *Fgfr2* mutation on the mandibular phenotype and covariance. *Fgfr2* mutations have been shown to significantly contribute to covariance in the skulls of perinatal mice. The hypotheses here further test whether *Fgfr2* mutations affect the pattern and magnitude of covariance in the mandible over ontogeny ( $\mathbf{H}_{MTA}$  and  $\mathbf{H}_{MTB0-1}$ ). The combination of a transgenic model and an ontogenetic sample facilitates hypotheses that further test whether *Fgfr2* influence on covariance is detectable through growth and development or whether it is masked by other influences, such as masticatory demands ( $\mathbf{H}_{MTB2}$ ).

#### 4.1.1. Genotype Shape and Size Variation

PCA plots were computed within each age group, comparing mandibular shape differences between the WT and HT mice. There is a large amount of overlap in shape space along both PC1 (36.04%) and PC2 (13.41%) for the embryonic genotypes (Figure 4.1). Indeed, shape differences visualized between these two groups was quite mild. In general the Crouzon mice display an antero-posteriorly shortened angle and condyle while the medio-lateral breadth between the two condyles and coronoid processes was greater than that of their wild-type litter mates. The alveolus was also slightly shortened

in the HT mice. Despite the overlap in shape space and the mild shape differences displayed in the embryonic mice, Procrustes distances between the two genotypes are significantly different (Figure 4.1).

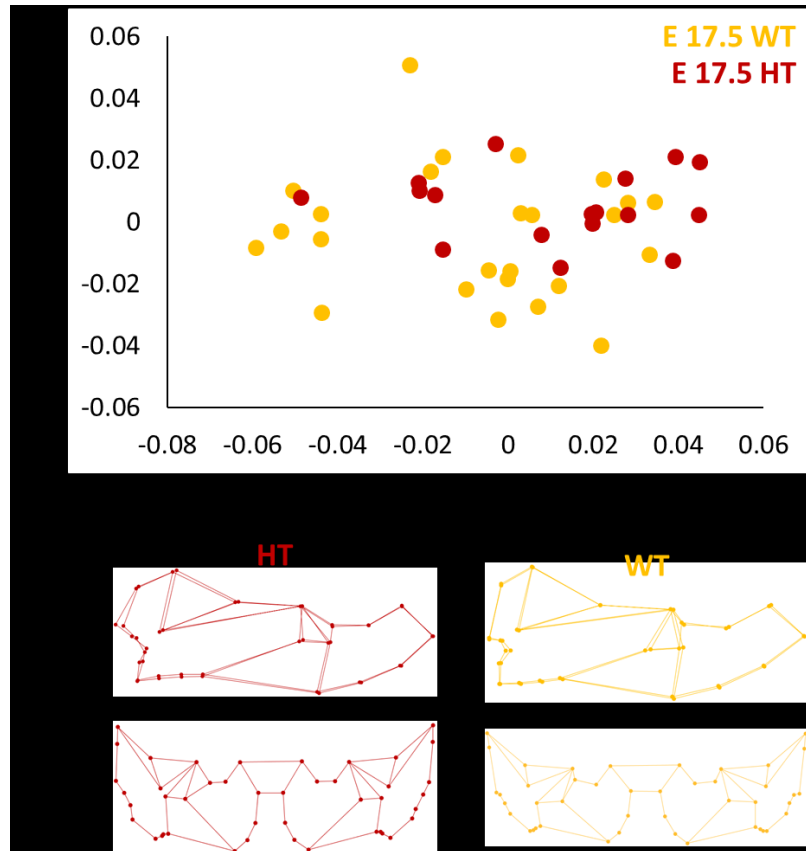


**Figure 4.1** PCA scatterplot of WT and HT embryonic mice (E17.5). Shape differences can be seen below in the wireframes demonstrating differences between genotypes. Wireframes illustrate sample mean configuration. WT and HT mandible shape was significantly different ( $p < 0.0001$ ; Procrustes Distance = 0.0247).

Mandibular shape disparity was much greater in the peri-weaning mice. PCA scatterplots displayed clear differences in shape space along PC1 (60.21%) though there was greater overlap along PC2 (9.48%) (Figure 4.2). Peri-weaning Crouzon mice had a posteriorly displaced incisor alveolus, both at the anterior and posterior aspect. They also had a relatively taller condyle and coronoid process while the angle was relatively shorter and more inferiorly oriented. The angle was also relatively taller in the supero-inferior dimension. Both the molar and incisal alveolus were relatively longer in the WT mice while the condyle and angle were shifted posteriorly. The net effect was an overall longer and more slender mandible in the WT mice. In addition, the medio-lateral distance among landmarks was much wider in HT peri-weaning mice which had a much more flared gonial angle. These shape differences were also reflected in the Procrustes distance calculations which were significantly different among the two groups of peri-weaning mice ( $p < 0.0001$ ).

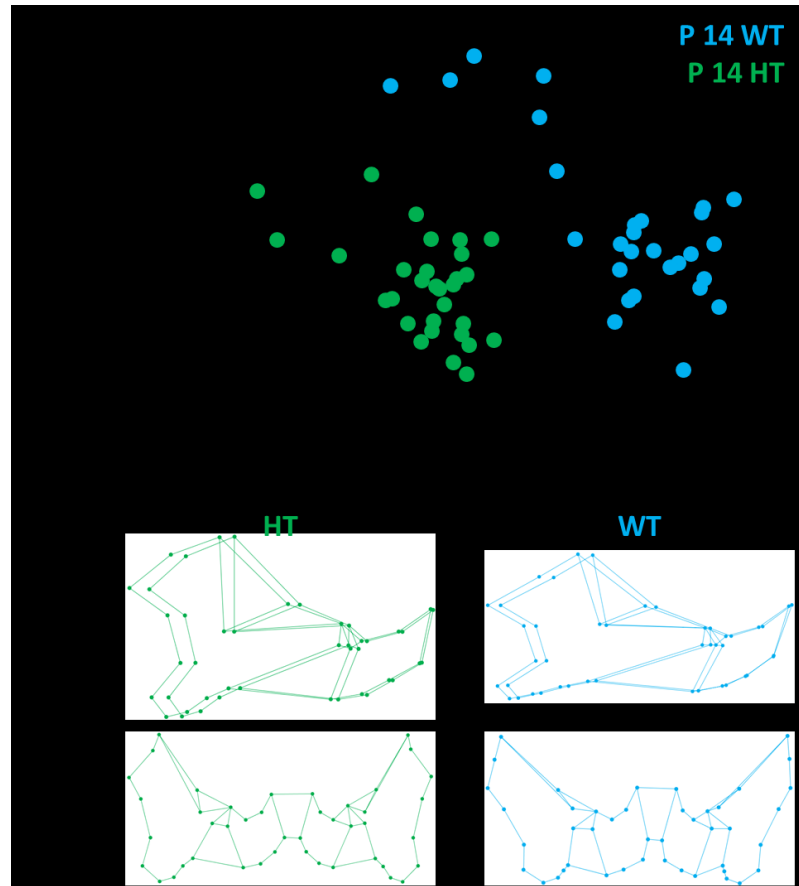


**Figure 4.2 PCA scatterplot of WT and HT embryonic mice (P14). Shape differences can be seen below in the wireframes demonstrating differences between genotypes. Wireframes illustrate sample mean configuration. WT and HT mandible shape was significantly different ( $p < 0.001$ ; Procrustes Distance = 0.0682).**

Shape differences seen between the adult mice were even more exaggerated than those seen in the peri-weaning mice. PCA scatterplots showed that the Crouzon mandibles occupied a much larger area of variation along PC1 (64.79%) than their wild-type littermates, though a clear separation was still visible (Figure 4.3). The PC2 axis (7.12%) had complete overlap among the genotypes. As shape varied over PC1 HT adults possessed an even stouter overall mandibular shape. The incisal alveolus was even more foreshortened and inflected superiorly. In contrast the posterior aspect of the molar alveolus was displaced posteriorly, creating a disproportionality longer molar row. The



adult wild-type littermates on the other hand possessed a slender alveolus in both the antero-posterior and super-lateral direction. In addition, the WT ramus was situated at a more oblique angle while the HT ramus was positioned more vertically. These ramal differences lent to a shorter distance in between the coronoid and posterior condyle. Likewise, the posterior border of the ramus and the angle were again displaced anteriorly. The WT adult condyle, on the other hand, was positioned very far posteriorly along with the ramal border and angle. Also, as seen in the peri-weaning mice, the WT adult mice had much more slender angle. Bi-lateral width continued to be greater in the HT adults to an even greater degree than the peri-weaning age group. HT mice displayed an overall wider mandible than the WT mice. Lastly, the shape differences observed in the PCA scatterplot and the wireframe deformations were supported by a significant difference in Procrustes distances ( $p < 0.0001$ ).

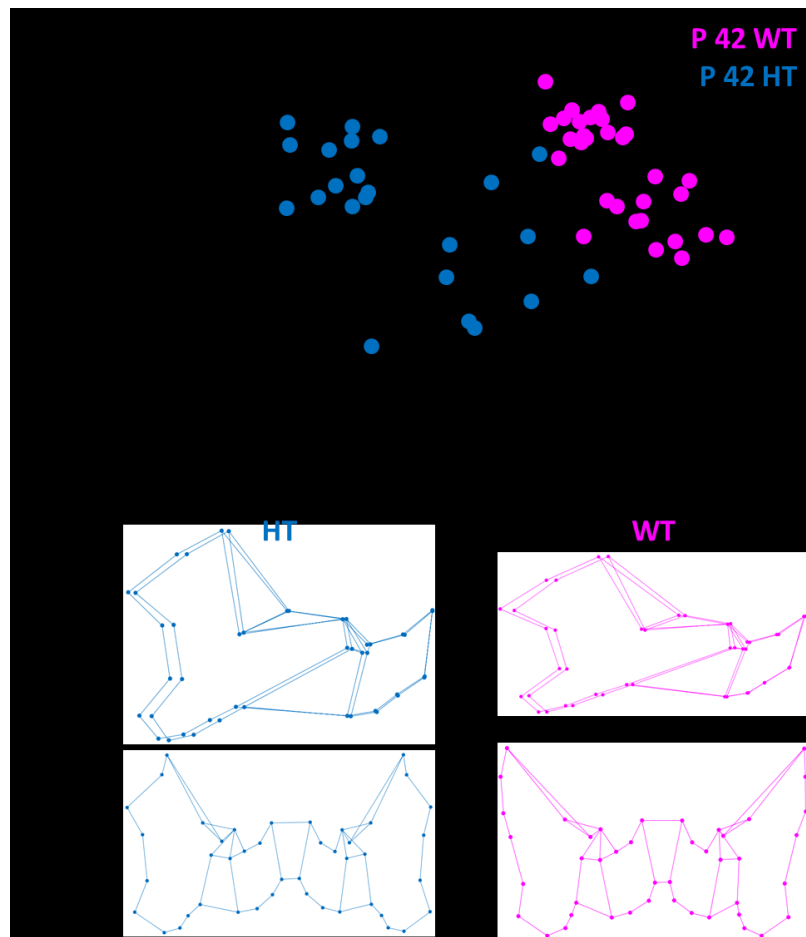


**Figure 4.3 PCA scatterplot of WT and HT embryonic mice (P42). Shape differences can be seen below in the wireframes demonstrating differences between genotypes. Wireframes illustrate sample mean configuration. WT and HT mandible shape was significantly different ( $p < 0.001$ ; Procrustes Distance = 0.0892).**

Two-tailed t-tests were performed comparing log centroid size ( $\ln CS$ ) to determine if size was significantly different between genotypes within each age group (Figure 4.4). Mandibular centroid size differences were found between WT and HT mice at the peri-weaning and adult developmental stages. Centroid size differences were not found to be significant between embryonic WT and HT mandibles. Boxplots comparison show that peri-weaning and adult WT mice possess significantly larger mandibles than their HT cohorts.

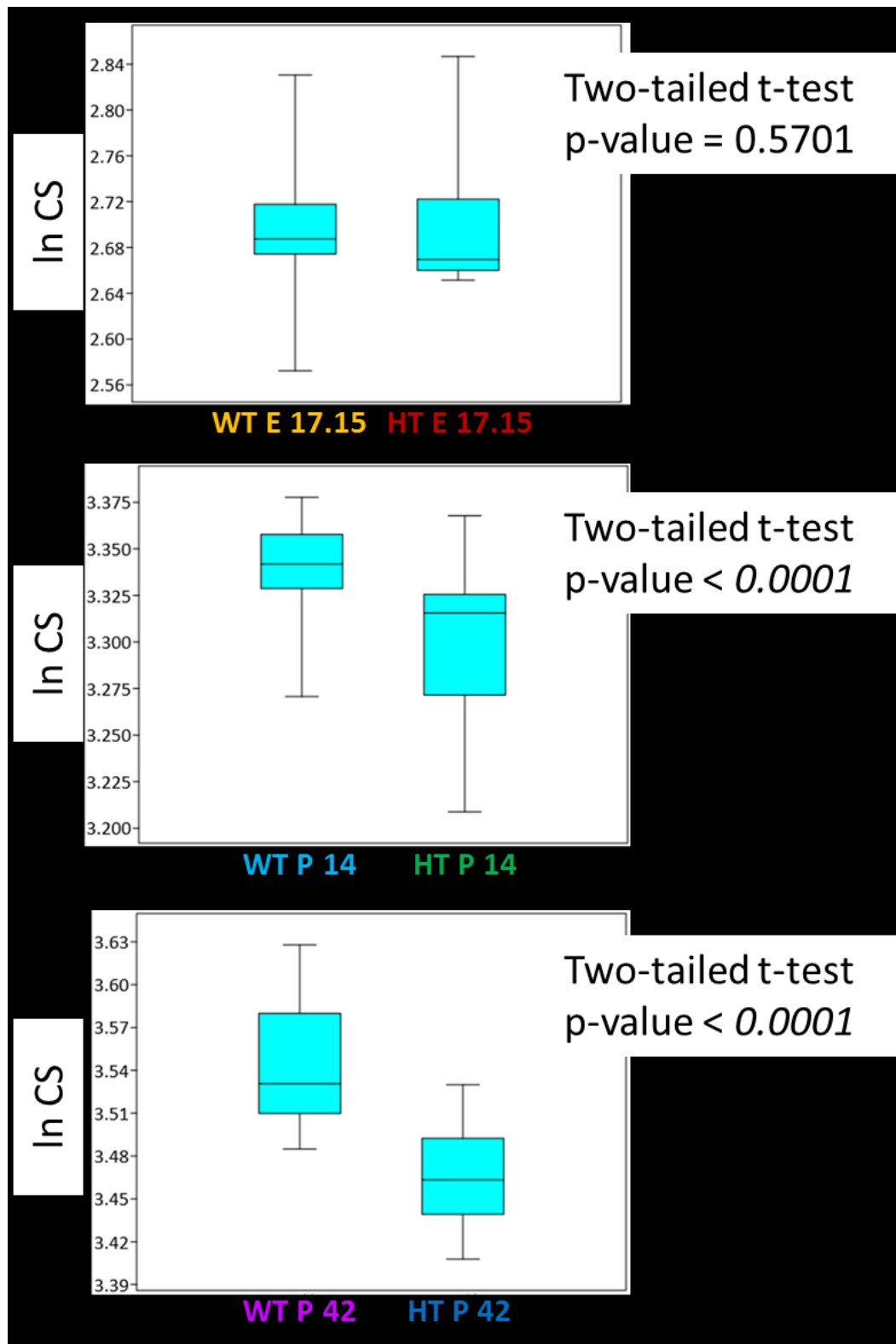


Figure 4.4 Box-plots comparing mandibular size (ln CS) between WT and HT mice within each age range. Two-tailed t-test were conducted to determine significant differences in size for A) embryonic (E 17.5) mice; B) peri-weaning (P 14) mice and; C) adult (P 42) mice

Given that both size and shape differences were found among wild-type and Crouzon mice, it is possible that size was in fact driving the degree of variation seen between the genotypes. Multivariate regressions were performed by regressing Procrustes coordinates of WT and HT mice on  $\ln$  CS within each age cohort (see Mitteroecker and Bookstein, 2009). Regressions were conducted to determine if size was significantly predicting shape among the mandibles at the three developmental stages. Significant correlations ( $p < 0.05$ ) were found between for all regressions suggesting that there is an allometric effect of size on shape between the wild-type and mutant mice. In order to correct for size, residual scores produced from the multivariate regressions were used as scaled data to supplement the original raw data. All analyses were run using both raw and scaled data.

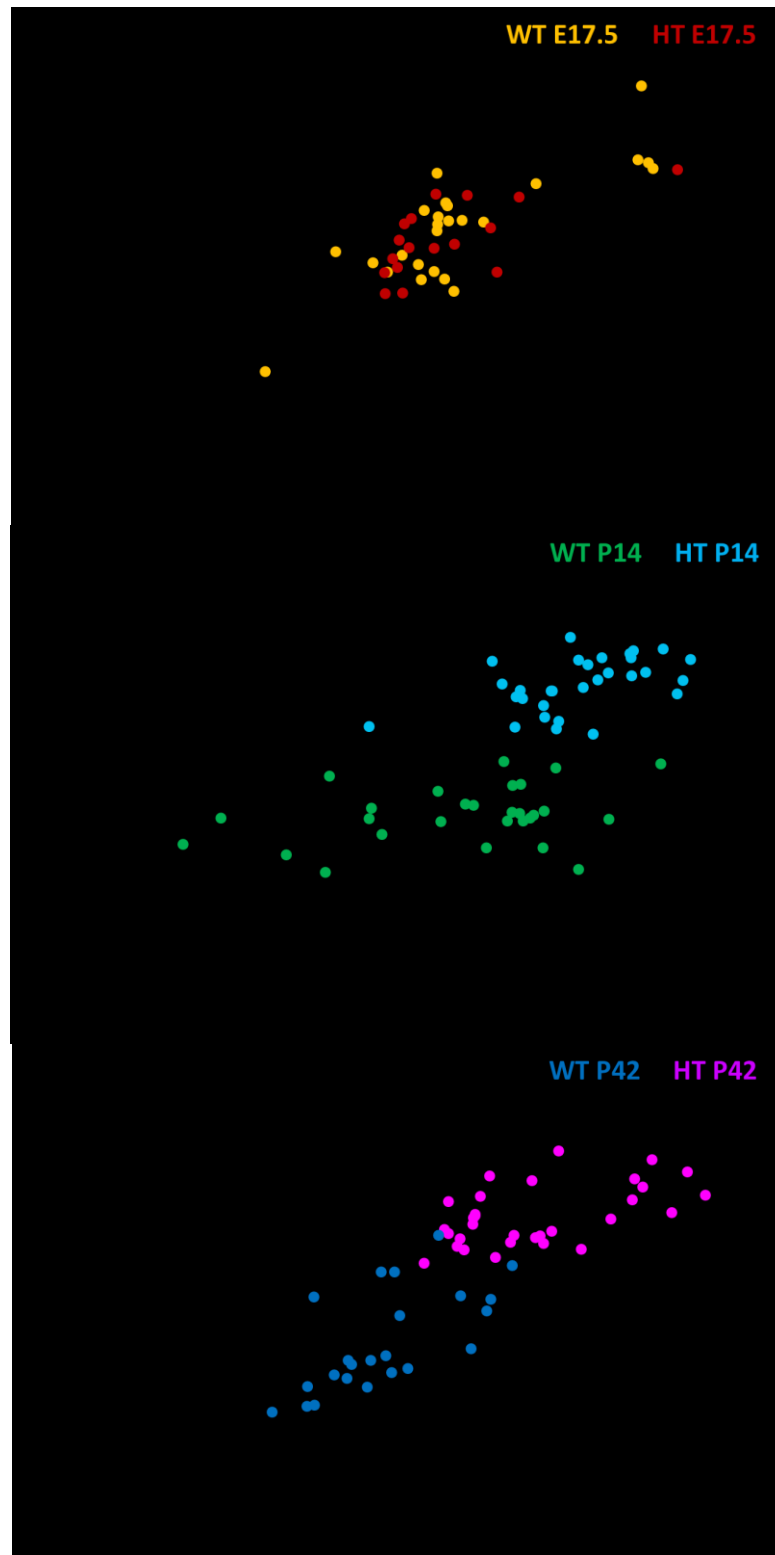


Figure 4.4 Scatterplots representing WT and HT mandibular shape change associated with static allometry within each age cohort. Shape scores were calculated from multivariate regressions of Procrustes coordinates on  $\ln$  CS (see Drake and Klingenberg, 2008).

#### 4.1.2. Patterns of Covariance across Genotypes

Patterns of covariance were investigated by comparing matrix correlations between genotypes within each age range in order to determine if the Crouzon mutation altered the way in which mandibular traits covaried. Patterns of covariance were also investigated by conducting a pooled within-group 2-Block PLS analysis (alveolar and ramal units) to see how the patterns of covariance were different/ similar between each genotype. Covariance matrix comparisons and 2-Block PLS analyses were also conducted for the JHU-only samples. Results were comparable with the whole sample so they will not be reported on here.

##### *Variance/ Covariance Matrix Correlations*

Patterns of covariance over the entire mandible were similar among genotype within each age cohort. V/CV repeatability scores from both raw and scaled data were relatively high within each age group and genotype ( $r > 0.80$ ) suggesting that measurement error was negligible enough to accurately represent the pattern of covariance present within each group. All matrix repeatability tests and observed and adjusted matrix correlation are displayed in Table 4.1. Results are significant in each circumstance ( $p < 0.0001$ ), suggesting that global mandibular covariance patterns are highly similar between WT and HT mice at each developmental stage. Comparable results with the scaled data suggest that patterns are similar regardless of the influence of allometry.

Table 4.1 Covariance matrix repeatability, observed and adjusted correlations compared between WT and HT age-cohorts. Bold values, on the diagonal, are matrix repeatability correlations, below the diagonal are observed correlation values, and above the diagonal are adjusted correlation values. All matrix correlations were significantly similar ( $p < 0.0001$ ). Matrix correlation comparisons using only the JHU bred mice resulted in statistically significant similarity among matrices. In each case, the JHU bred matrix repeatability, observed and adjusted correlations did not differ greatly from the whole-sample dataset.

RAW						
	E 17.5 WT	E 17.5 HT	P 14 WT	P 14 HT	P 42 WT	P42 HT
E 17.5 WT	<b>0.836422</b>	0.806730				
E 17.5 HT	0.6930504	<b>0.8823633</b>				
P 14 WT			<b>0.896805</b>	0.650160		
P14 HT			0.502335	<b>0.8969586</b>		
P42 WT					<b>0.885786</b>	0.655539
P42 HT					0.5833786	<b>0.8940778</b>
SCALED						
	E 17.5 WT	E 17.5 HT	P 14 WT	P 14 HT	P 42 WT	P42 HT
E 17.5 WT	<b>0.8790241</b>	0.807737				
E 17.5 HT	0.6983574	<b>0.8503836</b>				
P 14 WT			<b>0.8936888</b>	0.550972		
P14 HT			0.4829937	<b>0.8598795</b>		
P42 WT					<b>0.885217</b>	0.583764
P42 HT					0.5166177	<b>0.8847356</b>

### *Two-Block PLS*

2-Block PLS analyses were performed to determine how the Crouzon and WT mice share patterns of covariation in the mandible, using the Bi-modular model. Analyses were conducted on pair-wise comparisons of the wild-type and Crouzon genotypes within each specific age group and were pooled for genotype in order to reduce the influence of mean shape difference among WT and HT mice (Mitteroecker and Bookstein, 2008; Singh *et al.*, 2012). Scatterplots of PLS analyses were generated display the how pattern of covariation in the mandible overlapped between WT and HT mice.

As discussed previously, PLS results can be improperly biased by a difference in the degree of variance between the samples used. Therefore, the distribution of variance was calculated and then compared between WT and HT mice within each age group to determine if one group possessed a significantly greater amount of variance than the other. HT mice were found to have significantly greater amounts of variance in the peri-weaning and adult mice. Embryonic mice were not significantly different (Table 4.2). In the case of the peri-weaning and adult mice HT mice possess significantly greater amounts of variance in mandibular shape than their WT counterparts. Therefore, the Crouzon sample may be unduly influencing the signal of coordinated shape change among the alveolar and ramal regions in the peri-weaning and adult developmental stages. Interpretations are made with caution.

**Table 4.2 Calculations of observed variance for each separate age group. Bold values along the diagonal are the observed variance (SS) measures with each age. Above the diagonal are the observed absolute value differences ( $\Delta V$ ) in the variances between age groups in pair-wise comparisons.**

	Variance estimate (WT)	Variance estimate (HT)	$\Delta V$
<b>E 17.5 (raw)</b>	0.00237	0.00207	0.0003
<b>P 14 (raw)</b>	0.00110	0.00219	0.0011*
<b>P 42 (raw)</b>	0.00143	0.00502	0.0028*
<b>E 17.5 (scaled)</b>	0.00211	0.00201	0.0001
<b>P 14 (scaled)</b>	0.00069	0.00169	0.0007*
<b>P 42 (scaled)</b>	0.00122	0.00432	0.0028*

\* Indicates a significant difference in  $\Delta V$ .



PLS analyses showed that covariance between the alveolar region and the ramus was largely described along the first two PLS axes for each age group (Table 4.3 and 4.4). The same was true for raw and scaled data. As was seen in the previous 2-Block PLS analyses, the percent of covariance represented below PLS2 lies well below 5% therefore only results from the first two axes are documented here. For each age group PLS1 (80-91%) explained the largest amount of covariance between the alveolar and ramal modules, which were significantly correlated in each instance ( $r > 0.94$ ;  $p < 0.001$ ). Similarly, PLS2 (10-2%) represented a significant ( $r > 0.80$ ;  $p < 0.001$ ) extent of the coordinated shape change seen in the mouse mandible at each age range. However, this analysis was largely completed to describe the coordinated shape change shared between WT and HT that was associated with the greatest amount of covariance. Therefore, shape change solely along PLS1 will be focused on hereafter.

**Table 4.3 Pairwise correlation of 2-Block PLS scores from raw data within WT and HT age-cohorts. PLS scores are between the alveolar and ramal in the mandible, including the total percent of covariance along the first (PLS1) and second (PLS2) axes, and the accompanying correlation coefficient and significance values. PLS analyses were conducted within each age range and compared between WT and HT mice.**

<b>PLS1</b>			
	Total percent of covariance	r	p-value
<b>E17.5 (raw)</b>	79.815%	0.95563	< 0.001
<b>P14 (raw)</b>	91.112%	0.93412	< 0.001
<b>P42 (raw)</b>	90.696%	0.96348	< 0.001
<b>PLS2</b>			
<b>E17.5 (raw)</b>	10.269%	0.88093	< 0.001
<b>P14 (raw)</b>	2.730%	0.80154	< 0.001
<b>P42 (raw)</b>	4.647%	0.80509	< 0.001

**Table 4.4 Pairwise correlation of 2-Block PLS scores from scaled data within WT and HT age-cohorts. PLS scores are between the alveolar and ramal in the mandible, including the total percent of covariance along the first (PLS1) and second (PLS2) axes, and the accompanying correlation coefficient and significance values. PLS analyses were conducted within each age range and compared between WT and HT mice.**

<b>PLS1</b>			
	Total percent of covariance	r	p-value
<b>E17.5 (scaled)</b>	83.797%	0.96129	< 0.001
<b>P14 (scaled)</b>	93.184%	0.94201	< 0.001
<b>P42 (scaled)</b>	88.086%	0.96419	< 0.001
<b>PLS2</b>			
<b>E17.5 (scaled)</b>	7.366%	0.87389	< 0.001
<b>P14 (scaled)</b>	2.188%	0.80281	0.001
<b>P42 (scaled)</b>	5.582%	0.82486	< 0.001

Scatterplots of PLS1 scores from raw data show the relationship between the alveolar and ramal blocks for each age group (Figure 4.6). Specimens tend to cluster together in all plots, suggesting that WT and HT mice do not differ substantially in mandibular patterns of covariance. The overlap of both genotypes for each age group suggest that shape change associated with integration between the alveolus and ramus is occurring at the same rate across cohorts. However, both peri-weaning and adult HT mice occupy a larger portion of PLS1 axes, suggesting that they possess a broader range of covariation. It is likely that the greater dispersal along PLS1 seen in the Crouzon mandibles reflects their greater degree of variance, as shown above.

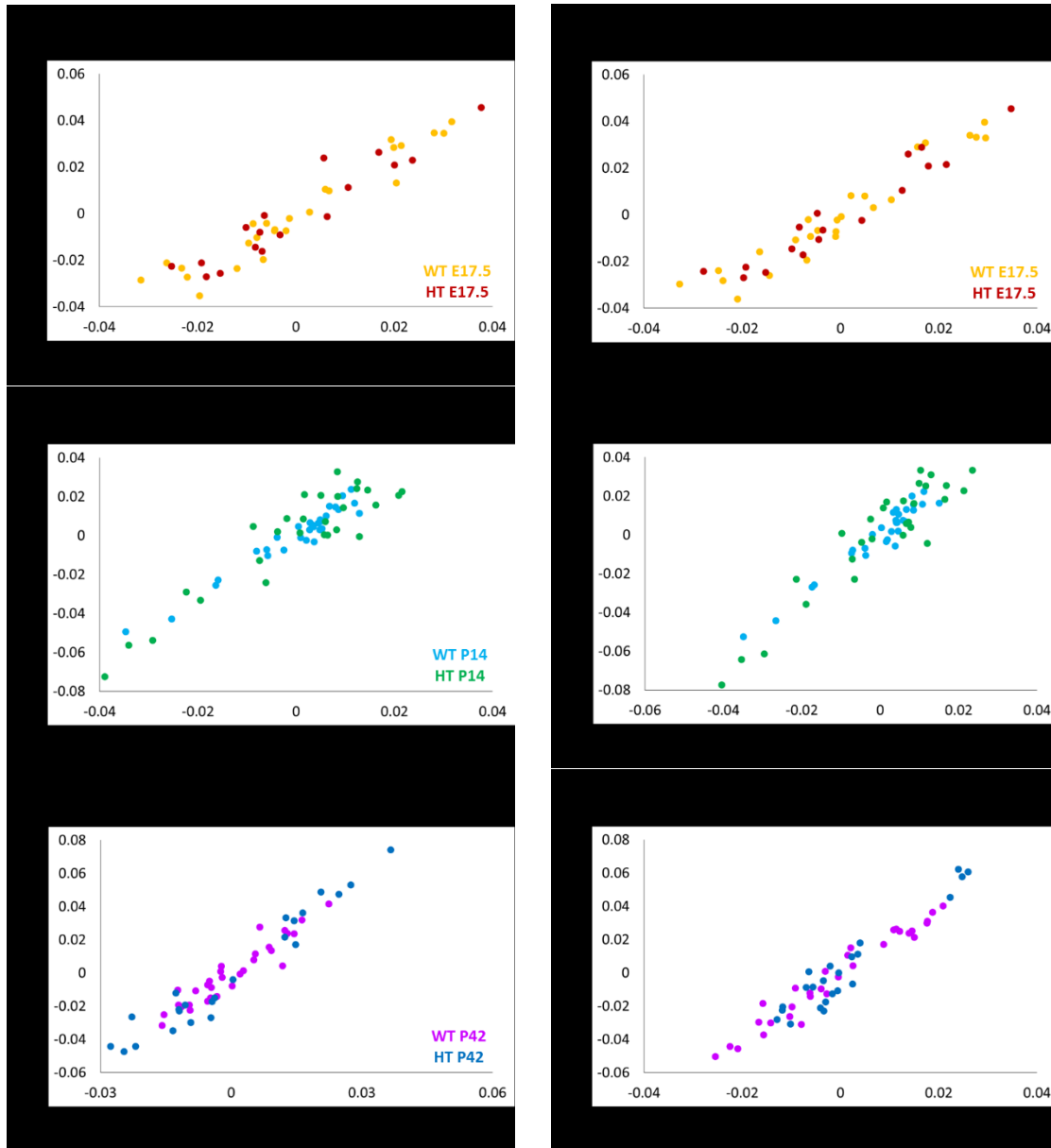


**Figure 4.6** Scatterplots of WT and HT age-cohorts for PLS1 axes scores. Scatterplots evaluate the amount of covariance shared in the Bi-modular model. Shape changes associated with patterns of integration Both raw (A – C) and scaled (D – F) datasets.

After removing allometric effects, PLS scatterplot distributions were remarkably similar for the scaled data. WT and HT mice display a considerable degree of overlap along PLS1 axes (Figure 4.6). Alveolar and ramal modules are covarying in similar ways among the WT and HT mandibles even with size removed. Again, peri-weaning and adult HT mice have wider distributions along axes of covariance which is likely a result of the larger distribution of variance found in these mice.

Figure 4.7 depicts shape changes associated with the greatest amount of covariance (PLS1 axes) for the raw and scaled data. Coordinated shape change of specimens loading highly on PLS1 are represented and a quite similar between the raw and scaled data. Beginning with the raw results for embryonic mice, the mandible covaries in much the same way between the WT and HT mice. In those specimens that load highly along PLS1, the entire incisal alveolus is displaced anteriorly as is the masseteric insertion point. At the same time the condyle, posterior border of the mandible and the angle are displaced posteriorly. Additionally, the ramus posterior to the molar row becomes narrower. Coordinated shape change after the influence of size is removed does not alter the pattern in which the alveolar and ramal regions are integrated. Covariance along the higher levels of PLS1 therefore reflects a mandible that elongates in both the alveolus and ramus and has a narrower distance between the articular condyles. This is the case whether or not there is an allometric effect.

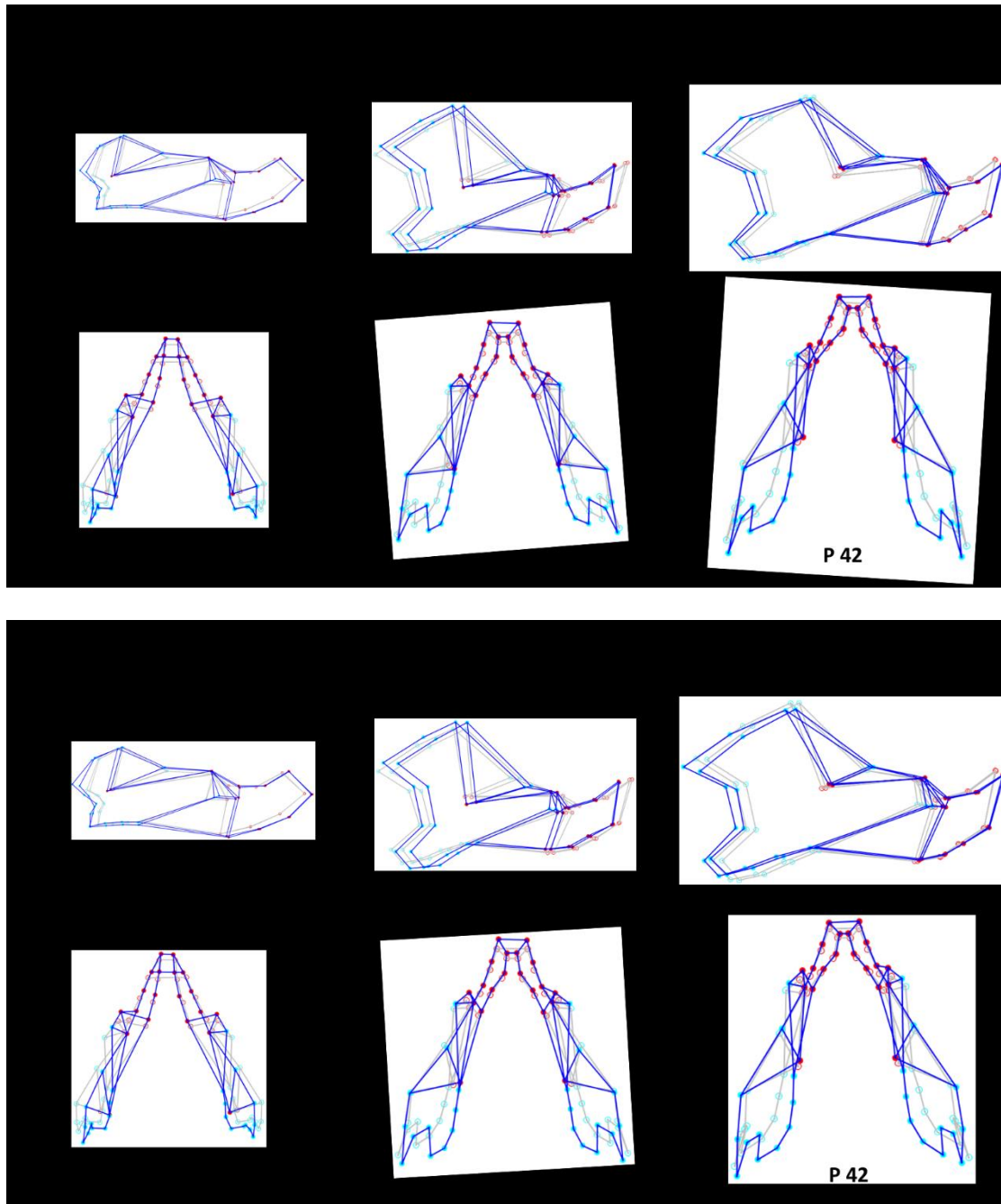


**Figure 4.7 Wireframes depicting the pattern of shape change associated with the greatest amount of covariance between the alveolar and ramal region in WT and HT age-cohort mandibles for the A) Raw PLS1 analyses and B) Scaled PLS1 analysis.**

Peri-weaning mice are similar, as well. In both WT and HT mice, those that load highly on PLS1 possess an anterior aspect of the incisal alveolus that is foreshortened. This is paired with slight anterior shift in the posterior aspect of the condyle and posterior border of the ramus. While the antero-posterior dimensions of the alveolus and ramus are modifying in conjunction with each other there are also coordinated changes in the supero-inferior direction. The junction between the coronoid and the molar alveolus displaces inferiorly while the molar row itself is shift inferiorly, however there is no change in placement of the inferior border of the corpus. At the same time the condyle and tip of the coronoid are laterally translated.

Scaled PLS analyses of the peri-weaning mice produced differences integrated shape patterns isolated to the ramus (Figure 4.6). Namely, the ramus loses some supero-inferior height between the angle and the tip of the coronoid. In fact, the inferior margin of the coronoid and the posterior aspect of the molar row are both shifted superiorly, further reducing the height of the coronoid. Lastly, the angle does not extend as far posteriorly in the scaled data, suggesting a shorter angular process. Alveolar morphological change, then, is similar in both scaled and unscaled data. However, associated shape changes in the scaled ramus result in a relative reduction in areas of muscular insertion.

Adult Crouzon and wild-type mandibles were highly integrated between the alveolus and ramus, resulting in a posteriorly displaced condyle and angle matched with an anteriorly displaced incisal tip. The molar row was superiorly translated along with a larger insertion area for the masseter by moving the attachment site anteriorly. Also,

correlated decreases in width of the posterior border of the ramus and the gonial angle are present.

Raw and scaled adult PLS analyses contrasted in a manner similar to seen in the peri-weaning mice. Differences were largely relegated to the ramus, in which height was again reduced from the tip of the coronoid to the angle. However, this reduction was more prominent in the inferiorly displaced condyle. Shape changes in the adult angle occurred in the supero-inferior dimension which also resulted in reduction of height. Lastly, depth of the body was decreased when compared to the raw data because the molar row no longer displaced superiorly.

#### 4.1.3. Magnitude of Covariance across Genotypes

Scaled variance of eigenvalues was used to compare the level of integration or covariance between Crouzon and wild-type mice within the mandible as a whole or within specific modules. Figures 4.8 – 4.10 show the way in which genotypes differ in magnitude of integration at each level. WT embryonic mice consistently exhibited significantly greater magnitudes of integration compared to their HT counterparts in all but one instance. HT mice had significantly higher degrees of covariance in the angle of the mandible than the WT mice. The same trend could be seen in the peri-weaning mice. Except for the angle, WT mice always possessed greater amounts of integration. Interestingly, the adult mice displayed a completely different SVE results. Here, the HT mandible consistently possesses statistically greater SVE values for each landmark configuration compared. Not only was magnitude constantly larger in HT mandibles, the

SVE values were almost always twice or more those found in WT mice. This suggests a dramatic ontogenetic shift in integration within the mandible between the wild-type and mutant mice.

#### Bi-module Configuration (2 partitions)

#### Mesenchymal Configuration (5 partitions)

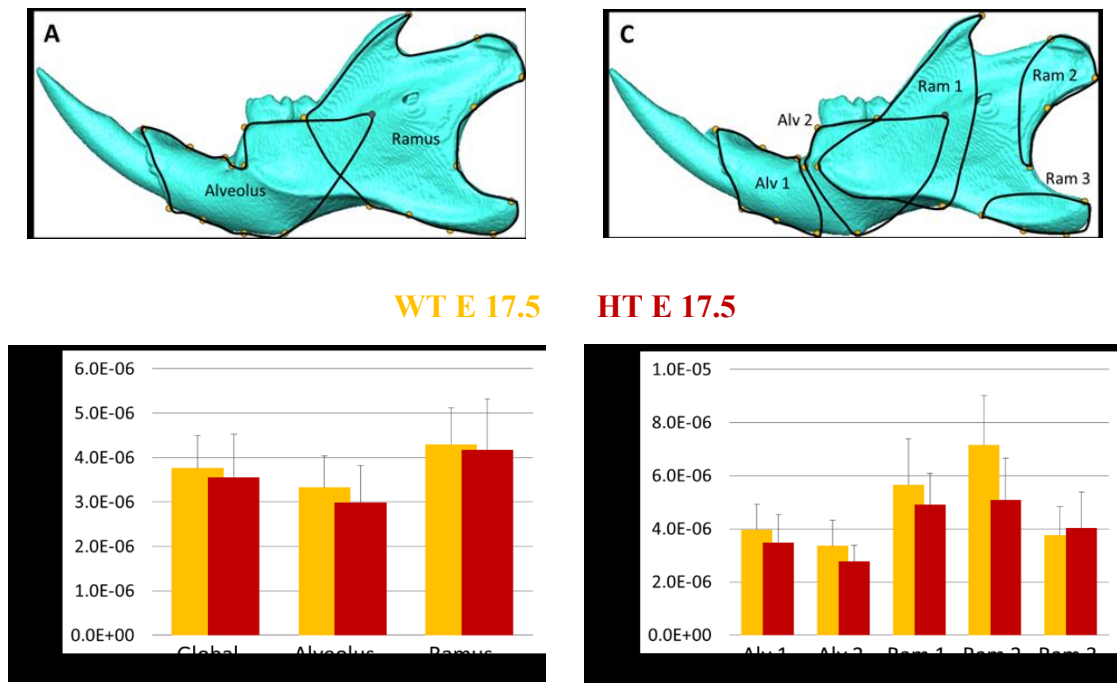


**Figure 4.8 Raw SVE scores for WT and HT embryonic (E 17.5) mice.** Three different landmark configurations were used based on the global mandible, landmarks representing the Bi-module configuration and the Mesenchymal configuration. SVE was calculated for each module and subsequently compared between WT and HT embryonic (E 17.5) mice using a bootstrap permutation test. All pair-wise comparisons were significantly different after Bonferroni correction ( $\alpha = 0.006$ ;  $p < 0.0001$ ). A) Example of Bi-module landmark configuration with alveolar (1,  $k=22$ ) and ramal (2,  $k=22$ ) partitions; B) Bar-graph showing global and Bi-modular raw SVE scores between genotype comparisons; C) Example of Mesenchymal landmark configuration with two alveolar (1,  $k=12$ ; 2,  $k=8$ ) and three ramal (1,  $k=8$ ; 2,  $k=8$ ; 3,  $k=8$ ) partitions; D) Bar-graph showing Mesenchymal SVE scores for genotype comparisons.



### Bi-module Configuration (2 partitions)

### Mesenchymal Configuration (5 partitions)

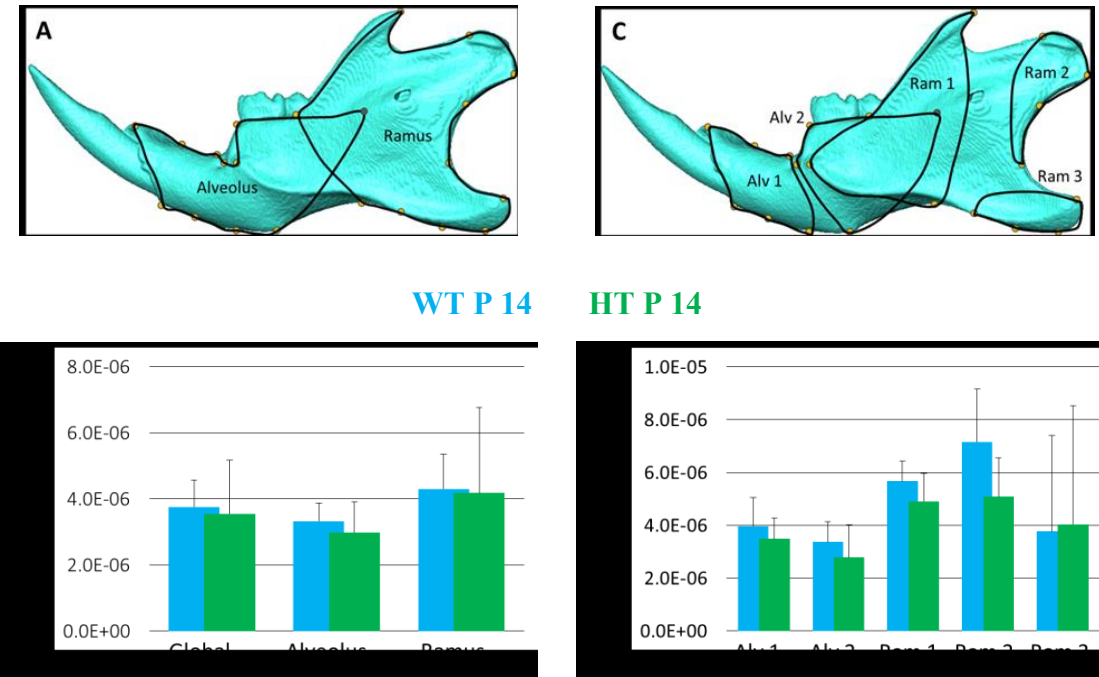
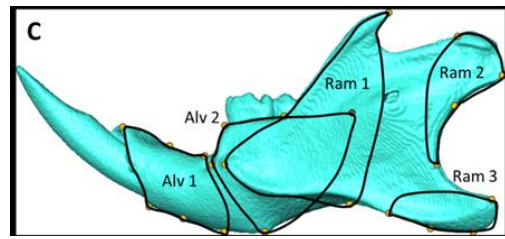
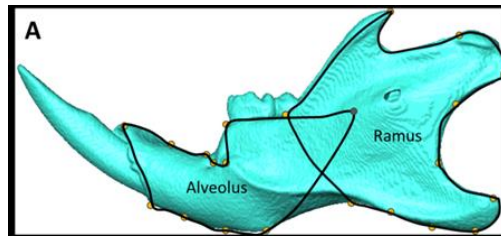


**Figure 4.9** Raw SVE scores for WT and HT peri-weaning (P 14) mice. Three different landmark configurations were used based on the global mandible, landmarks representing the Bi-module configuration and the Mesenchymal configuration. SVE was calculated for each module and subsequently compared between WT and HT peri-weaning (P 14) mice using a bootstrap permutation test. All pair-wise comparisons were significantly different after Bonferroni correction ( $\alpha = 0.006$ ;  $p < 0.0001$ ). A) Example of Bi-module landmark configuration with alveolar (1,  $k=22$ ) and ramal (2,  $k=22$ ) partitions; B) Bar-graph showing global and Bi-modular raw SVE scores between genotype comparisons; C) Example of Mesenchymal landmark configuration with two alveolar (1,  $k=12$ ; 2,  $k=8$ ) and three ramal (1,  $k=8$ ; 2,  $k=8$ ; 3,  $k=8$ ) partitions; D) Bar-graph showing Mesenchymal SVE scores for genotype comparisons.

## Bi-module Configuration (2 partitions)

## Mesenchymal Configuration (5 partitions)



WT P 42

HT P 42

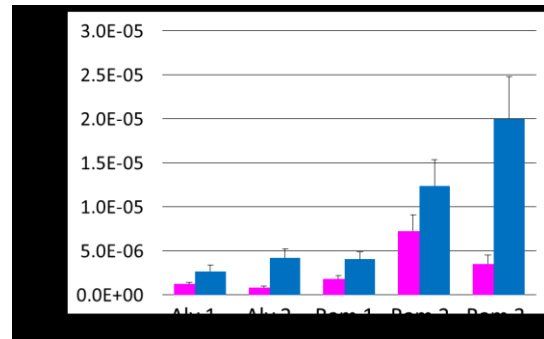
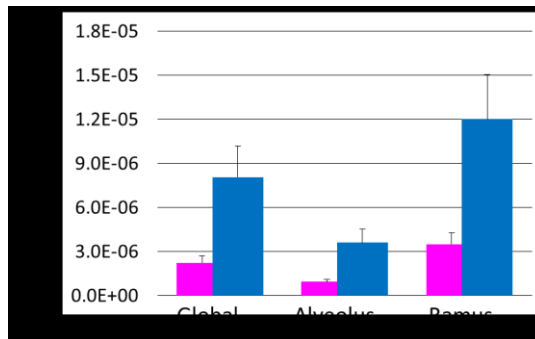


**Figure 4.10** Raw SVE scores for WT and HT adult (P 42) mice. Three different landmark configurations were used based on the global mandible, landmarks representing the Bi-module configuration and the Mesenchymal configuration. SVE was calculated for each module and subsequently compared between WT and HT adult (P 42) mice using a bootstrap permutation test. All pair-wise comparisons were significantly different after Bonferroni correction ( $\alpha = 0.006$ ;  $p < 0.0001$ ). A) Example of Bi-module landmark configuration with alveolar (1,  $k=22$ ) and ramal (2,  $k=22$ ) partitions; B) Bar-graph showing global and Bi-modular raw SVE scores between genotype comparisons; C) Example of Mesenchymal landmark configuration with two alveolar (1,  $k=12$ ; 2,  $k=8$ ) and three ramal (1,  $k=8$ ; 2,  $k=8$ ; 3,  $k=8$ ) partitions; D) Bar-graph showing Mesenchymal SVE scores for genotype comparisons.

Scaled data were not similar to the raw SVE results. It was particularly striking that once allometric effects were removed HT mandibles most often possessed greater magnitudes of covariance in the embryonic, peri-weaning and adult mice (Figure 4.11-4.13). Interestingly, as age increased so did the difference between SVE values among the WT and HT mice. This suggests that size is an integrating factor in the WT mice and possibly more so than in the HT mice given the difference in results

#### Bi-module Configuration (2 partitions)

#### Mesenchymal Configuration (5 partitions)

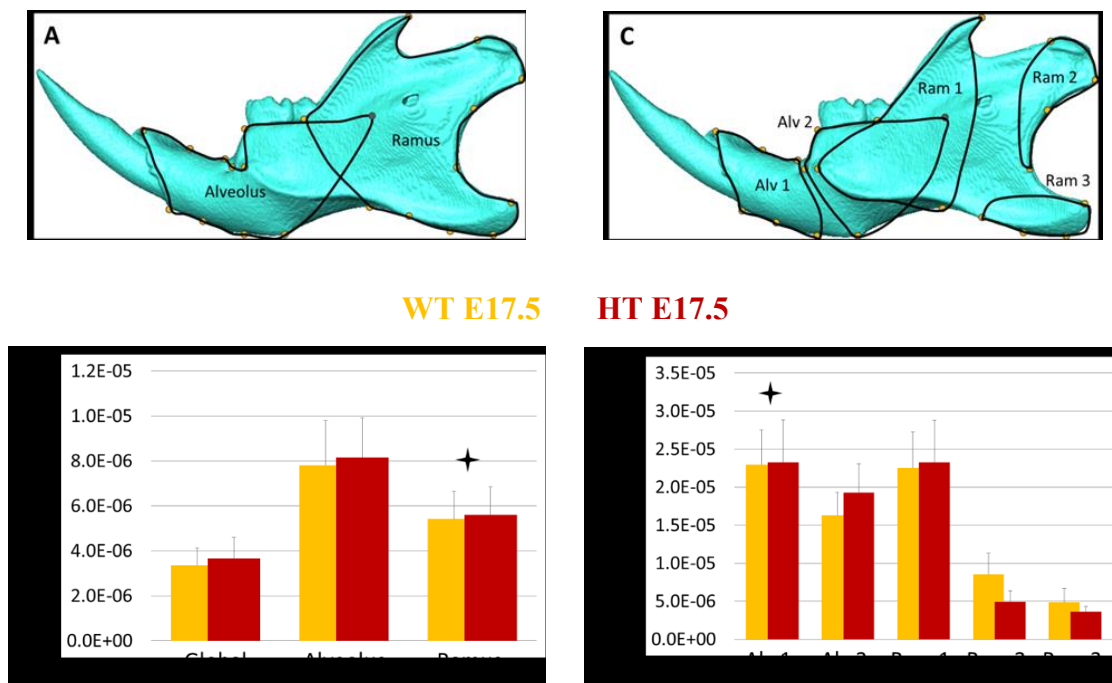


**Figure 4.11** Scaled SVE scores for WT and HT embryonic (E17.5) mice. Three different landmark configurations were used based on the global mandible, landmarks representing the Bi-module configuration and the Mesenchymal configuration. SVE was calculated for each module and subsequently compared between WT and HT embryonic (E17.5) mice using a bootstrap permutation test. An asterisk signifies a non-significant difference among groups ( $p = 0.0006$ , after Bonferroni correction). A) Example of Bi-module landmark configuration with alveolar (1,  $k=22$ ) and ramal (2,  $k=22$ ) partitions; B) Bar-graph showing global and Bi-modular raw SVE scores between genotype comparisons; C) Example of Mesenchymal landmark configuration with two alveolar (1,  $k=12$ ; 2,  $k=8$ ) and three ramal (1,  $k=8$ ; 2,  $k=8$ ; 3,  $k=8$ ) partitions; D) Bar-graph showing Mesenchymal SVE scores for genotype comparisons.

### Bi-module Configuration (2 partitions)

### Mesenchymal Configuration (5 partitions)

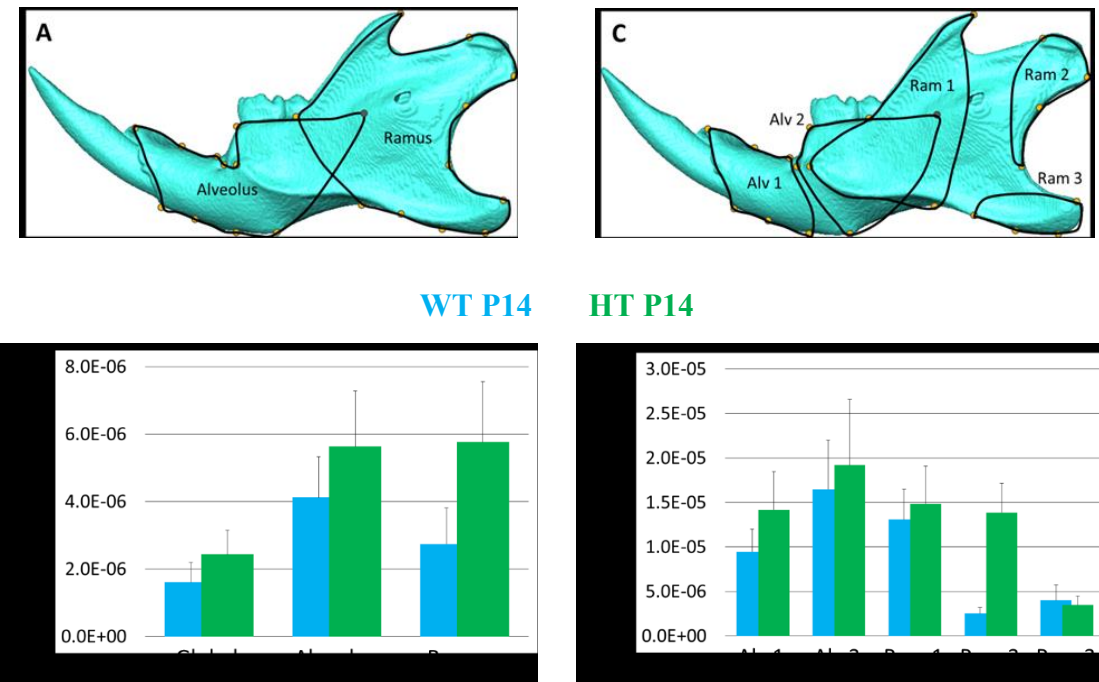


**Figure 4.12** Scaled SVE scores for WT and HT peri-weaning (P14) mice. Three different landmark configurations were used based on the global mandible, landmarks representing the Bi-module configuration and the Mesenchymal configuration. SVE was calculated for each module and subsequently compared between WT and HT peri-weaning (P14) mice using a bootstrap permutation test. An asterisk signifies a non-significant difference among groups ( $p < 0.05$ ). A) Example of Bi-module landmark configuration with alveolar (1,  $k=22$ ) and ramal (2,  $k=22$ ) partitions; B) Bar-graph showing global and Bi-modular raw SVE scores between genotype comparisons; C) Example of Mesenchymal landmark configuration with two alveolar (1,  $k=12$ ; 2,  $k=8$ ) and three ramal (1,  $k=8$ ; 2,  $k=8$ ; 3,  $k=8$ ) partitions; D) Bar-graph showing Mesenchymal SVE scores for genotype comparisons.

### Bi-module Configuration (2 partitions)

### Mesenchymal Configuration (5 partitions)

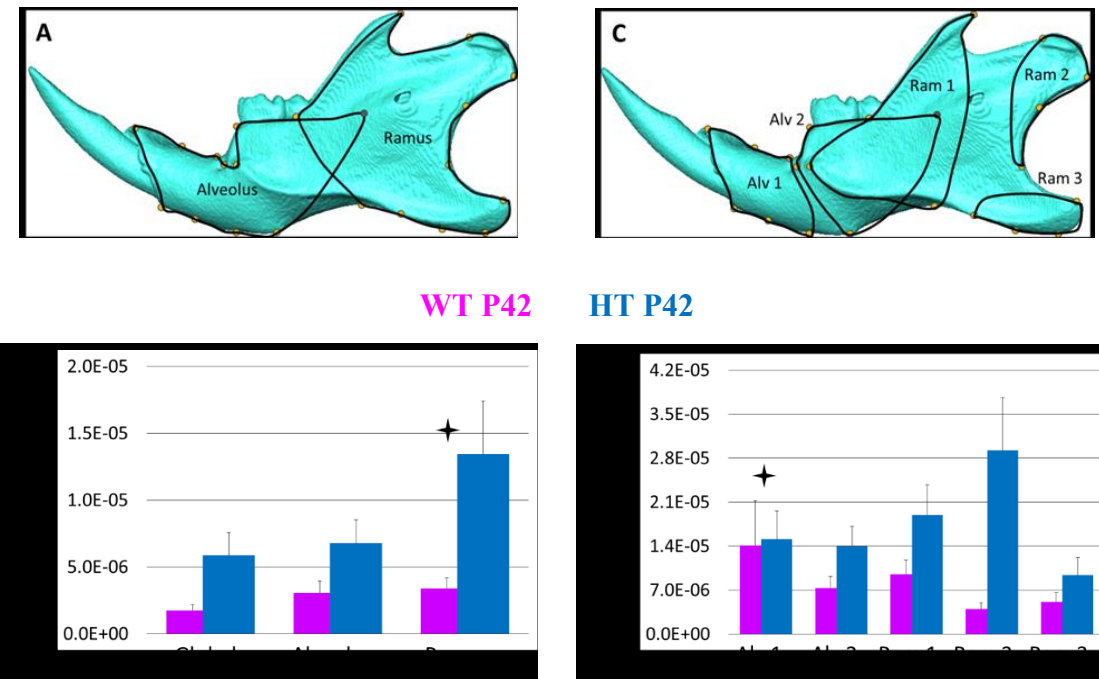


**Figure 4.13 Scaled SVE scores for WT and HT adult (P42) mice. Three different landmark configurations were used based on the global mandible, landmarks representing the Bi-module configuration and the Mesenchymal configuration. SVE was calculated for each module and subsequently compared between WT and HT adult (P42) mice using a bootstrap permutation test. An asterisk signifies a non-significant difference among groups ( $p = 0.0006$ , after Bonferroni correction). A) Example of Bi-module landmark configuration with alveolar (1,  $k=22$ ) and ramal (2,  $k=22$ ) partitions; B) Bar-graph showing global and Bi-modular raw SVE scores between genotype comparisons; C) Example of Mesenchymal landmark configuration with two alveolar (1,  $k=12$ ; 2,  $k=8$ ) and three ramal (1,  $k=8$ ; 2,  $k=8$ ; 3,  $k=8$ ) partitions; D) Bar-graph showing Mesenchymal SVE scores for genotype comparisons.**

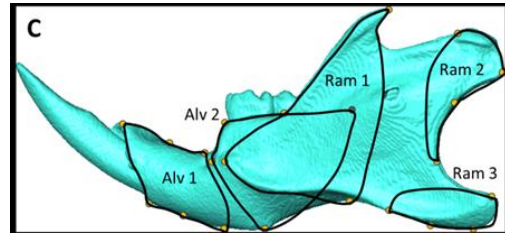
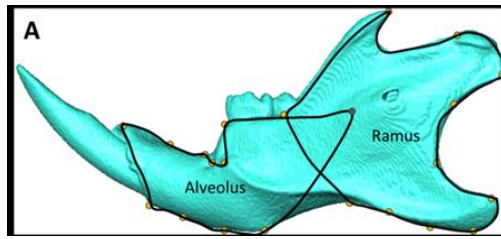
### *JHU Mice*

Discrepancies also appear among colony samples when comparing raw data. Results from SVE comparisons between WT and HT mice of the JHU-only sample drastically changed. SVE values for HT JHU-only mice become significantly larger than the WT JHU-only mice in many instances (Figure 4.14 and 4.16). Removing variance introduced by the WashU sample increases the degree of covariance in the embryonic HT mandibles overall. It also increases in the Mesenchymal ramal modules.

Analyses using the whole sample showed that in embryonic and peri-weaning mice, WT were more integrated than HT mice in most cases. In the JHU-only analyses however, HT mice possess significantly greater magnitudes of covariance than their WT littermates. Interestingly, results from the adult mice do not differ greatly between sample types (Figure 4.X). One explanation may be that variance contributed by the WT WashU mice increases the covariance in the larger JHU-only WT sample. It is also possible that patterns of covariance are ever so slightly different between the HT colonies and that this diminishes the SVE values for the whole sample because covariance is distributed over more principal component axes.

### Bi-module Configuration (2 partitions)

### Mesenchymal Configuration (5 partitions)



WT E 17.5

HT E 17.5

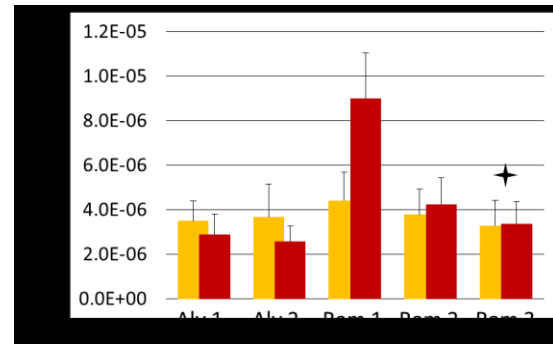
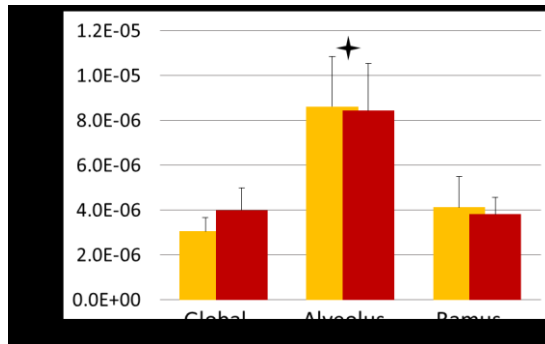


**Figure 4.14 SVE scores for JHU bred WT and HT embryonic (E 17.5) mice. Three different landmark configurations were used based on the global mandible, landmarks representing the Bi-module configuration and the Mesenchymal configuration. SVE was calculated for each module and subsequently compared between WT and HT embryonic (E 17.5) mice using a bootstrap permutation test. An asterisk signifies a non-significant difference among groups ( $p = 0.0006$ , after Bonferroni correction). A) Example of Bi-module landmark configuration with alveolar (1,  $k=22$ ) and ramal (2,  $k=22$ ) partitions; B) Bar-graph showing global and Bi-modular raw SVE scores between genotype comparisons; C) Example of Mesenchymal landmark configuration with two alveolar (1,  $k=12$ ; 2,  $k=8$ ) and three ramal (1,  $k=8$ ; 2,  $k=8$ ; 3,  $k=8$ ) partitions; D) Bar-graph showing Mesenchymal SVE scores for genotype comparisons.**

### Bi-module Configuration (2 partitions)

### Mesenchymal Configuration (5 partitions)

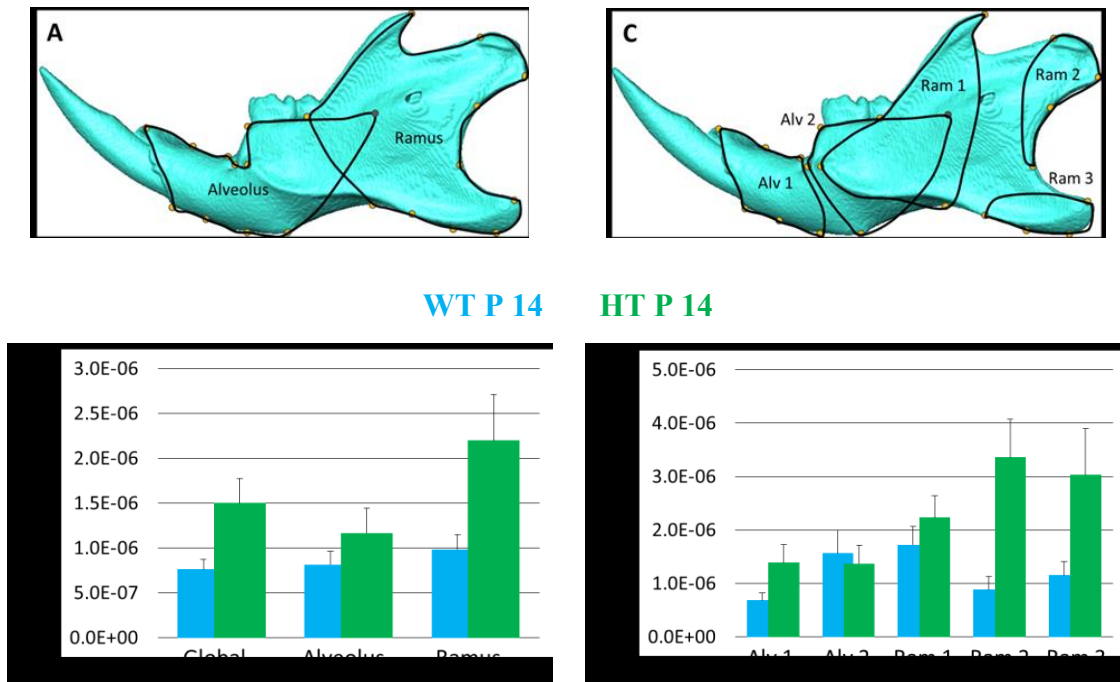


**Figure 4.15** SVE scores for JHU bred WT and HT peri-weaning (P 14) mice. Three different landmark configurations were used based on the global mandible, landmarks representing the Bi-module configuration and the Mesenchymal configuration. SVE was calculated for each module and subsequently compared between WT and HT peri-weaning (P 14) mice using a bootstrap permutation test. All pair-wise comparisons were significantly different after Bonferroni correction ( $\alpha = 0.006$ ;  $p < 0.0001$ ). A) Example of Bi-module landmark configuration with alveolar (1,  $k=22$ ) and ramal (2,  $k=22$ ) partitions; B) Bar-graph showing global and Bi-modular raw SVE scores between genotype comparisons; C) Example of Mesenchymal landmark configuration with two alveolar (1,  $k=12$ ; 2,  $k=8$ ) and three ramal (1,  $k=8$ ; 2,  $k=8$ ; 3,  $k=8$ ) partitions; D) Bar-graph showing Mesenchymal SVE scores for genotype comparisons.



### Bi-module Configuration (2 partitions)

### Mesenchymal Configuration (5 partitions)

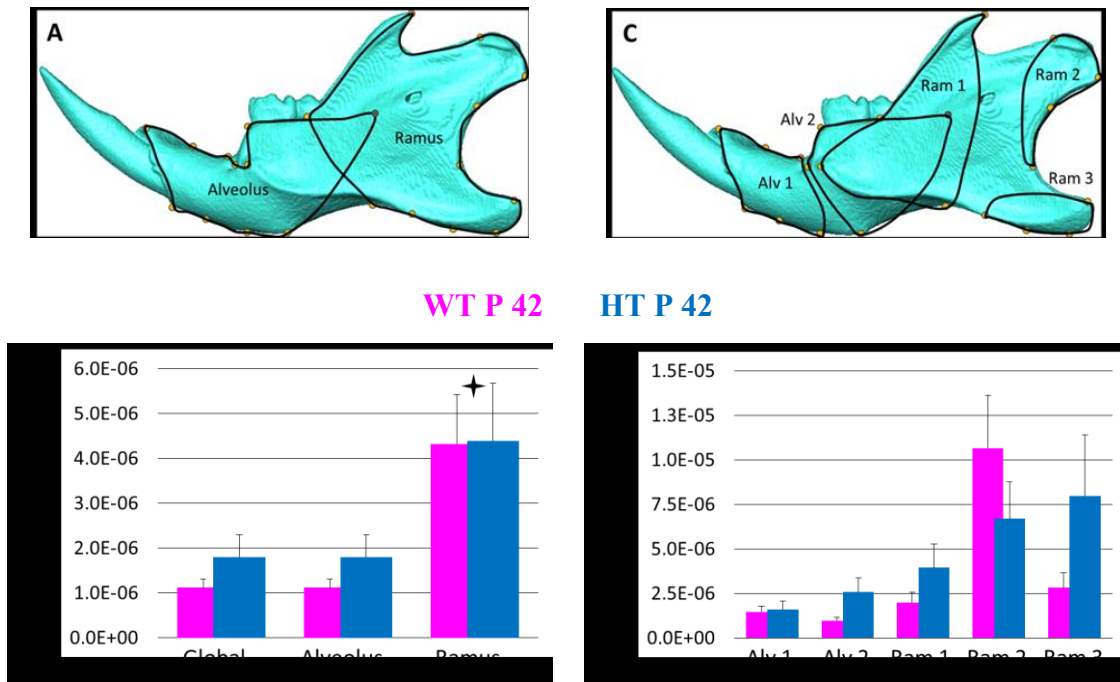
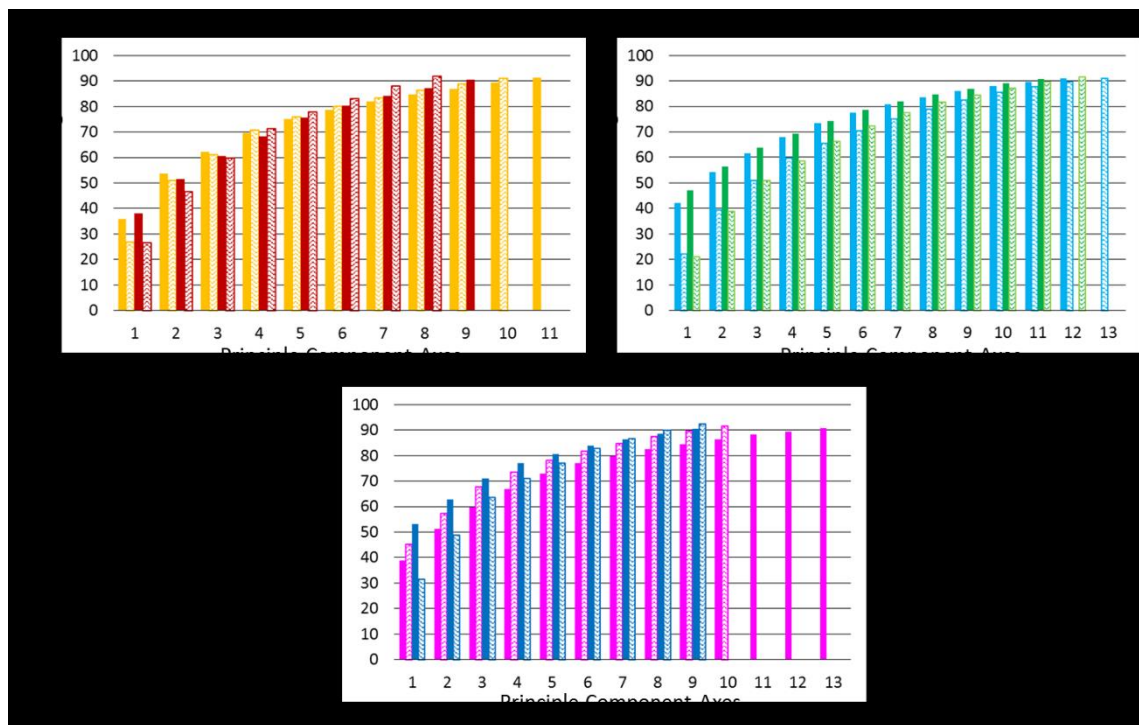


**Figure 4.16** SVE scores for JHU bred WT and HT adult (P 42) mice. Three different landmark configurations were used based on the global mandible, landmarks representing the Bi-module configuration and the Mesenchymal configuration. SVE was calculated for each module and subsequently compared between WT and HT adult (P 42) mice using a bootstrap permutation test. An asterisk signifies a non-significant difference among groups ( $p = 0.0006$ , after Bonferroni correction). A) Example of Bi-module landmark configuration with alveolar (1,  $k=22$ ) and ramal (2,  $k=22$ ) partitions; B) Bar-graph showing global and Bi-modular raw SVE scores between genotype comparisons; C) Example of Mesenchymal landmark configuration with two alveolar (1,  $k=12$ ; 2,  $k=8$ ) and three ramal (1,  $k=8$ ; 2,  $k=8$ ; 3,  $k=8$ ) partitions; D) Bar-graph showing Mesenchymal SVE scores for genotype comparisons.

In order to assess why so many discrepancies were found in the SVE data depending on which sample was used, the greatest amount of variance within each sample was investigated through principal component analyses of the global landmark configuration. Figure 4.17 shows how many principal component axes explain ~90% of variance for each age group, genotype and colony. There is a clear difference between the WT and HT sample. PCA percentages of both colonies and the JHU-only sample show that the degree of variance is distributed over a smaller number of axes in the HT mice.

This negates the explanation that when using both colonies, WashU HT mice introduce a degree of variance that clouds the magnitude of covariance. Because covariance matrices did not differ among WT or HT mice, whether using either colonies or just the JHU sample, it is unlikely that a difference in the pattern in which traits covary is causing this discrepancy. A comparison of magnitude between colonies within each age group may be beneficial; however, the WashU sample size is quite small that it may be difficult to retrieve reliable results.



WT E 17.5    HT E 17.5    WT P 14    HT P 14    WT P 42    HT P 42

**Figure 4.17** Histogram showing the distribution (up to 90%) of the percent of variance over principle component axes for mouse colonies. A) E 17.5 WT and HT mice; B) P 14 WT and HT mice; and C) P 42 WT and HT mice. Solid bars represent data from both mouse colonies. Lined bars represent data from the JHU only mouse colony. Percentages are cumulative values.

## 4.2. Discussion

### 4.2.1 Dynamic interaction of shape and size between the WT and HT mice.

PCA plots, as well as tests of Procrustes distance and size differences among WT and HT mouse mandibles, reveal a dynamic relationship of size and shape between these two genotypes. Both size and shape develop greater degrees of divergence as the mice age. Embryonic mice are the most similar in size and shape of the age groups. Though Procrustes distances were significantly different between genotype they were much smaller than those seen in the older mandibles. This is further exemplified in the overlap between WT and HT mice. Furthermore, mandibular size (ln CS) is not significantly different between the two. Procrustes distance is also significantly different in the peri-weaning and adult mandibles and that distance becomes greater at each age interval. The same trend is discernable in size differences. The wild-type mice continue to outpace Crouzon mandibles in size. WT mandibles are significantly larger and become even bigger from peri-weaning to adulthood.

Shape differences among WT and HT mice follow the sparse orthodontic research that exists on the Crouzon mandible in humans. Kreiborg (1981a) noted a decrease in mandibular length which was also found in a morphometric analysis of overall shape in Crouzon mice (Perlyn *et al.*, 2006a). Another morphometric analysis by Cutting *et al.*, (1995) documented lateral flaring of the ramus, anterior displacement of the coronoid notch and labial surface concavity in human adult Crouzon mandibles. In the morphological analyses completed here the Crouzon mandible possessed an antero-medially shorter body overall with a relatively narrower distance between the condyle and coronoid. The Crouzon mandible is deeper supero-inferiorly along the molar row

and has a wider bi-condylar distance. The ramus in HT mice is taller and the angle is more robust. Lastly, orthodontic research related to growth of the mandible in patients with Crouzon syndrome have noted an anterior rotation of the mandible which was not seen in the specimens here (Meazzini *et al.*, 2005, but see Wery *et al.*, 2015). The lack of perceived anterior rotation is likely due to two factors: first, anterior rotation in orthodontic studies is often related to the mandibles position relative to the basicranium and mid-face which were not included in from the study here and therefore could not be assessed. Second, the relationship between the cranial base and mandible will be inherently different between mice and humans because the cranial base is highly flexed in the latter. Thus, the resultant change in orientation seen in the mandible of human Crouzon patients may not necessarily be reflected in the mice that possess a much flatter basicranium (Lieberman *et al.*, 2000; 2008).

Kreiborg (1981b) claimed that normal growth of the mandible seen in adolescent Crouzon patients suggests that any difference in mandibular size is related to occlusal tracking of the retracted maxilla. However, Eswarakumar *et al.*, (2004) stated that any decrease in size is related to overall decrease in bone size noted throughout the rest of the skull due to disturbance in osteogenesis inflicted by the mutation. Pre- and post-operative studies of facial growth in patients that have experienced corrective surgery (e.g. Le Fort III osteogenic distraction) also report conflicting claims regarding the dependence that mandibular growth has on maxillary growth (Kaban *et al.*, 1987; David *et al.*, 1990; Meazzini *et al.*, 2005; Ahmed *et al.*, 2009; Shetye *et al.*, 2010; Wery *et al.*, 2015). It is likely that a portion of mandibular size and shape effects in the Crouzon mouse sample used here is dependent on maxillary and basicranial growth. However, due to the

continued growth of the mandible, even with the presence of a retrognathic maxilla, it is unlikely to be completely dependent. Thus other avenues of shape change must be considered here.

### *Possibilities Creating Mandibular Shape Divergence*

Several scenarios may result in the exacerbation of differences in mandibular size and shape between WT and HT mice. It is possible that this difference is due to timing of the disturbance in bone growth, to continued facial growth or perhaps due to the addition of deviant distribution of mechanical loads. Secondary cartilaginous scaffolds at the angle, coronoid and condyle are still present in the embryonic mice so it is clear that bone growth and ossification is not yet complete at this stage. It is possible that disturbance in bone growth caused by the *Fgfr2*<sup>+/C342Y</sup> mutation is not severe enough at this point to create size discrepancies among the mice. However, it does already produce at least a small divergence in shape. The larger discrepancies witnessed as age progresses could merely be a consequence of a later onset of perturbation of bone growth in the mandible. This would certainly comply with the arguments made by Eswarakumar *et al.*, (2004) and the inhibited growth seen in the rest of the cranium. A more accurate analysis would require a histological examination of osteogenic proliferation and differentiation in the mandible at these stages.

Interdependence between the mandible and the basicranium and face has been documented across Mammalia (e.g., Bastir and Rosas, 2005; Bastir *et al.*, 2006). Furthermore, mammals are known for prolonged facial growth in relation to basicranial growth (Baughan *et al.*, 1979; Buschang *et al.*, 1983; Enlow and Hans, 1996). Ongoing

changes in mandibular shape and size and the divergence between the two genotypes used here may be partially related to continued craniofacial growth. For instance, the bi-condylar width of the HT mandibles is likely the result of wider basicranial distances found among Crouzon skulls (Perlyn *et al.*, 2006a). In order to maintain a viable articulation at the temporomandibular joint, width of the mandible must match width of the cranium. In a ontogenetic study of *Fgfr2*<sup>+/*C342Y*</sup> mouse skulls DeLeon *et al.*, (2009) suggest that the primary defect contributing to craniofacial dysmorphology resides in the anterior cranial base (but see Martínez-Abadías *et al.*, 2013). Pre-natal fusion of sutures in the cranial base contribute to the brachycephaly that emerges later during post-natal ontogeny. In the face, this results in maxillary retraction during post-natal growth. Analyses of dysmorphic traits in other FGFR mutations (*Fgfr2*<sup>+/*S252W*</sup> and *Fgfr2*<sup>+/*P253R*</sup>) have pointed to localized suture closure within the face itself as another factor contributing to facial retraction or even cleft palate (Martínez-Abadías *et al.*, 2010). Certainly, a portion of shape variance seen in the Crouzon mandible is related to the early and ongoing dysmorphic cranial growth. However, the mandible possesses its own growth trajectory and it is unlikely that mandibular size and shape is solely dependent on the maxilla and cranial base.

Another factor that may play a role in the accumulated divergence of mandibular size and shape is the introduction of biomechanical loads on the mandible. The pattern of bone resorption and deposition depends largely on the orientation of muscle and bone involved in mechanical loading, as well as the type of mechanical loading that occurs (i.e. compression vs strain). Contrasts between WT and HT mandible size and shape have already been established by the peri-weaning developmental stage used suggesting that

alterations between WT and HT mandibles occur pre-weaning. Such an early divergence may alter the position of muscular attachment and direction in which stress and strain are distributed through the mandible. The introduction of mechanical loads may continue to alter the already divergent shapes. In actuality, the persistent changes in mandibular size and shape are likely a constellation of all these factors.

#### 4.2.2 Only Magnitude of Covariance is Altered Between Wild-type and Crouzon Mice

The second set of developmental hypotheses ( $H_{MTA-B}$ ) revolved around discernable modification of covariance structure in the Crouzon mice relative to the wild-type controls.  $H_{MTA}$  null hypothesis of complete dissimilarity between WT and HT patterns of covariance mice of all age groups can be fully rejected given the high and significant matrix correlation values. Similarly,  $H_{MTB0}$  tested the null hypothesis that magnitudes of mandibular covariance would be similar between WT and HT mice throughout ontogeny and can also be rejected because SVE analyses revealed consistent differences in the magnitude of covariance in every age group and at all modular levels. The following sub-hypotheses were more nuanced.  $H_{MTB1}$  conjectured that magnitude would be significantly greater in HT mandibles and thereby smaller in WT mice.  $H_{MTB2}$  went further and stated that significance would disappear as post-natal influences of developing dentition and diet changed covariance in the mandible. Results for these hypotheses varied depending on whether the raw, scaled or JHU-only data sets and are discussed in more detail below.

*Fgfr2<sup>+ / C342Y</sup> and wild-type mice possessed similar patterns of covariance*

Variance/ Covariance matrix comparisons among age-matched WT and HT mice were all statistically significant and generally well correlated. Thus the null hypothesis of complete dissimilarity is rejected; despite the *Fgfr2<sup>+ / C342Y</sup>* mutation patterns of covariance were similar. This suggests that coordinated shape change is maintained within the mandible. In other words, the same traits within the mandible are covarying in the same manner across genotypes.

Previous comparisons of covariance matrices between adult transgenic mice and their wild-type littermates have shown differing results. Hallgrímsson *et al.*, (2007) compared patterns of covariance in the cranium of a number of mutant and wild-type littermate pairings. In each case V/CV matrix correlations were quite low (0.33- 0.34) were not found to be similar. Jamniczky and Hallgrímsson (2009) later conducted a study in which both pattern of covariance was compared in rodent crania that agrees with the results found here. The sample was unique among many of the studies mentioned here in that it included a large sample of multiple wild mice, along with wild-type and mutant laboratory mice. Patterns of covariance were found to be statistically indistinguishable between wild mice and laboratory mice, including mutants, suggesting that patterns of covariance are relatively conserved.

Martínez-Abadías *et al.*, (2011) looked at two other FGF/FGFR mutations *Fgfr2<sup>+ / S252W</sup>* and *Fgfr2<sup>+ / P253R</sup>*. In a similar comparison of matrix correlations, cranial patterns of covariance were maintained between mutant and non-mutant littermates. Disturbances in development, whether it be in neural crest migration, osteogenic or chondrogenic differentiation, somatic growth, etc., will not affect the structure of



covariance in the same way. Covariance-generating processes may either affect each of the traits in a structure equally or could have a stronger influence on one trait over another. Results are persistent between this study and others; *Fgfr2* mutants and wild-type littermates possess similar patterns of covariance in the cranium and mandible.

Taking a closer look at Bi-modular model, the ramus and alveolus are integrated in the same way across genotypes. Interestingly, the pattern of shape change associated with largest axes of covariance seems to represent key characteristics of developmental stages. PLS analyses revealed that integrated shape change in embryonic mice was related to antero-posterior axis of the mandible relative to width, simply highlighting the initial attainment of size as dental buds are developing and osteogenesis continues at the secondary cartilages. Peri-weaning mice demonstrate expansion of ramal processes and change in curvature of the incisal alveolus. This may reflect persistent growth of the ramus and dental eruption. Lastly, adult integrated morphology results in shape change largely in depth of the molar alveolus and further enlargement of the ramus. This may be relaying the effect of fully grown molar roots and the effect of mechanical loading.

#### *Signals of integration are complex in the Crouzon mandible*

According to the Palimpsest model, if a developmental factor is significantly contributing to patterns of covariance, than any added amount of variance due to the introduction of some perturbation would channel that variance along the axes of covariance. Additive amounts of variance concentrated along axes that explain the largest measures of covariance would then inherently increased the strength of covariance

detectable (Hallgrímsson *et al.*, 2009). Indeed, in the Jamniczky and Hallgrímsson (2009) study referred to above, they found that mice possessing separate craniofacial mutations also had significantly greater magnitudes of integration when compared to wild muroids and wild-type lab mice. Results from the analyses completed here only partially agree with earlier studies.

Alternative hypotheses presented in this project originally speculated that *Fgfr2* mutation would be significantly greater magnitudes of integration, especially in the younger specimens. However, looking at results derived from the raw data set, this is not the case. Sub-adult HT mice possesses significantly weaker amounts of integration in the mandible as a whole and within smaller modules. Not until adulthood do the HT mice display greater magnitudes of covariance, in which SVE values were almost always twice as great as their WT counterparts. This would suggest that the perturbation generated by the *Fgfr2* mutation is significantly contributing to the pattern of covariance but only later in ontogeny.

Unscaled data do not support the hypothesis that differences between HT and WT mice would be stabilized because of the introduction of adult diet. It was presumed that the introduction of a covariance generating factor that would be comparable between the two genotypes, chewing the same diet, would prompt similar degrees of coordinated bone remodeling in response to similar biomechanical loads. Comparable loads and coordinated bone remodeling would produce similar levels of integration within the mandible and mask any previous differences in magnitude. However this was not the case. Conversely, these results do support early outcomes from this study that demonstrated continued separation in size and shape of the mandible between the WT

and HT mice. In the previous section it was conjectured that divergence could be due to the introduction of function on mandibles that had differencing lever mechanics due to size and shape discrepancies, differences in muscular insertion, as well as occlusion.

Different ontogenetic trends in the strength of covariance in the mandible are produced when two separate sources of variance are removed from the dataset, size and the influence of colony. When the effect of allometry is removed, scaled data show that HT mice consistently possess greater amounts of integration in the mandible, suggesting that the influence of the *Fgfr2* is present at all developmental stages, rather than just in adult hood. This would agree with other analyses of covariance in the skull of mice with *Fgfr2* mutations. Martínez-Abadías *et al.*, (2011) found that two *Fgfr2* mutations demonstrated greater degrees of covariance in the skull than their wild-type littermates. Data for their project was scaled in the same manner as the data here. That paper in combination with this study would suggest that in fact *Fgfr2* signaling developmental pathway is significantly contributing to the generation of covariance within the entire cranium, both skull and mandible.

Similarly, colony choice significantly impacts the results and conclusion of this study. The JHU-only sample results also demonstrate larger magnitudes of covariance in the HT mandibles within each ontogenetic stage. Future analyses should determine whether use of specimens from multiple colonies conflates the signal of covariance structure. Furthermore, this reinforces the importance of using an ontogenetic sample when investigating the structure covariance because the trends found in the adult sample may not represent what is occurring during growth and development.

#### 4.2.3 Summary

The *Fgfr2*<sup>+/*C342Y*</sup> mutation manifests in the mouse mandible in a similar manner as that to human patients with Crouzon syndrome. Dysmorphic morphology is also combined with an overall reduction in size. Despite these differences, the pattern of covariance is maintained within the mandible between wild-type and Crouzon mice suggesting that the way in which mandibular traits covary is conserved. Magnitude on the other hand, does seem to be affected by the mutation though the extent to which is unclear. Whether interpreting raw or scaled data, magnitude of covariance is at one point larger in HT mice further supporting the important role FGF/FGFR signaling pathways in the development of the head. Whether using raw, scaled or colony-specific data, timing of this trend is the largest discrepancy making further interpretations difficult. Future analyses will need to explore the role of colony and size on the strength of covariance in the Crouzon mandible to further clarify these relationships.

#### *Future Directions*

- 1) Integrate mandibles from other colonies using both WT and HT to determine if colony continues to have a significant effect on the magnitude of covariance.
- 2) Explore the degree of integration present between the basicranium and face with the mandible in Crouzon mice.



## Chapter 5: Results and Discussion – Functional Hypotheses

### 5.1. Results

#### 5.1.1. Shape Variation

A PCA scatterplot of all pooled primate genera can be seen in Figure 5.1. The majority of shape variation is explained along PC1 (70.728%) and a clear delineation of each genus can be seen. PC2 explains 8.08% of variation in this sample; however, only *C. torquatus* and *P. pithecia* separate along PC2. Interestingly, the two primate species with the hardest documented diets (*Cebus* and *Pithecia*) tend to group closest on PC1 while their phylogenetic cohorts are widely separated. Variation in shape along PC1 is concentrated in the height of the coronoid and condyle and bi-condylar width. Additionally it concentrates on the depth, curvature and flare of the gonial angle; as well as antero-posterior displacement of the symphysis and mandibular foramen. Cebid mandibles, with higher PC1 scores, are both wider and shorter than Pitheciines with a longer mandibular corpus. Pitheciines, in contrast, possess a much rounder, deeper gonial angle, as well as a shallower symphysis.

Procrustes distance comparisons between members of each separate cohort determined that shape differences were, in fact, significant ( $p < 0.001$ ). Wireframe deformations of shape change on PC1 within each cohort are shown in Figure 5.2 along with Procrustes distances. Within cebids, shape differences generally reflect the robusticity and gracility commonly associated with *Cebus* and *Saimiri*, respectively. *Cebus* possesses a taller mandibular ramus and corpus with a pronounced gonial angle. In addition, the corpus is foreshortened and rotated superiorly.

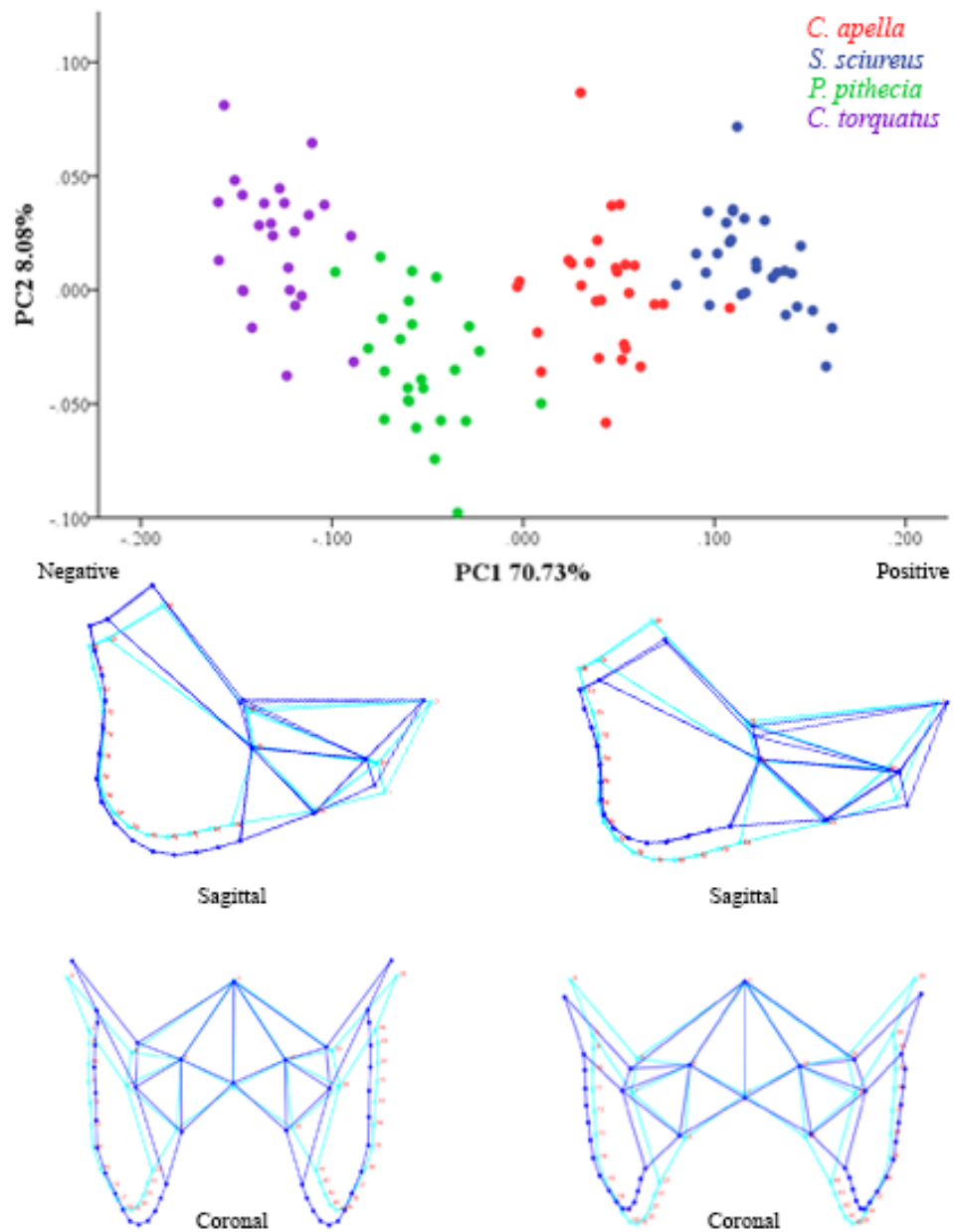


Figure 5.1 Principal Component Analysis scatterplot of PC1 and PC2 scores for all primates. Corresponding wireframe deformations are shown below in both sagittal and coronal view. In the wireframes, the light blue lines represent the average shape while dark blue demonstrates either the most positive (right) or negative (left) extreme shape changes.

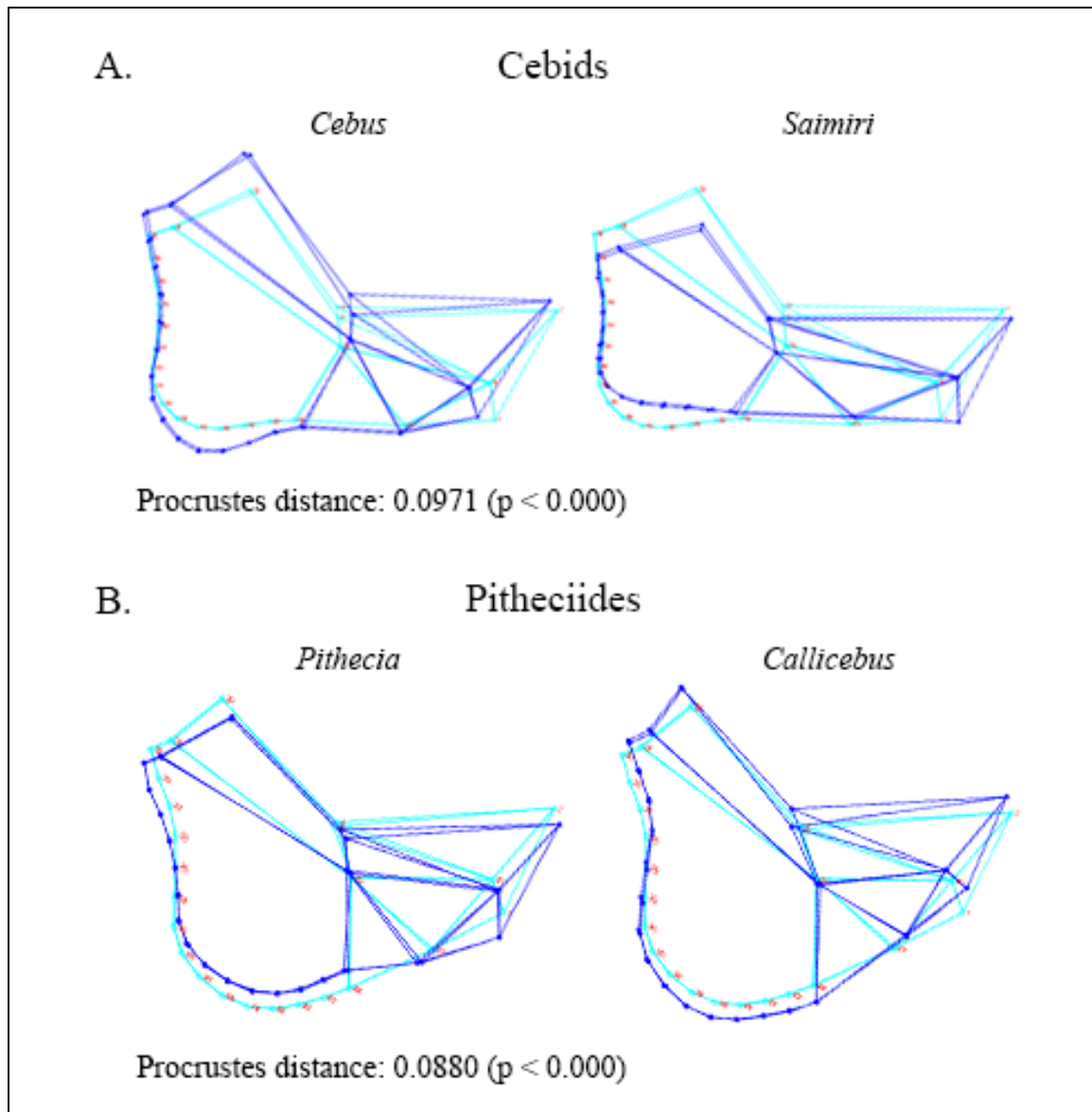


Figure 5.2 Shape changes within sister-taxa cohorts. A. Wireframe deformations demonstrating extreme shape changes between *Cebus apella* and *Saimiri sciureus* with Procrustes distance and significance reported below. B. Wireframe deformations demonstrating extreme shape changes between *Pithecia pithecia* and *Callicebus torquatus* with Procrustes distance and significance reported below.



Procrustes distances are also significantly different among *Pithecia* and *Callicebus* ( $p < 0.001$ ). The corpus of *P. pithecia* is longer than *C. torquatus* and is rotated inferiorly resulting in a wider angle between the coronoid and dental row. The inferior border of the corpus and symphysis is shallower in *C. torquatus* than *P. pithecia*. Lastly, *P. pithecia* has a less pronounced curve of the angle and a posteriorly displaced condyle, creating a larger antero-posterior distance between the coronoid and condyle.

Species-specific differences were also identified in relative centroid sizes, which are widely distributed across the genera (Figure 5.3A). *Cebus* average mandibular size is larger than the other primates, while *S. sciureus* has the smallest average mandible of the group. Bonferonni post-hoc tests from an ANOVA of centroid size revealed size differences were significant between all the primates used in this study. Sexually dimorphism in centroid size was also discovered in all but the *C. torquatus* specimens, in which male mandibles were consistently larger (Figure 5.3B). Such a large distribution of size and the presence of sexual dimorphism could influence both shape differences as well as amount of variation within each sample. While this information is interesting and important for many reasons, it may introduce unwanted effects for answering the hypotheses of this study. In particular, any undue increase in variation of shape, whether due to allometric effects or sexual dimorphism in size or shape, could conflate the statistical analyses conducted here.

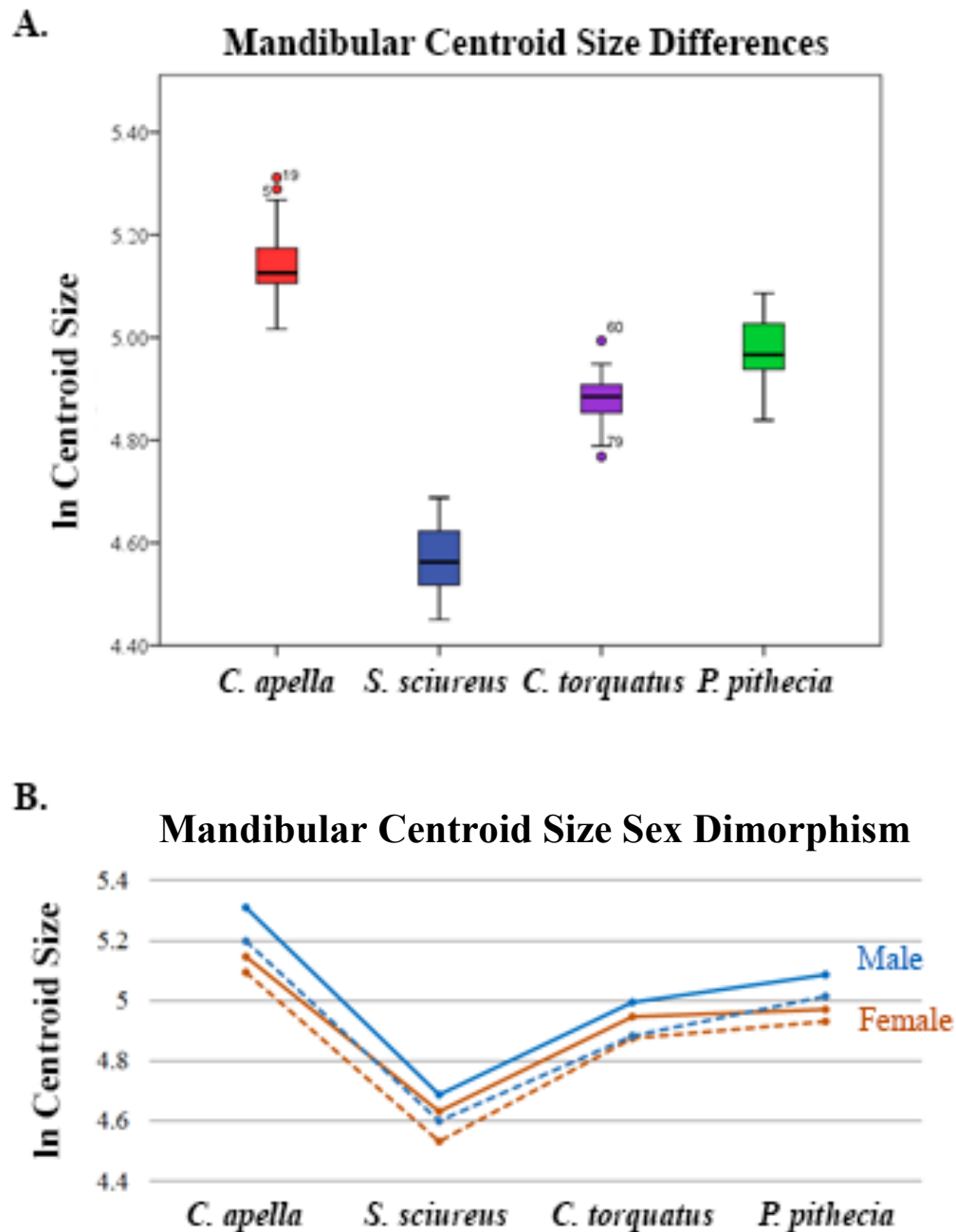


Figure 5.3 Images demonstrating ln CS differences between primate taxa and between within-taxa sex. There were significant differences in mandibular ln centroid size among all genera, as well, as between sex. A) Boxplot of each sample's centroid sizes with 25% standard deviation whiskers. Post-hoc Bonferroni analyses revealed that all genera were significantly different from each other at  $p < 0.000$ . B) Sex differences were significant in all genera, except for *C. torquatus*. Average ln centroid size is represented by the dashed line; the largest values within each sex are represented by the solid line. Significance was tested through one-way ANOVA.

A MANCOVA controlling for sex and ln CS was conducted in order to determine whether sexual dimorphism or allometry had a significant effect on mandibular shape as a whole. The first 35 principal component scores, which described 99% of the variation in this sample, were used as the dependent shape variables. Results showed that sex and centroid size did not significantly contribute to mandibular shape in the majority of the primate samples (Table 5.1). However, the sex factor was revealed to have a significant effect on *Cebus* mandibular shape ( $p = 0.023$ ; Table 5.1). This not only suggests that male and female capuchins possess disparate mandibular morphology but also that these differences could be increasing within-taxon variance to a large degree. Therefore, supplementary analyses were done with both size and sex corrected data for all *C. apella* specimens. Results did not differ between the original data and the sex-corrected data, the sex-corrected data are therefore not shown here.

**Table 5.1 MANCOVA results investigating the influence of sex and allometry on mandibular shape in each primate genus. PC scores representing 99% of shape were used as dependent variables, log centroid size (ln CS) as covariate and sex as the factor. P-values are given for the interaction of size and sex, as well as the influence of both size and sex after the non-significant interaction term has been removed. Only *Cebus* shows a significant influence of sex on shape. No other sample approached significance.**

Species	ln CS*Sex	ln CS	Sex
<i>C. apella</i>	0.573	0.126	0.023
<i>S. sciureus</i>	0.590	0.645	0.378
<i>C. torquatus</i>	0.651	0.117	0.755
<i>P. pithecia</i>	0.694	0.270	0.440

### 5.1.2 Patterns of Covariance

#### *Variance/Covariance Matrix Correlations*

V/CV matrices were generated in order to evaluate and contrast overall, global patterns of covariance structure in the mandible of the primates used here. Three pair-wise comparisons were carried out among the Cebids, Pitheciines and between the two hard-diet primates, *C. apella* and *P. pithecia*. Repeatability of covariance matrices were calculated for each separate genus, falling within 0.857 to 0.872. Measurement error is substantially low, allowing for confident subsequent analyses. All matrix repeatability tests and observed and adjusted matrix correlations are displayed in Table 5.2. Results are significant in each circumstance, alpha level being less than 0.0001, suggesting that global mandibular covariance patterns are significantly similar between cohort comparisons. Observed correlation values were relatively high for *Cebus* – *Saimiri* ( $R = 0.68$ ) and *Pithecia* – *Callicebus* ( $R = 0.66$ ).

**Table 5.2 Covariance matrix repeatability, observed and adjusted correlations for *Cebus* – *Saimiri* and *Pithecia* – *Callicebus*. Bold values are repeatability correlations, below the diagonal are observed correlation values and above the diagonal are adjusted.**

	<i>C. apella</i>	<i>S. sciureus</i>	<i>P. pithecia</i>	<i>C. torquatus</i>
<i>C. apella</i>	<b>0.871963</b>	0.7895459		
<i>S. sciureus</i>	0.682354	<b>0.8565766</b>		
<i>P. pithecia</i>			<b>0.867151</b>	0.761210
<i>C. torquatus</i>			0.659582	<b>0.865832</b>

### *Two-Block PLS*

Two-Block PLS analyses were performed on the pooled within-species covariance matrices using the Bi-modular configuration (Mitteroecker and Bookstein, 2008; Singh *et al.*, 2012). Analyses were conducted on pair-wise comparisons of the cebid cohort and pitheciid cohort to investigate differences in mandibles that are exposed to diets of varying mechanical properties. In addition, PLS analyses were also run between *Cebus* and *Pithecia* mandibles in a pair-wise comparison to determine if specific masticatory behavior in a hard diet, such as incisal versus molar row loading, will differentially affect integration or modularity. Supplemental analyses distinguishing sex in *Cebus* were also done, though as before, no difference in results was noted; they are not reported here.

Strong covariance within a cohort can be unduly influenced by a disproportionately larger degree of variance attributed to one genus over the other. To determine if this factor was skewing PLS analyses the distribution of variance was calculated for each genus and then compared between genera of each cohort (Table 5.3). Results show similar amounts of dispersion about the mean and that no one genus had a significantly greater amount of variance. Therefore, in all following results each genus is be interpreted as contributing the same overall amount of variance.

In general, a high total percentage of raw and scaled covariance between the alveolus and ramus in each pairwise comparison was described in the first two PLS scores. PLS1 (62-70%) accounted for the maximum covariance in the dataset for each comparison. The percent of covariance explained by PLS2 was also significant (range of 13-22%) in each case (Table 5.4). Covariation represented on further axes decreases

exponentially. Therefore, only the results and coordinated shape changes of the first two PLS axes will be reported here.

**Table 5.3** Calculations of observed variance for each separate primate genus, the difference between variance within each cohort ( $\Delta V$ ) and the upper 95% of difference from 900 permutation bootstrap. Comparisons were conducted between cohorts (*Cebus* – *Saimiri* and *Pithecia* – *Callicebus*). Bold values are genera variance estimates, above the diagonal are the  $\Delta V$  values between genera and below the diagonal are upper 95% bound estimates. When the 95% bound exceeds that of the  $\Delta V$ , those comparisons can be interpreted as non-significant.

	<i>C. apella</i>	<i>S. sciureus</i>	<i>P. pithecia</i>	<i>C. torquatus</i>
<i>C. apella</i>	<b>0.00386</b>	0.00686		
<i>S. sciureus</i>	0.00080*	<b>0.00317</b>		
<i>P. pithecia</i>			<b>0.00709</b>	0.00011
<i>C. torquatus</i>			0.00488*	<b>0.00721</b>

\* Indicates non-significant difference in  $\Delta V$ . Note that none of the comparisons show a significant difference in variance.

**Table 5.4** Pairwise correlation of 2-Block PLS scores between the alveolar and ramal regions in the mandible. Results are shown here, including the total percent of covariance along the first (PLS1) and second (PLS2) axes, and the accompanying correlation coefficient and significance values. PLS analyses were conducted for each cohort.

	PLS1			PLS2		
	% total covariance	r	p-value	% total covariance	r	p-value
Cebid	62.525%	0.8646	<0.0001	19.772%	0.8282	<0.0001
Pitheciin	67.801%	0.8833	<0.0001	17.486%	0.7978	0.0006

Scatterplots of PLS1 and PLS2 scores relay the relationship between the alveolar and ramal blocks for each cohort with both raw and scaled data (Figures 5.4 and 5.5). Specimens tend to cluster together in all plots, suggesting that primates do not differ substantially in mandibular patters of covariance. Scatterplots were generated based on group-centered scores, so that the influence of different average species shape could be

removed. The obvious visual overlap in genera suggests then, that shape change associated with integration between the alveolus and ramus is occurring at the same rate across cohorts.

Cebids displayed a moderate degree of covariance in the Bi-modular model on the first pair of PLS axes, representing 62.52% of total covariance with a statistically significant correlation. Shape changes from lower to higher scores along PLS1 correspond to an anteriorly displaced masseteric insertion and an elongate and superiorly tilted mandibular corpus associated with a postero-inferiorly and medially projecting gonial angle (Figure 5.4). Related patterns of shape change between the alveolus and ramus were markedly different along the second axis. Specimens that scored highly displayed a shortened superior-inferior distance between the coronoid and mandibular angle, and a postero-inferiorly rotated condyle, while the axis of both right and left mandibular rami are tilted so that the condyle is positioned more laterally. These ramal shape changes are associated with a posteriorly displaced masseteric insertion and an elongate, inferiorly rotated corpus. Changes in width are also jointly affected in the alveolus and ramus, with bi-coronoid, bi-condylar and bi-corpus distances increased (Figure 5.4). Major correlations of shape change within the Cebid mandible, representing about 81% of covariance are occurring in changes of the height and position of the gonial angle in the ramus paired with change in position of the masseteric insertion and orientation of the corpus.

Areas of associated shape change, orientation of the corpus and position of the gonial angle in the Pitheciinae sample were similar to that seen in Cebidae, though the way in which they changed was unique to that cohort. PLS1 axes accounted for 65.74%

of covariance and were highly correlated (0.893). Specimens which loaded higher in the PLS scatter reflect a foreshortened alveolus and a posteriorly tilted symphysis in conjunction with a postero-superiorly shifted coronoid and laterally flared gonial angle. Shape changes along PLS2 on the other hand, showed a foreshortened alveolus with a superiorly tilted symphysis in association with an anteriorly shifted coronoid and condyle and an angle with a much greater curvature. Again, bi-corpus, and coronoid width were closely related along PLS2 axes, with addition changes in symphyseal width. However, unlike cebids, these aspects are narrower in pitheciids (Figure 5.5). In addition, it seems that correlated shape changes along this axis were also decreasing the angle between the dental row and the coronoid.



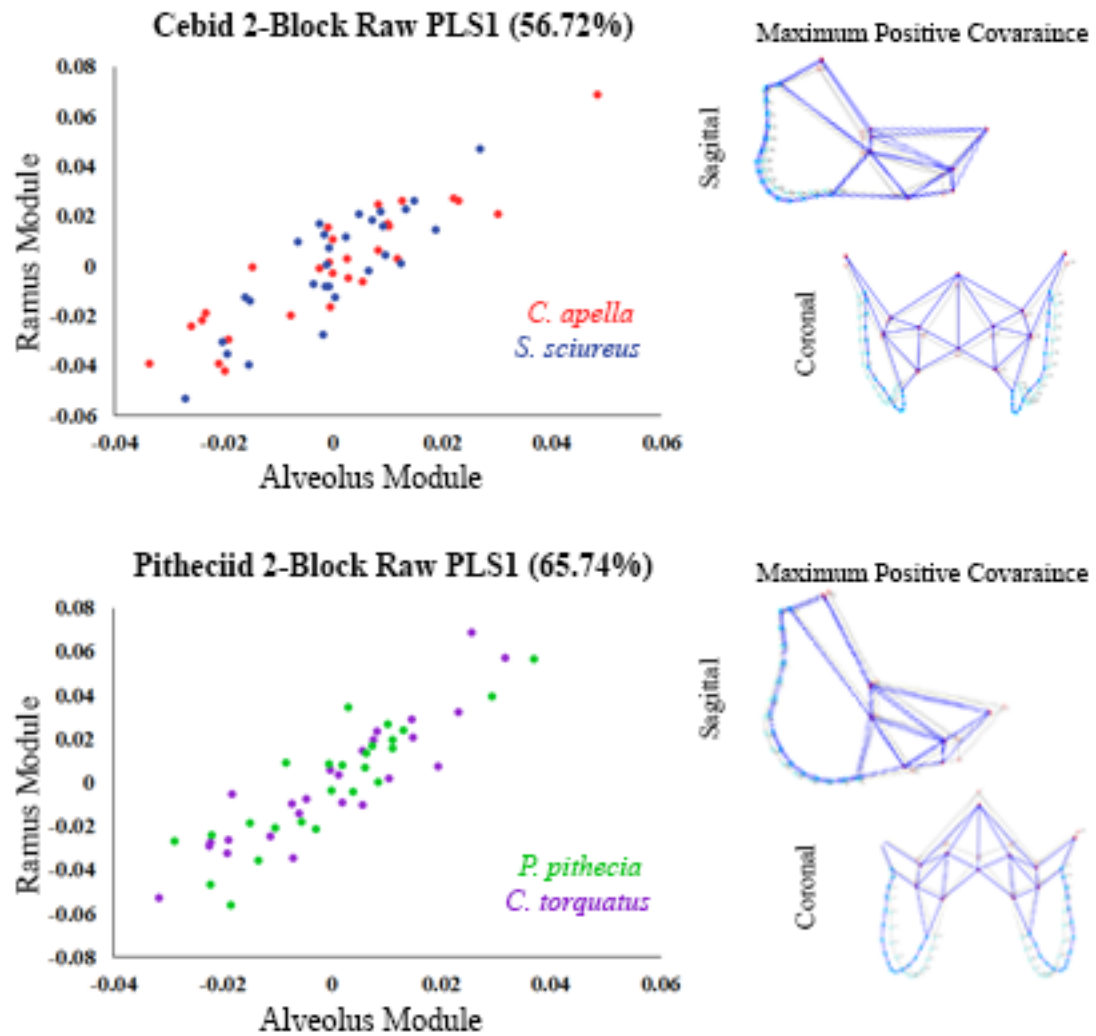


Figure 5.4 Scatterplots of PLS1 scores from 2-Block PLS analyses of *Cebus* – *Saimiri* and *Pithecia* – *Callicebus*. Scatterplots evaluate the amount of covariance shared in the Bi-modular model within all each pair-wise comparisons.

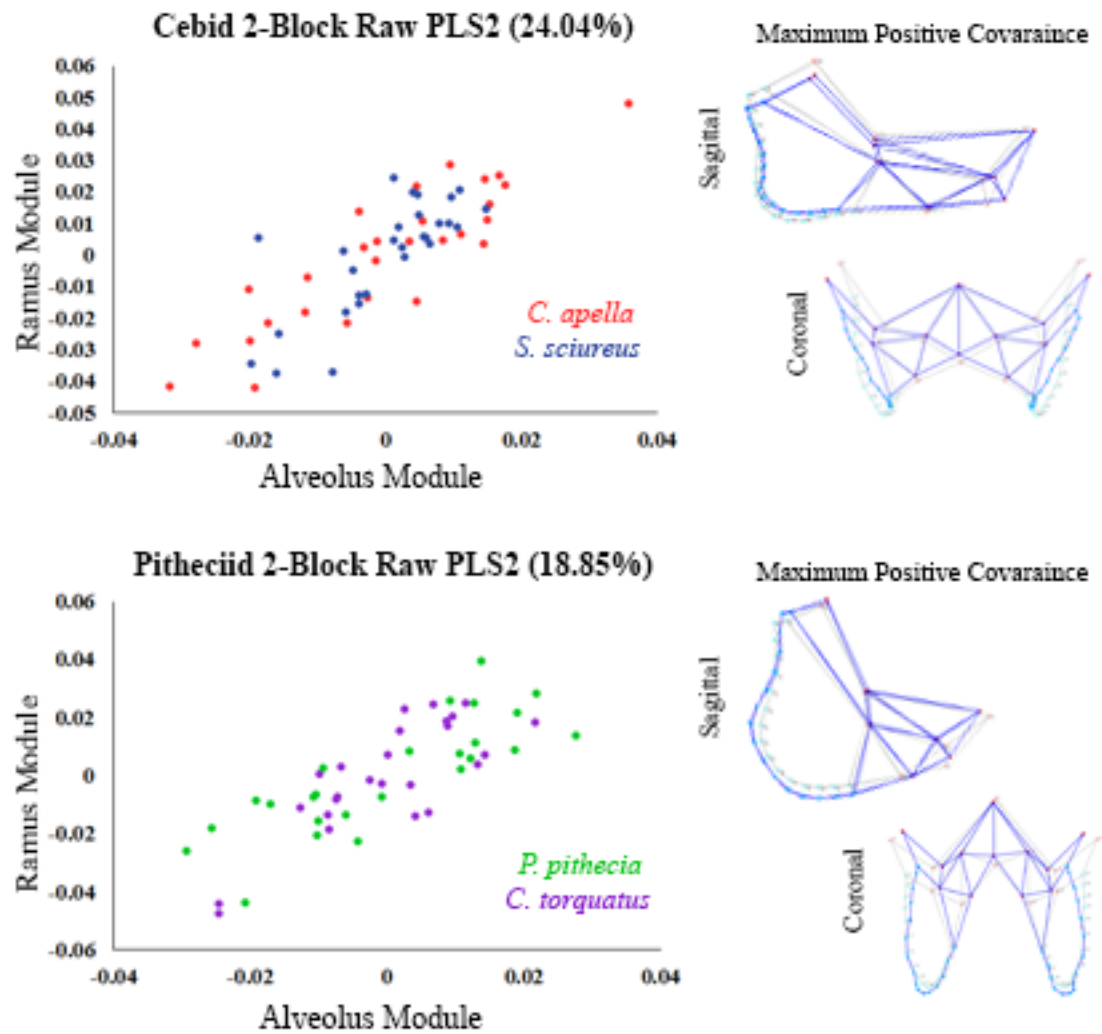


Figure 5.5 Scatterplots of PLS2 scores from 2-Block PLS analyses of *Cebus* – *Saimiri* and *Pithecia* – *Callicebus*. Scatterplots evaluate the amount of covariance shared in the Bi-modular model within all each pair-wise comparisons.

### 5.1.3. Magnitude

Scaled variance of eigenvalues was used to compare the level of integration or covariance between primates and within particular structures. Results varied across cohort comparisons. Figure 5.6 shows that *C. apella* possessed significantly greater ( $p < 0.05$ ) SVE scores than *S. sciureus* for the global landmark configuration, as well as all other landmark configurations. Differences between *C. apella* and *S. sciureus* were most pronounced in the alveolar modules, especially in the symphyseal region where SVE scores were nearly two times greater in *Cebus*.

The Pitheciine results were quite different, showing that *Callicebus*, the less-  
durophagous primate of the comparison, most often possessed the greatest SVE values (Figure 5.7). Again, SVE scores showed a large discrepancy between these primates in the alveolar region, particularly concentrated within the symphysis. Levels of integration did not show a particularly strong differentiation in the ramus for these two primates. Looking at the Bi-modular model, the covariance in shape of the entire ramus was similar. However, when broken down into the separate modules, *Callicebus* displayed significantly more covariance within the gonial angle than *Pithecia*. This trend was not present in the other two ramal modules.

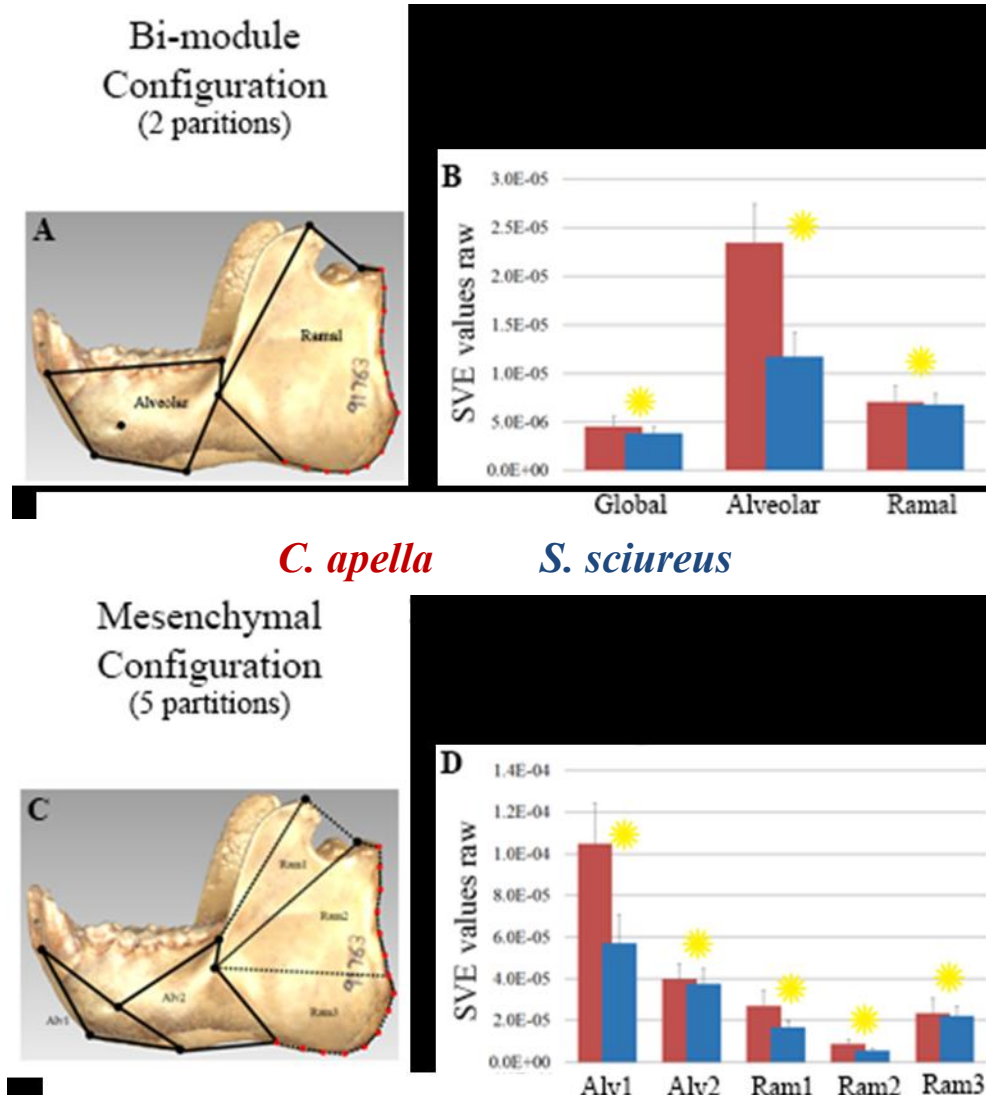


Figure 5.6 SVE scores for the Cebid cohort using three different landmark configurations based on the global mandible, landmarks representing the Bi-module configuration and the Mesenchymal configuration. SVE was calculated for each module and subsequently compared between *C. apella* and *S. sciureus* using a bootstrap permutation test. An asterisk signifies a significant difference among groups ( $p < 0.006$  after Bonferroni correction). A) Example of Bi-module landmark configuration with alveolar (1,  $k=10$ ) and ramal (2,  $k=36$ ) partitions; B) Bar-graph showing global and Bi-modular raw and scaled SVE scores Cebid comparisons; C) Example of Mesenchymal landmark configuration with two alveolar (1,  $k=4$ ; 2,  $k=8$ ) and three ramal (1,  $k=8$ ; 2,  $k=18$ ; 3,  $k=16$ ) partitions; D) Bar-graph showing Mesenchymal SVE scores for Cebid comparisons.

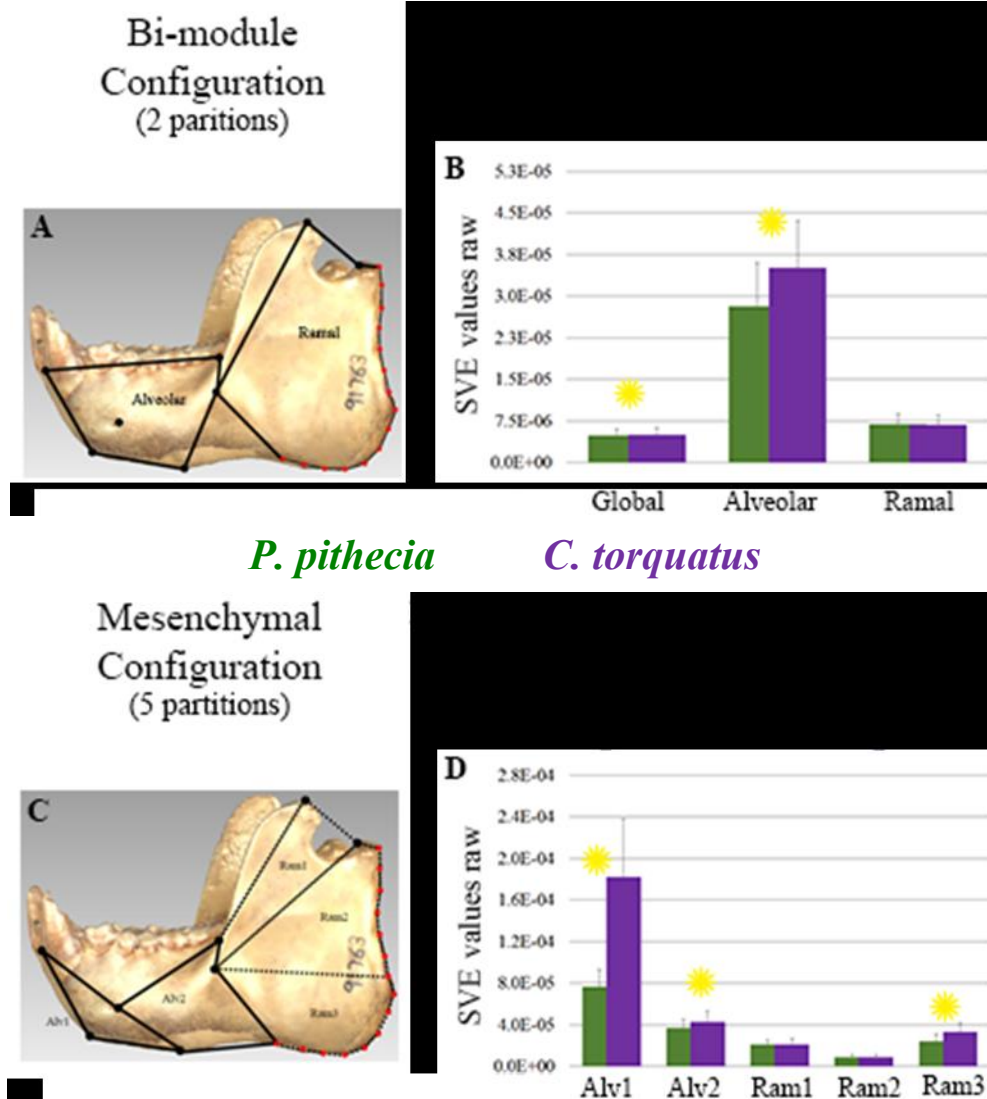


Figure 5.7 SVE scores for the Pitheciine cohort using three different landmark configurations based on the global mandible, landmarks representing the Bi-module configuration and the Mesenchymal configuration. SVE was calculated for each module and subsequently compared between *P. pithecia* and *C. torquatus* using a bootstrap permutation test. An asterisk signifies a significant difference among groups ( $p < 0.006$  after Bonferroni correction). A) Example of Bi-module landmark configuration with alveolar (1,  $k=10$ ) and ramal (2,  $k=36$ ) partitions; B) Bar-graph showing global and Bi-modular raw and scaled SVE scores for Pitheciine comparisons; C) Example of Mesenchymal landmark configuration with two alveolar (1,  $k=4$ ; 2,  $k=8$ ) and three ramal (3,  $k=8$ ; 4,  $k=18$ ; 5,  $k=16$ ) partitions; D) Bar-graph showing Mesenchymal SVE scores for Pitheciine comparisons.

### *R<sub>v</sub> Coefficients*

$R_v$  coefficients were calculated within each genus to determine levels of modularity within both the Bi-modular and Mesenchymal models (Table 5.4). In each of the Bi-modular analyses, the  $R_v$  coefficient was lower than the majority of randomly generated alternative partitions, ranging between 0.527 – 0.625. This confirms that the Bi-modular configuration is present in the primate mandible. Even with significant RV results in each of the four primate genera, the two Pitheciins displayed the highest degrees of association between the ramus and alveolus. *Callicebus* in particular had 20 instances in which other modular landmark configurations better fit the covariance structure and possessed the highest  $R_v$  coefficient ( $R_v = 0.625088$ ). In contrast, *Saimiri*, the other non-durophagous primate, has the lowest amount of integration between the two modules (0.526746). These results are consistent with the hypothesis that the mandible can be divided into two large modules. However, the distribution of  $R_v$  coefficients was moderately high indicating a fairly weak representation of modularity using the Bi-modular model.

The Mesenchymal model resulted in a better indication of modular structure in the primate mandible than the Bi-modular model for all of the primates analyzed here.  $R_v$  coefficient distribution ranged from 0.411 – 0.452, representing moderate to fairly low integration across modules. In addition, for all of the primates, *a priori* Mesenchymal model configurations had  $R_v$  values significantly ( $p < 0.001$ ) less than the values of all random partitions (Table 5.5).

**Table. 5.5** Table of  $R_v$  coefficients from each primate genus.  $R_v$  coefficient scores and p-values (from permutation test) for all hypothetical modules in each genus, representing both raw and scaled data sets. Numbers in parentheses indicate how many of the randomly generated modules resulted in  $R_v$  coefficients lower than the *a priori* hypothesized modules.

Genus	Bi-module model		Mesenchymal model	
	$R_v$ coefficient	p-value	$R_v$ coefficient	p-value
<i>C. apella</i>	0.576739 (2)	0.0002	0.430277 (0)	0.0000
<i>S. sciureus</i>	0.526746 (1)	0.0001	0.452129 (0)	0.0000
<i>P. pithecia</i>	0.614067 (11)	0.0010	0.420772 (0)	0.0000
<i>C. torquatus</i>	0.625088 (20)	0.0020	0.411634 (0)	0.0000

## 5.2 Discussion

New world monkeys (NWM) inhabit a wide range of ecologically diverse environments which is further exemplified by the variety of food resources they exploit. For instance, as highlighted here, some NWM have uniquely adapted to ingest and masticate seeds and fruits possessing resistant mechanical properties. Differences in feeding habits are reflected in their masticatory apparatus morphology. However, empirical studies explicitly testing the relationships between diet and mandibular functional morphology have led to incongruent results (Norconk *et al.*, 2009; Vinyard *et al.*, 2011). This study proposed several hypotheses relating to covariance structure as a factor influencing the morphological diversity of mandibular shape in NWM.

$H_{FXA0}$  hypothesized that NWM would share dissimilar pattern of global covariance. Rejection of this null hypothesis was expected suggesting that patterns of covariance are significantly similar as a function of shared functional demands required of all mandibular morphology, regardless of diet. Regarding magnitude of covariance among taxa, the null hypothesis ( $H_{FXB0}$ ) tested that magnitudes of covariance are similar between primates despite dietary differences. Alternative hypotheses ( $H_{FXB1}$ ) are that that

magnitudes of covariance would differ between primates exhibiting different dietary regimes. More specifically, I expected that mandibles generating large bite-forces and withstanding food reaction forces would demonstrate larger magnitudes of trait covariance (integration) than mandibles of those primates experiencing moderate to low habitual bite forces. Thus, habitually exerting larger occlusal loads and muscle forces would equate to a more integrated mandible while mandibles that undergo relatively small or infrequent loads would be more modular.

#### 5.2.1 Mandibular Morphological Diversity

Few geometric morphometric shape analyses have been conducted on NWM mandibular form (Rosenberger *et al.*, 2013); a much greater emphasis has been placed on traditional morphometrics, essential in elucidating phylogenetic, functional and ecomorphological information in this clade (see Norconk *et al.*, 2009 for review). PCA results of the mandibular morphology clearly separate not only each genus but each clade, as well. It is interesting that the more robust members, *Cebus* and *Pithecia* cluster together while the two gracile species occupy opposite ends of morphospace. The largest component of shape variation could be interpreted as representing diet and mandibular shape unique to each clade. Cebid corpus shape is characteristically uniform and untapered mesiodistally with a horizontally projecting gonial angle, often attributed to the basal state of platyrrhine mandibular morphology (Kay *et al.*, 2013). In contrast, the depth of the more derived pitheciine mandibular corpus is increased moving distally with an exorbitant gonial angle flare paired with a taller condyle/coronoid complex. Distinctive gonial angle position between cebids and pitheciines could result from muscle



force orientation, producing fundamentally different adductor resultant vectors in either clade. However, in a study looking at a larger number of pitheciids and cebid muscle resultant forces, Perry *et al.*, (2011) demonstrated no significant differences between these clades.

A number of field studies have observed fruit eating and seed-predation (frugivory-granivory) in pitheciine primates (Kinzey, 1992; Kinzey and Norconk, 1993; Palacios *et al.*, 1997; Lambert and Garber, 1998; Norconk *et al.*, 1998; Norconk and Conklin-Brittain, 2004; Alvarez and Heymann, 2012; Hawes and Peres, 2013). *Pithecia* participates in sclerocarpic foraging, meaning that they commonly breach hard husks that cover soft seeds (Kinzey and Norconk, 1993; Norconk *et al.*, 1998; Norconk, 2009). *Callicebus* has been noted to eat both fleshy fruits and immature seeds but is not considered to be a specialized sclerocarpic seed predator (Kinzey, 1978; Palacios, 1997; Alvarez and Heymann, 2012). However, they have been documented to scrap at hard-husked fruits in order to gain access to the softer seeds inside (Kinzey, 1977). These behaviors have lead some morphologists to suggest that the narrow pitheciine symphyses reflect an incisal adaptation to sclerocarpic foraging (Rosenberger and Tejedor, 2013). The incisor-canine battery is especially adapted to create an efficient gouging mechanism to open hard fruit pericarps (Kinzey and Norconk, 1993; Norconk *et al.*, 2009; Deane, 2012).

Documented feeding behavior in *Cebus* and *Saimiri* agree with mandibular shape seen here and asserted in previous research. *Cebus apella* is well-known to exploit mechanically resistant fruits and seeds, especially during the dry season (Terborgh, 1983; Galetti and Pedroni, 1994) whether by manipulating the foods with tools or breaching

them with dentition (Izawa and Mizuno, 1977; Janson and Boinski, 1992; Anapol, 1994; Norconk *et al.*, 2009; Visalberhi *et al.*, 2008). The ability to masticate such food is related to *Cebus*' robust mandibular morphology (Anapol, 1994; Norconk *et al.*, 2009).

Characteristic *Cebus* mandibular shape was apparent in this analysis, with a deep, well buttressed mandibular corpus to accommodate heavy occlusal loads and larger molar dentition. The coronoid process and angular process are longer and/or wider allowing for greater areas of muscular insertion, congruent with generating larger bite forces.

However, at this time, no research correlating muscular size and insertion area in platyrrhines is known. Future analyses would benefit from a comparison of these metrics. The *Saimiri* mandible, in contrast to robust capuchins, is long, slender and more gracile in general, reflecting the mandible of a species which prefers softer fruits and insects (Janson, 1992; Pinheiro *et al.*, 2013; Rothman *et al.*, 2014). Width of the corpus, condyle and coronoid are more exaggerated in *Saimiri* when compared to *Cebus*, possibly reflecting palatal and basicranial width.

Differences in robusticity are also present between *Pithecia* and *Callicebus*, though not as starkly apparent as between the cebids. *Pithecia* mandibular corpus depth is greater and the distance between the TMJ and tooth row is not as pronounced, two factors representative of a mandibular morphology selected to generate and withstand obdurate diets. Though *Callicebus* is not considered a specialized seed-predator, some of the incipient traits associated with increasingly derived pitheciin sclerocarpy are present, such as an enlarged posterior angle (Norconck *et al.*, 2009). Both pitheciines demonstrate narrower symphyses when compared to cebids, though to a much greater degree in *Callicebus*. Mating style in titi monkeys is based on a pair-bonded system, therefore

*Callicebus* does not have sexual dimorphism. Thus, their incisal canine complex has been referred to as structural trade-off between the dietary and mating strategies (Rosenberger, 1990) and is consequently narrower than that found in other pitheciines.

#### 5.2.2. Covariance Patterns Are Conserved Across Primate Groups.

Covariance patterns were shared in all cohort comparisons evinced by similarity in VCV matrix correlations and 2-Block PLS scatterplots. Therefore, the first hypothesis ( $H_{FXA}$ ) can be fully rejected. Furthermore, these results agree with several previous analyses of NWM crania (Cheverud, 1996b; Ackermann and Cheverud, 2000; Marroig and Cheverud 2001) as well as other studies of other vertebrate crania (Young and Badyaev, 2006; Goswami 2007; Goswami and Polly, 2010a; Jamniczky *et al.*, 2014; but see Beldade and Brakefield, 2003).

Results from this study support the notion that generally shared functional demands in the jaw will lead to a similar covariance pattern. Strain magnitudes are generally experienced ubiquitously through the mandible during ingestion, mastication or other para-masticatory behaviors. At the same time forces are also regionally specific, such as occlusal load at bite point, force from muscular contraction and joint reaction force at the temporomandibular joint. However, these are commonalities associated with bite force in most primate jaw architecture. Logically then, though the forces may differ in magnitude and region, each mandible must be able to function as a unit to both generate and withstand these forces. Patterns of trait covariance would then reflect these shared demands, as seen in this analysis, whether through internal developmental or external functional influences.

Adult mandibular structure has commonly been described as a Bi-module structure comprised of an alveolar unit which houses the dentition and receives occlusal loads, and a ramal unit which acts as a scaffold for muscular attachment and joint reaction force (Klingenberg *et al.*, 2001, 2003; Zelditch *et al.*, 2008, 2009; Meloro *et al.*, 2011; Piras *et al.*, 2013). Though these are modular units, as stated above there must be some degree of integration between them in order for the jaw to function. Indeed, significant levels of integration between these units were detected, among all pair-wise comparisons. Furthermore, visualization of scatterplots of alveolar and ramal PLS axes bolsters the hypothesis that covariance patterns are shared. Lastly, trait covariance between the alveolus and ramus was dictated by an overarching theme, whereby the mandible was lengthened or shortened as a whole. This trend was apparent in all of the PLS1 analyses.

Despite smaller underlying differences, the overall pattern of covariance is the same in all groups. More specifically, the ramal and alveolar shape changes were proportional in that as one lengthened or shortened so did the other. As mentioned previously, the mandible acts as a lever and therefore must have a lever arm and a load arm. The ratio of these two arms (load arm/lever arm) is directly related to mandibular mechanical advantage. Regardless of shape change, as long as a functioning ratio is maintained, mechanical advantage is not lost (Vinyard, 2008; Swiderski and Zelditch, 2010). Though linear functional estimates were not calculated for these particular analyses, PLS analyses do suggest that load arm ratios, which reside in the relationship between the ramus and alveolus, are being maintained. Thus the largest integrating effect in the Bi-modular model across the board reflects the conservation of mechanical

advantage. Future studies would benefit from calculating functional measurements, such as mechanical advantage, to see if they are correlated with the covariance structure demonstrated here.

Interestingly, the second largest axis of integration also revealed a uniform pattern in each cohort comparison. Here a clear relationship between position of the condyle and coronoid and width of the mandibular body can be seen. These patterns are probably due to the mandible tracking articulation at the TMJ and occlusion with the maxillary dentition. Integration between the mandible and cranium is clearly important for successful masticatory as well as respiratory needs. However, it is not the leading factor influencing the pattern of covariance within the mandible. Other studies have suggested a nested degree of integration between the mandible and cranium, positing that while integrative patterns within the mandible can be independent from the cranium underlying trait covariance across the skull still exists (Bastir and Rosas, 2005; Bastir *et al.*, 2006; Wellens *et al.*, 2013; Alarcón *et al.*, 2014).

Simultaneous conservation of patterns of covariance and the range of morphological diversity observed in platyrrhine mandibles, both here and elsewhere, may at first seem contradictory. Yet, several previous studies have noted these relationships. It is widely held that shared developmental and genetic factors work to maintain patterns of covariance processes (Lande 1980; Cheverud 1984, 1996a; Wagner and Altenberg, 1996; Ackermann and Cheverud, 2000; Klingenberg *et al.*, 2003 Marroig *et al.*, 2004; Hallgrímsson *et al.*, 2007). These factors include genetic pleiotropic signaling pathways, somatic bone and cartilaginous growth or mechanical tissue interactions. Mitteroecker and Bookstein (2008) termed these effects as “common factors” suggesting that they

were shared across primate crania and would therefore be represented as shared in the covariance structure.

Stabilizing selection is also an important aspect that could be guiding a common covariance structure across the primate mandible (Estes and Arnold, 2007; Jamniczky and Hallgrímsson, 2009). As previously stated, stabilizing selection acts to remove outliers that may be deleterious to the population fitness, thereby increasing the number of individuals existing near the population mean and thus reducing variance overall. Several investigations of the patterns of covariance in the crania across NWM and Mammalia in general have demonstrated that, despite large evolutionary time-spans between taxa, the pattern of covariance remains similar (Oliviera *et al.*, 2009; Porto *et al.*, 2009; Shirai and Marroig, 2010). The stasis of covariance patterns has been attributed to stabilizing selection acting on shared developmental and functional processes. Thus the sample of NWM mandibles used here mirrors the conserved patterns of covariance demonstrated in the NWM cranium.

The level of comparative observation conducted here should also be considered. Comparative studies at this level (inter-generic) possibly reflect larger clade-specific phylogenetic, and thus genetic, patterns of integration. Though the correlation of morphological integration and phylogeny has not always been clearly supported across large taxonomic groups (Cheverud, 1989; Stepan, 1997, Goswami, 2007) pair-wise taxonomic covariance (or correlation) matrix comparisons rarely differ significantly. Still, it is possible that similar comparisons conducted at lower taxonomic level (intra-generic) may reveal more nuanced covariance structures.

The design of the hypotheses asserted was not intended to address phylogenetic questions. It is expected that in analyses comprising a larger taxonomic range of NWM, interspecific covariance patterns would remain similar within the mandible. However, it is arguable that covariance matrices designed to correlate patterns of mandibular covariance with either diet or phylogeny could result in differing patterns among groups.

A recent analysis of jaw divergence in cichlid fish by Jamniczky *et al.*, (2014) has also concluded that covariance pattern is conserved across the masticatory region despite differences in morphology and functional demands. Where differences are seen is in the modular structure of the masticatory apparatus and the magnitude of integration within each module (Albertson *et al.*, 2005; Cooper *et al.*, 2011) which has largely been attributed to the extreme complexity of the in-lever out-lever system in fish (Hu *et al.*, 2014).

### 5.2.3. Magnitude of Integration Differs Amongst Primate Mandibles.

The second group of hypotheses is partially supported by the results here (**H<sub>FXB</sub>**). Namely, covariance magnitude differences are present among all the pair-wise comparisons, as originally expected. However, the *a priori* hypotheses suggesting that primates with obdurate diets possess greater values of overall magnitude were not consistently supported. In fact, results portray a unique divergence in magnitude of overall integration in each setting. Moreover, those primates that demonstrated greater global integration did not necessarily also possess consistently larger or smaller magnitudes at the two modular levels tested here.

Of all the comparisons, only the Cebids demonstrated the originally hypothesized pattern. In contrast, *Callicebus* most often displayed greater degrees of integration when compared to *Pithecia*, except for comparisons between the ramal modules in which there was no significant difference. The easiest explanation for the disagreement in results may involve the relative amount of force being exerted between the two primate cohorts. *Cebus* is well known to generate masticatory loads at a level well beyond that of *Saimiri*, whereas *Pithecia* bite forces are located at a relatively intermediate level for platyrrhine seed-predators (Norconk *et al.*, 2009; Kay *et al.*, 2013; Norconk *et al.*, 2013). Therefore, the level of integration is selected for and exacerbated *in vivo* due to the greatly increased functional exertion in the *Cebus* mandible. The pitheciine distribution of magnitude may then be reflecting another modulating factor, similar to the patterns of integration seen in the 2Block PLS analyses.

#### *Developmental-functional impact on modularity*

Two interesting trends can be found when comparing the modular magnitudes. First, in all of the pair-wise comparisons the Bi-modular alveolar and anterior alveolar modules (Alv1) show the greatest degree of difference in covariance magnitude. *Callicebus* in particular has an anterior alveolar SVE value that exceeds *Pithecia* over two-fold. Second, the only instances in which insignificant differences appeared were in the ramal modules of the pitheciine comparison. As discussed before, many factors distinguish the alveolar from the ramal region, any or all of which could be contributing to constraint in the ramus while the alveolar region demonstrates the ability to vary between taxa. It is important to keep in mind that the strength of covariance magnitude is



only in relation to the pairwise comparison. For instance, even though *S. sciureus* demonstrated a significantly smaller SVE value compared to *C. apella* this does not mean that the magnitude is inherently weak in *S. sciureus*.

In light of functional interpretation, similarity of ramal SVE values suggests that mechanical interactions between muscle and bone, as well as joint force reaction at the TMJ are creating the same degree of covariance in these primates (except the cebids) despite dietary disparity. At the same time dental growth and occlusal loads within the alveolus are disproportionately affecting one genus over the other. It is tempting to suggest that bone-muscle interaction or even the area on which muscle must be attached is not different enough to impact trait covariance.

An ontogenetic analysis could elucidate the underlying factors contributing to magnitude differences by determining the developmental timing of magnitude divergence, convergence or lack thereof between our primate samples. Genus specific timings for bone ossification, dental development, muscle-bone interaction, etc. can lead to greater diversity and levels of integration/modularity (Zelditch, 2005; Young *et al.*, 2007; Young and Badyaev, 2010; Goswami *et al.*, 2012). For instance, if alveolar magnitude differences are the same early in ontogeny and then diverge after the onset of adult function, it would suggest on early developmental regulation of shape variance. However, the overlying aspect of strain from occlusal load would then differentially affect trait covariance causing a later divergence. Plasticity in alveolar bone growth then would be highly advantageous to capitalize on varied or unprecedented food resources. Another likely scenario would be that among primates different magnitude are detected in the alveolus earlier in ontogeny but remain the same between rami. Spatiotemporal

differences between these two modules of the mandible may allow them to vary independent of each other, leading to differential amenability to selection.

#### *Evolutionary consequence of varying magnitude intensities*

Evolutionary studies of morphological variation across large taxonomic groups, including NWM, have also found a discrepancy between the fixed covariance patterns and the plasticity of covariance magnitudes. Porto *et al.*, (2009) completed a study in which overall pattern of covariance, magnitude of integration and the modularity index were compared across a diverse group of metatherian and eutherian crania, including primates. For clarification, as described in Chapter 3, the modularity index measures the relative modularity within each taxon relative to the overall integration within the same taxon. They found, as in other studies and this project, that within eutherians the pattern of covariance remained similar across taxa despite great morphological variation. In contrast, overall magnitude of integration between traits differed. Primates in particular demonstrated both high and low levels of integration. Furthermore, using the modularity index, they found that those taxa in which overall integration was highest possessed the lowest amount of modularity. Conversely, those taxa in which integration was weak demonstrated a stronger degree of modularity. Similar studies using comparable samples and statistical techniques confirm these results (Oliveira *et al.*, 2009; Shirai and Marroig, 2010)

In a companion paper, Marroig *et al.*, (2009) used the same sample and data as Porto *et al.*, (2009) to apply theoretical models of selection and evolvability to the covariance structure within the skull. The intent was to determine the way in which the

magnitude of integration would direct evolutionary responses to simulated selective vectors. They found that skulls with higher overall integration (and lower modularity ratios) were less amenable to selective pressures while skulls with higher levels of modularity (and weaker overall integration) were significantly more responsive to simulation selection vectors. The work of Melo and Marroig (2014) ties in nicely to these results as it suggests that directional selection may drive populations to develop greater amounts of modularity while stabilizing selection drives the patterns of covariance that are present in a population.

Taken together these studies support common theoretical tenets concerning how the structure of covariance directs evolutionary responses. First, as has been repeatedly stated here, conserved patterns of covariance are largely credited to stabilizing selection. However, the plasticity of magnitude is thought to allow for the diversity seen across mammalian taxa. Second, greater overall integration occurs in tandem with lower overall modularity while skulls that are more modular demonstrate weaker integration. At the same time more modularity is significantly associated with a greater ability to respond to selective pressures. Thus, these analyses agree with the notion that modularity increases evolvability. Furthermore, stabilizing selection retains the pattern of covariance and possibly the intensity of integration.

The mandibles studied here mirror the aforementioned analyses in that the pattern of covariance is indeed conserved between different clades. However, NWM are renowned for dietary specialization and morphological diversity due to masticatory behaviors. It is possible that the morphological differences found in the mandible among platyrrhines are largely due to the plasticity of magnitude. Thus mandibular magnitude

allows morphological variation to adapt to selective pressures while simultaneously maintaining the way in which traits are correlated.

It would seem contradictory however, that *C. apella* which is under strong adaptive pressure to generate and withstand disproportionately large masticatory loads, has the largest overall magnitudes of integration. If directional selection drives parcellation of modules, for instance due to modification in pleiotropic signaling pathways, then one might expect tufted capuchin mandibles to demonstrate greater levels of modularity. While *C. apella* mandibles had the greatest amount of integration at all levels, it was not feasible to determine the relative proportion of modularity to integration from the methods used here (SVE comparisons). Future analyses utilizing the modularity index may in fact show higher levels of modularity in this primate species when compared to other primates that do not engage in a specialized diet.

Still, the importance of finding highly organized covariance structure in the primate exhibiting the largest occlusal loads should not be diminished. Porto *et al* (2008) and others (Oliveria *et al.*, 2009; Shirai and Marroig, 2010) conducted their analyses on the skull, a structure that is known to be highly developmentally regulated, with relatively clear nested modular design. The mandible has been shown to depart from this structure and to demonstrate more complex organization of covariance that is highly reflective of adaptation to diet and in vivo functional overlay (Monteiro *et al.*, 2005; Young *et al.*, 2007; Zelditch *et al.*, 2008, 2009; Monteiro and Nogueira, 2010; ; Molero *et al.*, 2011; Piras *et al.*, 2013). It is possible that the results found here correspond to a unique mandibular structure, which is highly influenced by function.

#### 5.2.4 The Mandible Has A Hierarchical Covariance Structure.

Several previous analyses have attempted to explore and determine the best fit modular structure of the mandible across a variety of vertebrate groups and taxonomic levels using different methodological approaches (Monteiro *et al.*, 2005; Young and Badyaev, 2006; Zelditch *et al.*, 2008, 2009; Monteiro and Nogueira, 2010; Molero *et al.*, 2011; Piras *et al.*, 2013). Both Mesenchymal and Bi-module models were observed, as well as many studies with inconclusive results. In smaller comparative samples with questions geared towards functional relationships, however, the Bi-module model is predominately evident. This is usually explained as a result of functional interactions correlated with adult feeding demands overriding the developmental modular design to integrate two larger units. The modules may be responding to either muscle and joint force or bite point force as separate units but are still integrated as a whole to generate and dissipate adult forces.

Based on these previous studies, it might predicted that mandibular modularity would be best reflected as the alveolar and ramal organization in these adult primates, especially in the seed-predating primates. Though results from this analysis did find evidence for significant Bi-modular configuration in platyrrhine mandibles it was not better represented in the hard-diet primates. In addition, Mesenchymal model  $R_v$  coefficients were also significantly evident and, based on low  $R_v$  coefficients, are perhaps better representative of the mandibular covariance structure.

$R_v$  coefficients from both models were found to be significant, making it difficult to argue or determine whether one covariance organization is better suited to platyrrhine mandibles than the other because no statistical analysis was completed to compare the

two directly. At most, the relative strength of integration, as determined by the  $R_v$  value, can be discussed. In general, Bi-modular  $R_v$  were moderate to high while Mesenchymal were moderate to low suggesting greater modularity in the Mesenchymal model. Mesenchymal models were also the best fit when compared to randomly generate hypothetical modular structures, in all instances. When the Bi-modular model was applied, in contrast, most instances resulted in some randomly generated modules with a better fit, though not enough to make it insignificant. One might speculate then, with caution, that the Mesenchymal model is the best representative of the covariance structure here.

Another interesting trend was that the clades grouped together in terms of magnitude of covariance between each constituent part. In other words, cebids had the lowest levels of integration (small  $R_v$ ) in the Bi-modular model but the highest in the Mesenchymal (largest  $R_v$ ). The opposite was true for the pitheciins. Again, cautious speculation would interpret these results to suggest that taxonomic relationships are regulating common magnitudes of integration. If phylogenetic relatedness is the influencing factor here that might suggest that developmental regulation of covariance is continuing to strongly mediate integration in the mandible despite functional influences. Because the  $R_v$  results can only be discussed in degrees, the only really conclusive or convincing argument to be made here is that the mandible, much like the cranium is a structure composed of nested modular structures. When decomposed at specific levels, modules related to developmental signaling, muscle-bone interaction or any other covariance generating system can be detected. But these modules are not isolated or completely autonomous, they will covary with other units to differing degrees. The

challenge is to decipher how those different magnitudes may constrain or enable adaptability. Regarding the mandible as a nested hierarchical structure is concordant with the inherent assumptions behind the Palimpsest model.

#### 5.2.5 Summary

This study further supports earlier analyses and contributes new information to the field. Phenotypic covariance patterns are remarkably similar among the mandibles of this small group of platyrrhines, despite taxonomic distance or dietary diversity, in line with previous studies looking at NWM crania and other non-primate mandibles. Additionally, even though covariance patterns were similar across groups, covariance magnitudes did differ. Again, this agrees with data on NWM crania which demonstrate the same trend. However, it was expected that hard-diet primates would consistently possess the greatest magnitude of integration in both cohorts. Only *Cebus* followed this trend suggesting that differences in magnitudes seen here may only be partially explained by diet. In conclusion, the mandible of NWM, an extremely ecomorphologically diverse taxonomic group, is a hierarchically nested modular structure, much like the cranium. Cross-taxonomic similarities in covariance pattern reveal a conserved developmental signal which would normally suggest constraint in the wake of natural selection. However, ubiquitous significant differences in the intensity of trait covariance at multiple levels further the argument that covariance magnitude and complex inter-related modular systems increase adaptability, allowing the NWM mandible to occupy a diverse morphological space.

### *Future Directions*

- 1) Incorporate biomechanical metrics to determine the amount of covariance explained by bite force and mechanical advantage.
- 2) Test if the covariance magnitudes estimated here remain as significant when compared to other module magnitudes within the same population (per Porto *et al.*, 2009; 2013).
- 3) Collect ontogenetic samples to test whether shape variance correlates with magnitude differences over ontogeny.
- 4) Test hypotheses on a larger sample of NWM mandibles to generate more inclusive results and test phylogenetic hypotheses.





## Chapter 6: Overall Conclusions

### 6.1 Interpretations of Mandibular Covariance from both Samples

The samples used here were disparate in multiple ways. Samples were derived from separate orders, Rodentia (mice) and Primates (primates), consisted of ontogenetic (mice) and adult samples (primates), consisted of laboratory (mice) and natural populations (primates) and were constructed at the intra-population (mice) and inter-population levels (primates). Furthermore, each sample was constructed to address specific outstanding questions in the literature. The mouse sample was designed to address questions related to hypotheses surrounding the ontogenetic structure of covariance. Additionally, these hypotheses addresses questions relating to the influence of function as a covariance generating factor experienced in later ontogeny. The primate sample was constructed to address questions related to how covariance differs in the mandible of primates under separate functional demands. However, each of the hypotheses proposed in this study are inter-related and the analyses applied to each sample were nearly identical, such that the results from each sample can be widely interpreted together. Four main conclusions from the results found here stand-out: 1) the mandible is a nested hierarchical structure; 2) pattern of covariance is conserved while magnitude of covariance is plastic; 3) covariance changes over ontogeny, and; 4) function influences covariance. Each of these conclusions is discussed further below.

### 6.1.1 The Mandible is a Nested Hierarchical Structure

In accordance with the Palimpsest Model the structure of covariance in the mandible is hierarchical. Meaning that the organization of covariance will include both integration between units on a larger scale and modular organization within units on a smaller scale. This is evidenced by the presence of both Bi-modular and Mesenchymal modules found in the mouse and primate mandibles. Similar nested-hierarchical structures are present in the crania of Mammalia at large. Extreme instances of integration or modularity would likely prove disadvantageous to evolution at the population level. Possessing a nested-hierarchy of covariance allows the mandible to respond dynamically to selective pressures while still coordinating interactions between developmentally/ functionally interdependent units.

Dynamic organization of integration and modularity largely also reflects the multiple influences on the mandible. Covariance generating processes are present at several levels from pleiotropic genetic signaling, tissue-to-tissue induction processes, muscle-to-bone interactions, overall somatic growth, etc. Each of these processes contributes to the covariance of the mandible and asserts its influence at multiple anatomical levels and developmental periods. Thus when attempting to reconstruct covariance in the mandible it is important to design hypotheses with this multi-level organization in mind.

### 6.1.2 Pattern of Covariance is conserved while Magnitude of Covariance is Plastic

Similar to the multi-level organization of integration and modularity, there is also a dynamic relationship between patterns and magnitudes of covariance. Samples used here showed similar discrepancies between the pattern and magnitude of covariance found in several studies of crania across largely diverse taxa. Here, pattern of covariance was found to be similar in age-matched wild-type and Crouzon mice, as well as in the primate sample. Magnitude on the other hand was significantly different in all age-matched mice and within each pair-wise comparison of primates.

Like the skull, the mandible is clearly under stabilizing selection due to developmental and functional constraints. This is even further evidenced by the fact that patterns of covariance were not distinguishable between wild-type mice and Crouzon mice. Furthermore, patterns of covariance were not different in primates despite extreme differences in masticatory forces applied to the mandible in different primates. Thus, developmental and functional constraints dictate the way in which traits must be correlated in order to grow properly and function efficiently.

Magnitude on the other hand, differed significantly in both the age-matched mice and between primates that habitually exploit a hard-diet and those primates that do not. Mandibular magnitudes, again, mirror those in the skull in that they vary with much more frequency. NWM are a highly diverse group of primates in which the masticatory apparatus has been adapted to particular dietary regimes, evidenced by the morphological diversity apparent in their mandibles. Plasticity in mandibular magnitudes is a likely candidate to assist in the diversification of mandibular shape in primates. Furthermore, considering the close phylogenetic relationships of the pair-wise comparisons conducted

here (*Cebus* – *Saimiri* and *Pithecia* – *Callicebus*) it is likely that that plasticity in magnitude aids morphological variation to respond to selective pressures in short evolutionary time periods (Porto *et al.*, 2009; Armbruster *et al.*, 2014).

The ratio of modularity within specific modules relative to the overall integration/modularity within the mandible is also of great importance, especially in the primate sample. Differences in these ratios may explain why *Cebus apella* was the only hard diet primate to demonstrate large overall integration. It may also distinguish between those primates that have a mandible adapted to a specialized diet from those that do not. Future studies should incorporate analyses utilizing the modularity index.

#### 6.1.3 Covariance Changes over Ontogeny

Another major tenet of the Palimpsest model states that covariance will change over ontogeny as new covariance generating factors overlay other covariance generating factors from earlier developmental stages. These include, as stated above, from pleiotropic genetic signaling, tissue-to-tissue induction processes, muscle-to-bone interactions and overall somatic growth among others. The objectives of the developmental mouse model explicitly attempted to determine if, when and to what degree did patterns and magnitudes of covariance change over ontogeny. Indeed, pattern and magnitude of covariance were modified as the mouse mandible advanced in age, supporting the Palimpsest model.

Interestingly, as seen among the age-matched samples, pattern of covariance was more conserved, occurring only between late developmental stages, while change in magnitude occurred throughout ontogeny. Patterns of covariance found here do not agree with previous studies which identified shifts earlier in ontogeny within the crania.

Differences between those studies and this could be due to either data collection techniques or the fact that the mandible has a more prolonged growth trajectory compared to most of the cranium. Late ontogenetic shifts in mandibular patterns of covariance may also be due to functional demands brought on by the introduction of an adult diet, as discussed below. Magnitude on the other hand continues to vary significantly among mandibles but in a relatively consistent pattern that shows embryonic mice possessing the largest amounts of integration and the adults possessing the least.

Importantly, it should be reiterated here that the use of Procrustes superimposition does reallocate variance across landmarks. This may bias the signal of variance as landmarks that are not biologically prone to variability will demonstrate increased variance and vice-versa after Procrustes analysis. Thus, one possible way to explain the late-onset change in patterns of covariance among developing mice is methodology. If landmark variance is objectively flawed, the method used here may not reliably detect biological shifts in the way landmarks covary. Hence, important changes in covariance among the younger mice may be masked in the analyses conducted here. As mentioned in Chapter 3: Materials and Methods, Euclidean Distance Matrix Analysis (EDMA) is a distance based methodology that creates a coordinate-free way to employ landmark data in analyses of shape differences, variance and covariance among biological groups. Future analyses will incorporate EDM to test hypotheses of covariance.

The timing of different changes in covariance may have an important impact on when selection can act on the mandible. Early developmental constraints in the pattern of covariance may prevent a response to selective pressure possibly to due factors such as dental development or tracking cranial growth. However, there seems to be a break in

covariance patterns from weaning to adulthood which may in fact demonstrate a significant influence of diet/function which induces changes in mandibular traits correlations. Similarly, constraint on magnitude of integration seems to be relaxed as mice approach adulthood. Perhaps it is beneficial for the structure of covariance to vary during late ontogeny as adult diets are first being experienced which may also suggest that adaptive pressures for efficient masticatory complex occur in later developmental stages, as well.

#### 6.1.4 Function Influences Covariance

Post-weaning changes in the patterns of covariance among mice paired with the greater magnitude of integration found in *C. apella* suggest that function is a significant covariance generating factor in the mandible. Functional causes of integration may be the result of external forces such as muscle-to-bone interactions, peak occlusal loads and the resultant coordinated remodeling of bone that likely cause greater covariance between traits. It is also possible that the patterns of covariance related to diet and function are the result of long-term adaptive influence in the mandible. The hypotheses tested here were not explicitly designed to address these questions, neither is it suggested that the short-term or long-term functional influence on covariance is mutually exclusive.

Greater overall integration in the *C. apella* mandible could be interpreted as the result of *in vivo* functional requirements that need to be met in order to successfully ingest its specialized hard-diet. The recruitment of larger muscular forces along with the structural ability to withstand those forces could result in greater coordination during bone remodeling for a more robust mandible. Yet, considering that *P. pithecia* does not

demonstrate significantly greater integration within the mandible compared to *C. torquatus* may negate that premise. However, in the context of NWM that masticate mechanically resistant foods, *P. pithecia* is considered to be intermediate so that the greater amount of integration found in *C. apella* may be the result of a specialized hard diet. Whether these trends might be found only at the individual-level or as a population-level feature could determine whether higher amounts of integration are also an adaptive response to function. Future analyses will incorporate other *Cebus spp.* If the magnitudes are found to differ among *C. apella* and other capuchins it may suggest that *C. apella* is specifically adapted for their diet.

Another confounding factor may again stem from the use of Procrustes superimposition to calculate and analyze variance and covariance. Partitioning variance among all landmarks may dilute signals of magnitude in *P. pithecia* mandible, making it difficult to discern any difference from *C. torquatus*. EDMA analyses may rectify the discrepancy found when both “hard diet” primates are compared to their “softer-diet” cohorts. Future analyses of integration will therefore include distance based procedures and analyses of EDMA mean form.

In contrast, larger amounts of integration were not found among the adult-mice as was originally proposed. The change in mechanical forces may not be significant enough to generate significant increases in the strength of integration within a population. However, changes in the pattern of integration do seem to track with the introduction of an adult diet. It may be that rearranging the way in which traits covary is relatively more important for intra-population functional constraints and influences on covariance rather than the strength with which they covary. This may be true in species that are not



specialized for a mechanically difficult diet. This is especially important considering that other experimental analyses have demonstrated that the mandibles of mice fed hard-diets were more likely to be better integrated than those fed a soft-diet (Anderson *et al.*, 2014).



## Literature Cited

- Ackermann RR, Cheverud JM. 2000. Phenotypic covariance structure in tamarins (genus *Saguinus*): A comparison of variation patterns using matrix correlation and common principal component analysis. *Am J Phys Anthropol* 111(4):489-501.
- Ackermann RR. 2005. Ontogenetic integration of the hominoid face. *J Hum Evol* 48(2):175-197.
- Adams DC, Otárola-Castillo E. 2013. Geomorph: An R package for the collection and analysis of geometric morphometric shape data. *Methods in Ecology and Evolution* 4(4):393-399.
- Ahmed I, Afzal A. 2009. Diagnosis and evaluation of Crouzon syndrome. *J Coll Physicians Surg Pak* 19(5):318-320.
- Alarcón JA, Bastir M, García-Espona I, Menéndez-Núñez M, Rosas A. 2014. Morphological integration of mandible and cranium: Orthodontic implications. *Arch Oral Biol* 59(1):22-29.
- Albertson RC, Streelman JT, Kocher TD, Yelick PC. 2005. Integration and evolution of the cichlid mandible: The molecular basis of alternate feeding strategies. *Proc Natl Acad Sci USA* 102(45):16287-16292.
- Alfaro JWL, Silva JSE, Rylands AB. 2012. How different are robust and gracile capuchin monkeys? An argument for the use of *Sapajus* and *Cebus*. *Am J Primatol* 74(4):273-286.
- Alvarez SJ, Heymann EW. 2012. Brief Communication: a preliminary study of the influence of physical fruit traits of fruit handling and seed fate by white-handed titi monkeys (*Callicebus lugens*). *Am J Phys Anthropol* 147:482-488.

- Anapol F, Lee S. 1994. Morphological adaptation to diet in platyrrhine primates. *Am J Phys Anthropol* 94(2):239-261.
- Anderson PS, Renaud S, Rayfield EJ. 2014. Adaptive plasticity in the mouse mandible. *BMC Evolutionary Biology* 14(1):85.
- Armbruster WS, Pélabon C, Bolstad GH, Hansen TF. 2014. Integrated phenotypes: understanding trait covariation in plants and animals. *Philosophical Transactions of the Royal Society B: Biological Sciences*, 369(1649), 20130245.
- Atchley WR. 1987. Developmental quantitative genetics and the evolution of ontogenies. *Evolution* 41(2): 316-330.
- Atchley WR. 1993. Genetic and developmental aspects of variability in the mammalian mandible. *The Skull* 1:207-247.
- Atchley WR, Hall BK. 1991. A model for development and evolution of complex morphological structures. *Biological Reviews* 66(2):101-157.
- Atchley WR, Plummer AA, Riska B. 1985. Genetic analysis of size-scaling patterns in the mouse mandible. *Genetics* 111(3):579-595.
- Atchley WR, Plummer AA, Riska B. 1985. Genetics of mandible form in the mouse. *Genetics* 111(3):555-577.
- Baba ML, Darga LL, Goodman M. 1979. Immunodiffusion systematics of the primates. *Folia Primatol* 32(3):207-238.
- Bachmayer DI, Ross RB, Munro IR. 1986. Maxillary growth following LeFort III advancement surgery in Crouzon, Apert, and Pfeiffer syndromes. *American Journal of Orthodontics and Dentofacial Orthopedics* 90(5):420-430.

- Badyaev AV, Foresman KR. 2004. Evolution of morphological integration. I. Functional units channel stress-induced variation in shrew mandibles. *Am Nat* 163(6):868-879.
- Badyaev AV, Foresman KR, Young RL. 2005. Evolution of morphological integration: Developmental accommodation of stress-induced variation. *Am Nat* 166(3):382-395.
- Badyaev AV. 2005. Stress-induced variation in evolution: From behavioral plasticity to genetic assimilation. *Proc Biol Sci* 272(1566):877-886.
- Bailey DW. 1986. Genes that affect morphogenesis of the murine mandible: Recombinant-inbred strain analysis. *J Hered* 77(1):17-25.
- Bastir M, Rosas A. 2005. Hierarchical nature of morphological integration and modularity in the human posterior face. *Am J Phys Anthropol* 128(1):26-34.
- Bastir M, Rosas A, O'Higgins P. 2006. Craniofacial levels and the morphological maturation of the human skull. *J Anat* 209(5):637-654.
- Baughan B, Demirjian A, Levesque G, Lapalme-Chaput L. 1979. The pattern of facial growth before and during puberty, as shown by French-Canadian girls. *Ann Hum Biol* 6(1):59-76.
- Beecher RM, Corruccini RS. 1981. Effects of dietary consistency on craniofacial and occlusal development in the rat. *Angle Orthod* 51(1):61-69.
- Beecher RM, Corruccini RS, Freeman M. 1983. Craniofacial correlates of dietary consistency in a nonhuman primate. *J Craniofac Genet Dev Biol* 3(2):193-202.
- Beldade P, Brakefield PM. 2003. Concerted evolution and developmental integration in modular butterfly wing patterns. *Evol Dev* 5(2):169-179.

- Bertrand S, Camasses A, Somorjai I, Belgacem MR, Chabrol O, Escande ML, Pontarotti P, Escriva H. 2011. Amphioxus FGF signaling predicts the acquisition of vertebrate morphological traits. *Proc Natl Acad Sci USA* 108(22):9160-9165.
- Biewener AA, Bertram JE. 1993. Skeletal strain patterns in relation to exercise training during growth. *J Exp Biol* 185:51-69.
- Boell L, Tautz D. 2011. Micro-evolutionary divergence patterns of mandible shapes in wild house mouse (*Mus musculus*) populations. *BMC Evol Biol* 11:306-2148-11-306.
- Bookstein FL. 1991. Morphometric tools for landmark data: Geometry and biology. Cambridge University Press.
- Bookstein FL. 1997. Landmark methods for forms without landmarks: Morphometrics of group differences in outline shape. *Medical image analysis*. 1(3), 225-243.
- Bookstein FL, Gunz P, Mitterøcker P, Prossinger H, Schæfer K, Seidler H. 2003. Cranial integration in *Homo*: Singular warps analysis of the midsagittal plane in ontogeny and evolution. *J Hum Evol* 44(2):167-187.
- Bonner JT. 1988. The evolution of complexity by means of natural selection. Princeton, NJ: Princeton University Press.
- Boubli JP, Rylands AB, Farias IP, Alfaro ME, ALFARO JL. 2012. *Cebus* phylogenetic relationships: A preliminary reassessment of the diversity of the untufted capuchin monkeys. *Am J Primatol* 74(4):381-393.
- Bouvier M. 1986. A biomechanical analysis of mandibular scaling in old world monkeys. *Am J Phys Anthropol* 69(4):473-482.
- Bouvier M. 1986. Biomechanical scaling of mandibular dimensions in new world monkeys. *Int J Primatol* 7(6):551-567.

- Bouvier M, Hylander WL. 1981. Effect of bone strain on cortical bone structure in macaques (*Macaca mulatta*). *J Morphol* 167(1):1-12.
- Bresnick S, Schendel S. 1995. Crouzon's disease correlates with low fibroblastic growth factor receptor activity in stenosed cranial sutures. *J Craniofac Surg* 6(3):245-248.
- Breuker CJ, Debat V, Klingenberg CP. 2006. Functional evo-devo. *Trends in Ecology & Evolution* 21(9):488-492.
- Burgio G, Baylac M, Heyer E, Montagutelli X. 2012. Exploration of the genetic organization of morphological modularity on the mouse mandible using a set of interspecific recombinant congenic strains between C57BL/6 and mice of the *Mus spretus* species. *G3-Genes Genomes Genetics* 2(10):1257-1268.
- Buschang PH, Baume RM, Nass GG. 1983. A craniofacial growth maturity gradient for males and females between 4 and 16 years of age. *Am J Phys Anthropol* 61(3):373-381.
- Carinci F, Avantaggiato A, Curioni C. 1994. Crouzon syndrome: Cephalometric analysis and evaluation of pathogenesis. *The Cleft Palate-Craniofacial Journal* 31(3):201-209.
- Chernoff B, Magwene P. 1999. Morphological integration: Forty years later. In: Olson EC, Miller RL, editors. *Morphological integration*. Chicago: University of Chicago Press. p 319–348.
- Cheverud JM. 1982. Phenotypic, genetic, and environmental morphological integration in the cranium. *Evolution* 36(3): 499-516.
- Cheverud JM. 1984. Quantitative genetics and developmental constraints on evolution by selection. *J Theor Biol* 110(2):155-171.

- Cheverud JM. 1989. A comparative analysis of morphological variation patterns in the papionins. *Evolution* 43(8): 1737-1747.
- Cheverud JM. 1996. Developmental integration and the evolution of pleiotropy. *Am Zool* 36(1):44-50.
- Cheverud JM, Ehrich TH, Vaughn TT, Koreishi SF, Linsey RB, Pletscher LS. 2004. Pleiotropic effects on mandibular morphology II: Differential epistasis and genetic variation in morphological integration. *Journal of Experimental Zoology Part B: Molecular and Developmental Evolution* 302(5):424-435.
- Cheverud JM, Hartman SE, Richtsmeier JT, Atchley WR. 1991. A quantitative genetic analysis of localized morphology in mandibles of inbred mice using finite element scaling analysis. *J Craniofac Genet Dev Biol* 11:122-137.
- Cheverud JM, Leamy LJ. 1985. Quantitative genetics and the evolution of ontogeny. III. Ontogenetic changes in correlation structure among live-body traits in random bred mice. *Genet Res* 46(03):325-335.
- Cheverud JM, Routman EJ, Irschick DJ. 1997. Pleiotropic effects of individual gene loci on mandibular morphology. *Evolution* 51(6): 2006-2016.
- Cheverud J. 1996. Quantitative genetic analysis of cranial morphology in the cotton-top (*Saguinus oedipus*) and saddle-back (*S. fuscicollis*) tamarins. *J Evol Biol* 9(1):5-42.
- Cole TM. 1992. Postnatal heterochrony of the masticatory apparatus in *Cebus apella* and *Cebus albifrons*. *J Hum Evol* 23(3):253-282.
- Cobb SN, O'Higgins P. 2007. The ontogeny of sexual dimorphism in the facial skeleton of the African apes. *J Hum Evol* 53:176–190.



- Cooper WJ, Wernle J, Mann K, Albertson RC. 2011. Functional and genetic integration in the skulls of Lake Malawi cichlids. *Evolutionary Biology* 38(3):316-334.
- Corner BD, Lele S, Richtsmeier JT. 1992. Measuring precision of three-dimensional landmark data. *J Quant Anthropol* 3:347-359.
- Corruccini RS, Beecher RM. 1982. Occlusal variation related to soft diet in a nonhuman primate. *Science* 218(4567):74-76.
- Costaras-Volarich M, Pruzansky S. 1984. Is the mandible intrinsically different in Apert and Crouzon syndromes? *Am J Orthod* 85(6):475-487.
- Coulier F, Pontarotti P, Roubin R, Hartung H, Goldfarb M, Birnbaum D. 1997. Of worms and men: An evolutionary perspective on the fibroblast growth factor (FGF) and FGF receptor families. *J Mol Evol* 44(1):43-56.
- Daegling DJ. 1989. Biomechanics of cross-sectional size and shape in the hominoid mandibular corpus. *Am J Phys Anthropol* 80(1):91-106.
- Daegling DJ. 1992. Mandibular morphology and diet in the genus *Cebus*. *Int J Primatol* 13(5):545-570.
- Daegling DJ. 1996. Growth in the mandibles of African apes. *J Hum Evol* 30(4):315-341.
- Daegling DJ. 2002. Bone geometry in cercopithecoid mandibles. *Arch Oral Biol* 47(4):315-325.
- Daegling DJ. 2007. Relationship of bone utilization and biomechanical competence in hominoid mandibles. *Arch Oral Biol* 52(1):51-63.
- Daegling DJ, Grine FE. 2007. Mandibular biomechanics and the paleontological evidence for the evolution of human diet. In: Ungar PS, editor. *Evolution of the*

human diet: the known, the unknown, and the unknowable. New York: Oxford University Press. p 106–131.

Daegling DJ, Hotzman JL. 2003. Functional significance of cortical bone distribution in anthropoid mandibles: An in vitro assessment of bone strain under combined loads. *Am J Phys Anthropol* 122(1):38-50.

Daegling DJ, McGraw WS. 2007. Functional morphology of the mangabey mandibular corpus: Relationship to dental specializations and feeding behavior. *Am J Phys Anthropol* 134(1):50-62.

Daegling D, McGraw W. 2000. Gnathic morphology and feeding ecology in papionin primates. *American Journal of Physical Anthropology*, 30 (Supplement), 134.

Dean CA, Rohlf FJ, Slice DE. 2004. Geometric morphometrics: ten years of progress following the 'revolution'. *Italian Journal of Zoology* 71(1):5-16.

David DJ, Sheen R. 1990. Surgical correction of Crouzon syndrome. *Plast Reconstr Surg* 85(3):344-354.

de Oliveira FB, Porto A, Marroig G. 2009. Covariance structure in the skull of catarrhini: A case of pattern stasis and magnitude evolution. *J Hum Evol* 56(4):417-430.

Deane A. 2012. Platyrrhine incisors and diet. *Am J Phys Anthropol* 148:249-261.

Dechow PC, Hylander WL. 2000. Elastic properties and masticatory bone stress in the macaque mandible. *Am J Phys Anthropol* 112(4):559-574.

Dechow PC, Wang Q, Peterson J. 2010. Edentulation alters material properties of cortical bone in the human craniofacial skeleton: functional implications for craniofacial structure in primate evolution. *Anat Rec* 293(4):618-629.

- DeLeon VB, Richtsmeier JT. 2009. Fluctuating asymmetry and developmental instability in sagittal craniosynostosis. *The Cleft Palate-Craniofacial Journal* 46(2):187-196.
- DeLeon VB, Zumpano MP, Richtsmeier JT. 2001. The effect of neurocranial surgery on basicranial morphology in isolated sagittal craniosynostosis. *The Cleft Palate-Craniofacial Journal* 38(2):134-146.
- Demes B, Creel N. 1988. Bite force, diet, and cranial morphology of fossil hominids. *J Hum Evol* 17(7):657-670.
- Drake AG, Klingenberg CP. 2010. Large-scale diversification of skull shape in domestic dogs: Disparity and modularity. *Am Nat* 175(3):289-301.
- Duarte LC, Monteiro LR, Von Zuben FJ, Dos Reis SF. 2000. Variation in mandible shape in *Thrichomys apereoides* (Mammalia: Rodentia): Geometric analysis of a complex morphological structure. *Syst Biol* 49(3):563-578.
- Ehrich TH, Vaughn TT, Koreishi SF, Linsey RB, Pletscher LS, Cheverud JM. 2003. Pleiotropic effects on mandibular morphology I. Developmental morphological integration and differential dominance. *Journal of Experimental Zoology Part B: Molecular and Developmental Evolution* 296(1):58-79.
- Enlow DH, Hans MG. 1996. *Essentials of facial growth*. Philadelphia, PA: WB Saunders Company.
- Estes S, & Arnold SJ. 2007. Resolving the paradox of stasis: models with stabilizing selection explain evolutionary divergence on all timescales. *The American Naturalist*, 169(2), 227-244.
- Eswarakumar VP, Horowitz MC, Locklin R, Morriss-Kay GM, Lonai P. 2004. A gain-of-function mutation of *Fgfr2c* demonstrates the roles of this receptor variant in osteogenesis. *Proc Natl Acad Sci USA* 101(34):12555-12560.

- Eswarakumar VP, Ozcan F, Lew ED, Bae JH, Tome F, Booth CJ, Adams DJ, Lax I, Schlessinger J. 2006. Attenuation of signaling pathways stimulated by pathologically activated FGF-receptor 2 mutants prevents craniosynostosis. *Proc Natl Acad Sci USA* 103(49):18603-18608.
- Fish JL, Sklar RS, Woronowicz KC, Schneider RA. 2014. Multiple developmental mechanisms regulate species-specific jaw size. *Development* 141(3):674-684.
- Fleagle JG, Mittermeier RA, Skopec AL. 1981. Differential habitat use by *Cebus apella* and *Saimiri sciureus* in central Surinam. *Primates* 22(3):361-367.
- Ford SM. 1986. Systematics of the New World monkeys. In: Swindler DR, Erwin J, editors. *Comparative primate biology*, Vol.1. Systematics, evolution, and anatomy. New York: Alan R. Liss, Inc. p 73–135.
- Galetti M, Pedroni F. 1994. Seasonal diet of capuchin monkeys (*Cebus apella*) in a semideciduous forest in south-east Brazil. *Journal of Tropical Ecology* 10(1):27-39.
- Galvin BD, Hart KC, Meyer AN, Webster MK, Donoghue DJ. 1996. Constitutive receptor activation by Crouzon syndrome mutations in fibroblast growth factor receptor (FGFR)2 and FGFR2/Neu chimeras. *Proc Natl Acad Sci U S A* 93(15):7894-7899.
- Garber PA, Bicca-Marques JC, Azevedo-Lopes MAO. 2008. In: Garber PA, Estrada A, Bicca-Marques JC, Heymann EW, Strier KB editors. *South American primates: Comparative perspectives in the study of behavior, ecology, and conservation*. Chicago: Springer Science & Business Media. p 365 – 388.
- Garber PA, Leigh SR. 1997. Ontogenetic variation in small-bodied new world primates: Implications for patterns of reproduction and infant care. *Folia Primatol* 68(1):1-22.
- Garcia G, Hingst-Zaher E, Cerqueira R, Marroig G. 2014. Quantitative genetics and modularity in cranial and mandibular morphology of *Calomys expulsus*. *Evolutionary Biology* 41(4):619-636.

- Gonzalez PN, Hallgrímsson B, Oyhenart EE. 2011. Developmental plasticity in covariance structure of the skull: Effects of prenatal stress. *J Anat* 218(2):243-257.
- Gonzalez PN, Lotto FP, Hallgrímsson B. 2014. Canalization and developmental instability of the fetal skull in a mouse model of maternal nutritional stress. *Am J Phys Anthropol* 154(4):544-553.
- Gonzalez PN, Oyhenart EE, Hallgrímsson B. 2011. Effects of environmental perturbations during postnatal development on the phenotypic integration of the skull. *Journal of Experimental Zoology Part B: Molecular and Developmental Evolution* 316(8):547-561.
- Goswami A. 2006. Cranial modularity shifts during mammalian evolution. *Am Nat* 168(2):270-280.
- Goswami A. 2007. Phylogeny, diet, and cranial integration in Australodelphian marsupials. *PLoS One* 2(10):e995.
- Goswami A, Polly P, Mock O, Sánchez-Villagra M. 2012. Shape, variance and integration during craniogenesis: Contrasting marsupial and placental mammals. *J Evol Biol* 25(5):862-872.
- Goswami A., Smaers JB, Soligo C, Polly PD. 2014. The macroevolutionary consequences of phenotypic integration: from development to deep time. *Philosophical Transactions of the Royal Society of London B: Biological Sciences*, 369(1649), 20130254.
- Goswami A, Polly PD. 2010. The influence of modularity on cranial morphological disparity in Carnivora and primates (Mammalia). *PLoS One* 5(3):e9517.
- Greaves WS. 1978. The jaw lever system in ungulates: a new model. *J Zool* 184(2):271-285.

Griffin JN, Compagnucci C, Hu D, Fish J, Klein O, Marcucio R, Depew MJ. 2013. Fgf8 dosage determines midfacial integration and polarity within the nasal and optic capsules. *Dev Biol* 374(1):185-197.

Groves CP. 2001. *Primate taxonomy*. Washington, DC: Smithsonian Institution Press.

Gunz P, Mitteroecker P, Bookstein F. 2005. Semilandmarks in three dimensions. In: Slice D, editor. *Modern morphometrics in physical anthropology*. New York, NY: Kluwer Academic/Plenum Publishers. p 73–98.

Hall BK. 1999. *Evolutionary developmental biology*, Kluwer Academia Publishers. Dordrecht.

Hall BK. 2003. Unlocking the black box between genotype and phenotype: Cell condensations as morphogenetic (modular) units. *Biology and Philosophy* 18(2):219-247.

Hallgrímsson B. 1999. Ontogenetic patterning of skeletal fluctuating asymmetry in rhesus macaques and humans: Evolutionary and developmental implications. *Int J Primatol* 20(1):121-151.

Hallgrímsson B, Brown JJ, Ford-Hutchinson AF, Sheets HD, Zelditch ML, Jirik FR. 2006. The brachymorph mouse and the developmental-genetic basis for canalization and morphological integration. *Evol Dev* 8(1):61-73.

Hallgrímsson B, Jamniczky H, Young NM, Rolian C, Parsons TE, Boughner JC, Marcucio RS. 2009. Deciphering the palimpsest: Studying the relationship between morphological integration and phenotypic covariation. *Evolutionary Biology* 36(4):355-376.

Hallgrímsson B, Lieberman DE, Young NM, Parsons T, Wat S. 2007. Evolution of covariance in the mammalian skull. In: *Novartis Foundation Symp* 284:164 – 185.

- Hallgrímsson B, Willmore K, Dorval C, Cooper DM. 2004. Craniofacial variability and modularity in macaques and mice. *Journal of Experimental Zoology Part B: Molecular and Developmental Evolution* 302(3):207-225.
- Hansen TF. 2003. Is modularity necessary for evolvability? Remarks on the relationship between pleiotropy and evolvability. *Biosystems* 69(2):83-94.
- Hansen TF, Houle D. 2004. Evolvability, stabilizing selection and the problem of stasis. In: Pigliucci M, Preston K, editors. *Phenotypic integration: studying the ecology and evolution of complex phenotypes*. Oxford, UK: Oxford University Press. p 130–150.
- Hartwig WC. 1996. Perinatal life history traits in new world monkeys. *Am J Primatol* 40(2):99-130.
- Harvati K, Singh N, Lopez EN. 2011. A three-dimensional look at the Neanderthal mandible. In: Condemi S, Weniger G-C, editors. *Continuity and Discontinuity in the People of Europe: One Hundred Fifty Years of Neanderthal Study*. New York, NY: Springer. pp 179–192.
- Hawes JE, Peres CA. 2014. Ecological correlates of trophic status and frugivory in Neotropical primates. *Oikos* 123(3):365-377.
- Herring SW. 1993. Formation of the vertebrate face epigenetic and functional influences. *Am Zool* 33(4):472-483.
- Herring SW, Rafferty KL, Liu ZJ, Marshall CD. 2001. Jaw muscles and the skull in mammals: The biomechanics of mastication. *Comparative Biochemistry and Physiology Part A: Molecular & Integrative Physiology* 131(1):207-219.
- Herring SW, Lakars TC. 1982. Craniofacial development in the absence of muscle contraction. *J Craniofac Genet Dev Biol* 1(4):341-357.

- Hershkovitz P. 1977. Living New World monkeys (Platyrrhini). Chicago: University of Chicago Press.
- Heymann EW, Nadjafzadeh MN. 2013. Insectivory and prey foraging techniques in *Callicebus*—a case study of *Callicebus cupreus* and a comparison to other pitheciids. In: Barnett AA, Veiga LM, Ferrari SF, Norconk MA, editors. Evolutionary biology and conservation of Titis, Sakis and Uacaris. Cambridge, UK: Cambridge University Press. p 215–224.
- Holmes MA, DeLeon VB, Perlyn C. 2011. Dysmorphology in the mandible of a Crouzon mouse model. The FASEB Journal 25(Supplement):64.4.
- Holmes MA, Ruff CB. 2011. Dietary effects on development of the human mandibular corpus. Am J Phys Anthropol 145(4):615-628.
- Holmes MA. 2013. The influence of dentition on the developing mandible in a mouse model. The FASEB Journal 27(Supplement):963.7.
- Holton NE, Franciscus RG, Ravosa MJ, Southard TE. 2014. Functional and morphological correlates of mandibular symphyseal form in a living human sample. Am J Phys Anthropol 153(3):387-396.
- Hoover KC, Williams FL. *In press*. Variation in regional diet and mandibular morphology in prehistoric Japanese hunter–gatherer–fishers. Quaternary International.
- Hu Y, Albertson RC. 2014. Hedgehog signaling mediates adaptive variation in a dynamic functional system in the cichlid feeding apparatus. Proc Natl Acad Sci USA 111(23):8530-8534.
- Heuzé Y, Martínez-Abadías N, Stella JM, Arnaud E, Collet C, Fructuoso GG, Alamar M, Lo LJ, Boyadjiev SA, Di Rocco F, Richtsmeier JT. 2014a. Quantification of facial skeletal shape variation in fibroblast growth factor receptor-related



craniosynostosis syndromes. Birth Defects Research Part A: Clinical and Molecular Teratology 100 (4): 250-259.

- Heuzé Y, Singh N, Basilico C, Jabs EW, Holmes G, Richtsmeier JT. 2014b. Morphological comparison of the craniofacial phenotypes of mouse models expressing the Apert *FGFR2*<sup>S252W</sup> mutation in neural crest-or mesoderm-derived tissues. Bone 63():101-109.
- Hughes SE. 1997. Differential expression of the Fibroblast Growth Factor Receptor (FGFR) multigene family in normal human adult tissues. J Histochem Cytochem 45(7):1005-1019.
- Huiskes R. 2000. If bone is the answer, then what is the question? J Anat 197(02):145-156.
- Hünemeier T, Gómez-Valdés J, Azevedo S, Quinto-Sánchez M, Passaglia L, Salzano FM, Sánchez-Mejorada G, Alonzo VA, Martínez-Abadías N, Bortolini M. 2014. FGFR1 signaling is associated with the magnitude of morphological integration in human head shape. Am J Hum Biol 26(2):164-175.
- Hylander WL. 1975. The human mandible: Lever or link? Am J Phys Anthropol 43(2):227-242.
- Hylander WL. 1978. Incisal bite force direction in humans and the functional significance of mammalian mandibular translation. Am J Phys Anthropol 48(1):1-7.
- Hylander WL. 1979. The functional significance of primate mandibular form. J Morphol 160(2):223-239.
- Hylander WL, Johnson KR. 1994. Jaw muscle function and wishboning of the mandible during mastication in macaques and baboons. Am J Phys Anthropol 94(4):523-547.

- Iriarte-Diaz J, Reed DA, Ross CF. 2011. Sources of variance in temporal and spatial aspects of jaw kinematics in two species of primates feeding on foods of different properties. *Integr Comp Biol* 51(2):307-319.
- Iseki S, Wilkie AO, Heath JK, Ishimaru T, Eto K, Morriss-Kay GM. 1997. Fgfr2 and osteopontin domains in the developing skull vault are mutually exclusive and can be altered by locally applied FGF2. *Development* 124(17):3375-3384.
- Izawa K, Mizuno A. 1977. Palm-fruit cracking behavior of wild black-capped capuchin (*Cebus apella*). *Primates* 18(4):773-792.
- Jamniczky HA, Hallgrímsson B. 2009. A comparison of covariance structure in wild and laboratory muroid crania. *Evolution* 63(6):1540-1556.
- Jamniczky HA, Harper EE, Garner R, Cresko WA, Wainwright PC, Hallgrímsson B, Kimmel CB. 2014. Association between integration structure and functional evolution in the opercular four-bar apparatus of the threespine stickleback, *Gasterosteus aculeatus* (Pisces: Gasterosteidae). *Biol J Linn Soc* 111(2):375-390.
- Janson CH, Boinski S. 1992. Morphological and behavioral adaptations for foraging in generalist primates: The case of the cebines. *Am J Phys Anthropol* 88(4):483-498.
- Jojić V, Blagojević J, Vujošević M. 2012. Two-module organization of the mandible in the yellow-necked mouse: A comparison between two different morphometric approaches. *J Evol Biol* 25(12):2489-2500.
- Jones AG, Arnold SJ, Bürger R. 2003. Stability of the G-matrix in a population experiencing pleiotropic mutation, stabilizing selection, and genetic drift. *Evolution*, 57(8): 1747-1760.
- Jones AG, Arnold SJ, Bürger R. 2007. The mutation matrix and the evolution of evolvability. *Evolution*, 61(4): 727-745.

- Jones AG, Bürger R, Arnold SJ. 2014. Epistasis and natural selection shape the mutational architecture of complex traits. *Nature communications*, 5:3709
- Jones DC, Zelditch ML, Peake PL, German RZ. 2007. The effects of muscular dystrophy on the craniofacial shape of *Mus musculus*. *J Anat* 210(6):723-730.
- Jones KE, Ruff CB, Goswami A. 2013. Morphology and biomechanics of the pinniped jaw: Mandibular evolution without mastication. *Anat Rec* 296(7):1049-1063.
- Kaban LB, Conover M, Mulliken JB. 1986. Midface position after Le Fort III advancement: A long-term follow-up study. *Cleft Palate J* 23(s1).
- Kay RF, Meldrum DJ, Takai M. 2013. Pitheciidae and other platyrrhine seed predators. In: Barnett AA, Veiga LM, Ferrari SF, Norconk MA, editors. *Evolutionary biology and conservation of Titis, Sakis and Uacaris*. Cambridge, UK: Cambridge University Press. p 3-12.
- Kay RF. 1984. On the use of anatomical features to infer foraging behavior in extinct primates. In: Rodman PS, Cant JGH, editors. *Adaptations for foraging in nonhuman primates: contributions to an organismal biology of prosimians, monkeys, and apes*. New York, NY: Columbia University Press. p 21–53.
- Kay RF. 1990. The phyletic relationships of extant and fossil pitheciinae (Platyrrhini, Anthropoidea). *J Hum Evol* 19(1):175-208.
- Kay RF. 2015. Biogeography in deep time—What do phylogenetics, geology, and paleoclimate tell us about early platyrrhine evolution? *Mol Phylogenet Evol* 82:358-374.
- Kinzey WG. 1974. Ceboid models for the evolution of hominoid dentition. *J Hum Evol* 3(3):193-203.

- Kinzey WG. 1977. Diet and feeding behavior of *Callicebus torquatus*. In: Clutton-Brock TH, editor. Primate Ecology: Studies of Feeding and Ranging Behavior in Lemurs, Monkeys and Apes. New York, NY: Academic Press. pp 127-151.
- Kinzey WG. 1978. Feeding behavior and molar features in two species of titi monkey. Recent Advances in Primatology 1:373-385.
- Kinzey WG. 1992. Dietary and dental adaptations in the pitheciinae. Am J Phys Anthropol 88(4):499-514.
- Kinzey WG, Norconk MA. 1993. Physical and chemical properties of fruit and seeds eaten by *Pithecia* and *Chiropotes* in Surinam and Venezuela. Int J Primatol 14(2):207-227.
- Klingenberg CP. 2005. Developmental constraints, modules, and evolvability. In: Hallgrímsson B, Hall BK, editors. Variation: A Central Concept in Biology. San Diego: Academic Press. p 213–230.
- Klingenberg CP. 2008a. Morphological integration and developmental modularity. Annual Review of Ecology, Evolution, and Systematics: 115-132.
- Klingenberg CP. 2008b. Novelty and “Homology-free” morphometrics: What’s in a name? Evolutionary Biology 35(3):186-190.
- Klingenberg CP. 2009. Morphometric integration and modularity in configurations of landmarks: Tools for evaluating a priori hypotheses. Evol Dev 11(4):405-421.
- Klingenberg CP. 2010. Evolution and development of shape: Integrating quantitative approaches. Nature Reviews Genetics 11(9):623-635.
- Klingenberg CP, Debat V, Roff DA. 2010. Quantitative genetics of shape in cricket wings: Developmental integration in a functional structure. Evolution 64(10):2935-2951.

- Klingenberg CP, Leamy LJ. 2001. Quantitative genetics of geometric shape in the mouse mandible. *Evolution* 55(11):2342-2352.
- Klingenberg CP, Mebus K, Auffray J. 2003. Developmental integration in a complex morphological structure: How distinct are the modules in the mouse mandible? *Evol Dev* 5(5):522-531.
- Klingenberg CP. 2014. Studying morphological integration and modularity at multiple levels: Concepts and analysis. *Philos Trans R Soc Lond B Biol Sci* 369(1649):20130249.
- Klingenberg CP, Leamy LJ, Cheverud JM. 2004. Integration and modularity of quantitative trait locus effects on geometric shape in the mouse mandible. *Genetics* 166(4):1909-1921.
- Klingenberg CP, Leamy LJ, Routman EJ, Cheverud JM. 2001. Genetic architecture of mandible shape in mice: Effects of quantitative trait loci analyzed by geometric morphometrics. *Genetics* 157(2):785-802.
- Klingenberg CP, Marugan-Lobon J. 2013. Evolutionary covariation in geometric morphometric data: Analyzing integration, modularity, and allometry in a phylogenetic context. *Syst Biol* 62(4):591-610.
- Kohn L, Cheverud J. 1992. Issues in evaluating repeatability of an imaging system for use in anthropometry. *Proceedings of the Electronic Imaging of the Human Body Working Group, Crew System Ergonomics Information Analysis Center, Dayton, OH.*
- Kreiborg S. 1981. Craniofacial growth in Plagiocephaly and Crouzon syndrome. *Scandinavian Journal of Plastic and Reconstructive Surgery and Hand Surgery* 15(3):187-197.

- Kreiborg S, Aduss H. 1986. Pre-and postsurgical facial growth in patients with Crouzon's and Apert's syndromes. *Cleft Palate J* 23(Suppl 1):78-90.
- Kreiborg S. 1981. Crouzon syndrome. A clinical and roentgen-cephalometric study. *Scand J Plast Reconstr Surg Suppl* 18:1-198.
- Kreiborg S, Bjork A. 1981. Craniofacial asymmetry of a dry skull with Plagiocephaly. *Eur J Orthod* 3(3):195-203.
- Lambert JE, Garber PA. 1998. Evolutionary and ecological implications of primate seed dispersal. *Am J Primatol* 45:9-28.
- Lande R. 1980. The genetic covariance between characters maintained by pleiotropic mutations. *Genetics* 94(1):203-215.
- Lande R, Arnold SJ. 1983. The measurement of selection on correlated characters. *Evolution*, 37(6):1210-1226.
- Leamy L. 1994. Morphological integration of fluctuating asymmetry in the mouse mandible. *Genetica* 89:141-155.
- Leamy LJ, Routman EJ, Cheverud JM. 1997. A search for quantitative trait loci affecting asymmetry of mandibular characters in mice. *Evolution* 51 (3):957-969.
- Ledogar JA, Winchester JM, St Clair EM, Boyer DM. 2013. Diet and dental topography in pitheciine seed predators. *Am J Phys Anthropol* 150(1):107-121.
- Leigh SR. 1992. Patterns of variation in the ontogeny of primate body size dimorphism. *J Hum Evol* 23(1):27-50.
- Lele S, Richtsmeier JT. 2001. An invariant approach to statistical analysis of shapes. New York, NY: Chapman & Hall.

- Lieberman DE. 1995. Testing hypotheses about recent human evolution from skulls: Integrating morphology, function, development, and phylogeny. *Curr Anthropol* 36 (2):159-197.
- Lieberman D. 2000. Ontogeny, homology and phylogeny in the hominid craniofacial skeleton. The problem of the browridge. In: O'Higgins P, Cohn M, editors. *Development, growth and evolution: implications for the study of hominid skeletal evolution*. London: Academic Press. p 85–122.
- Lieberman DE, Hallgrímsson B, Liu W, Parsons TE, Jamniczky HA. 2008. Spatial packing, cranial base angulation, and craniofacial shape variation in the mammalian skull: Testing a new model using mice. *J Anat* 212(6):720-735.
- Lieberman DE, Krovitz GE, Yates FW, Devlin M, Claire MS. 2004. Effects of food processing on masticatory strain and craniofacial growth in a retrognathic face. *J Hum Evol* 46(6):655-677.
- Lieberman DE, Wood BA, Pilbeam DR. 1996. Homoplasy and early *Homo*: An analysis of the evolutionary relationships of *H. habilis* sensu stricto and *H. rudolfensis*. *J Hum Evol* 30(2):97-120.
- MacKinnon KC. 2013. Ontogeny of social behavior in the genus *Cebus* and the application of an integrative framework for examining plasticity and complexity in evolution. In: Clancy K, Hinde K, Rutherford J, editors. *Building babies*. New York, NY: Springer. p 387-408.
- Makedonska J, Wright BW, Strait DS. 2012. The effect of dietary adaption on cranial morphological integration in capuchins (order Primates, genus *Cebus*). *PloS One* 7(10):e40398.
- Marcucio RS, Young NM, Hu D, Hallgrímsson B. 2011. Mechanisms that underlie co-variation of the brain and face. *Genesis* 49(4):177-189.
- Marroig G, Cheverud J. 2005. Size and shape in marmosets skulls: Allometry and heterochrony in the morphological evolution of small critters. *Am J Phys Anthropol* 40 (Supplement) 145.

- Marroig G, Cheverud JM. 2001. A comparison of phenotypic variation and covariation patterns and the role of phylogeny, ecology, and ontogeny during cranial evolution of new world monkeys. *Evolution* 55(12):2576-2600.
- Marroig G, Cheverud JM. 2004. Cranial evolution in sakis (*Pithecia*, Platyrrhini) I: Interspecific differentiation and allometric patterns. *Am J Phys Anthropol* 125(3):266-278.
- Marroig G. 2007. When size makes a difference: Allometry, life-history and morphological evolution of capuchins (*Cebus*) and squirrels (*Saimiri*) monkeys (Cebinae, Platyrrhini). *BMC Evol Biol* (7):20.
- Marroig G, Shirai LT, Porto A, de Oliveira FB, De Conto V. 2009. The evolution of modularity in the mammalian skull II: evolutionary consequences. *Evolutionary Biology*, 36(1), 136-148.
- Martínez-Abadías N, Heuze Y, Wang Y, Jabs EW, Aldridge K, Richtsmeier JT. 2011. FGF/FGFR signaling coordinates skull development by modulating magnitude of morphological integration: Evidence from Apert syndrome mouse models. *PLoS One* 6(10):e26425.
- Martínez-Abadías N, Motch SM, Pankratz TL, Wang Y, Aldridge K, Jabs EW, Richtsmeier JT. 2013. Tissue-specific responses to aberrant FGF signaling in complex head phenotypes. *Developmental Dynamics*, 242(1):80-94.
- Martínez-Abadías N, Percival C, Aldridge K, Hill CA, Ryan T, Sirivunnabood S, Wang Y, Jabs EW, Richtsmeier JT. 2010. Beyond the closed suture in Apert syndrome mouse models: Evidence of primary effects of FGFR2 signaling on facial shape at birth. *Developmental Dynamics* 239(11):3058-3071.
- Mavropoulos A, Ammann P, Bresin A, Kiliaridis S. 2005. Masticatory demands induce region-specific changes in mandibular bone density in growing rats. *Angle Orthod* 75(4):625-630.



- McFadden L, McFadden K, Precious D. 1986. Effect of controlled dietary consistency and cage environment on the rat mandibular growth. *Anat Rec* 215(4):390-396.
- Meazzini MC, Mazzoleni F, Caronni E, Bozzetti A. 2005. Le Fort III advancement osteotomy in the growing child affected by Crouzon's and Apert's syndromes: Presurgical and postsurgical growth. *J Craniofac Surg* 16(3):369-377.
- Melo D, Marroig G. 2015. Directional selection can drive the evolution of modularity in complex traits. *PNAS*, 112(2), 470-475.
- Meloro C, Raia P, Carotenuto F, Cobb SN. 2011. Phylogenetic signal, function and integration in the subunits of the carnivoran mandible. *Evolutionary Biology* 38(4):465-475.
- Menegaz R. 2013. Ecomorphological Implications of Primate Dietary Variability: An Experimental Model. PhD Thesis: University of Missouri, Columbia.
- Menegaz RA, Sublett SV, Figueroa SD, Hoffman TJ, Ravosa MJ, Aldridge K. 2010. Evidence for the influence of diet on cranial form and robusticity. *Anat Rec* 293(4):630-641.
- Mitteroecker P. 2009. The developmental basis of variational modularity: Insights from quantitative genetics, morphometrics, and developmental biology. *Evolutionary Biology* 36(4):377-385.
- Mitteroecker P, Bookstein F. 2008. The evolutionary role of modularity and integration in the hominoid cranium. *Evolution* 62(4):943-958.
- Mitteroecker P, Bookstein F. 2009. The ontogenetic trajectory of the phenotypic covariance matrix, with examples from craniofacial shape in rats and humans. *Evolution* 63(3):727-737.

- Mitteroecker P, Gunz P, Bernhard M, Schaefer K, Bookstein FL. 2004. Comparison of cranial ontogenetic trajectories among great apes and humans. *J Hum Evol*, 46(6):679-698.
- Mitteroecker P, Gunz P. 2009. Advances in geometric morphometrics. *Evolutionary Biology* 36(2):235-247.
- Mitteroecker P, Bookstein F. 2007. The conceptual and statistical relationship between modularity and morphological integration. *Syst Biol* 56(5):818-836.
- Monteiro LR, Bonato V, Dos Reis SF. 2005. Evolutionary integration and morphological diversification in complex morphological structures: Mandible shape divergence in spiny rats (Rodentia, *Echimyidae*). *Evol Dev* 7(5):429-439.
- Monteiro LR, Nogueira MR. 2010. Adaptive radiations, ecological specialization, and the evolutionary integration of complex morphological structures. *Evolution* 64(3):724-744.
- Mooney MP, Siegel MI, Gest TR. 1985. Prenatal stress and increased fluctuating asymmetry in the parietal bones of neonatal rats. *Am J Phys Anthropol* 68(1):131-134.
- Morriss-Kay GM, Wilkie AO. 2005. Growth of the normal skull vault and its alteration in craniosynostosis: Insights from human genetics and experimental studies. *J Anat* 207(5):637-653.
- Moss M, Meehan M. 1970. Functional cranial analysis of the coronoid process in the rat. *Acta Anat* 77(1):11-24.
- Moitch Perrine SM, Cole TM, Martínez-Abadías N, Aldridge K, Jabs EW, Richtsmeier JT. 2014. Craniofacial divergence by distinct prenatal growth patterns in *Fgfr2* mutant mice. *BMC Dev Biol* 14:8-213X-14-8.

- Muenke M, Schell U. 1995. Fibroblast-growth-factor receptor mutations in human skeletal disorders. *Trends in Genetics* 11(8):308-313.
- Muñoz-Muñoz F, Sans-Fuentes M, López-Fuster M, Ventura J. 2011. Evolutionary modularity of the mouse mandible: Dissecting the effect of chromosomal reorganizations and isolation by distance in a Robertsonian system of *Mus musculus domesticus*. *J Evol Biol* 24(8):1763-1776.
- Needham J. 1933. On the dissociability of the fundamental processes in ontogenesis. *Biol Rev*, 8:180-223
- Nonaka K, Nakata M. 1988. Genetic and environmental factors in the longitudinal growth of rats: III. Craniofacial shape change. *J Craniofac Genet Dev Biol* 8(4):337-344.
- Norconk MA, Conklin-Brittain NL. 2004. Variation on frugivory: the diet of Venezuelan white-faced sakis. *Int J Primatol* 25(1):1-26.
- Norconk MA, Grafton BW, Conklin-Brittain NL. 1998. Seed dispersal by Neotropical seed predators. *Am J Primatol* 45:103-126.
- Norconk M, Grafton B, McGraw S, Veiga L, Ferrari S, Norconk M. 2013. Morphological and ecological adaptations to seed predation—A primate-wide perspective. In: Barnett AA, Veiga LM, Ferrari SF, Norconk MA, editors. *Evolutionary biology and conservation of Titis, Sakis and Uacaris*. Cambridge, UK: Cambridge University Press. p: 55-71.
- Norconk MA, Veres M. 2011. Physical properties of fruit and seeds ingested by primate seed predators with emphasis on sakis and bearded sakis. *Anat Rec* 294(12):2092-2111.
- Norconk MA, Wright BW, Conklin-Brittain NL, Vinyard CJ. 2009. Mechanical and nutritional properties of food as factors in platyrrhine dietary adaptations. In: Garber PA, Estrada A, Bicca-Marques JC, Heymann EK, Strier KB, editors.

South American primates: comparative perspectives in the study of behavior, ecology, and conservation. New York: Springer. Springer. p 279-319.

Olson E, Miller R. 1958. Morphological integration. Chicago: University of Chicago Press.

Ornitz DM, Marie PJ. 2002. FGF signaling pathways in endochondral and intramembranous bone development and human genetic disease. *Genes Dev* 16(12):1446-1465.

Palacios E, Rodriguez A, Defler TR. 1997. Diet of a group of *Callicebus torquatus lugens* (Humboldt, 1812) during the annual resource bottleneck in Amazonian Columbia. *Int. J Primatol* 18(4):503-522.

Parsons KJ, Márquez E, Albertson RC. 2012. Constraint and opportunity: The genetic basis and evolution of modularity in the cichlid mandible. *Am Nat* 179(1):64-78.

Percival CJ, Green R, Marcucio R, Hallgrímsson B. 2014. Surface landmark quantification of embryonic mouse craniofacial morphogenesis. *BMC Developmental Biology* 14(1):31.

Perelman P, Johnson WE, Roos C, Seuánez HN, Horvath JE, Moreira M, Kessing B, Pontius J, Roelke M, Rumpler Y. 2011. A molecular phylogeny of living primates. *PLoS Genet* 7(3):e1001342.

Perez SI, Bernal V, Gonzalez PN. 2006. Differences between sliding semi-landmark methods in geometric morphometrics, with an application to human craniofacial and dental variation. *J Anat* 208(6):769-784.

Perlyn CA, DeLeon VB, Babbs C, Govier D, Burell L, Darvann T, Kreiborg S, Morriss-Kay G. 2006a. The craniofacial phenotype of the Crouzon mouse: Analysis of a model for syndromic craniosynostosis using three-dimensional MicroCT. *The Cleft Palate-Craniofacial Journal* 43(6):740-748.

- Perlyn CA, Morriss-Kay G, Darvann T, Tenenbaum M, Ornitz DM. 2006b. A model for the pharmacological treatment of crouzon syndrome. *Neurosurgery* 59(1):210-5.
- Perry JMG, Hartstone-Rose A, Logan RL. 2011. The jaw adductor resultant and estimated bite force in primates. *Anatomy Research International* vol. 2011, Article ID 929848: 1-11.
- Pierce SE, Agielczyk KD, Rayfield EJ. 2008. Patterns of morphospace occupation and mechanical performance in extant crocodilian skulls: A combined geometric morphometric and finite element modeling approach. *J Morphol* 269:840–864
- Pinheiro T, Ferrari SF, Lopes MA. 2013. Activity budget, diet and use of space by two groups of squirrel monkeys (*Saimiri sciureus*) in eastern Amazonia. *Primates* 54(3):301-308.
- Piras P, Maiorino L, Teresi L, Meloro C, Lucci F, Kotsakis T, Raia P. 2013. Bite of the cats: Relationships between functional integration and mechanical performance as revealed by mandible geometry. *Syst Biol* 62(6):878-900.
- Podolsky RD. 1990. Effects of mixed-species association on resource use by *Saimiri sciureus* and *Cebus apella*. *Am J Primatol* 21(2):147-158.
- Polanski JM. 2011. Morphological integration of the modern human mandible during ontogeny. *Int J Evol Biol* 2011:545879.
- Porto A, de Oliveira FB, Shirai LT, De Conto V, Marroig G. 2009. The evolution of modularity in the mammalian skull I: Morphological integration patterns and magnitudes. *Evolutionary Biology* 36(1):118-135.
- Porto A, Shirai LT, de Oliveira FB, Marroig G. 2013. Size variation, growth strategies and the evolution of modularity. *Evolution*, 67:3305-3322.

- R Development Core Team. 2008. R: A language and environment for statistical computing. Available at: [http:// www.r-project.org/](http://www.r-project.org/).
- Raff RA, Sly BJ. 2000. Modularity and dissociation in the evolution of gene expression territories in development. *Evol Dev* 2(2):102-113.
- Ramaesh T, Bard JB. 2003. The growth and morphogenesis of the early mouse mandible: A quantitative analysis. *J Anat* 203(2):213-222.
- Ravosa MJ. 1996. Jaw morphology and function in living and fossil old world monkeys. *Int J Primatol* 17(6):909-932.
- Ravosa MJ, López EK, Menegaz RA, Stock SR, Stack MS, Hamrick MW. 2008. Adaptive plasticity in the mammalian masticatory complex: You are what, and how, you eat. In: Vinyard DJ, Ravosa MJ, Wall CE, editors. *Primate Craniofacial Biology and Function*. New York: Springer Academic Publishers.p:293-328.
- Ravosa MJ, Kunwar R, Stock SR, Stack MS. 2007. Pushing the limit: Masticatory stress and adaptive plasticity in mammalian craniomandibular joints. *J Exp Biol* 210(4):628-641.
- Ray DA, Xing J, Hedges DJ, Hall MA, Laborde ME, Anders BA, White BR, Stoilova N, Fowlkes JD, Landry KE. 2005. Alu insertion loci and platyrrhine primate phylogeny. *Mol Phylogenet Evol* 35(1):117-126.
- Reitsma JH, Ongkosuwito EM, Buschang PH, Prah-Andersen B. 2012. Facial growth in patients with Apert and Crouzon syndromes compared to normal children. *The Cleft Palate-Craniofacial Journal* 49(2):185-193.
- Renaud S, Hardouin E, Pisanu B, Chapuis J. 2013. Invasive house mice facing a changing environment on the Sub-Antarctic Guillou island (Kerguelen archipelago). *J Evol Biol* 26(3):612-624.

- Renaud S, Gomes Rodrigues H, Ledevin R, Pisanu B, Chapuis J, Hardouin EA. 2015. Fast evolutionary response of house mice to anthropogenic disturbance on a Sub-Antarctic island. *Biol J Linn Soc* 114(3):513-526.
- Renaud S, Auffray JC, de la Porte S. 2010. Epigenetic effects on the mouse mandible: Common features and discrepancies in remodeling due to muscular dystrophy and response to food consistency. *BMC Evol Biol* 10:28-2148-10-28.
- Richtsmeier JT, Cole III TM, Lele SR. 2005. An invariant approach to the study of fluctuating asymmetry: Developmental instability in a mouse model for Down syndrome. In: Slice D, editor. *Modern morphometrics in physical anthropology*. New York, NY: Kluwer Academic/Plenum Publishers p 187-212.
- Richtsmeier JT, DeLeon VB. 2009. Morphological integration of the skull in craniofacial anomalies. *Orthodontics & Craniofacial Research* 12(3):149-158.
- Richtsmeier JT, Aldridge K, DeLeon VB, Panchal J, Kane AA, Marsh JL, Yan P, Cole TM. 2006. Phenotypic integration of neurocranium and brain. *J Exp Zool B Mol Dev Evol* 306(4):360-378.
- Riedl R, Jefferies RPS. 1978. *Order in living organisms: A systems analysis of evolution*. Wiley New York.
- Riska B, Atchley WR, Rutledge JJ. 1984. A genetic analysis of targeted growth in mice. *Genetics* 107(1):79-101.
- Robinson JG, Redford KH. 1986. Body size, diet, and population density of Neotropical forest mammals. *Am Nat* 128 (5):665-680.
- Rohlf FJ, Corti M. 2000. Use of two-block partial least-squares to study covariation in shape. *Syst Biol* 49(4):740-753.

- Rohlf FJ, Slice D. 1990. Extensions of the Procrustes method for the optimal superimposition of landmarks. *Syst Zool* 39(1):40-59.
- Roseman CC, Kenny-Hunt JP, Cheverud JM. 2009. Phenotypic integration without modularity: Testing hypotheses about the distribution of pleiotropic quantitative trait loci in a continuous space. *Evolutionary Biology* 36(3):282-291.
- Rosenberger AL. 1984. Fossil new world monkeys dispute the molecular clock. *J Hum Evol* 13(8):737-742.
- Rosenberger AL, Tejedor MF. 2013. The misbegotten: Long lineages, long branches and the interrelationships of *Aotus*, *Callicebus* and the saki-uacaris In: Barnett AA, Veiga LM, Ferrari SF, Norconk MA, editors. *Evolutionary biology and conservation of Titis, Sakis and Uacaris*. Cambridge, UK: Cambridge University Press. p 13-22.
- Rosenberger AL, Klukkert ZS, Cooke SB, Rímoli R. 2013. Rethinking antillothrix: The mandible and its implications. *Am J Primatol* 75(8):825-836.
- Rosenberger AL, Setoguchi T, Shigehara N. 1990. The fossil record of callitrichine primates. *J Hum Evol* 19(1):209-236.
- Ross CF, Iriarte-Diaz J, Nunn CL. 2012. Innovative approaches to the relationship between diet and mandibular morphology in primates. *Int J Primatol* 33(3):632-660.
- Ross C. 1991. Life history patterns of new world monkeys. *Int J Primatol* 12(5):481-502.
- Rothman JM, Raubenheimer D, Bryer MA, Takahashi M, Gilbert CC. 2014. Nutritional contributions of insects to primate diets: implications for primate evolution. *J Hum Evol* 71:59-69.



- Ryan TM, Colbert M, Ketcham RA, Vinyard CJ. 2010. Trabecular bone structure in the mandibular condyles of gouging and nongouging platyrrhine primates. *Am J Phys Anthropol* 141(4):583-593.
- Rylands AB, Mittermeier RA. 2009. The diversity of the New World primates (Platyrrhini): an annotated taxonomy. In: Garber PA, Estrada A, Bicca-Marques JC, Heymann EK, Strier KB, editors. *South American primates: comparative perspectives in the study of behavior, ecology, and conservation*. New York: Springer. p 23-54.
- Schneider H, Schneider M, Sampaio I, Harada M, Stanhope M, Czelusniak J, Goodman M. 1993. Molecular phylogeny of the New World monkeys (Platyrrhini, Primates). *Mol Phylogenet Evol* 2(3):225-242.
- Schneider H, Canavez FC, Sampaio I, Moreira MÂM, Tagliaro CH, Seuánez HN. 2001. Can molecular data place each Neotropical monkey in its own branch? *Chromosoma* 109(8):515-523.
- Schneider H, Sampaio I. 2015. The systematics and evolution of New World primates—A review. *Mol Phylogenet Evol* 82:348-357.
- Schneider H, Sampaio I, Harada M, Barroso C, Schneider M, Czelusniak J, Goodman M. 1996. Molecular phylogeny of the New World monkeys (Platyrrhini, Primates) based on two unlinked nuclear genes: IRBP intron 1 and  $\epsilon$ -globin sequences. *Am J Phys Anthropol* 100:153-180.
- Schwartz-Dabney CL, Dechow PC. 2003. Variations in cortical material properties throughout the human dentate mandible. *Am J Phys Anthropol* 120 (3):252-277.
- Scott JE, McAbee KR, Eastman MM, Ravosa MJ. 2014. Teaching an old jaw new tricks: Diet-induced plasticity in a model organism from weaning to adulthood. *J Exp Biol* 217(Pt 22):4099-4107.

- Shetye PR, Davidson EH, Sorkin M, Grayson BH, McCarthy JG. 2010. Evaluation of three surgical techniques for advancement of the midface in growing children with syndromic craniosynostosis. *Plast Reconstr Surg* 126(3):982-994.
- Shirai LT, Marroig G. 2010. Skull modularity in Neotropical marsupials and monkeys: Size variation and evolutionary constraint and flexibility. *Journal of Experimental Zoology Part B: Molecular and Developmental Evolution* 314(8):663-683.
- Sholts S, Flores L, Walker P, Wärmländer S. 2011. Comparison of coordinate measurement precision of different landmark types on human crania using a 3D laser scanner and a 3D digitizer: Implications for applications of digital morphometrics. *International Journal of Osteoarchaeology* 21(5):535-543.
- Singh N, Harvati K, Gunz P, Hublin J. 2007. A 3D geometric morphometric study of morphological integration in the primate mandible. *Am J Phys Anthropol* 134(45 (Supplemental)):219.
- Singh N. 2014. Ontogenetic study of allometric variation in *Homo* and *Pan* mandibles. *Anat Rec* 297(2):261-272.
- Singh N, Harvati K, Hublin J, Klingenberg CP. 2012. Morphological evolution through integration: A quantitative study of cranial integration in *Homo*, *Pan*, *Gorilla* and *Pongo*. *J Hum Evol* 62(1):155-164.
- Smith RJ, Jungers WL. 1997. Body mass in comparative primatology. *J Hum Evol* 32(6):523-559.
- Slice DE. 2007. Geometric morphometrics *Annu. Rev. Anthropol.* 36(1):261-281.
- Spencer M.A., Demes B. 1993. Biomechanical analysis of masticatory system configuration in Neandertals and Inuits. *Am J Phys Anthropol* 91 (1):1-20.

- Spyropoulos MN, Tsolakis AI, Alexandridis C, Katsavrias E, Dontas I. 2002. Role of suprahyoid musculature on mandibular morphology and growth orientation in rats. *American Journal of Orthodontics and Dentofacial Orthopedics* 122(4):392-400.
- Steppan SJ. 1997. Phylogenetic analysis of phenotypic covariance structure. II. Reconstructing matrix evolution. *Evolution* 51(2):587-594.
- Stone AI. 2006. Foraging ontogeny is not linked to delayed maturation in squirrel monkeys (*Saimiri sciureus*). *Ethology* 112(2):105-115.
- Stringer C. 2003. Human evolution: Out of Ethiopia. *Nature* 423(6941):692-695.
- Swiderski DL, Zelditch ML. 2010. Morphological diversity despite isometric scaling of lever arms. *Evolutionary Biology* 37(1):1-18.
- Swiderski DL, Zelditch ML. 2013. The complex ontogenetic trajectory of mandibular shape in a laboratory mouse. *J Anat* 223(6):568-580.
- Tanaka E, Sano R, Kawai N, Langenbach GE, Brugman P, Tanne K, van Eijden TM. 2007. Effect of food consistency on the degree of mineralization in the rat mandible. *Ann Biomed Eng* 35(9):1617-1621.
- Taylor AB. 2002. Masticatory form and function in the African apes. *Am J Phys Anthropol* 117(2):133-156.
- Taylor AB, Eng CM, Anapol FC, Vinyard CJ. 2009. The functional correlates of jaw-muscle fiber architecture in tree-gouging and nongouging callitrichid monkeys. *Am J Phys Anthropol* 139:353-367.
- Taylor AB, Vinyard CJ. 2009. Jaw-muscle fiber architecture in tufted capuchins favors generating relatively large muscle forces without compromising jaw gape. *J Hum Evol* 57(6):710-720.

- Terborgh J. 1983. Five Neotropical primates: A study in comparative ecology. Princeton, NJ: Princeton University Press.
- Turner CH, Burr DB. 1993. Basic biomechanical measurements of bone: A tutorial. *Bone* 14(4):595-608.
- Vinyard CJ. 2008. Putting shape to work: Making functional interpretations of masticatory apparatus shapes in primates. In: Vinyard CJ, Ravosa MF, Wall CE, editors. *Primate Craniofacial Function and Biology*. New York, NE: Springer. p 357-385.
- Vinyard CJ, Ryan TM. 2006. Cross-sectional bone distribution in the mandibles of gouging and non-gouging *Platyrrhini*. *Int J Primatol* 27(5):1461-1490.
- Vinyard CJ, Taylor AB. 2010. A preliminary analysis of the relationship between Jaw-Muscle architecture and jaw-muscle electromyography during chewing across primates. *Anat Rec* 293(4):572-582.
- Vinyard CJ, Wall CE, Williams SH, Hylander WL. 2003. Comparative functional analysis of skull morphology of tree-gouging primates. *Am J Phys Anthropol* 120(2):153-170.
- Vinyard CJ, Payseur BA. 2008. Of "mice" and mammals: Utilizing classical inbred mice to study the genetic architecture of function and performance in mammals. *Integr Comp Biol* 48(3):324-337.
- Vinyard CJ, Wall CE, Williams SH, Hylander WL. 2008. Patterns of variation across primates in jaw-muscle electromyography during mastication. *Integr Comp Biol* 48(2):294-311.
- Vinyard CJ, Williams SH, Wall CE, Doherty AH, Crompton AW, Hylander WL. 2011. A preliminary analysis of correlations between chewing motor patterns and mandibular morphology across mammals. *Integr Comp Biol* 51(2):260-270.

- Visalberghi E, Sabbatini G, Spagnoletti N, Andrade F, Ottoni E, Izar P, Fragaszy D. 2008. Physical properties of palm fruits processed with tools by wild bearded capuchins (*Cebus libidinosus*). *Am J Primatol* 70:884-891.
- Vogl C, Atchley WR, Xu S. 1994. The ontogeny of morphological differences in the mandible in two inbred strains of mice. *J Craniofac Genet Dev Biol* 14(2):97-110.
- von Cramon-Taubadel N. 2011. Global human mandibular variation reflects differences in agricultural and hunter-gatherer subsistence strategies. *Proc Natl Acad Sci USA* 108(49):19546-19551.
- Wagner G. 1990. A comparative study of morphological integration in *Apis mellifera* (Insecta, Hymenoptera). *J Zool Syst Evol Res* 28(1):48-61.
- Wagner GP. 1996. Homologues, natural kinds and the evolution of modularity. *Am Zool* 36(1):36-43.
- Wagner GP, Altenberg L. 1996. Perspective: Complex adaptations and the evolution of evolvability. *Evolution* 50(3):967-976.
- Wagner GP, Kenney-Hunt JP, Pavlicev M, Peck JR, Waxman D, Cheverud JM. 2008. Pleiotropic scaling of gene effects and the 'cost of complexity'. *Nature* 452(7186):470-472.
- Wagner GP, Pavlicev M, Cheverud JM. 2007. The road to modularity. *Nature Reviews Genetics* 8(12):921-931.
- Wainwright PC, Alfaro ME, Bolnick DI, Hulsey CD. 2005. Many-to-one mapping of form to function: A general principle in organismal design? *Integr Comp Biol* 45(2):256-262.

- Wellens H, Kuijpers-Jagtman A, Halazonetis D. 2013. Geometric morphometric analysis of craniofacial variation, ontogeny and modularity in a cross-sectional sample of modern humans. *J Anat* 222(4):397-409.
- Wery M, Nada R, van der Meulen J, Wolvius E, Ongkosuwito E. 2015. Three-dimensional computed tomographic evaluation of Le Fort III distraction osteogenesis with an external device in syndromic craniosynostosis. *British Journal of Oral and Maxillofacial Surgery* 53(3):285-291.
- Wildman DE, Jameson NM, Opazo JC, Soojin VY. 2009. A fully resolved genus level phylogeny of Neotropical primates (Platyrrhini). *Mol Phylogenet Evol* 53(3):694-702.
- Wilkie AO. 1997. Craniosynostosis: Genes and mechanisms. *Hum Mol Genet* 6(10):1647-1656.
- Willmore KE, Roseman CC, Rogers J, Cheverud JM, Richtsmeier JT. 2009. Comparison of mandibular phenotypic and genetic integration between baboon and mouse. *Evolutionary Biology* 36(1):19-36.
- Willmore KE, Leamy L, Hallgrímsson B. 2006. Effects of developmental and functional interactions on mouse cranial variability through late ontogeny. *Evol Dev* 8(6):550-567.
- Wright BW. 2005. Craniodental biomechanics and dietary toughness in the genus *Cebus*. *J Hum Evol* 48(5):473-492.
- Wright BW, Wright KA, Chalk J, Verderane P, Fragaszy D, Visalberghi E, Izar P, Ottoni EB, Constatntino P, Vinyard C. 2009. Fallback Foraging as a Way of Life: Using Dietary Toughness to Compare the Fallback Signal Among Capuchins and Implications for Interpreting Morphological Variation *Am J Phys Anthropol* 140(4):687-699.
- Young NM, Hallgrímsson B. 2005. Serial homology and the evolution of mammalian limb covariation structure. *Evolution* 59(12):2691-2704.

- Young RL, Badyaev AV. 2006. Evolutionary persistence of phenotypic integration: Influence of developmental and functional relationships on complex trait evolution. *Evolution* 60(6):1291-1299.
- Young RL, Badyaev AV. 2010. Developmental plasticity links local adaptation and evolutionary diversification in foraging morphology. *Journal of Experimental Zoology Part B: Molecular and Developmental Evolution* 314(6):434-444.
- Young RL, Haselkorn TS, Badyaev AV. 2007. Functional equivalence of morphologies enables morphological and ecological diversity. *Evolution* 61(11):2480-2492.
- Young RL, Sweeny MJ, Badyaev AV. 2010. Morphological diversity and ecological similarity: versatility of muscular and skeletal morphologies enables ecological convergence in shrews. *Functional Ecology* 24(3):556-565.
- Zelditch ML, Carmichael AC. 1989a. Growth and intensity of integration through postnatal growth in the skull of *Sigmodon fulviventer*. *J Mammal* 70 (3):477-484.
- Zelditch ML, Carmichael AC. 1989b. Ontogenetic variation in patterns of developmental and functional integration in skulls of *Sigmodon fulviventer*. *Evolution* 43 (4):814-824.
- Zelditch ML. 1988. Ontogenetic variation in patterns of phenotypic integration in the laboratory rat. *Evolution* 42(1):28-41.
- Zelditch ML, Lundrigan BL, Garland T. 2004. Developmental regulation of skull morphology. I. ontogenetic dynamics of variance. *Evol Dev* 6(3):194-206.
- Zelditch ML, Mezey J, Sheets HD, Lundrigan BL, Garland T. 2006. Developmental regulation of skull morphology II: Ontogenetic dynamics of covariance. *Evol Dev* 8(1):46-60.

Zelditch ML, Swiderski DL, Sheets HD. 2012. Geometric morphometrics for biologists: A primer. San Diego, CA: Elsevier Academic Press.

Zelditch ML, Wood AR, Bonett RM, Swiderski DL. 2008. Modularity of the rodent mandible: Integrating bones, muscles, and teeth. *Evol Dev* 10(6):756-768.

Zelditch ML, Wood AR, Swiderski DL. 2009. Building developmental integration into functional systems: Function-induced integration of mandibular shape. *Evolutionary Biology* 36(1):71-87.

Zelditch M. 2005. Developmental regulation of variation. In: Hallgrímsson B, Hall BK, editors. *Variation: A Central Concept in Biology*. San Diego: Academic Press. 249–276.

Zimble-DeLorenzo HS, Dobson FS. 2011. Demography of squirrel monkeys (*Saimiri sciureus*) in captive environments and its effect on population growth. *Am J Primatol* 73(10):1041-1050.

Zimble-DeLorenzo HS, Stone AI. 2011. Integration of field and captive studies for understanding the behavioral ecology of the squirrel monkey (*Saimiri* sp.). *Am J Primatol* 73(7):607-622.





## CURRICULUM VITAE

The Johns Hopkins University School of Medicine

Megan A. Holmes

October/ 13/ 2015

### **Educational History:**

Ph.D. expected	2015	Center for Functional Anatomy and Evolution Mentor: Valerie DeLeon, Ph.D.	Johns Hopkins School of Medicine
B.A.	2005	Anthropology	Florida Atlantic University

### **Professional Experience:**

Lead Instructor	2014 – Present	Physician Assistant Anatomy, Duke Physician Assistant Program, Duke School of Medicine.
Laboratory Instructor	2014 – Present	Body and Brain I & II, Doctor of Physical Therapy Program, Duke School of Medicine
Instructor	2013	Clinical Anatomy for Physician Assistants, Towson University/ CCBC Physician Assistant Program
Research Assistant	2008-2013	Dr. Valerie DeLeon, Johns Hopkins School of Medicine
Laboratory Instructor	2010, 2011, 2012	Gross Anatomy, Johns Hopkins School of Medicine
Laboratory Instructor	2009, 2010	Summer Institute in Anatomy, Johns Hopkins
Research Assistant	2006	Dr. Doug Broadfield, Florida Atlantic University Department of Anthropology
Teaching Assistant	2006	Reasons and Values, Florida Atlantic University Department of Philosophy
Research Assistant	2006	Florida Atlantic Field School in Ecuador, South America

Teaching Assistant      2005      Environment and Disease, Florida Atlantic  
University Department of Anthropology

**Research Grants:**

Marrow Research Grant (\$3,000)      Grant to conduct independent research.

**Publications, peer reviewed:**

Ruff CB, Garofalo E, **Holmes MA**. 2013. Interpreting skeletal growth in the past from a functional and physiological perspective. *American Journal of Physical Anthropology*, 150: 29-37.

**Holmes MA**, Ruff CB. 2011. Dietary effects on development of the human mandibular corpus. *American Journal of Physical Anthropology*, 145(4):615-628.

**Presentations:**

**Holmes MA**, DeLeon VD. 2014. The functional influence on trait covariance in platyrrhine mandibles. *American Journal of Physical Anthropology*, 151(S57): 158

**Holmes MA**. 2013. Tooth root and crown surface areas have different allometric relationships associated with diet in cercopithecines. *American Journal of Physical Anthropology*, 150(S56): 151

**Holmes MA**. 2013. The influence of dentition on the developing mandible in a mouse model. *The FASEB Journal*, 27: 963.7.

**Holmes MA**, Peburn T, DeLeon V. 2012. Molar surface area and mandibular mechanics: complex scaling relationships in primate masticatory systems. *The FASEB Journal*, 26:455.2.

**Holmes MA**, Ruff CB, Garofalo EM. 2011. Diet and ontogenetic changes in human mandibular strength. *American Journal of Physical Anthropology*, 141 (S50):130.

**Holmes MA**, Ruff C, DeLeon V, Brown K, Frolich B. 2010. Scaling in the primate masticatory apparatus. *The FASEB Journal*, 24: 1b10

**Holmes MA**, Garofalo EM, Ruff CB. 2010. Contrasting growth patterns in strength of the human mandible and long bones. *American Journal of Physical Anthropology*, 141(S50):130.

**Holmes MA**, McCarthy R, Mooney M, Siegel M. 2008. Developmental integration in the primate sphenoid and ethmomaxillary complex. *American Journal of Physical Anthropology*, 135(S46):119

McCarthy R, **Holmes MA**, Lucas L, O'Donnell K. 2007. Taxonomy of Middle Pleistocene humans: What is *Homo heidelbergensis*, anyway? *American Journal of Physical Anthropology*, 134(S45): 167